UNCLASSIFIED

AD NUMBER

AD826428

NEW LIMITATION CHANGE

TO

Approved for public release, distribution unlimited

FROM

Distribution: Further dissemination only as directed by Air Force Materials Lab., Nonmetallic Materials Div., Wright-Patterson AFB, OH 45433. Dec 1967, or higher DoD authority.

AUTHORITY

AFML ltr, 7 Dec 1972

THIS PAGE IS UNCLASSIFIED

AFML-TR-67-164

AD826428

JOINT AIR FORCE-NAVY SUPERSONIC RAIN EROSION EVALUATIONS OF MATERIALS

GEORGE F. SCHMITT, JR.

AIR FORCE MATERIALS LABORATORY

GEORGE J. TATNALL
KENNETH W. FOULKE

NAVAL AIR DEVELOPMENT CENTER

TECHNICAL REPORT AFML-TR-67-164

DECEMBER 1967

This document may be further distributed by any holder only with specific prior approval of the Elastomers and Coatings Branch (MANE), Nonmetallic Materials Division, Air Force Materials Laboratory, Wright-Patterson Air Force Base, Ohio 45433, or the Radome Antenna Section (AERT), Radar Division, Naval Air Development Center, Johnsville, Pennsylvania 18974.

AIR FORCE MATERIALS LABORATORY
AIR FORCE SYSTEMS COMMAND
WRIGHT-PATTERSON AIR FORCE BASE, OHIO

DISCLAIMER NOTICE

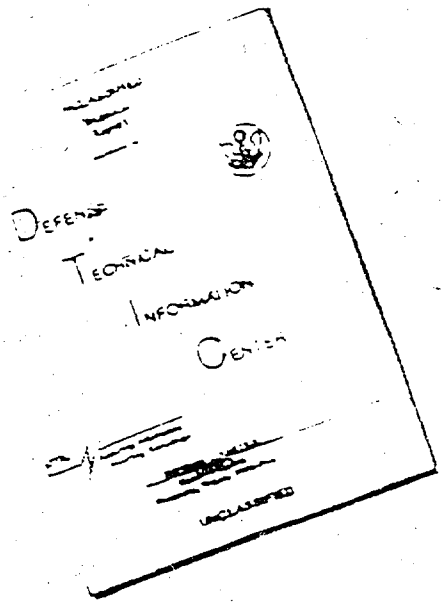

THIS DOCUMENT IS BEST QUALITY AVAILABLE. THE COPY FURNISHED TO DTIC CONTAINED A SIGNIFICANT NUMBER OF PAGES WHICH DO NOT REPRODUCE LEGIBLY.

REPRODUCED FROM
BEST AVAILABLE COPY

NOTICE

When Government drawings, specifications, or other data are used for any purpose other than in connection with a definitely related Government procurement operation, the United States Government thereby incurs no responsibility nor any obligation whatsoever; and the fact that the Government may have formulated, furnished, or in any way supplied the said drawings, specifications, or other data, is not to be regarded by implication or otherwise as in any manner licensing the holder or any other person or corporation, or conveying any rights or permission to manufacture, use, or sell any patented invention that may in any way be related thereto.

Copies of this report should not be returned unless return is required by security considerations, contractual obligations, or notice on a specific document.

200 - January 1968 - CO455 - 22-481

AFML-TR-67-164

JOINT AIR FORCE-NAVY SUPERSONIC RAIN EROSION EVALUATIONS OF MATERIALS

GEORGE F. SCHMITT, JR

AIR FORCE MATERIALS LABORATORY

GEORGE J. TATNALL
KENNETH W. FOULKE

NAVAL AIR DEVELOPMENT CENTER

This document may be further distributed by any holder only with specific prior approval of the Elastomers and Coatings Branch (MANE), Nonmetallic Materials Division, Air Force Materials Laboratory, Wright-Patterson Air Force Base, Ohio 45433, or the Radome Antenna Section (AERT), Radar Division, Naval Air Development Center, Johnsville, Pennsylvania 18974.

FOREWORD

This report was prepared by George F. Schmitt, Jr., Elastomers and Coatings Branch (MAME), Nonmetallic Materials Division, Air Force Materials Laboratory, Directorate of Laboratories, Air Force Systems Command, Wright-Patterson Air Force Base, Ohio, and by George J. Tatnall and Kenneth W. Foulke, Naval Air Development Center, Johnsville, Pennsylvania. This work was initiated under AFSC Project No. 7340 "Nonmetallic and Composite Materials," Task No. 734007 "Coatings for Energy Utilization, Control and Protective Functions," and NAVAIR SYMCOM Weptask RAV 03J 001/2021/R008-01-01, Problem Assignment 25.

This report covers work conducted from January 1966 to December 1966. The manuscript was released by the authors in March 1967 for publication.

The discussion of materials by brand names in this report is in no way to be taken as endorsement or criticism of them by the Government. They were selected as representative of certain classes of materials and their names are a convenient way of handling and discussing them. The Government incurs no liability or obligation to any supplier of materials from the information included in this report.

The authors express their appreciation for the support and cooperation of Bernard K. Jackson, 1/Lt USAF, Project Engineer, and the personnel of the Track Test Directorate, Air Force Missile Development Center, Holloman Air Force Base, New Mexico. Their efforts in firing the rocket sled tests were greatly responsible for the timely completion of this series.

Appreciation is also extended to the materials suppliers for their contributions of materials samples and material properties measurements to the program at no cost to the Government.

This technical report has been reviewed and is approved.

WARREN P. JOHNSON, Acting Chief
Elastomers & Coatings Branch
Nonmetallic Materials Division
Air Force Materials Laboratory

ABSTRACT

A comprehensive investigation of sixty-five dielectric and other materials for short exposure time rain erosion resistance at velocities of Mach 1.5, 2.0, 2.5 and 3.0 has recently been accomplished in a joint program of the Elastomers and Coatings Branch, Nonmetallic Materials Division, Air Force Materials Laboratory and the Radome-Antenna Section, Naval Air Development Center. This work was accomplished at the Holloman AFB Test Track Facility, New Mexico.

Multiple samples of each material were mounted in a wedge shaped holder attached to the forward end of a multi-staged rocket sled and exposed to the same rain environment by firing the sled through a 6,000 feet long artificial rainfield. The samples were exposed at five different impact angles and four different velocities and the quantitative rain erosion resistance determined as a function of velocity, time of exposure and impact angle. Although the exposure times were short the materials demonstrated real differences in their rain erosion resistance.

Materials evaluated included isotropic and sandwich ceramics, plastic laminates, nickel electroplated plastics, inorganic laminates, ceramic and elastomeric coated laminates, glasses, thermoplastics, sandwich plastics and metals. The results of these supersonic exposures are summarized and listed according to materials category.

Quantitative data in the form of weight loss per unit area and mean depth of penetration rate (MDPR) are presented. Equations describing the high velocity-short exposure time erosion rates of plastic laminates and fused silica ceramics have been developed. Data for most other materials have been plotted but not fitted to equations. Photographs of all rain-exposed specimens and descriptions of the 65 materials evaluated are included.

Distribution of this Abstract is unlimited.

TABLE OF CONTENTS

SECTION		PAGE
I	INTRODUCTION	1
II	SUMMARY	2
III	THE RAIN EROSION WEDGE	3
	1. Physical Description	3
	2. Aerodynamic Characteristics	6
	3. Drop Disintegration Effects	6
IV	HOLLOMAN TRACK FACILITY	10
	1. Track Description	10
	2. Rocket Sled	10
	3. Instrumentation	12
V	HOLLOMAN RAIN FIELD	13
	1. Description Of The System	13
	2. Rain Size And Distribution	13
	3. Firing Conditions	13
VI	MATERIALS EVALUATED	17
	1. Classes Of Materials	17
	2. Sample Processing	17
	3. Property Data	19
VII	RAIN EROSION DAMAGE DATA	21
	1. The Card Photographs	21
	2. The High Velocity-Short Exposure Time Rain Erosion Equation	21
	3. Rain Erosion Phenomenon	25
	4. Failure Mechanism In Materials	25
	5. Calibration Runs	25
VIII	EVALUATION RESULTS	31
	1. Class A - Isotropic Ceramics	32
	2. Class B - Sandwich Ceramics	50
	3. Class C - Plastic Laminates	54
	4. Class D - Inorganic Laminates	68

TABLE OF CONTENTS (CONTD)

SECTION		PAGE
	5. Class E - Ceramic Coated Laminates	72
	6. Class F - Elastomeric Coated Laminates	94
	7. Class G - Glasses	110
	8. Class H - Sandwich Plastics	116
	9. Class I - Thermal Plastics	126
	10. Class J - Metals	132
IX	DISCUSSION OF RESULTS	136
X	CONCLUSIONS	138
XI	FUTURE WORK	141
	REFERENCES	160

ILLUSTRATIONS

FIGURE		PAGE
1.	Supersonic Rain Erosion Wedge	4
2.	Sample Mounting and Cover Plate	5
3.	Rain Erosion Wedge Shock Wave Pattern (M = 2.85)	7
4.	Drop Disintegration Times vs Wedge Exposure Times	9
5.	Rain Erosion Rocket Sled (Mach 3.0 Configuration)	11
6.	Holloman Rain Field	14
7.	Particle Size Distribution of Natural Rainfall	15
8.	Drop Size Distribution at Holloman Track Rain Simulation System (System Pressure - 9 psi)	16
9.	Materials Suppliers Data Form	18
10.	Mean Depth of Penetration Rate vs Sine of the Impact Angle for PBI Laminates	22
11.	Slope and Intercept of the Rain Erosion Equation vs Velocity for PBI Laminates	24
12.	Mach 1.5 Calibration Run Data (1758.0 ft/sec)	26
13.	Mach 2.0 Calibration Run Data (2116.9 ft/sec)	27
14.	Mach 2.5 Calibration Run Data (2549.0 ft/sec)	28
15.	Mach 3.0 Calibration Run Data (3366.4 ft/sec)	29
16.	Sample Position Numbers in Wedge	30
17.	Rain Erosion Damage Data for 9606 Pyroceram	33
18.	Rain Erosion Damage Data for 9611 Pyroceram	35
19.	Rain Erosion Damage Data for Alsimag 753 Alumina	37
20.	Rain Erosion Damage Data for Wearox Alumina and AL-300 Alumina	38
21.	Rain Erosion Damage Data for Alsimag 754 Beryllia	41
22.	MDPR vs Sine Impact Angle - Alsimag 701 Cordierite	42
23.	Rain Erosion Damage Data for Alsimag 701 Cordierite	43
24.	MDPR vs Sine Impact Angle - GD/P Fused Silica	44

ILLUSTRATIONS (CONTD)

FIGURE		PAGE
25.	Rain Erosion Damage Data for Corning 7941 Fused Silica	45
26.	Rain Erosion Damage Data for GD/P Fused Silica (Type I)	46
27.	Rain Erosion Damage Data for GD/P Fused Silica (Type II)	47
28.	Rain Erosion Damage Data for GD/P Fused Silica (Type III)	48
29.	Rain Erosion Damage Data for 0.040 Inch Alumina/Alumina Foam/ 0.040 Inch Alumina	51
30.	Rain Erosion Damage Data for 0.020 Inch Alumina/Alumina Foam/ 0.020 Inch Alumina	52
31.	MDPR vs Sine Impact Angle - PBI (Imidite) Laminate	54
32.	Rain Erosion Damage Data for PBI (Imidite) Laminate	55
33.	MDPR vs Sine Impact Angle - Furane Epoxy Laminate	56
34.	Rain Erosion Damage Data for Furane Epoxy Laminate	57
35.	MDPR vs Sine Impact Angle - Epon 828 Epoxy Laminate	58
36.	Rain Erosion Damage Data for Epon 828 Epoxy Laminate	59
37.	MDPR vs Sine Impact Angle - Polyimide Laminate BMEC 1937 Sealer	60
38.	Rain Erosion Damage Data for Polyimide Laminate BMEC 1937 Sealer	61
39.	MDPR vs Sine Impact Angle - Polyimide Laminate - Skyguard 700	62
40.	Rain Erosion Damage Data for Polyimide Laminate - Skyguard 700	63
41.	MDPR vs Sine Impact Angle - Nomex Epoxy Laminate	64
42.	Rain Erosion Damage Data for Nomex Epoxy Laminate	65
43.	MDPR vs Sine Impact Angle - DC 2106 Silicone Laminate	66
44.	Rain Erosion Damage Data for DC 2106 Silicone Laminate	67
45.	MDPR vs Sine Impact Angle - Filament Wound Alumina - Silica/S Glass Laminate	68
46.	Rain Erosion Damage Data for Filament Wound Alumina - Silica/S Glass Laminate	69
47.	MDPR vs Sine Impact Angle - Aluminum Phosphate Laminate	70

ILLUSTRATIONS (CONT'D)

FIGURE		PAGE
48.	Rain Erosion Damage Data for Aluminum Phosphate Laminate	71
49.	Rain Erosion Damage Data for 0.020 Inch Precast Alumina/$AlPO_4$ Laminate	73
50.	Rain Erosion Damage Data for 0.040 Inch Precast Alumina/$AlPO_4$ Laminate	74
51.	Rain Erosion Damage Data for 0.020 Inch PS Alumina/$AlPO_4$ Laminate	77
52.	Rain Erosion Damage Data for 0.040 Inch PS Alumina/$AlPO_4$ Laminate	78
53.	Rain Erosion Damage Data for 0.020 Inch PS Alumina/Alumina - Silica S Glass Laminate	79
54.	Rain Erosion Damage Data for Sprayed Alumina/Silica Quartz Glass	80
55.	Rain Erosion Damage Data for Alumina/Polyimide Laminate	81
56.	Rain Erosion Damage Data for 0.020 Inch Flame Sprayed Alumina/ PBI Laminate	83
57.	Rain Erosion Damage Data for 0.040 Inch Flame Sprayed Alumina/ PBI Laminate	84
58.	Rain Erosion Damage Data for 0.030 Inch Rokide "A"/Polyimide Laminate	85
59.	Rain Erosion Damage Data for Rokide "A" Alumina/Polyimide Laminate Al_2O_3 Contains Cr_2O_3	86
60.	Rain Erosion Damage Data for 0.125 Inch Alumina/0.030 Inch RTV521/0.100 Inch Polyimide Laminate	89
61.	Rain Erosion Damage Data for Rokide "A" Alumina/828 Epoxy Laminate	91
62.	Rain Erosion Damage Data for Plasma Sprayed Alumina (0.030 Inch)/Epon 828 Laminate	93
63.	MDPR vs Sine Impact Angle -- 0.010 Inch Gaco/Epon 828 Epoxy Laminate	94
64.	Rain Erosion Damage Data for 0.010 Inch Gaco/Epon 828 Epoxy Laminate	95
65.	Rain Erosion Damage Data for 0.020 Inch Gaco/Epon 828 Epoxy Laminate	96

ILLUSTRATIONS (CONTD)

FIGURE		PAGE
66.	MDPR vs Sine Impact Angle - 0.010 Inch Neoprene/Dacron/ Epon 828 Epoxy Laminate	98
67.	Rain Erosion Damage Data for 0.010 Inch Neoprene/Dacron/ Epon 828 Epoxy Laminate	99
68.	Rain Erosion Damage Data for 0.020 Inch Neoprene/Dacron/ Epon 828 Epoxy Laminate	100
69.	Rain Erosion Damage Data for 0.030 Inch Neoprene/Dacron/ Epon 828 Epoxy Laminate	101
70.	MDPR vs Sine Impact Angle - 0.014 Inch Polyurethane/Epon 828 Epoxy Laminate	102
71.	Rain Erosion Damage Data for 0.014 Inch Polyurethane/Epon 828 Epoxy Laminate	103
72.	Rain Erosion Damage Data for 0.026 Inch Polyurethane/Epon 828 Epoxy Laminate	104
73.	Rain Erosion Damage Data for 0.038 Inch Polyurethane/Epon 828 Epoxy Laminate	105
74.	Rain Erosion Damage Data for 0.020 Inch Hycar/828 Epoxy Laminate	107
75.	Rain Erosion Damage Data for 0.030 Inch Hycar/828 Epoxy Laminate	108
76.	Rain Erosion Damage Data for 0313 Chemcor Glass	111
77.	Rain Erosion Damage Data for 9753 IR Glass	112
78.	Rain Erosion Damage Data for C106 CER-VIT Glass	113
79.	Rain Erosion Damage Data for 0315 Chemcor Glass	114
80.	Rain Erosion Damage Data for 0.010 Inch Gaco/0.040 Furane Epoxy Honeycomb	117
81.	Rain Erosion Damage Data for Polyimide Honeycomb	118
82.	Rain Erosion Damage Data for 0.020 Inch Titanium/Polyimide Honeycomb/0.020 Inch Titanium	119
83.	Rain Erosion Damage Data for 0.035 Inch Teflon/Nomex Epoxy Laminate	121
84.	Rain Erosion Damage Data for AC-2755 Cork/Epoxy Laminate	122

ILLUSTRATIONS (CONTD)

FIGURE		PAGE
85.	Rain Erosion Damage Data for 0.010 Inch Electro Plated Nickel/ Epon 828 Laminate	125
86.	Rain Erosion Damage Data for Polyphenylene Oxide	127
87.	MDPR vs Sine Impact Angle - Plexiglas	128
88.	Rain Erosion Damage Data for Plexiglas	129
89.	MDPR vs Sine Impact Angle - Teflon	130
90.	Rain Erosion Damage Data for Teflon	131
91.	Rain Erosion Damage Data for 2024-T3 Aluminum	133
92.	Rain Erosion Damage Data for 6061-T6 Aluminum	134
93.	Rain Erosion Damage Data for Annealed Copper	135

TABLES

TABLE		PAGE
I	Propulsion Systems	141
II	Run Record - Mach 1.5	142
III	Run Record - Mach 2.0	143
IV	Run Record - Mach 2.5	144
V	Run Record - Mach 3.0	145
VI	Materials List	145
VII	Materials Properties Summary	151
VIII	Constants for the Rain Erosion Equation	159

SYMBOLS

A, B, C, E, F, α, γ	constants of the high velocity-short time exposure rain erosion equation
D	drop diameter (in feet)
K_1, K_2, K_3	functions of velocity in rain erosion equation
MDP	mean depth of penetration or volume loss per unit area (cm)
MDPR	mean depth of penetration rate or erosion rate (volume loss/unit area/sec)
M	Mach number
ΔS	drop path length (inches)
t	exposure time in rain
t*	drop breakup time
v	velocity (ft/sec)
wt loss	weight loss per unit area
θ	impact angle
θ_D	point of change of slope of the high velocity-short time exposure rain erosion equation
ρ	material density (gm/cm^3)

SECTION I

INTRODUCTION

Supersonic aircraft and missiles may experience damage to radomes, leading edge surfaces, and structural members because of raindrop impingement. This phenomenon, known as rain erosion, has become increasingly severe as the velocity of these aerospace systems continues to increase.

The designers of radomes and aircraft have, in the past, relied on subsonic whirling arm erosion data extrapolated to higher velocities or on the qualification test of a mock-up radome by one firing through the rain field on a rocket sled track. These investigations have been used to supposedly predict the behavior and performance of materials upon repeated exposure in a supersonic rain environment.

With the increasing numbers of supersonic aircraft, a systematic comprehensive evaluation of nonmetallic, dielectric materials for structural applications was necessary to obtain erosion rates at supersonic velocities so that designers could develop efficient components which would withstand rain erosion under high speed, operational conditions.

The program undertaken by the U. S. Naval Air Development Center (NAVAIRDEVCEN), Radome Section, and the Air Force Materials Laboratory (AFML), Elastomers and Coatings Branch, was directed toward obtaining these erosion design criteria as a function of velocity, angle of impingement, rainfall intensity, and materials physical properties. Damage rates and volume loss per unit time were determined for 65 materials which may be used in supersonic aircraft or missile systems.

SECTION II

SUMMARY

Sixty-five different dielectric and other materials were evaluated for short-exposure time (four seconds or less depending on velocity), rain erosion resistance at velocities between Mach 1.5 and 3.0 by firing multistaged rocket sleds through a 6000-feet long artificial rain field at the Holloman Air Force Base Test Track Facility. A rain erosion wedge, designed to accommodate eight different materials for each sled run, was supported on the forward end of the rocket sled. By exposing each material to the same rain environment at five different impact angles and at four constant velocities, the quantitative rain erosion resistance of these materials was determined as a function of velocity, impact angle and time.

Material specimens 1.250 x 1.250 x 0.250 inches were used to obtain weight loss values per unit area. Data was reduced to the form of mean depth of penetration rate (MDPR) vs sin θ (the impact angle θ) for a family of supersonic velocities.

Where possible, general empirical rain erosion equations were fitted to the plotted data. For certain materials the data was not suitable for deriving equations but was plotted uncorrected through the experimental points. Several of the best performing materials yielded nonmeasurable damage rates. The damage increased exponentially with velocity and varied directly with the normal component of velocity.

Materials evaluated in this program included isotropic ceramics, sandwich ceramics, plastic laminates, inorganic laminates, ceramic-coated laminates, elastomeric-coated laminates, glasses, thermal plastics, sandwich plastics, and metals.

The Mach 1.5 results indicated that flame sprayed alumina coatings, the uncoated 8265 Furane epoxy and Epon 828 epoxy laminates, and all the elastomeric-coated laminates yielded good protection from the rain impingement at this velocity for a short exposure time. The elastomers (sprayed neoprene, molded boot neoprene, and boot urethane) were completely undamaged after one firing at Mach 1.5. Other materials which exhibited good erosion resistance at this velocity were a polyphenylene oxide plastic, an electroplated nickel coating over an epoxy laminate, a plasma sprayed alumina coating (treated with phosphoric acid) over an epoxy laminate, and a Rokide "A" flame sprayed alumina impregnated with epoxy resin over an epoxy laminate.

At Mach 2.0 and 2.5 materials which exhibited superior rain erosion resistance in addition to the isotropic alumina and beryllia were the polyphenylene oxide thermal plastic, an electroplated nickel coating over epoxy laminate, a plasma sprayed alumina coating treated with phosphoric acid over an epoxy laminate, and a Rokide "A" flame sprayed alumina impregnated with epoxy resin over an epoxy laminate. At Mach 2.0 other isotropic ceramics such as Pyroceram and fused silica were damaged sufficiently to limit their capability in this environment.

Of the materials investigated at Mach 3.0, those which best survived the rain environment with little damage were the highly dense alumina and beryllia isotropic ceramics. Other isotropic ceramics, sandwich ceramics, ceramic and elastomeric-coated laminates, glasses, and metals were severely to moderately damaged at this velocity.

SECTION III

THE RAIN EROSION WEDGE

1. PHYSICAL DESCRIPTION

a. Construction

The supersonic rain erosion wedge shown in Figure 1 was designed by NAVAIRDEVCEN for multiple sample testing of materials at velocities of Mach 1.5 or greater. Eight different materials can be evaluated for each run with samples of the same material mounted on both the left and right sides at each of the following angles: 13.5°, 30°, 45°, 60° and 90°. By providing for two specimens of the same material at the same impact angle but displaced vertically by four spaces, some normalizing effect is introduced to partially compensate for slight variations in the material, rain-fall distribution, and sample edge effects. A total of 80 samples are contained in the fully loaded wedge.

The basic construction consists of left and right side plates, top and bottom plates, and a base or back plate all of which were machined from 7075-T6 aluminum. Parts were doweled and secured with internal wrenching cap screws. A separate leading edge and all sample cover plates were made from stainless steel to retard rain erosion on the forward surfaces. Sample cover plates were secured with countersunk Allen head screws having nylon lock inserts.

Both top and bottom surfaces were inclined 15 degrees upward from the leading edge aft to induce a negative lift component and to relieve the afterbody for flow expansion. The base or aft end dimensions are 13-1/2 x 12-1/2 inches making the total frontal area 1.33 ft^2 with the added area resulting from inclination of the top and bottom surfaces. The loaded gross weight reading for firing ranges between 70 and 75 pounds depending upon the density of the samples.

Mounting holes were provided in both the bottom and back plates for quick-change attachment to the Holloman rocket sleds. NAVAIRDEVCEN assembly and detail drawings are listed in Reference 1.

b. Sample Mounting

Material samples 1.250 x 1.250 x 0.250 inches were mounted in wedge grooves behind stainless steel cover plates as shown by Figure 2. The exposed sample area dimensions are 1.00 x 1.00 inch at all impact angles. The stainless cover plates are 0.060 inch thick with leading edges chamfered parallel to the wedge center line, and aft edges chamfered at 45 degrees to the plate surface. All leading edges were beveled to minimize shielding by the cover plates; the back edges were chamfered to reduce the effects of a high pressure corner or cavity.

Most of the materials evaluated were backed with hard rubber pads of the same size as the test sample. Aluminum spacers were installed between samples to accept the concentrated loads when the cover plates were tightened. Dimensional differences between the spacer thickness and the sum of the rubber pad and sample thicknesses were such that the rubber was slightly compressed. This method was found to be undesirable for brittle materials, causing premature breakage on some materials in the early runs.

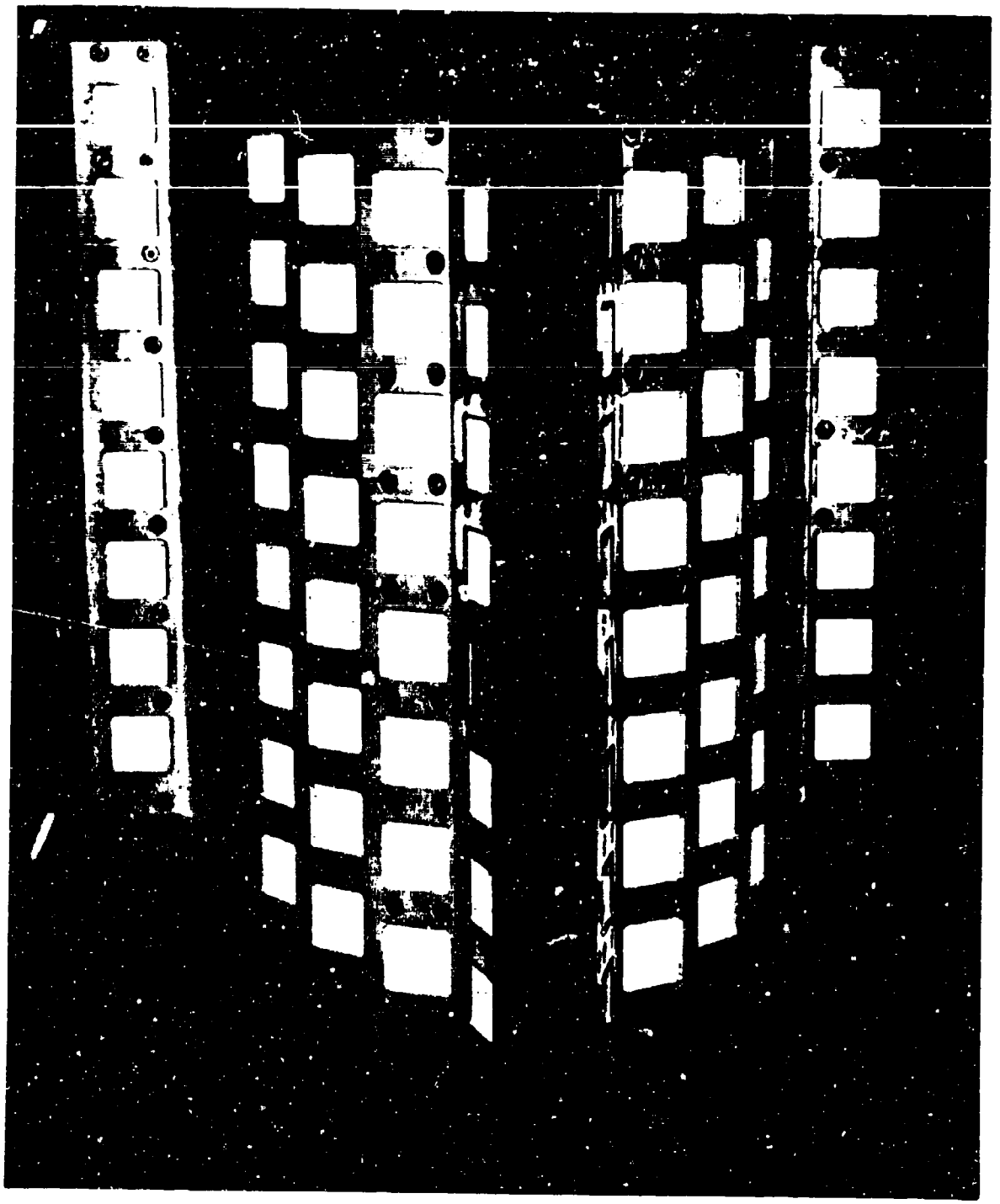

Figure 1. Supersonic Rain Erosion Wedge

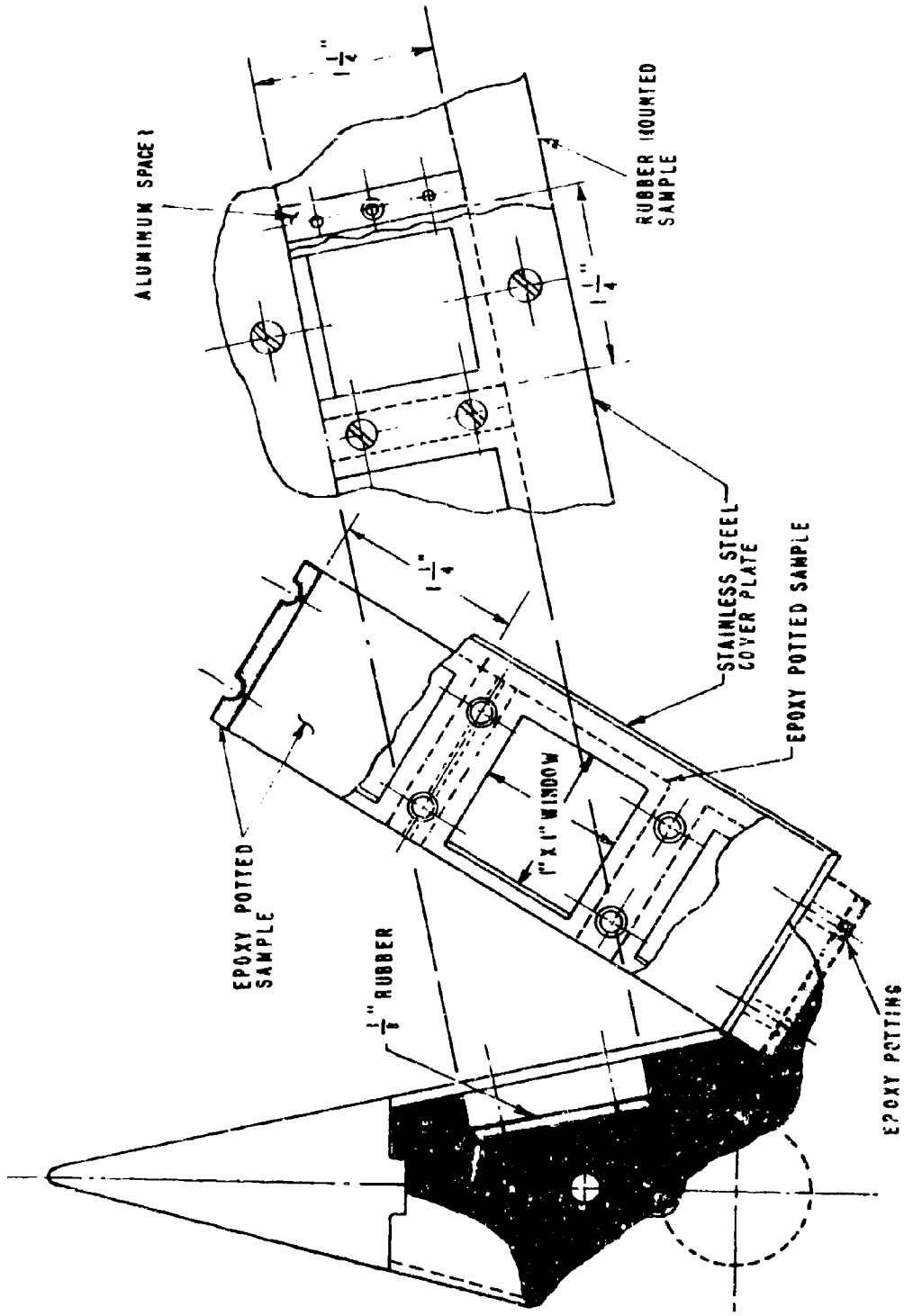

Figure 2. Sample Mounting and Cover Plate

A potting method was therefore developed for use with all brittle materials (Figure 2). In this type of sample mounting both the hard rubber backing and half the spacer width on each end were replaced with fiber reinforced epoxy potting. A complete set of 80 samples was potted in one model setup. Ten eight-sample-strips were then jig drilled and saw cut into individual pieces. All potted samples were numbered and weighed after potting and machining.

All samples had approximately 1/8 inch of unexposed edge on all four sides to prevent drop impact on the edges. This was done to minimize edge effects as well as to provide a method of securing them.

2. AERODYNAMIC CHARACTERISTICS

Three basic profiles or configurations were considered in designing the wedge for multiple sample testing: the circular leading edge, the hypocycloid or inverse of the circular leading edge, and the configuration as shown in Figure 3. It was determined that the latter profile produced the minimum form drag, the most oblique shock pattern and, therefore, the shortest paths between the first shock wave and the surfaces of the test samples.

A quarter scale model was made at the NAVAIRDEVCEN and run at the David Taylor Model Basin (DTMB) Supersonic Wind Tunnel at Mach Nos between 1.5 and 2.86 to determine the flow patterns and to measure the aerodynamic forces and moments. Force and moment data are reported in Reference 2.

The 15° inclination angle of the top and bottom surfaces produced a sizeable negative lift component at all Mach numbers which was a requirement of the sled designers. This force and moment data was used in the Holloman rocket sled performance computer program for the selection of launch station, booster propulsion, sustainer propulsion, and retarding mechanisms to achieve the specified performance within the rain field.

Shock wave patterns at M 2.86 are shown in Figure 3, and are typical of all Mach numbers between 1.5 and 3.0. In addition to the bow wave from the 15° half-angle leading edge, there are four major secondary compression waves. The fourth or last one is a normal detached shock wave creating supersonic flow behind the base.

Two major separated flow regions are indicated from Schlieren photographs. One is in the corner between the 15° and 60° samples; a second exists along the curved surface forward of the 90° sample. Two minor separated flow regions are shown in the corners forward of the 45° and 30° surfaces. Vertical bleeder slots were added just forward of the 90° samples on the curved surfaces. These slots reduced the size of the separated flow region over the curved surfaces and slightly reduced the drag coefficient by raising the base pressure.

Figure 3 also shows the path lengths, Δ_s, at full scale through which water drops must travel between penetration of the bow wave and impingement at the center of the sample surfaces. These path lengths vary between 2.25 and 3.50 inches with the exception of the 90° sample, the length of which is greater than double that of all other angles. The drop disintegration effect resulting from the longer path at 90° seriously affects the rain erosion rate at 90°.

3. DROP DISINTEGRATION EFFECTS

Any region of flow separation, a shock wave or combination of shock waves has some effect upon the water drops. In rain erosion testing the objective is to evaluate materials with such effects mimimized or to test as nearly as possible to free stream conditions.

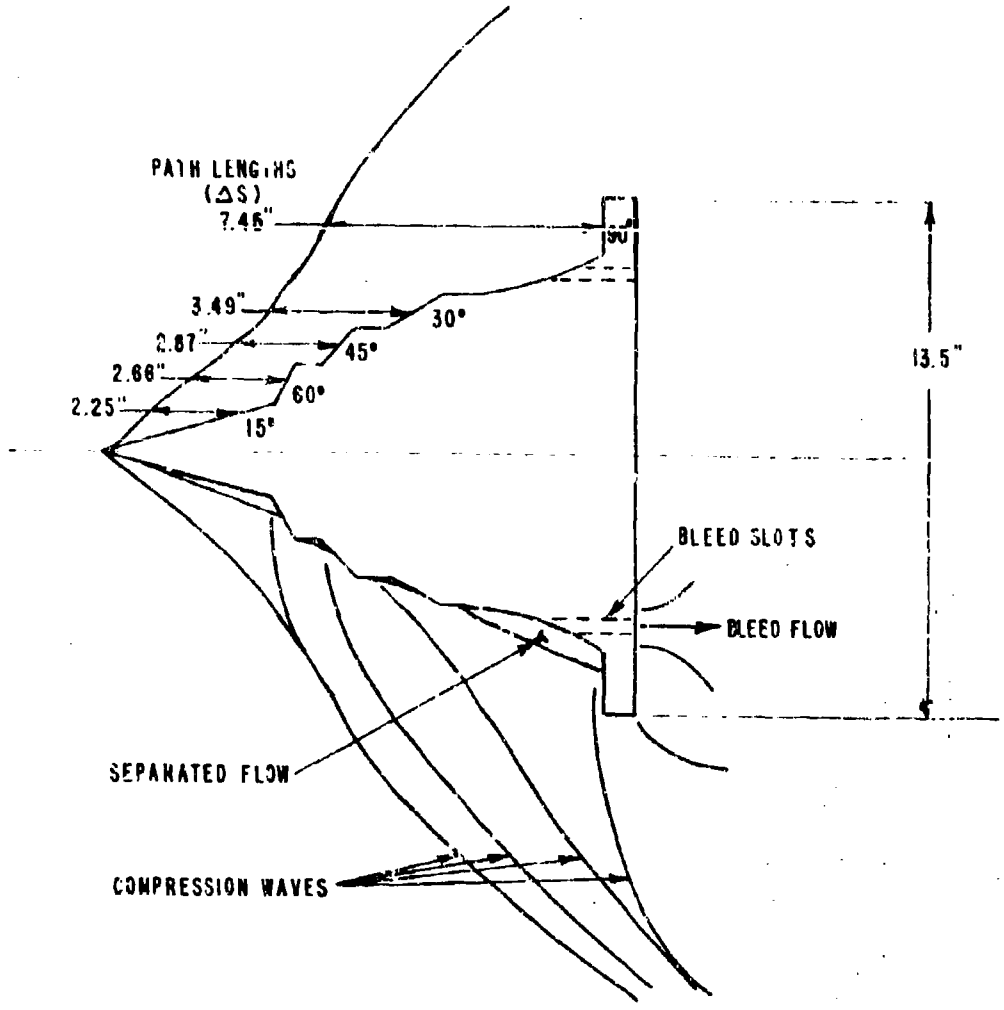

Figure 3. Rain Erosion Wedge Shock Wave Pattern (M = 2.85)

Conversely the vehicle designer or user of materials subject to rain erosion damage should take full advantage of techniques for the delay of erosion and prevention by the deliberate breakup of water drops before impingement.

Since there is no method of avoiding the generation of shock waves when testing in the atmosphere at supersonic velocities it is impossible to avoid this effect to some degree. In any test method the disintegration effects should be explored and understood. They should be carefully considered in the comparison of data from different test methods; in some cases they may completely invalidate the test data.

Disintegration or drop-breakup times have been investigated both in the United States and the United Kingdom. Experimental measurements obtained by Jenkins at the Royal Aircraft Establishment (Reference 3) are in good agreement with values obtained by Engel at the

U. S. Bureau of Standards (Reference 4). This work was performed in the high subsonic and transonic velocity range from which the empirical equation was derived for breakup time (t^*) in terms of drop diameter (D) in feet and velocity (V) in ft/sec.

$$t^* = \frac{20\,D}{V^{0.72}}$$

The time in the above equation corresponds to the time to reduce a drop of diameter D to droplets no larger than 0.1 mm. This equation can be applied to low supersonic speeds and should be particularly valid behind normal shock waves. Calculation of breakup times at velocities between 1500 and 3500 ft/sec for drop sizes between 1 and 3 mm diameter are plotted in Figure 4. At Mach 2.0 the time to break down a 1 mm drop to 0.1 mm is 0.00625 second; time required to break down a 2 mm drop to the same droplet size is about 0.0005 second.

Taking the path lengths of Figure 3 at Mach 2.85 for the full size wedge the exposure times were calculated using the time increments and local velocities between shock waves. These points (Figure 4) indicate that for angles of 15°, 45°, and 60° the exposure times are less than that required to disintegrate 1 mm drops and small compared with times required for disintegration of 2 and 3 mm drops. For the 30° angle specimens the exposure times are greater than required to break up the 1 mm drop and more seriously affect the 30° samples. The 90° sample disintegration path length time, much greater than for all other angles, is sufficient to break down all drops of 2.5 mm or less. This effect is quite obvious upon inspection of the 90° samples and is reflected in the very low weight losses at this angle. All 90° data is therefore considered invalid and is not included in the curves for weight loss.

Some efforts have been made to photograph water drops within the shock pattern with overhead cameras. To date this has been unsuccessful but could certainly provide valuable information for better interpretation of the data.

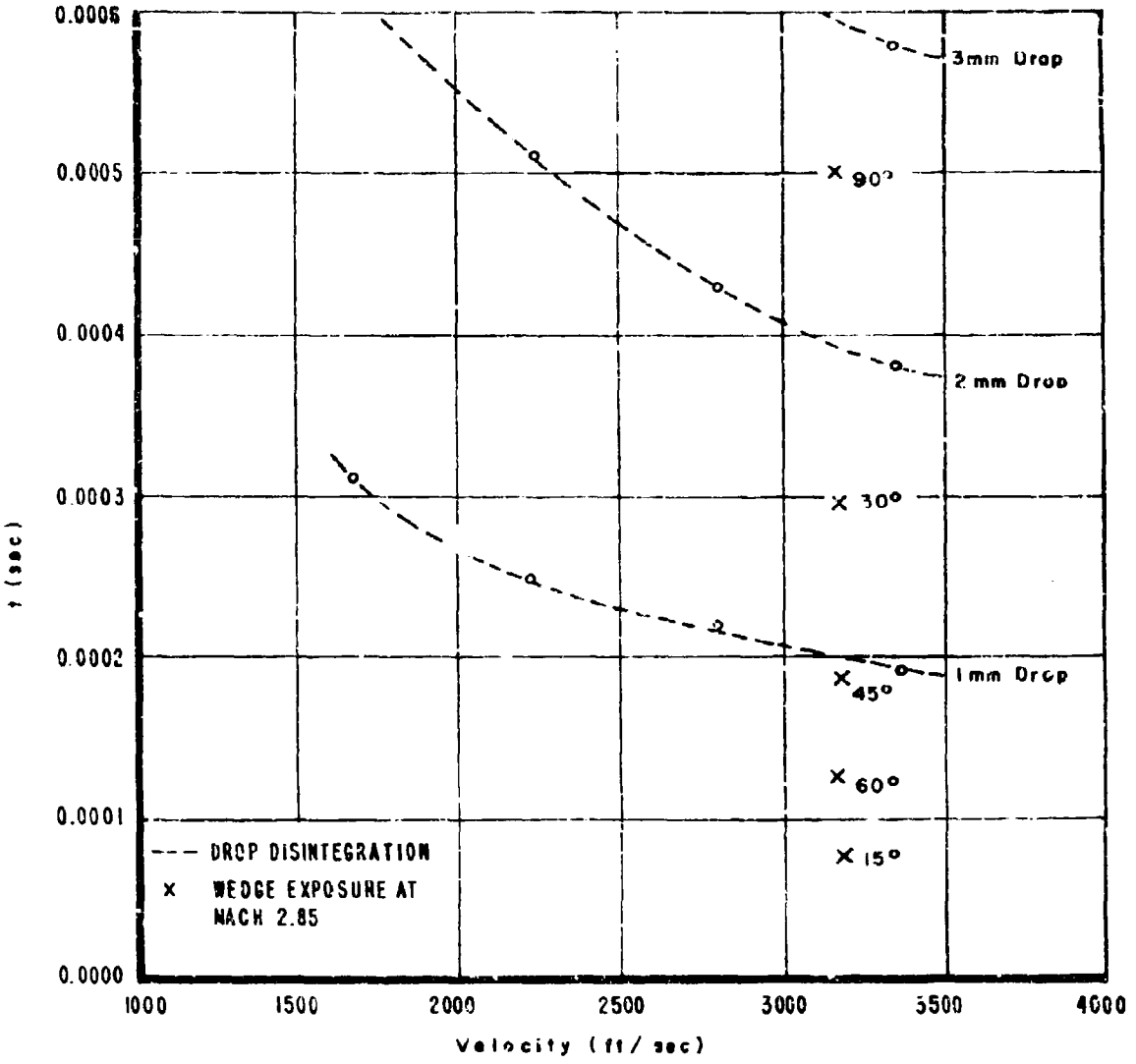

Figure 4. Drop Disintegration Times vs Wedge Exposure Times

SECTION IV

THE HOLLOMAN TRACK FACILITY

1. TRACK DESCRIPTION

The 35,500-foot test track operated by the Test Track Directorate of the Air Force Missile Development Center (AFMDC) is located at Holloman Air Force Base, New Mexico, on the eastern edge of the White Sands Missile Range. Direction of the track is within a few degrees of true north with the main breech located at the south end. The 6000-feet rain field zone is located toward the north end between stations 20, 700 and 26,700 feet. For details, see Reference 5.

The 171 lb/yd crane rails are spaced 7 feet on center. Alignment is maintained within a tolerance of ± 0.005 inch on the west rail and ± 0.010 inch on the east rail. Both rails are welded to provide one continuous joint-free track section for the entire 35,500 feet.

The track is equipped with four stationary blockhouses on the west side of the track including one at either end, one in the center, and one at track station 2970. A portable fire control trailer is also available for use in firing solid propulsion units from any point on the track. Both the north blockhouse and the fire control trailer were used in this series. A completely equipped, shielded, dust free telemetry ground station is located 2000 feet east of the mid-point of the track and visual observations of the firings are made from this station.

Two means of sled deceleration by water braking are available, and both were used in this program. Waterfilled polyethylene bags are laid directly on the track and the slippers on which the sled is mounted strike these bags slowing the vehicle to a stop. This method of braking was used to stop the sustainer stage at all Mach numbers. A momentum exchange brake (U-tube arrangement) was added to stop the booster on the Mach 2.0 runs and the second booster on the Mach 3.0 runs.

All firings were made between 0200 and 0700 to take full advantage of calm night air on the desert. Wind velocities normally begin to increase shortly after sunrise and usually reach 5 to 10 knots by midmorning. The advantage of night operations is apparent in achieving 30 launches over a six-month period with only two scheduled runs aborted because of weather.

2. ROCKET SLED

All rocket sled hardware was provided by the Holloman Track Test Directorate. The sustainer sled, originally designed for radome testing, was modified to support the rain erosion wedge and to house a cluster of seven M-58 sustainer motors. Separate pusher sleds were designed for the Genie and the Nike motors.

To accelerate to peak velocity and to sustain the desired Mach numbers in the rain field, staging was used in accordance with Table I. Three basic surplus engines were used in various combinations to achieve the required velocity performance. A photograph of the Mach 3.0 sled configuration is shown in Figure 5 with two Nike booster stages and two sustainer stages housed in the forward sled.

With the exception of some engine ignition malfunctions in the early firings, the staging used was satisfactory and produced relatively flat velocity profiles through the rain. Wind tunnel force coefficients for the wedge assisted in computer calculated sled performance, selection of launch points and deceleration coast-out distances.

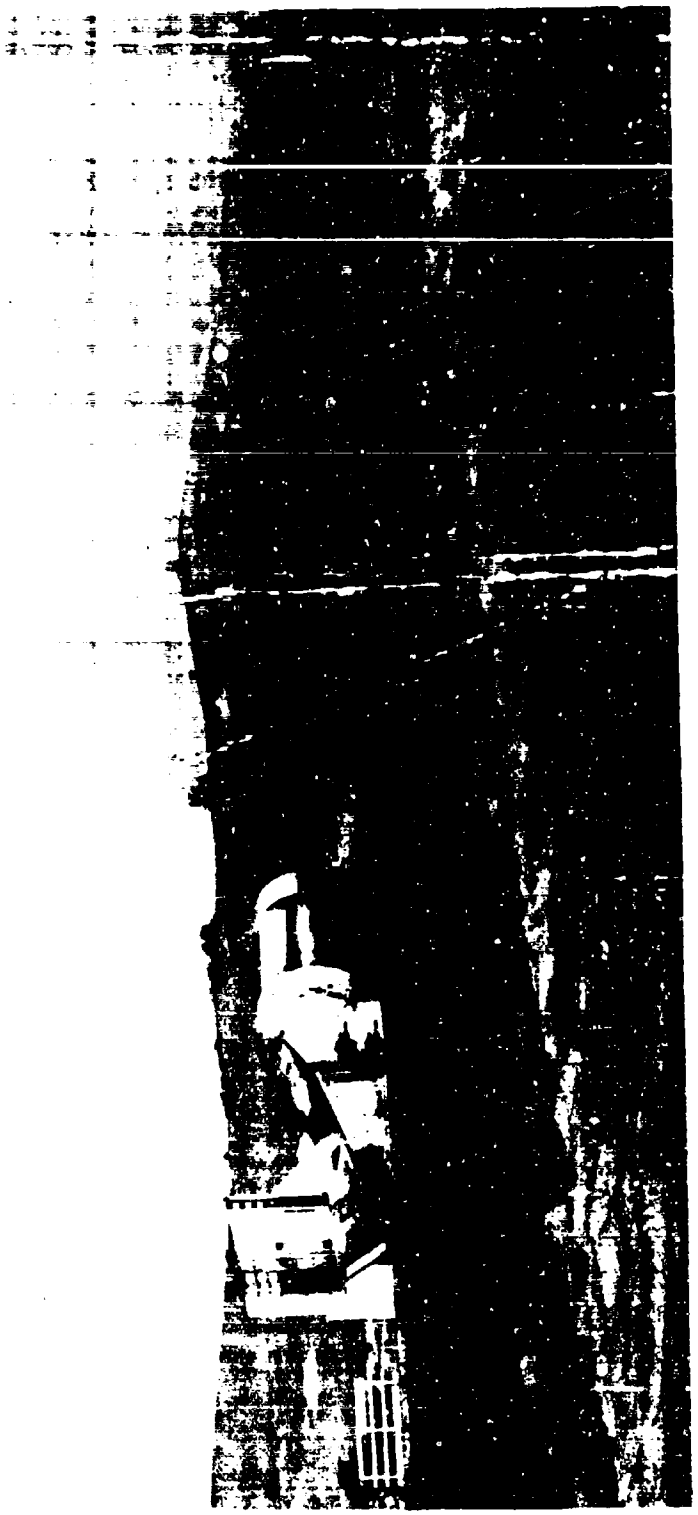

Figure 5. Rain Erosion Rocket Sled (Mach 3.0 Configuration)

A complete history of the 30 sled firings with dates, firing times, wind conditions, average velocities in the rain, and sample designations is listed in Tables II through V.

3. INSTRUMENTATION

Two measurements of sled velocity were made on the rain erosion runs. The space/time (VMS) technique (Reference 5) determines sled position, velocity and acceleration by defining the time interval of sled travel between very accurately spaced (13-foot intervals) light beam interrupters on the track. An RF modulation is created from the sled borne photo pickup as it passes these interrupter stations with conversion and transmission as RF. Accuracies in excess of 0.1 foot per second are attainable.

Twelve "spot velocity" checks on a sled can be made during a run using time interval counters. These are 1 megacycle counters which may be started and then stopped by means of a breakwire as a sled progresses across a specific distance. This technique was the primary one used for the rain erosion test series.

Photographic coverage for these runs included image motion cameras, limited shadowgraph photography, motion pictures and still documentary (before and after) photography. The image motion technique provides a full length view of the test wedge at 500-foot intervals through the rain field. These photographs were used to analyze the progressive erosion of materials with increasing rain exposure. Shadowgraph coverage was attempted in order to study the shock wave pattern around the wedge. Limited success was attained because of difficulties with shooting vertically from above the track and obtaining a well-defined shock front.

Documentary coverage with color and black and white still photos, before and after firings, of the test wedge, the vehicle, and propulsion systems and general scenes was also provided. The motion pictures taken during the runs further helped to document the series.

SECTION V

THE HOLLOMAN RAIN FIELD

1. DESCRIPTION OF THE SYSTEM

The present Holloman rain field simulation system consists of 6000 feet of rain between stations 20,700 and 26,700 on the 35,500-foot track. This provides up to 8800 feet for sled acceleration and 20,700 feet for deceleration when firing North to South. Vertical standpipes (rain dispensers) are spaced 9 feet on either side of the west rail with the nozzles located 31 inches above the track surface. Longitudinal spacing of the standpipes is 8 feet with the east and west nozzles staggered to provide a separation of only 4 feet between nozzles. A photograph of the rain field looking north is shown in Figure 6.

All nozzles are Spraying Systems Company Veejet 1/4 u 8070 mounted at 65 degrees from the horizontal on the standpipes. The standpipes are supplied through a manifold system in which each section feeds only 50 nozzles and provides individual pressure regulation. The manifold in turn is fed through a 6-inch main from a 20,000-gallon storage tank. A D-8 diesel engine powers a centrifugal pump capable of delivering up to 4800 gallons/minute flow rate to the sytem.

At the 2.5 inch/hour rainfall rate used for these tests the available water supply can be used for more than 10 minutes without refill of the tank. Under conventional operation the nozzles were operated for about 3 minutes/run. This is possible through a bypass system with no loss of water until T minus 60 seconds at which time remote control valves deliver pressure to the nozzles. A full water system at start assures uniform flow after 35 seconds.

A comprehensive description of the Holloman rain field, designed and installed by the Sandia Corporation, is reported in Reference 6.

2. RAIN SIZE AND DISTRIBUTION

The original intent of this program was to evaluate all materials at 1 inch/hour rainfall rate with a mean drop size between 1.8 and 2.0 mm. This rainfall rate agrees with Figure 7 which describes typical particle size distribution for natural rainfall rates up to 6 inches/hour.

Drop sampling at the Holloman Test Track using the oil system technique showed that a system pressure of 9 psi provided the required 1.9 mm mean drop size for a monorail sled on the west rail. The Veejet 1/4 u 8070 nozzles operated at 9 psi give a rainfall rate of 2.25 to 2.5 inches/hour with a cyclic gradient between the nozzle center and the edges of the fan shaped spray pattern. A characteristic drop size distribution curve is shown in Figure 8 for comparison with that of natural rain of Figure 7.

Firing of test samples through 6000 feet of rain at 2.5 inches/hour rainfall rate with a mean drop size of 1.9 mm produces a total energy absorption by any given sample. This same total energy would be absorbed by the same sample if the water system could have been operated at 1.9 mm mean drop size, a 1 inch/hour rate, but over 15,000 feet of track. The major difference between these two exposures would be the time of energy absorption or the rate of pressure pulses inducing short time stresses within the material.

3. FIRING CONDITIONS

Observation of wind effects upon the water system was made for random wind velocities and directions. Cutoff or abort conditions were established at 2 knots cross track and 3 to 4 knots down track. Wind readings were reported from three track stations, one at each end and one at the center of the rain field. Normally they were reported every 15 seconds between T minus 60 seconds and firing.

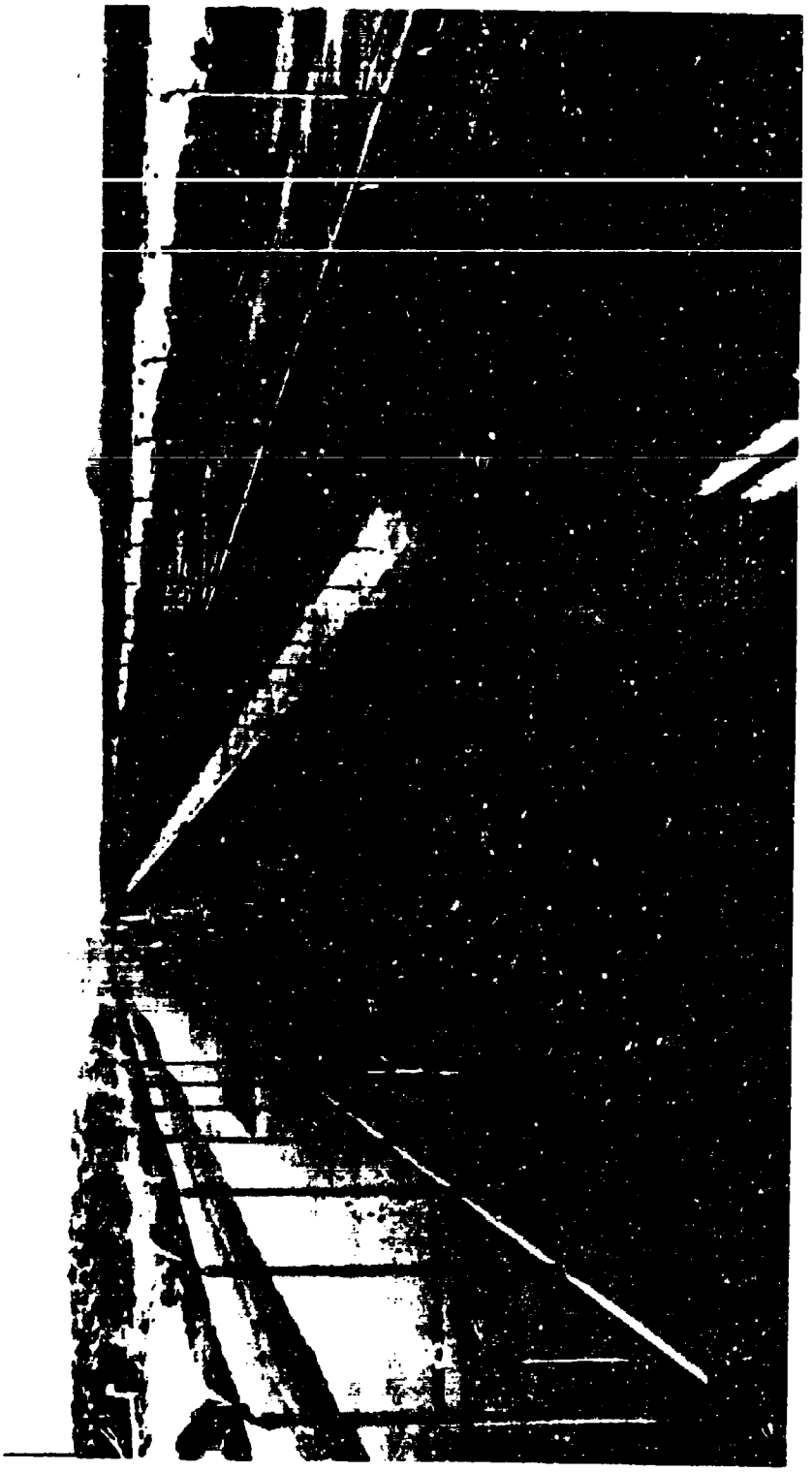

Figure 6. Holloman Rain Field

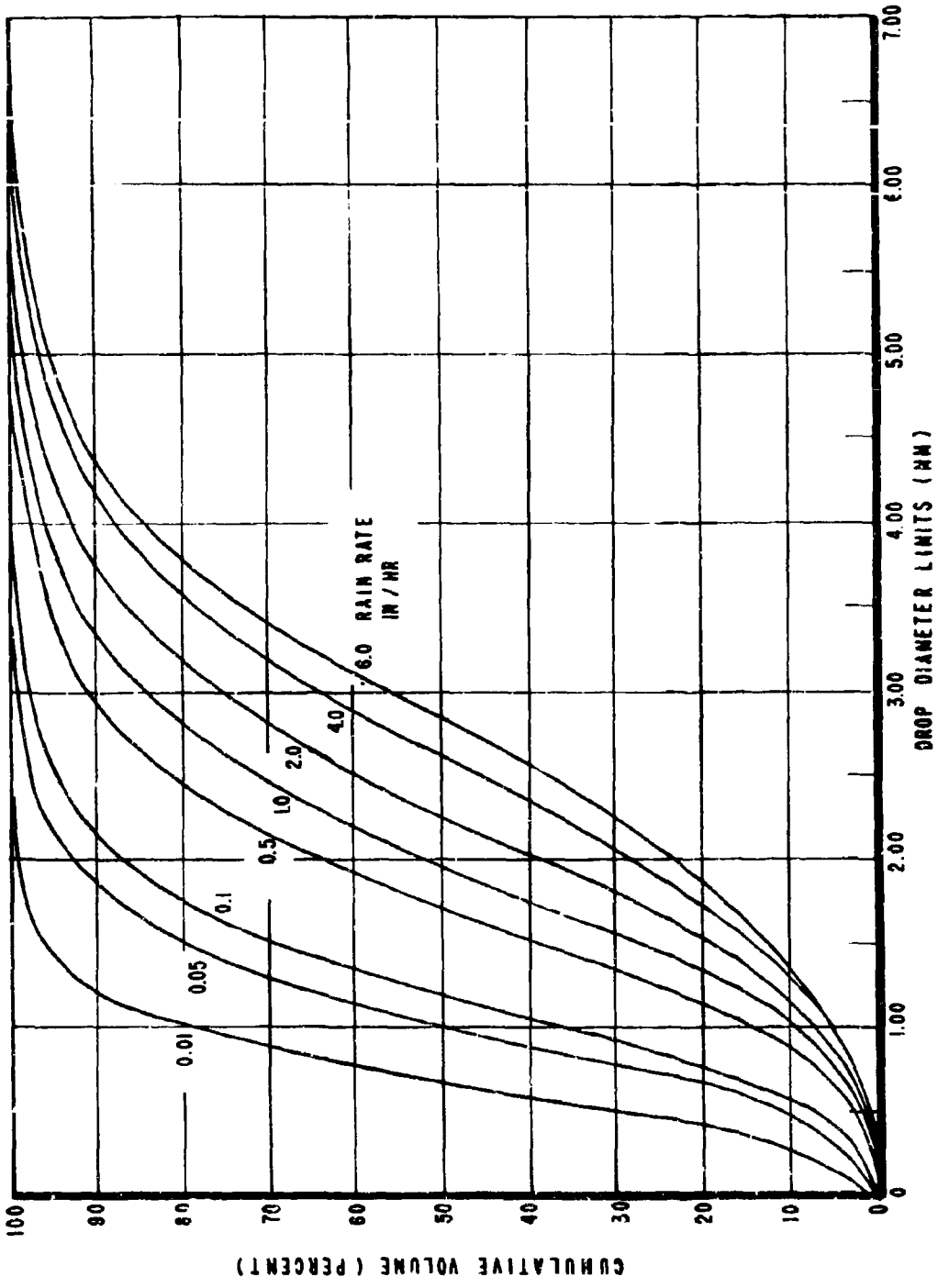

Figure 7. Particle Size Distribution of Natural Rainfall (Reference 7)

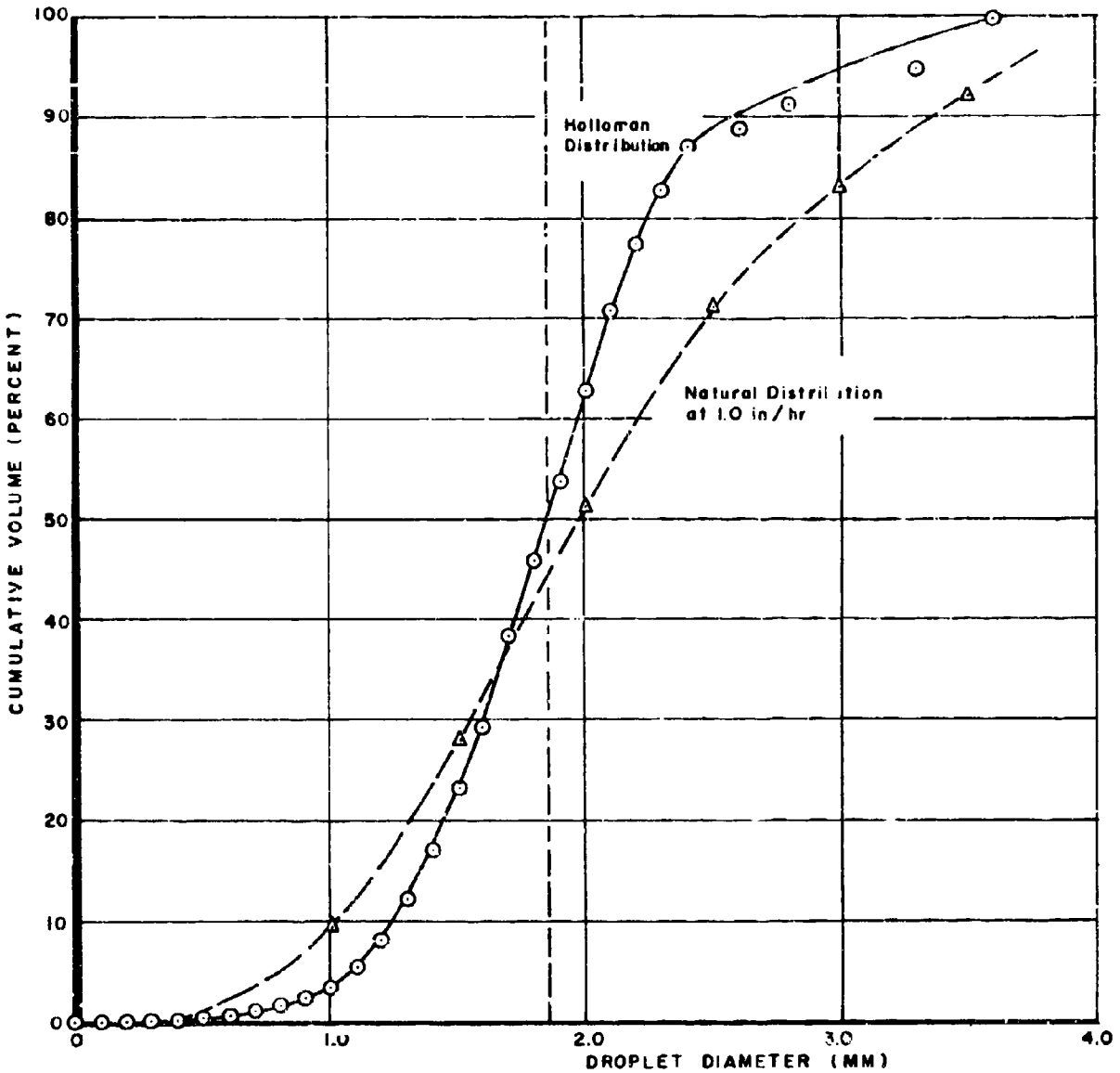

Figure 8. Drop Size Distribution at Holloman Track Rain Simulation System (System Pressure - 9 psi)

SECTION VI

MATERIALS EVALUATED

1. CLASSES OF MATERIALS

Materials selected for these evaluations were classified in 10 major categories according to material-type. Isotropic ceramics were selected because of their potential for high speed, high temperature radomes, their good erosion resistant properties (high density and strength), and their excellent dielectric properties. Sandwich ceramics, while lacking in the strength of solid ceramics, are a widely-considered and used structural material for advanced radome designs.

Plastic organic laminates such as epoxies, polyimide and polybenzimidazole are currently in extensive use as radome materials or are being planned for future applications. In a like manner, inorganic laminates are being evaluated for very high temperature systems.

Coated laminates represent still other structural materials which have found broad application. Considerable effort is now being conducted in developing dense, ceramic, rain erosion resistant coatings for a variety of laminate and metal substrates (Reference 8). The ceramic coatings are intended for use in a supersonic environment and hence needed evaluation as to their protective capability in rain. Elastomeric coatings are widely used for subsonic rain erosion protection, but little has been done to evaluate them supersonically in rain (other than an occasional proof test of a mock-up radome).

Increasing applications of glasses in supersonic systems for windshields, radome, and infrared windows dictated an evaluation of representative systems.

Unique structural systems such as plastic honeycombs with laminate or metal skins and laminates with cork, Teflon, or metal coatings also were evaluated because of possible use in a number of cases. Along this line, thermal plastics such as polyphenylene oxide and Teflon were evaluated as bulk materials, and polymethylmethacrylate (Plexiglas) was chosen because of extensive rain erosion research on it in the past.

The final class of materials was metals which were chosen as representative aircraft structural materials (for parts other than radomes) and as a base line on which to compare materials. Soft metals such as aluminum alloys and annealed copper were chosen so that some evidence of erosion would be present.

Keeping in mind the need for improved dielectric materials and the lack of supersonic erosion data on most of these materials, the various materials in each class were chosen, obtained from various suppliers, processed, arranged into runs, exposed at Holloman supersonically, and then post-processed and evaluated. See Table III for a listing of materials.

2. SAMPLE PROCESSING

Each material supplier was required to supply with his material a physical property data sheet which included porosity, density, hardness, and other pertinent physical and electrical properties. These were also furnished at no cost to the program. (See Figure 9.)

Prerun sample processing consisted first of inspecting received samples for damage and dimensional tolerances to avoid difficulty of installation into the test wedge at the test track. In only a very few cases were the samples oversize, requiring sanding or additional machine work.

RAIN EROSION MATERIAL EVALUATION

(JOINT AIR FORCE-NAVY PROGRAM AT HOLLOMAN AFB SLED TRACK)

REQUEST FOR RAIN EROSION TEST SAMPLES AND MATERIAL PROPERTY DATA

Supplier _____

Material _____

No. Samples Required _____

Test Velocit _____

Test Sample:

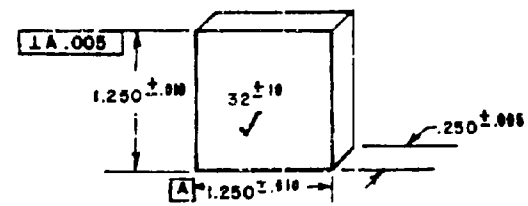

Material Properties

The following items are to be completed by the supplier under the appropriate column as per the corresponding test method. All values to be at room temperature.

PROPERTY	CERAMICS TEST METHOD	CERAMICS VALUE	PLASTICS TEST METHOD	PLASTICS VALUE	REMARKS
Porosity - %	ASTM - 373 - 56		FTM Std No. 406 MTD 5021		
Density - Gm/cc	ASTM - 373 - 56		FTM Std. No. 406 MTD 5011		
Hardness	Knoop (500 Gm load)		Barcol		
Modulus of Elasticity - psi	Sonic Resonance Method		Slope of Tan at Low End of Stress Strain Curve		
Shear Modulus - psi	Sonic Resonance Method		Not Applicable		
Shear Strength - psi	Not Applicable		FTM Std. No. 406 MTD 1040		
Flexural Strength - psi	Cyl. Spec. 4 Pt. Loading 100,000 psi/min		FTM Std. No. 406 MTD 1031		
Tensile Strength - psi	Supplier Method		FTM Std. No. 406 MTD 1011		
Compressive Strength - psi	Not Applicable		FTM Std. No. 406 MTD 1021		
Poissons Ratio	Sonic Resonance Method		Supplier Method		
Dielectric Constant (8.6-10.0 KMC)	ATC Rept. ARTC 4		ATC Rept. ARTC 4		
Loss Tangent (8.6-10.0 KMC)	ATC Rept. ARTC 4		ATC Rept. ARTC 4		

This Space for NAVAIRDEVCEN Use Only

Sample Code _____

Date Received _____

Remarks:

Figure 9. Materials Supplies Data Form

The sample materials were arranged into groups of eight where similar materials, insofar as possible, were evaluated on the same run. After assignment to a given run all samples were numbered and recorded in the Test Sample Log Book. The numbering system used included material class letter, class number, Mach number, run number, and serial number. The following example demonstrates the code numbering system:

C 3 - 1.5 - 4 - 10

The above number indicates this C3 sample to be an 828 Epoxy laminate (see Table VI) evaluated on the fourth run at Mach 1.5. The number 10 indicates that the sample is number 10 of 1 through 10 recorded in the log book to note the vertical position and impact angle.

After numbering, the samples were dried overnight at 150°F for removal of moisture. Samples were then weighed on a Mettler electronic balance, Model H-4. This instrument measures to the nearest milligram with 0.5 mg accuracy. Having recorded the sample weights in the Test Sample Log Book the specimens were packaged into special run boxes for shipment to Holloman Air Force Base. At the time of loading into the test wedge the position numbers for each specimen were recorded.

Upon completion of a firing the samples were removed by personnel from either the AFML or NAVAIRDEVCEN, packaged in the original run boxes and shipped back to the NAVAIRDEVCEN for post-run sample processing. The samples were then redried for 16 hours at 150°F and reweighed for weight loss. The post-firing weights were entered in the Test Sample Log Book. Weight loss (gm), weight loss per unit area (gm/cm^2), and MDP (cm) were calculated based on materials density. The MDP calculation assumes the damage to be uniform over the exposed area of one square inch.

The 10 samples of any specific material for a run were then mounted on 8 x 10-1/2 standard cards. The weight losses, MDPs, pertinent descriptive information, and velocity profiles through the 6000-foot rain field were added to the cards for each group of samples. The cards were photographed in both color and black and white. The black and white was required for this report; color prints were forwarded to each supplier for his samples. The completed cards were then cataloged in special card files as permanent records. These card files are available for observation at both AFML and NAVAIRDEVCEN for Government agencies or industries who are interested in rain erosion damage.

3. PROPERTY DATA

Applicable physical property data for all materials was submitted together with the samples. Standard ASTM test methods were specified where applicable in order to obtain all data on a common basis. Table VII presents the data as it was submitted by materials suppliers; it was not screened for conformance with standard test methods. As a long range objective of this program, an attempt is being made to correlate material properties with the damage experienced in the rain environment.

The following properties were selected as pertinent to erosion resistance and dielectric performance:

Porosity	Tensile Strength
Density	Compressive Strength
Hardness	Tear Strength
Modulus of Elasticity	Modulus @ 100% Elongation
Shear Modulus	Poisson's Ratio
Shear Strength	Dielectric Constant
Flexural Strength	Loss Tangent

It is pointed out that these materials were not prepared to optimize one particular property specifically, but rather as representative samples of their pertinent class of material. Therefore, because a particular material is considered low in a certain property does not indicate inferiority in any way for other applications.

SECTION VII

RAIN EROSION DAMAGE DATA

1. THE CARD PHOTOGRAPHS

All exposed samples were mounted on standard card forms after reweighing. Samples from the left side of the wedge were mounted in the lower row; right-side samples were mounted in the upper row. The forward or leading edge in all cases is on the left-hand side of the cards. The top row of numbers, above the samples, indicates the weight losses per unit area (gm/cm^2); the lower row of numbers presents the calculated MDPs in cm assuming uniform erosion over the exposed area.

Material description, test conditions, run number, date of test and test Mach number are listed in the lower left corner. The velocity profiles through the 6000-foot rain field for each run are drawn in the lower right corner of the cards. Average velocities for all runs were calculated for conversion of weight loss per unit area to mean depth of penetration rate (MDPR) using the following equation:

$$\text{MDPR} = \frac{\text{MDP}}{\text{sec}} = \frac{\text{Weight Loss/Unit Area}}{\rho t} = \frac{\text{Volume Loss / Unit Area}}{\text{Unit Time}}$$

$$\frac{\text{cm}}{\text{sec}} = \frac{\text{gm}}{\text{cm}^2} \times \frac{\text{cm}^3}{\text{gm}} \times \frac{1}{\text{sec}} = \frac{\text{cm}^3/\text{cm}^2}{\text{sec}}$$

Where ρ is the density of the eroded material, g/cm^3
t is the exposed time in the rain, sec

Rain erosion damage data for a material is plotted as MDPR vs sin θ for a family of velocities. This form was shown to best fit the data for some classes of materials. There are cases however where it does not apply. Ductile materials, for example, while severely dented or deformed within a very short exposure time, experienced no significant weight loss. Certain high strength but brittle ceramic materials showed no weight loss for the velocities and exposure times of the test. Other ceramics fractured and showed such a wide scatter of data points as to preclude their plotting into any reasonable curves.

2. THE HIGH VELOCITY - SHORT EXPOSURE TIME RAIN EROSION EQUATION

Some attempt has been made toward deriving equations to fit the MDPR dependence upon velocity and impact angle. Obviously it would be most desirable to develop a general equation which would fit most types of materials and for which specific constants and exponents could be determined for the individual materials. The data derived from evaluating 65 different materials which logically fit into 10 different material classes is now available for such curve fitting.

First efforts were devoted to a homogeneous group of materials which were eroded with a minimum difference in weight loss between left and right-side samples and which, in general, showed the best plots of MDPR vs sin θ. The plastic laminate (Class C) group was best suited for doing this because erosion results showed a minimum deviation of data points from straight lines and the most reasonable magnitude and slope change with velocity. The equation to best describe the rain erosion effect was derived purely on a mathematical curve fitting basis. Figure 10 (a PBI laminate) is a typical graph of the MDPR vs sin θ for the Class C

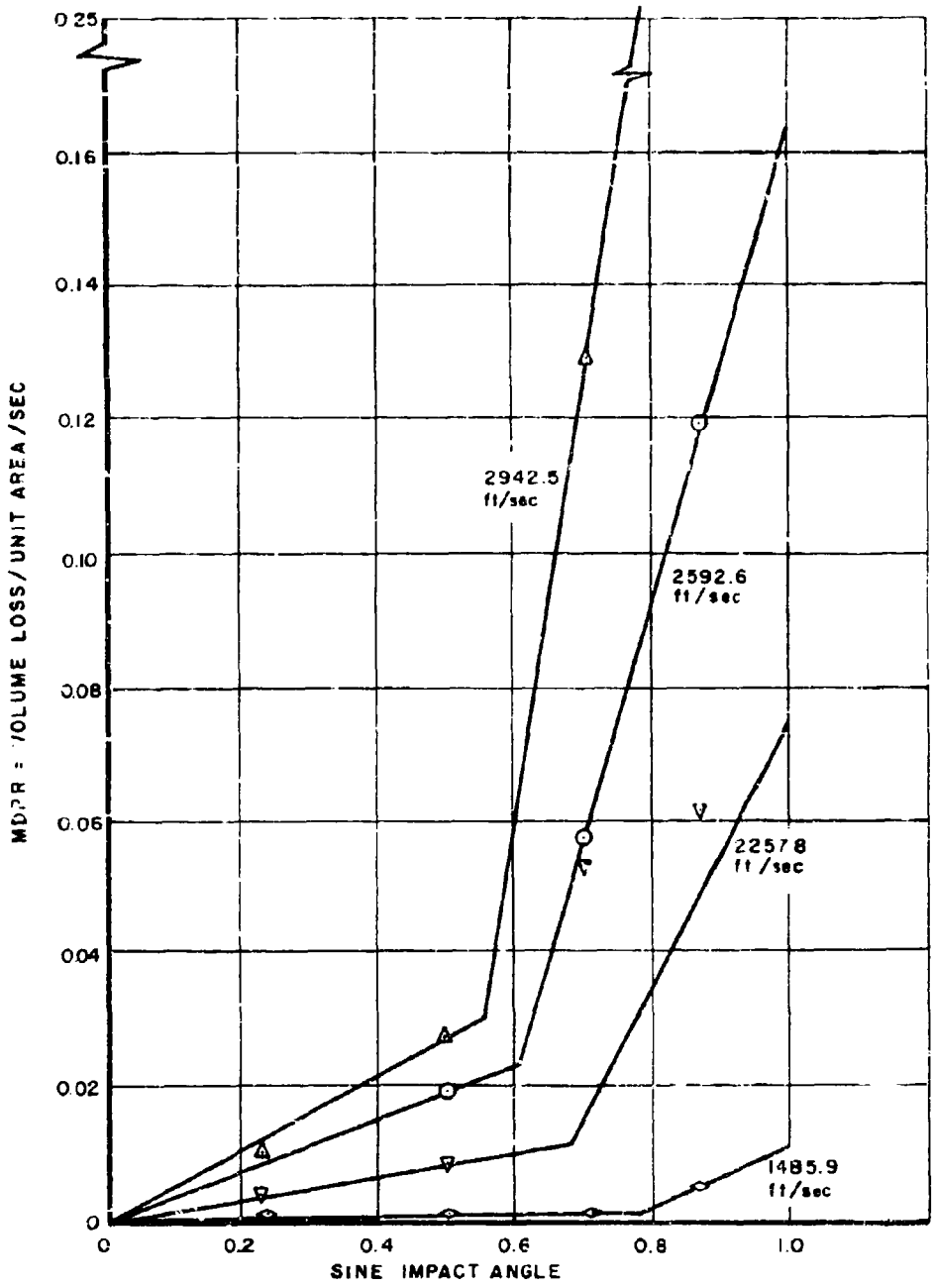

Figure 10. Mean Depth of Penetration Rate vs Sine of the Impact Angle for PBI Laminates

materials. For any specific test velocity the graph is a combination of two straight lines of different slopes intersecting at $\theta = \theta_D$. For $\sin\theta < \sin\theta_D$ the straight line is described by the equation:

$$MDPR = K_1 \sin\theta \tag{1}$$

For $\sin\theta > \sin\theta_D$ the straight line is described by the equation:

$$MDPR = K_2 \sin\theta + K_3 \tag{2}$$

In the above equations K_1, K_2, and K_3 are all functions of velocity $f(\nu)$. When K_1, K_2, and K_3 are plotted vs velocity on a semilog graph they produce straight lines as shown by Figure 11. From these three slopes the $f(\nu)$ describing K_1, K_2, and K_3 are determined. θ_D is then determined by equating $K_1 \sin\theta_D = K_2 \operatorname{Sin}\theta_D + K_3$. Therefore the functions are simple exponentials given as:

$$K_1 = A e^{\alpha\nu} \tag{3}$$

$$K_2 = B e^{\beta\nu} \tag{4}$$

$$K_3 = C e^{\gamma\nu} \tag{5}$$

$$\text{at } \theta_D \quad \sin\theta_D = \frac{K_3}{K_1 - K_2} \tag{6}$$

In Equations (3) and (4) the exponents α and β are equal. By substituting Equations (3) through (6) in Equations (1) and (2)

$$MDPR = A e^{\alpha\nu} \sin\theta \text{ for } \theta < \theta_D \tag{7}$$

$$MDPR = B e^{\alpha\nu} \sin\theta + C e^{\gamma\nu} \text{ for } \theta > \theta_D \tag{8}$$

$$\theta_D = C / A - B e^{(\gamma-\alpha)\nu}$$

A more simplified form of Equations (7) and (8) is:

$$MDPR = E e^{\alpha\nu} \sin\theta + F e^{\gamma\nu} \tag{9}$$

where

$$E = A \text{ and } F = 0 \text{ for } \theta < \frac{C}{A - B} e^{(\gamma-\alpha)\nu}$$

$$E = B \text{ and } F = C \text{ for } \theta > \frac{C}{A - B} e^{(\gamma-\alpha)\nu}$$

Values for constants E, F, α and γ have been evaluated for all Class C materials. These constants are listed in Table VIII. Of the many classes of materials tested, Equation (9) has been found to apply to the plastic laminates (Class C) and some of the ceramics. Further work is being conducted on the other classes to see if they may fit the general equation (9).

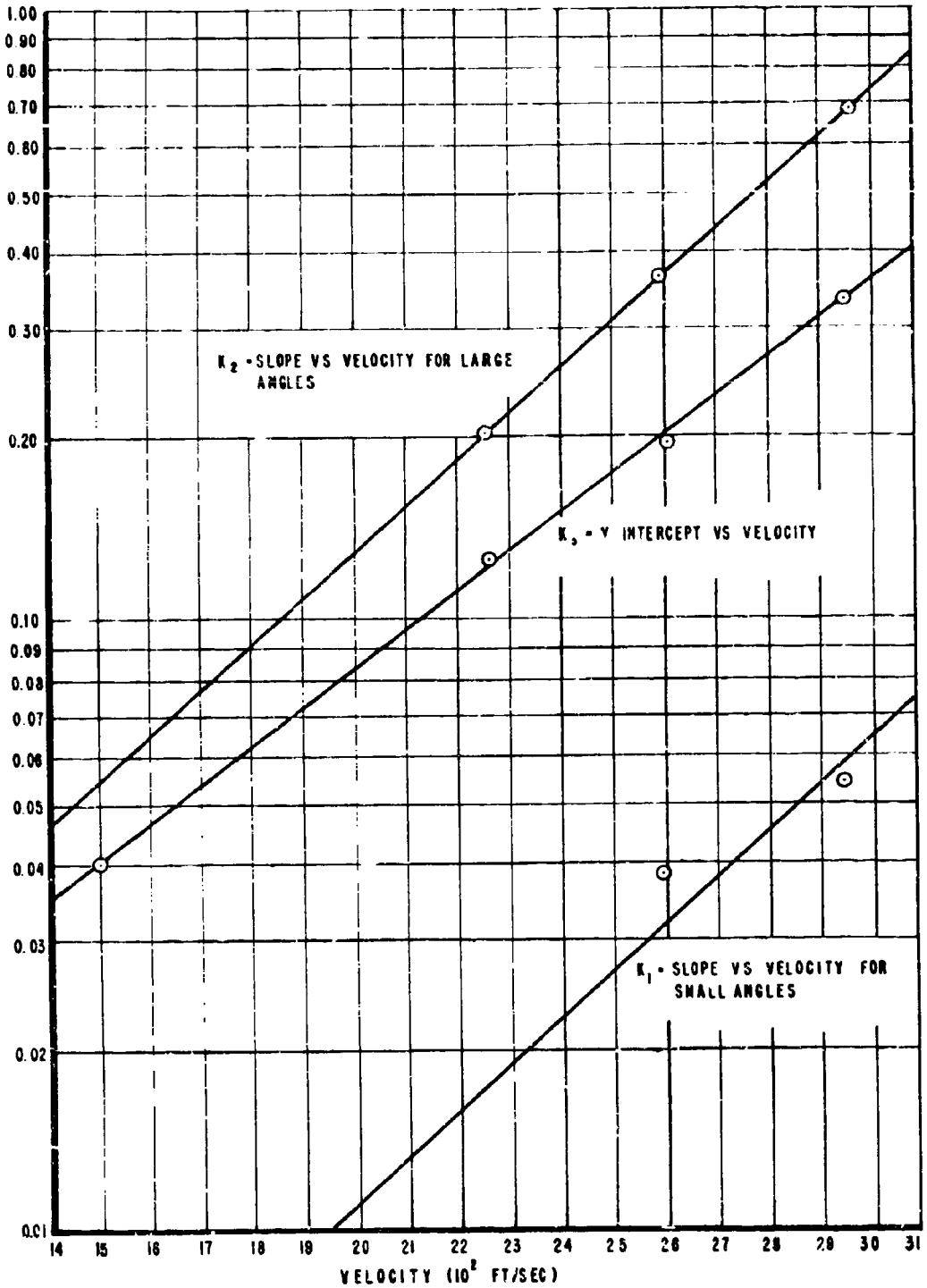

Figure 11. Slope and Intercept of the Rain Erosion Equation vs Velocity for PBI Laminates

3. RAIN EROSION PHENOMENON

The loss of material by rain erosion is a complex phenomenon which has been studied in recent years by the University of Cambridge and the Royal Aircraft Establishment among others. The radial flow velocities associated with water drop impact at 90° have been measured at 2 to 3 times the impact velocity. The dynamic or impact pressures on the face of materials at normal impact can be calculated by the water hammer equation:

$$p = \rho c v$$

where

c = compression wave or acoustic velocity

ρ = fluid density

v = impact velocity

At 3000 ft/sec this pressure is approximately 194,000 psi. It is these tremendous high pressure pulses which induce excessive tensile, compression, shear and combined stresses within a material, causing failure.

4. FAILURE MECHANISMS IN MATERIALS

The mechanism of failure within materials varies according to material type with elastomeric materials failing adhesively through transmission of the shear stress to the substrate breaking the bond. Plastic-like materials and soft metals deform under impact and flow plastically resulting in craters and pits. Isotropic ceramics and hard metals are eroded by work hardening and subsequent fracture of small imperfections in the surface. As these imperfections are removed, protrusions are formed against which the flowing liquid acts to exert a shear stress and turning moment, causing failure. All these mechanisms have been observed in this evaluation series.

5. CALIBRATION RUNS

To investigate the effects of sample position on sample damage both vertical and left/right, four standard or calibration runs were conducted. The wedges for these runs contained 80 samples of material cut from the same sheet of Plexiglas. Calibration runs were made at Mach 1.5, 2.0, 2.5, and 3.0. Data for these runs are shown in Figures 12 through 15. Vertical and left/right positions are shown in Figure 16. Left side losses are represented by the dashed lines; right side losses are shown by solid lines. In general the data is random at all velocities and for all angles with the left and right curves crossing without indicating any pattern or trend.

This random weight loss effect may be explained in terms of probabilities of drop size distribution experienced by any particular single exposed sample. It is not difficult to imagine that a sample on one side of the wedge could experience impact with a somewhat different total number of drops and average drop size than the other side when traveling 6000 feet through a tube of air in which random size water particles are dispersed.

It may be concluded from Figures 12 through 15 that there are no serious effects which make the samples position dependent. Positions 1 and 8, i. e., top and bottom, at 60° show somewhat greater losses than all samples at the same angle in positions 2 through 7. This becomes more serious at the high velocities and can be explained only as an end effect in which the wave pattern differs from that which is typical over the center section of the two-dimensional wedge. The normalizing tendency of staggering samples on either side of the wedge partially overcomes this effect.

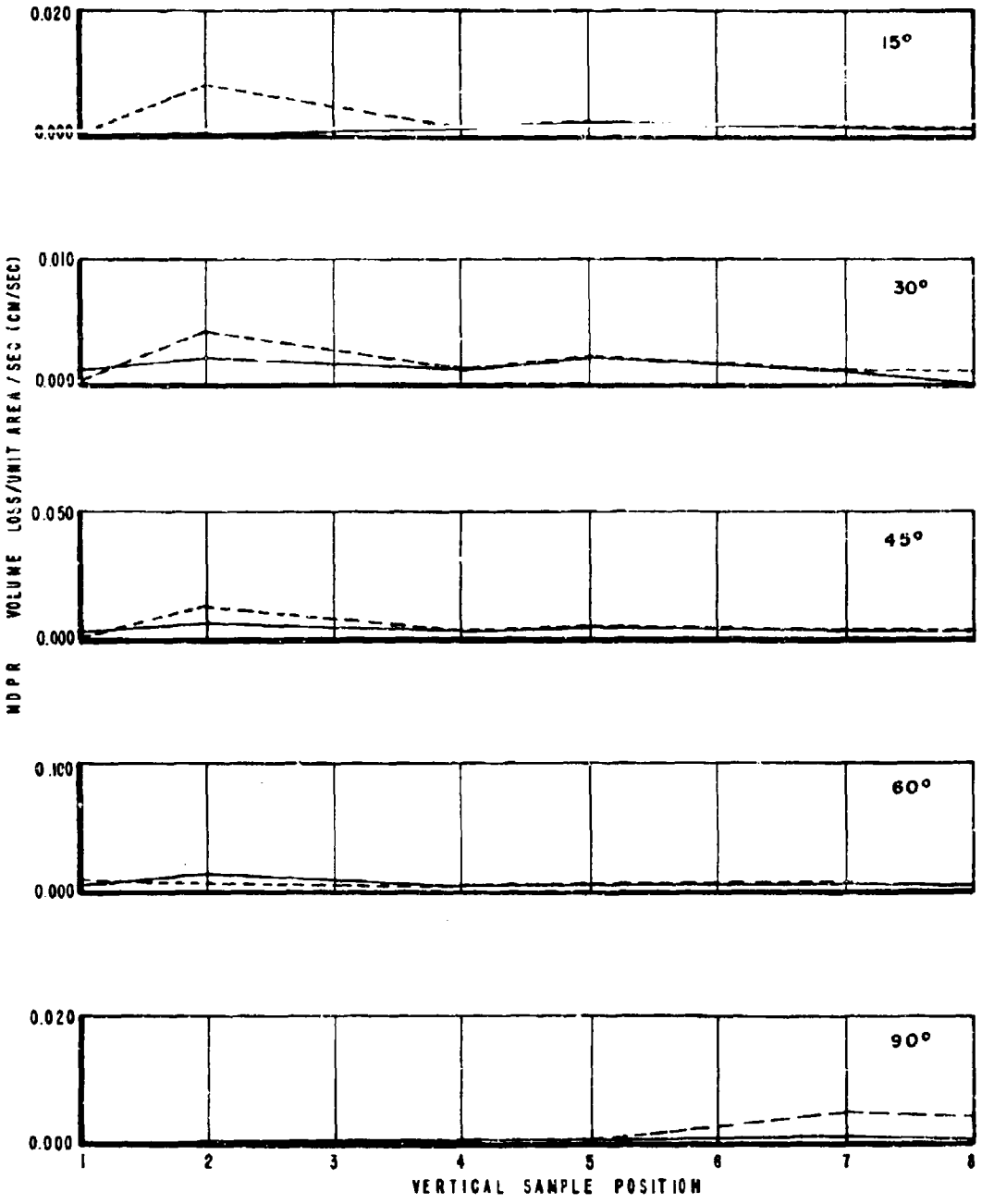

Figure 12. Mach 1.5 Calibration Run Data (1758.0 ft/sec)

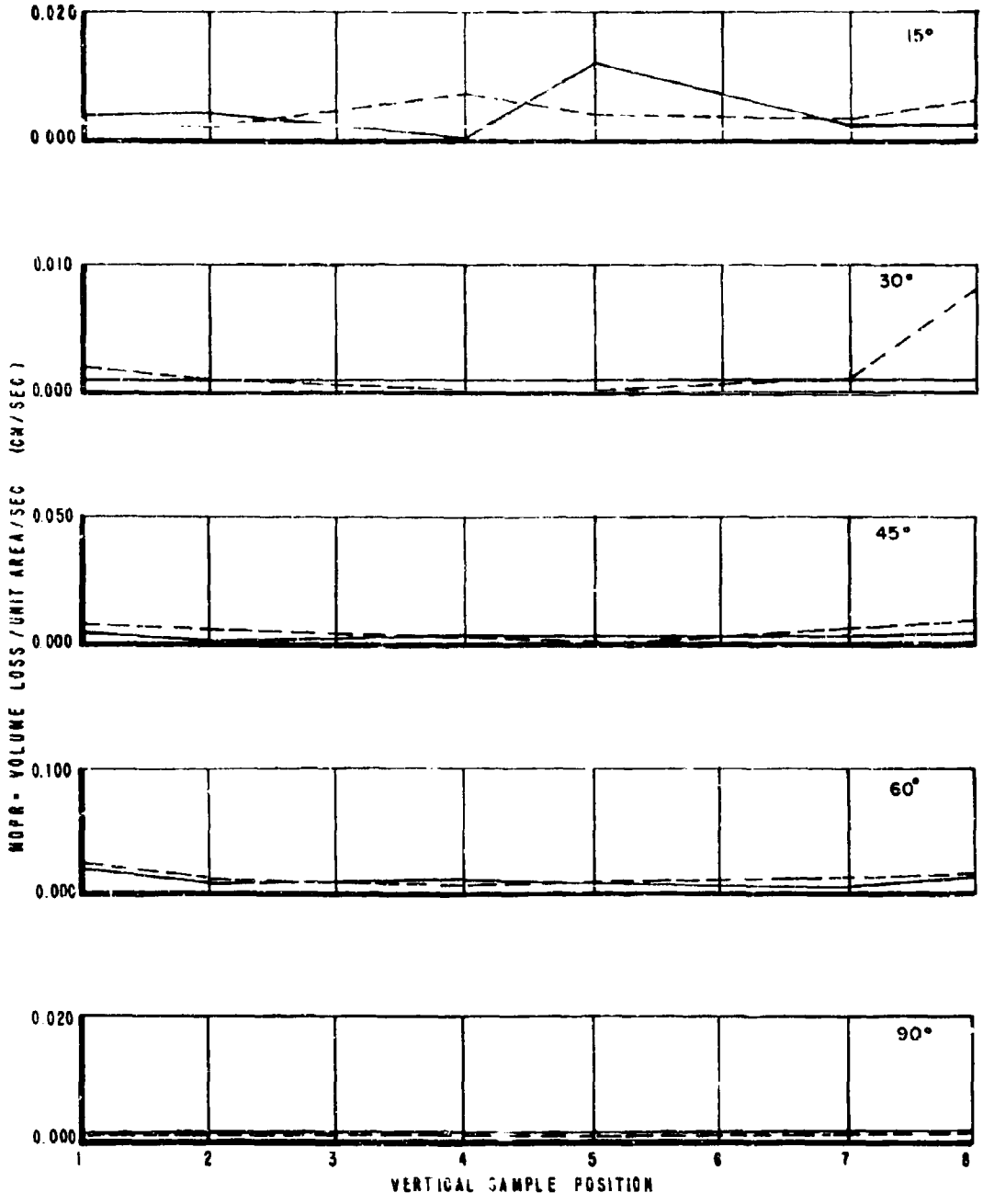

Figure 13. Mach 2.0 Calibration Run Data (2116.9 ft/sec)

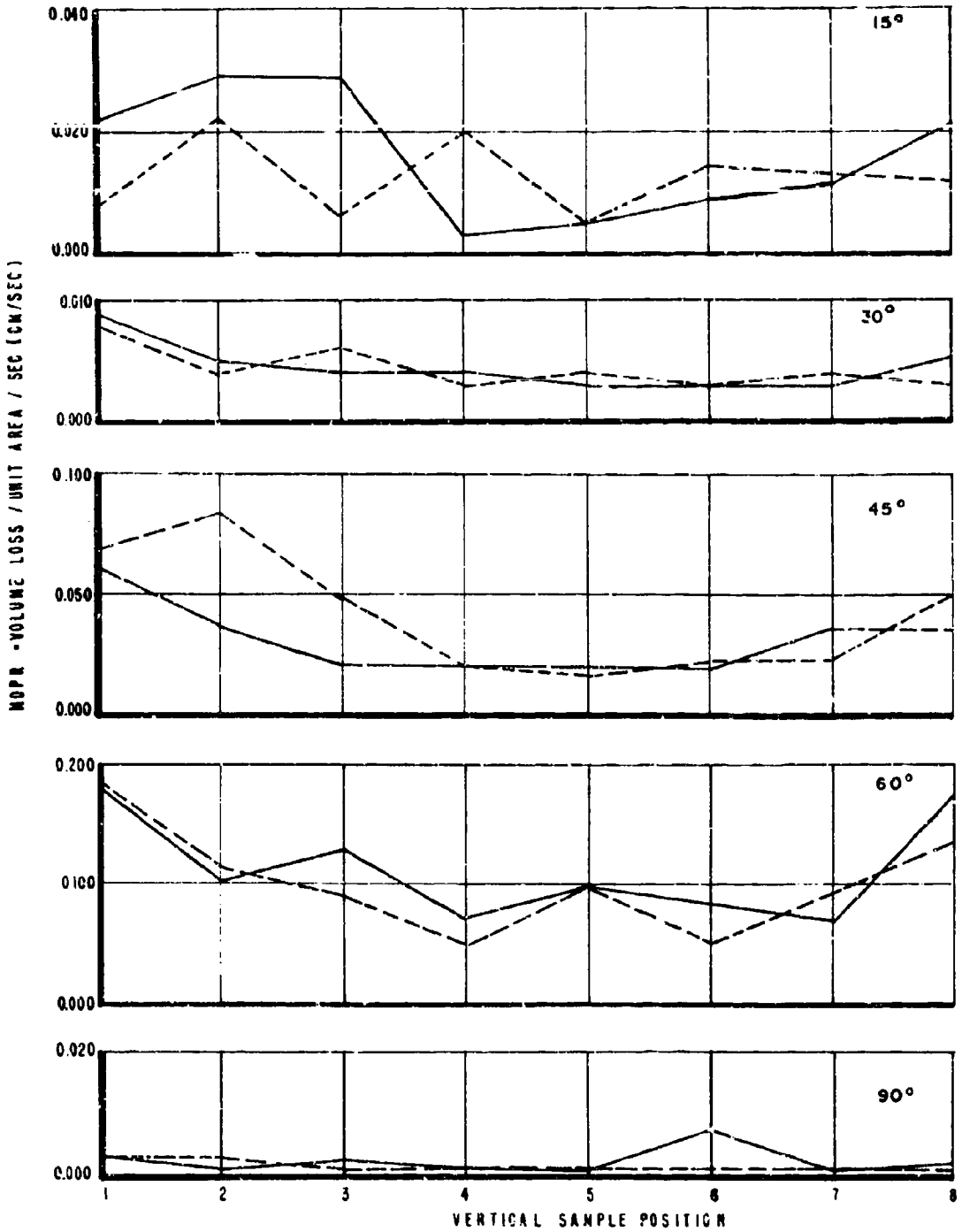

Figure 14. Mach 2.5 Calibration Run Data (2549.0 ft/sec)

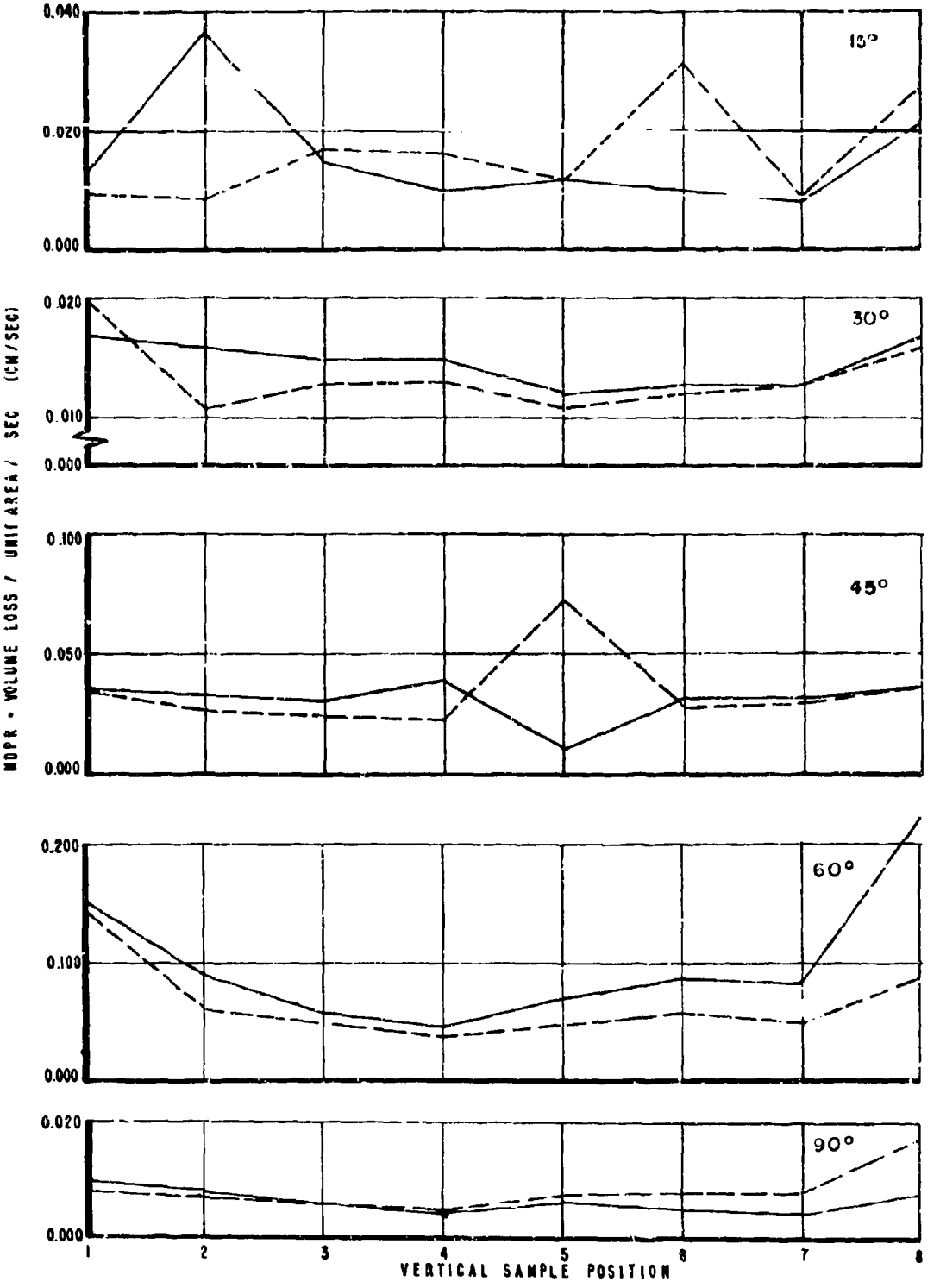

Figure 15. Mach 3.0 Calibration Run Data (3366.4 ft/sec)

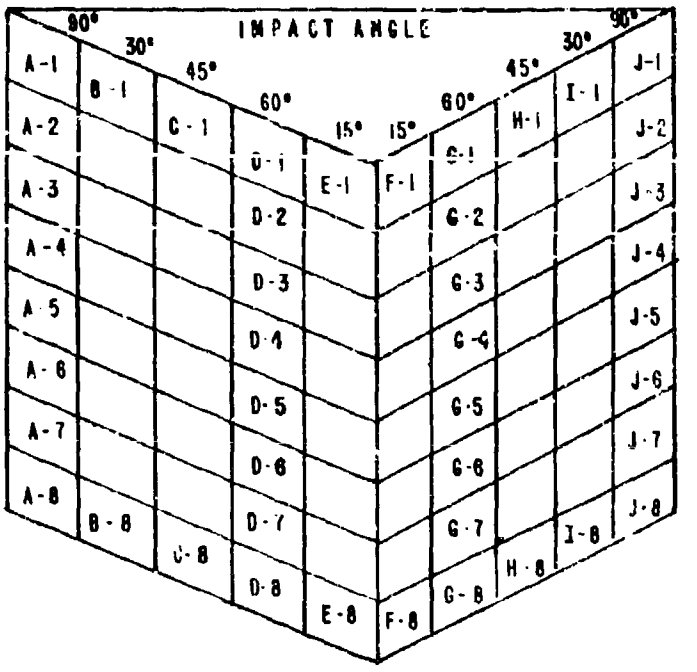

Note: The letters and numbers of the positions have no relation to the letters and numbers of the classes of materials

Figure 16. Sample Position Numbers in Wedge

When the 16 data points for Plexiglas, material 1-2, were averaged for the same impact angle and velocity before plotting the curve MDPR vs sin θ or erosion rate vs normal component of velocity, the same curve was produced as was obtained from a run in which only two data points per angle were available. This is an indication that two samples exposed to the same test conditions is not too small a sampling to yield reliable data.

SECTION VIII

EVALUATION RESULTS

Each of the materials is discussed individually. The presentation and evaluation includes a description of the material, an indication of important properties, results and treatment of erosion data, conclusions regarding the material and recommendations for its improvement.

It is again emphasized that these materials were not specifically designed or prepared for supersonic rain erosion resistance and any poor performance in the rain environment by no means indicates any criticism or disparity in their utility for other nonerosive applications. Further, any outstanding performance in the rain should not be taken as an endorsement of these materials by the Government; it is rather a function of the materials properties and their relationship to erosion resistance.

1. CLASS A - ISOTROPIC CERAMICS

A-1 Pyroceram 9606

Pyroceram 9606 is a glass-ceramic material developed by and proprietary to the Corning Glass Works. It has been used extensively for missile radomes in the supersonic range and remains one of the best available materials in terms of both cost and overall performance.

This material is centrifugally spun or cast in a female mold in the glass form after which it is rough machined. Final grinding is completed after conversion to the ceramic stage. Dielectric property tolerances are excellent because of the close control of batches, and finish machine tolerances to provide precision radomes.

It has zero porosity, good flexural strength, moderate thermal expansion properties and a high use temperature. It may therefore be considered to be good in thermal shock resistance, depending upon the wall thickness for a specific application.

Pyroceram 9606 is not as erosion resistant as highly dense alumina or beryllia but is more resistant than cordierite or fused silica of the isotropic ceramics. Specimens of Pyroceram 9606 were undamaged in all positions at velocities up through Mach 2.0 The 60° specimens were eroded at Mach 2.5 and 3.0 and the 45° specimens were also damaged at Mach 3.0. Otherwise the material exhibited good erosion resistance.

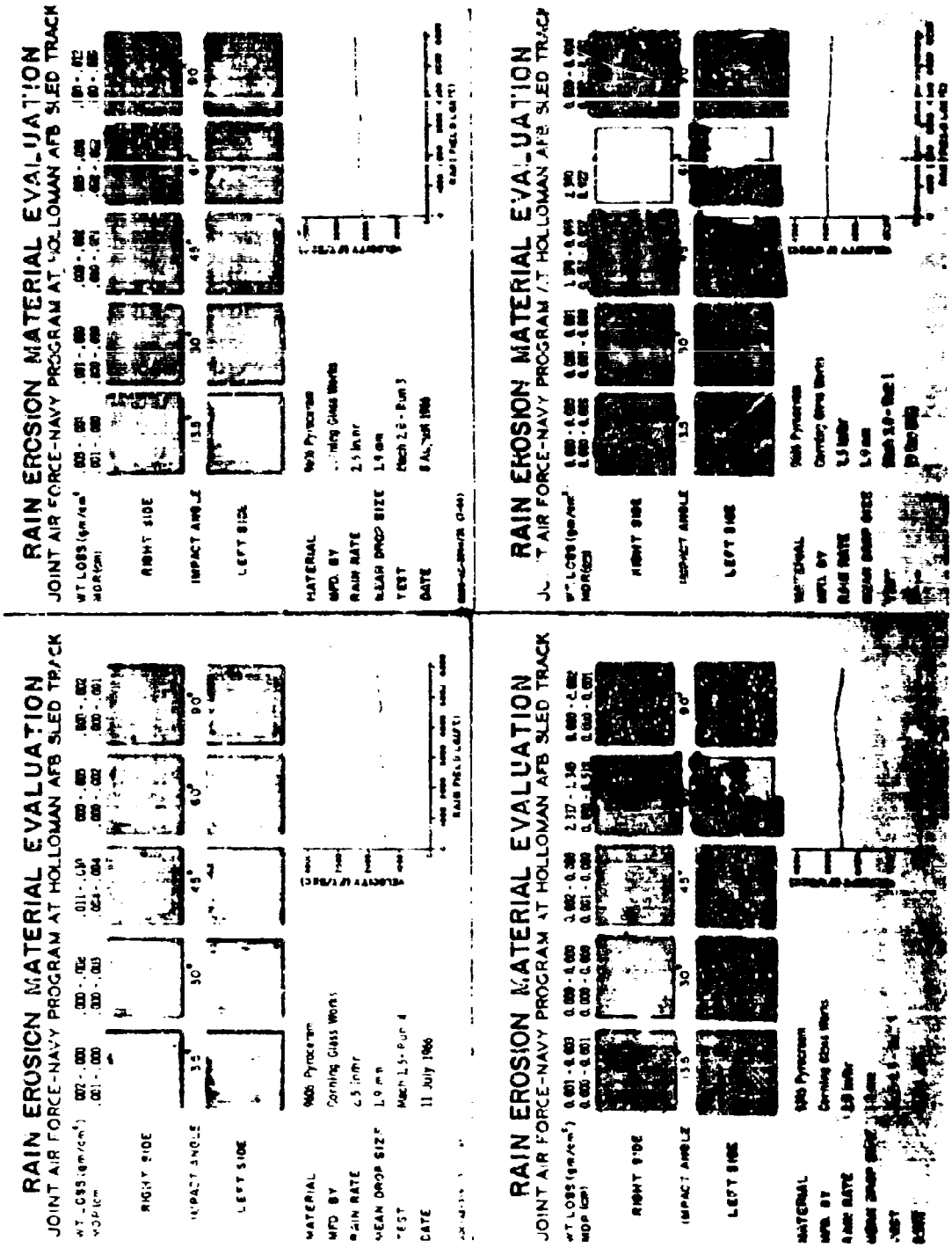

Figure 17. Rain Erosion Damage Data for 960C Pyroceram

A-2 Pyroceram 9611

This material is a developmental form of Pyroceram and has a higher density and dielectric constant than the 9606. It has zero porosity but lower flexural and tensile strength. Since it is both developmental and proprietary, very limited information is available.

This material, in general, performed better than the glasses tested but not as well as the 9606 Pyroceram, alumina, or beryllia. Up through Mach 2.0, performance was better than fused silica; at greater Mach numbers its performance was unsatisfactory at all impact angles. Upon failure the material dices similar to certain types of safety glass with small, round-edged pieces, but without noticeable surface erosion.

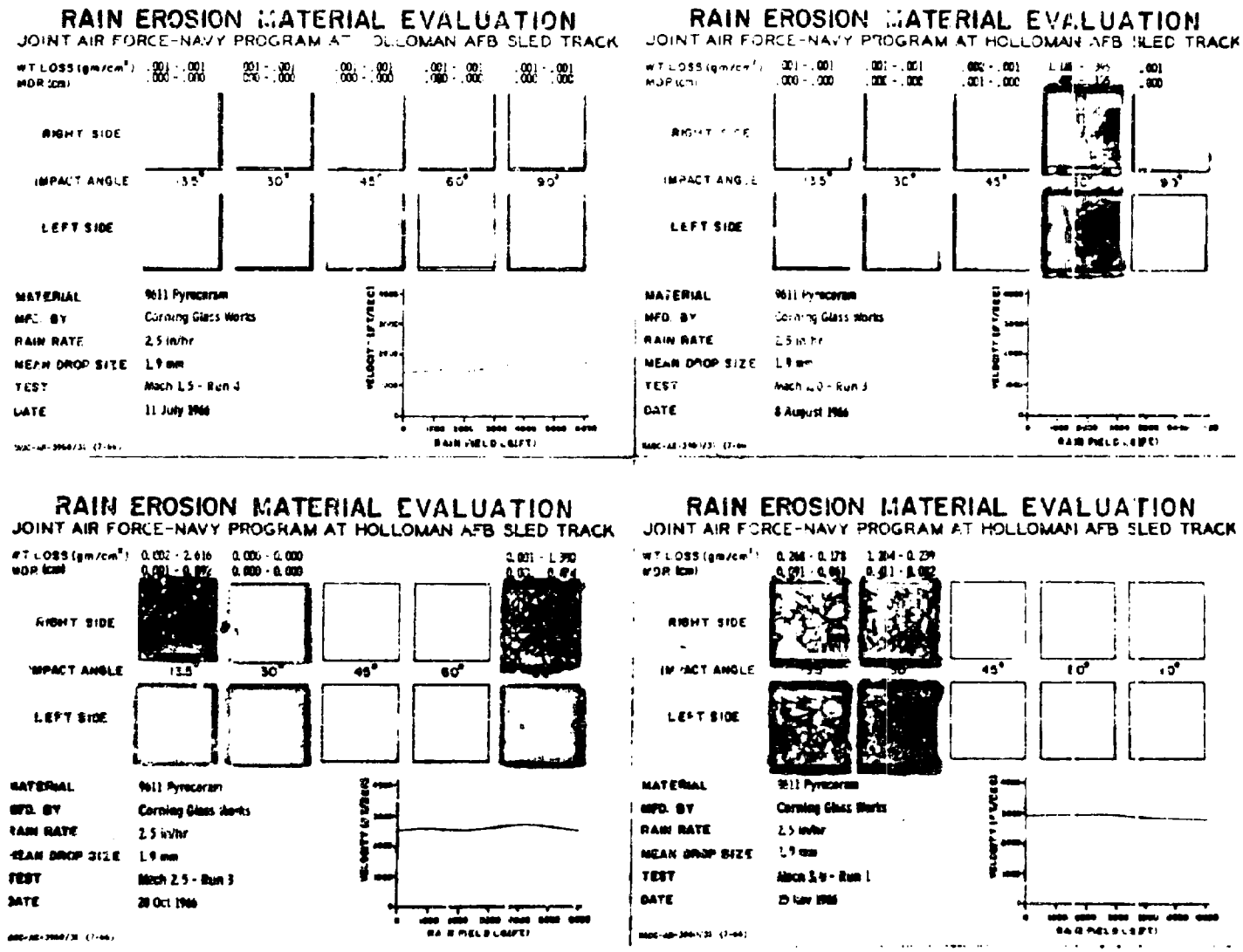

Figure 18. Rain Erosion Damage Data for 9611 Pyroceram

A-3, A-4, A-5 Alumina

Three representative high grade aluminas were furnished for evaluation by two suppliers. Alsimag No. 753 alumina from the American Lava Division of the 3-M Company was tested on the same run with Western Cold and Platinum Company Wesgo AL-300, and Wesgo Wearox aluminas. Properties of these three materials are similar (see table VII). All three are typical of the alumina materials currently in use on several missile systems.

As a radome material the high grade aluminas have the greatest hardness, elastic modulus, and flexural strengths of the isotropic ceramic materials considered in this program. Porosity is zero with dielectric constants ranging between 9.6 and 9.9. These materials make excellent radomes if the particular wall construction at the design frequency is within the allowable thermal stress limit. Cost is likely to be somewhat higher than for some other ceramics because of relatively high cost diamond grinding.

Of all dielectric materials evaluated these materials show the greatest rain erosion resistance. At Mach 2.0 and 2.5 no measurable damage was observed for the Alsimag 753 alumina; the Wesgo AL-300 and Wesgo Wearox were evaluated only at Mach 3.0. Since fracture did occur in the 753 and Wearox specimens at 60° at Mach 3.0, the AL-300 may be slightly superior in rain erosion resistance. It is likely that this difference results from a smaller grain size within the AL-300 material.

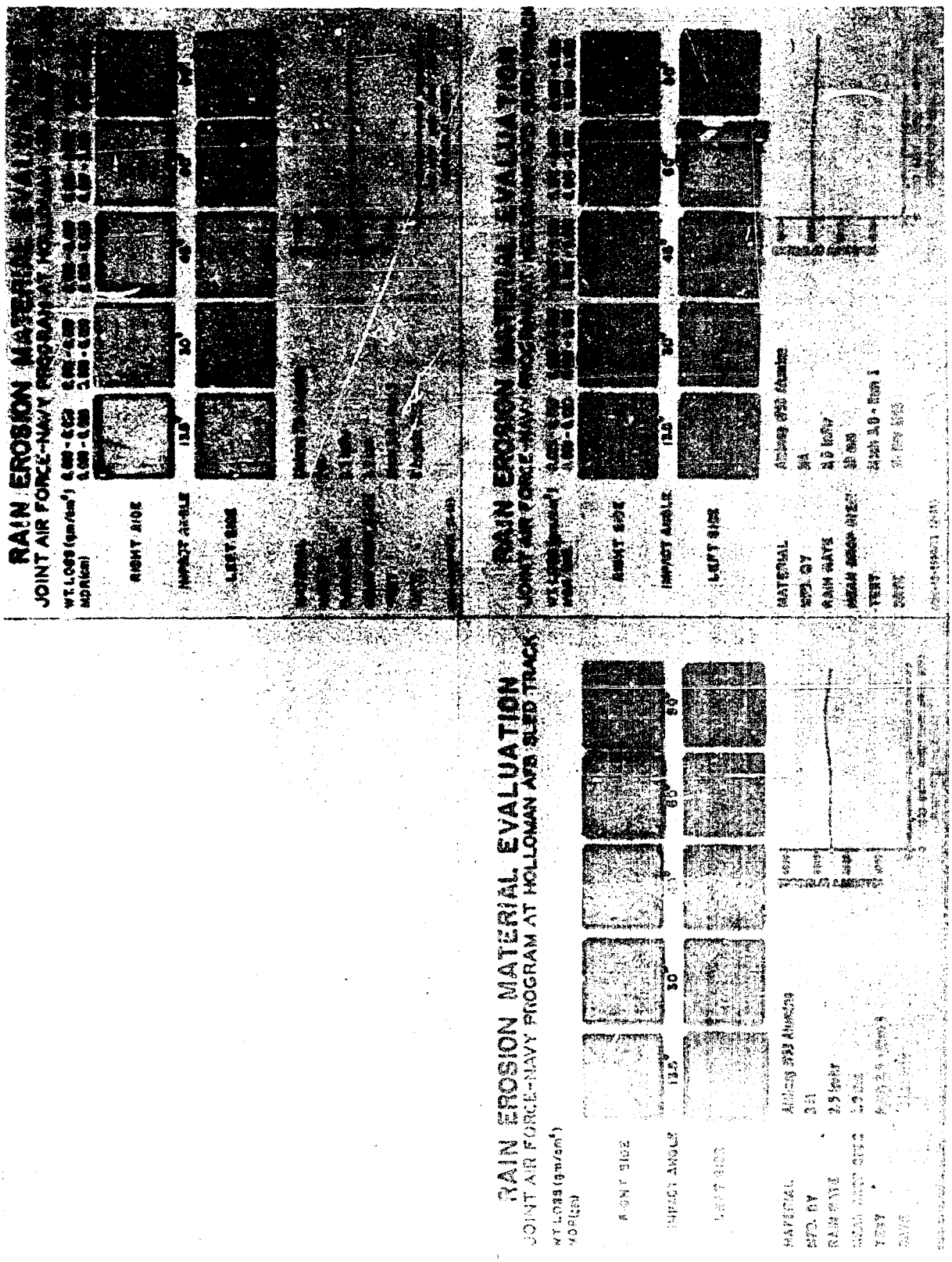

Figure 19. Rain Erosion Damage Data for Alsimag 753 Alumina

Best Available Copy

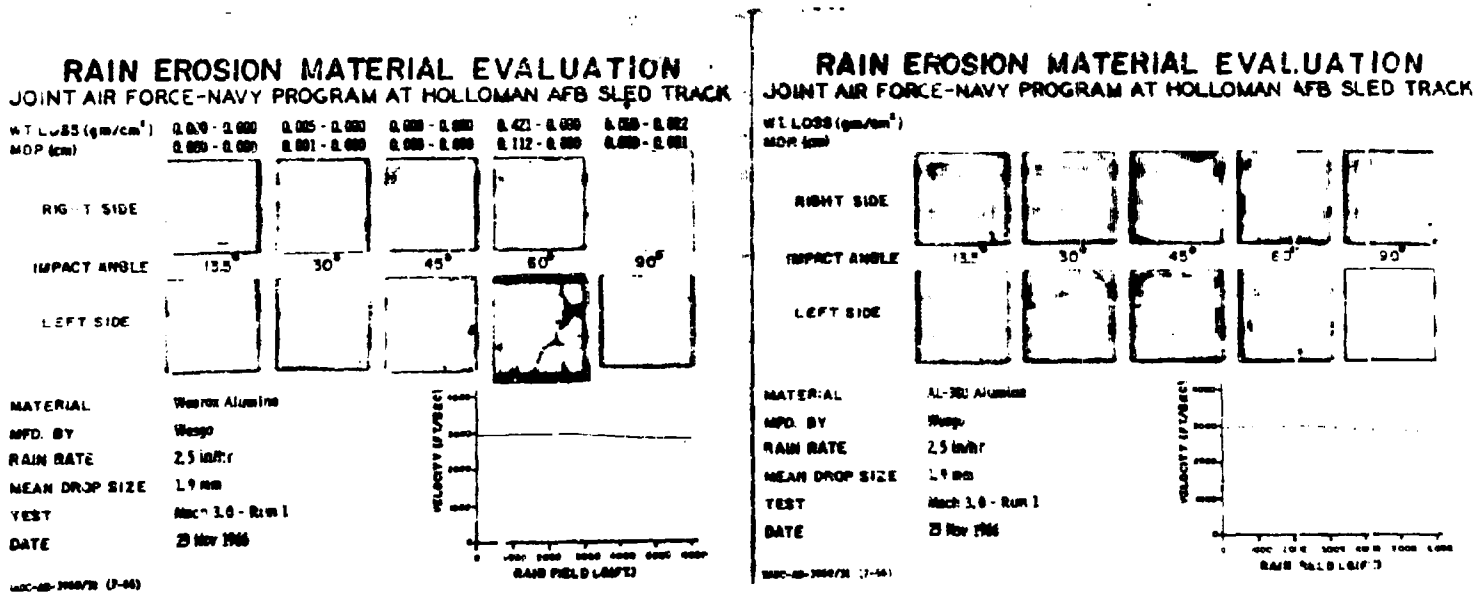

Figure 20. Rain Erosion Damage Data for Wearox Alumina and AL-300 Alumina

PRECEDING PAGE BLANK - NOT FILMED.

A-6 Beryllia Alsimag No. 754

Dense beryllia ceramics are manufactured by several companies in the United States. The number is very limited because of the toxic effects from working with the material in the powder, dust, or vapor form. Special processing facilities are required to protect the workers from these potential health hazards. This does not mean that beryllia should not be considered as a candidate radome material. It means only that the special facilities tend to raise the cost of products made from this material. These companies currently have the capability of manufacturing large size radome blanks. They do not however have the finish grinding capability; this finishing would have to be accomplished by companies having such grinding equipment.

Beryllia has an exceptionally high thermal conductivity, comparable to that of aluminum metal. Combined with fairly high flexural and tensile strength this material can be expected to provide good thermal shock resistance for many missile applications. Its dielectric properties are excellent and it is nonporous. The hardness approaches that of alumina which should make it very resistant to rain erosion.

The Alsimag 754 beryllia specimens were provided by American Lava Division of 3-M Company. The test specimens for 60° at Mach 2.0 were broken rather than eroded. This occurred before the brittle materials were potted and additional samples were not available for rerun. This is obvious from the samples showing no damage at Mach 2.5. Weight loss at Mach 3.0 is very minor indicating that beryllia may be rated second only to high grade alumina.

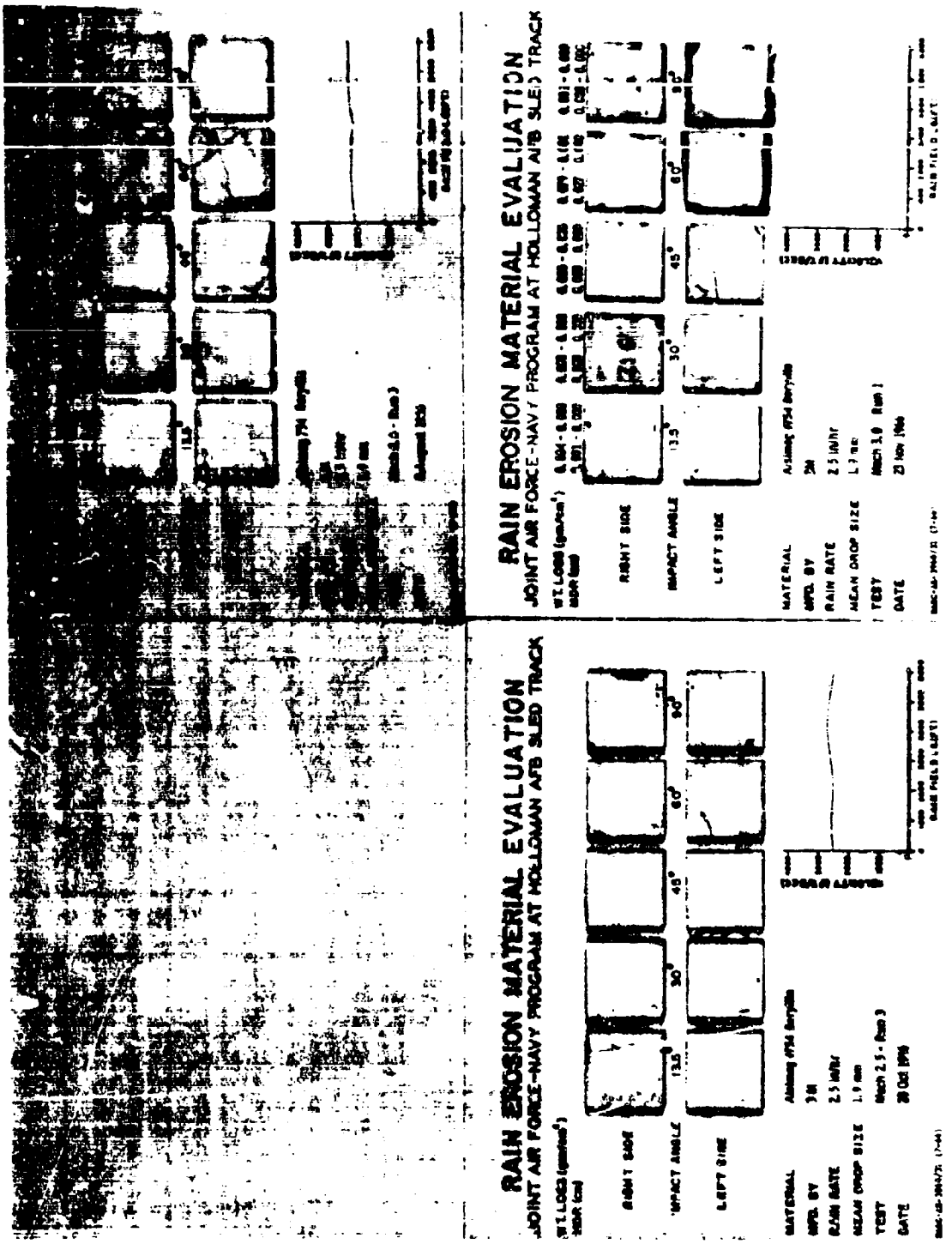

Figure 21. Rain Erosion Damage Data for Alsimag 754 Beryllia

A-7 Cordierite - Alsimag No. 701

Cordierite ($2MgO \cdot 2\ Al_2O_3 \cdot 5SiO_2$) is of interest for radome manufacture because it is non-proprietary, has good dielectric properties, is fairly hard and has medium strength by comparison with other ceramics. It has the disadvantage of being slightly porous and would, therefore, require a sublimation type sealer such as Teflon. This material has a relatively narrow firing range requiring precision firing control. Otherwise it can be manufactured essentially with the same slip casting or pressing processes as silica or alumina.

The cordierite evaluated in this program is the Alsimag No. 701 furnished by the American Lava Division of the 3-M Company. Generally cordierite can be rated between 9606 Pyroceram and 7941 fused silica in erosion resistance. The surface eroded measurably at 45° and 60° at higher velocities. All samples were potted including the Mach 2.0 specimens.

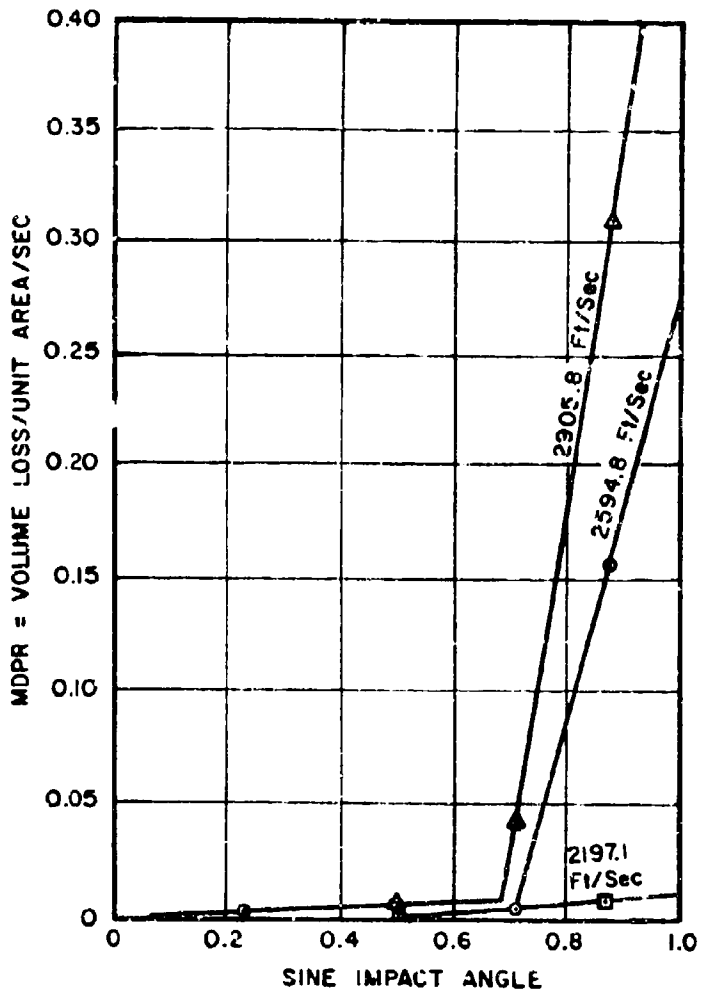

Figure 22. MDPR vs Sine Impact Angle - Alsimag 701 Cordierite

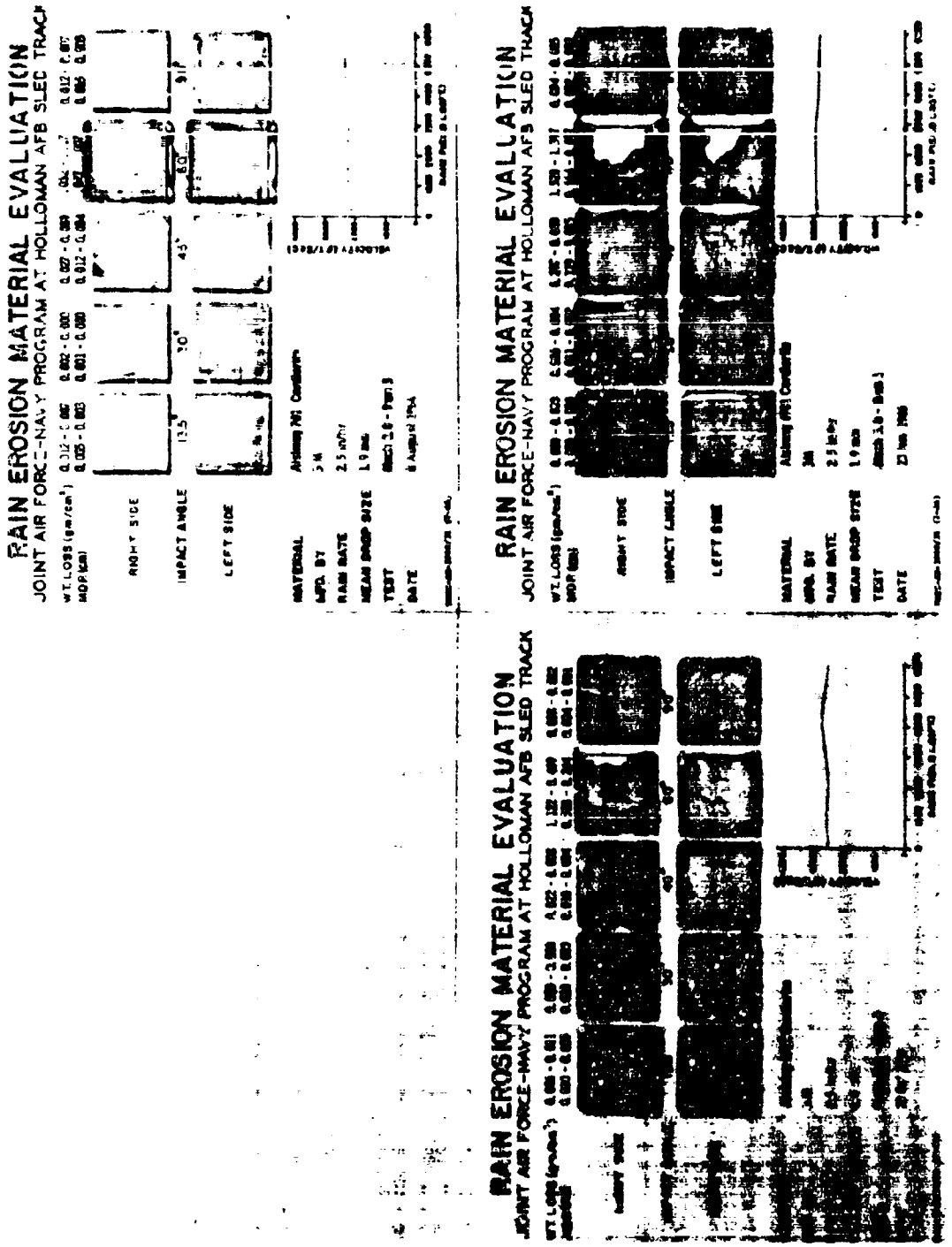

Figure 23. Rain Erosion Damage Data for Alsimag 701 Cordierite

A-8, A-9, A-10, A-11, A-12 Fused Silica

Five separate fused silica materials were furnished by three suppliers: (1) one from Corning 7941; (2) three from the Pomona Division of General Dynamics (GD/P); and (3) one from the Brunswick Corporation. Of the three silicas from GD/P, Type I was silicon coated, Type II Teflon coated, and Type III uncoated. All five may be considered as representative of the available materials from many suppliers. From the data of Table VII the 7941 is likely of higher strength than the others tested.

In spite of a serious porosity problem and lack of strength the fused silicas have the lowest dielectric constant, loss tangent, and thermal expansion of any of the ceramics. It is the best available material in thermal shock resistance, has a very high peak use temperature, and ablates clearly above the softening point. There are certain applications where fused silica may be the only material capable of meeting the thermal environment at very high heat flux levels. It may also be attractive for some applications from a cost standpoint.

In observing the results of fused silicas Types I, II and III the damage is very similar. The data has been combined to average the weight losses using six samples per angle instead of two. MDPR equations were developed for both 7941 and the GD/P silicas producing constants which indicate the GD/P silica is slightly more resistant than the 7941.

The fused silicas as a group are the poorest ceramic materials evaluated. When using this material for any missile radome the impact angles should be very small and metallic nose tips should be incorporated into the design where feasible.

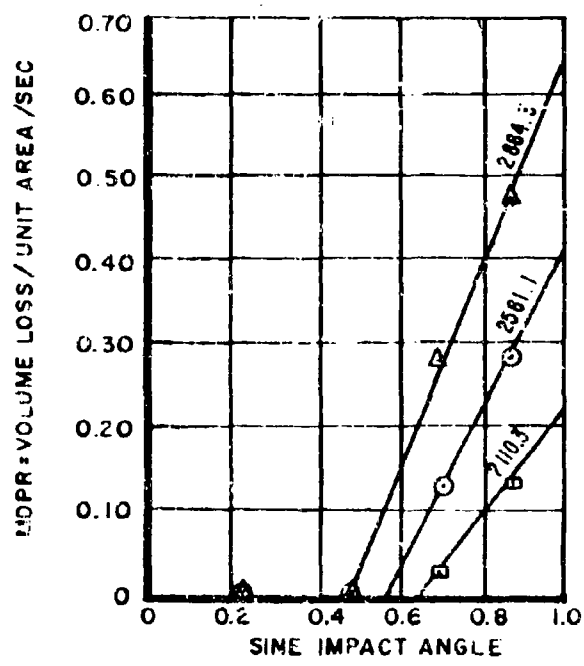

Figure 24. MDPR vs Sine Impact Angle - GD/P Fused Silica

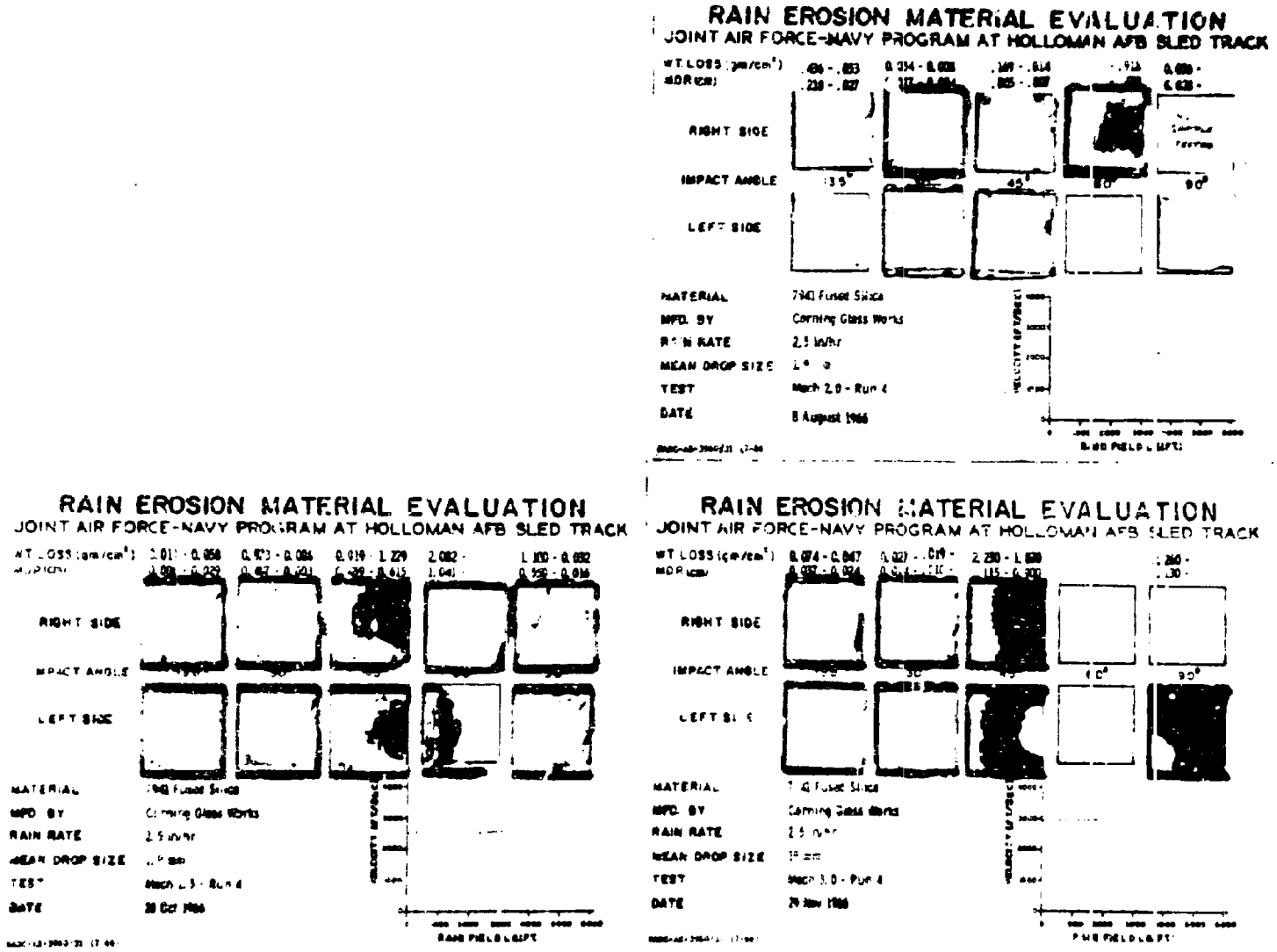

Figure 25. Rain Erosion Damage Data for Corning 7941 Fused Silica

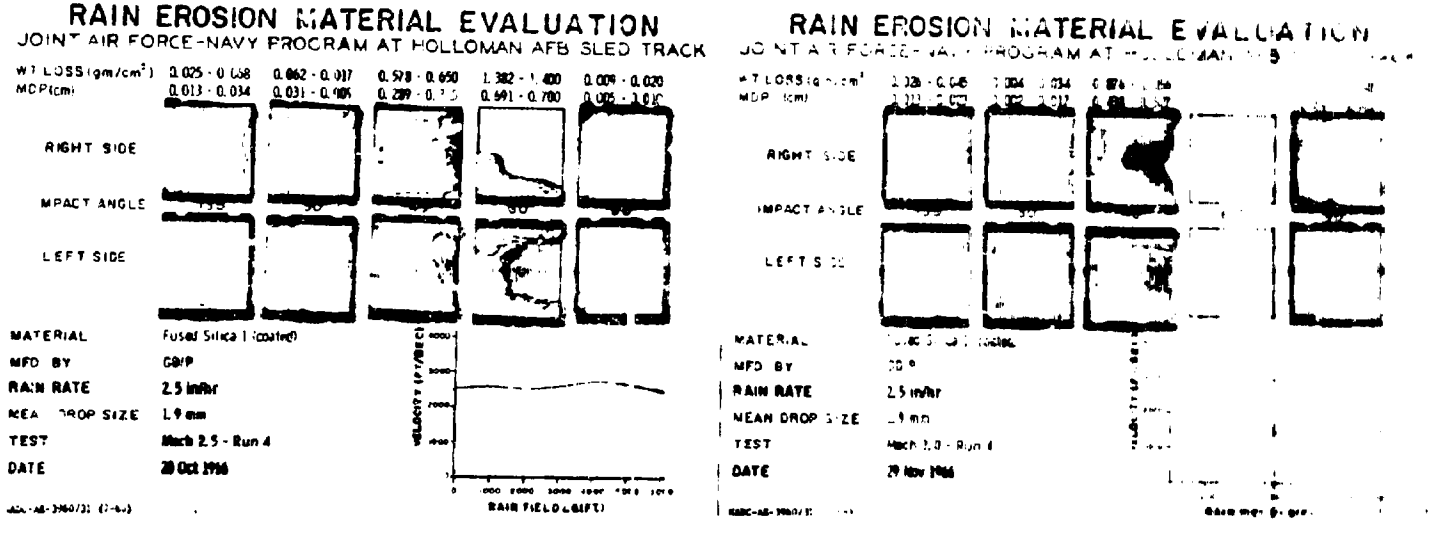

Figure 26. Rain Erosion Damage Data for GD/P Fused Silica (Type I)

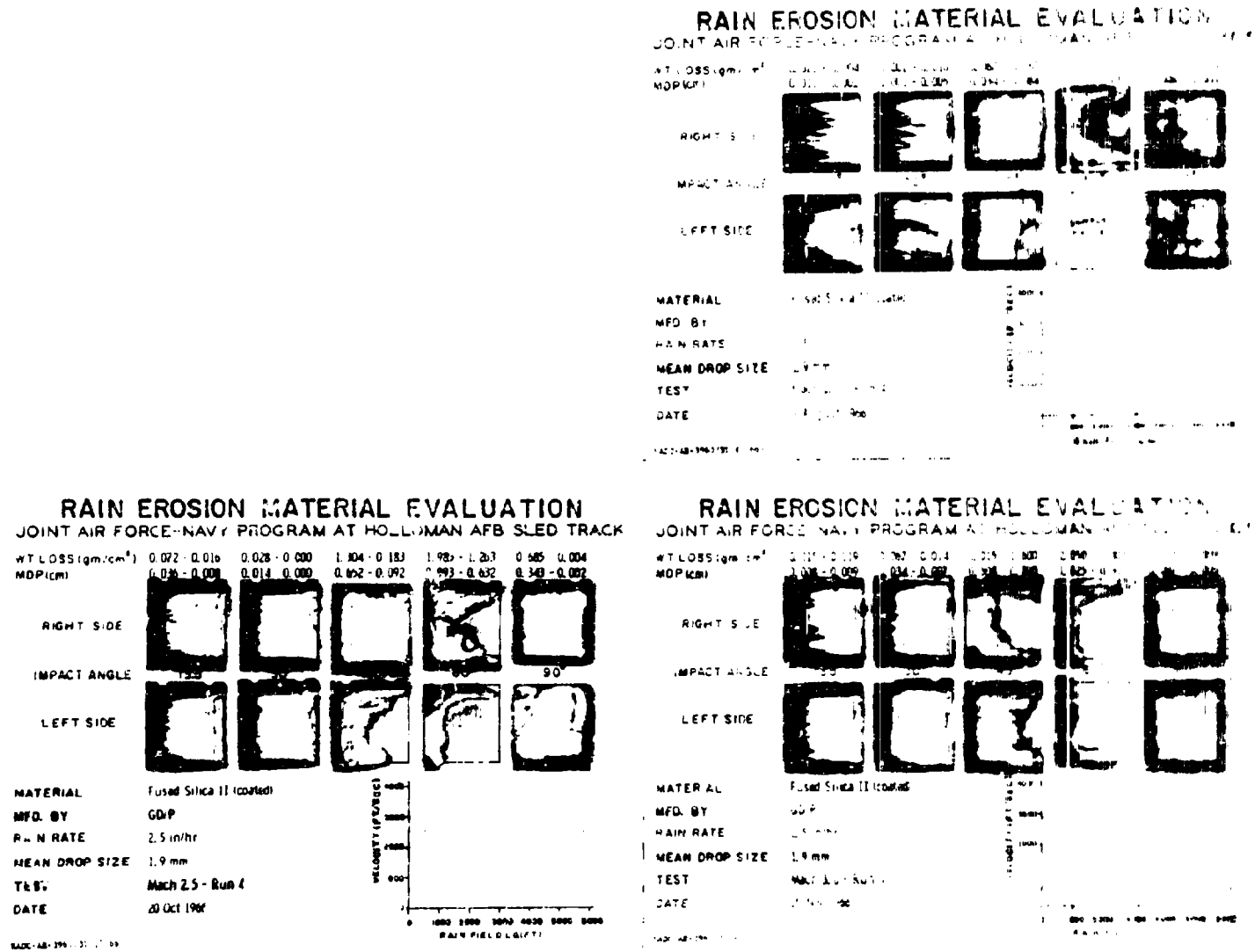

Figure 27. Rain Erosion Damage Data for GD/P Fused Silica (Type II)

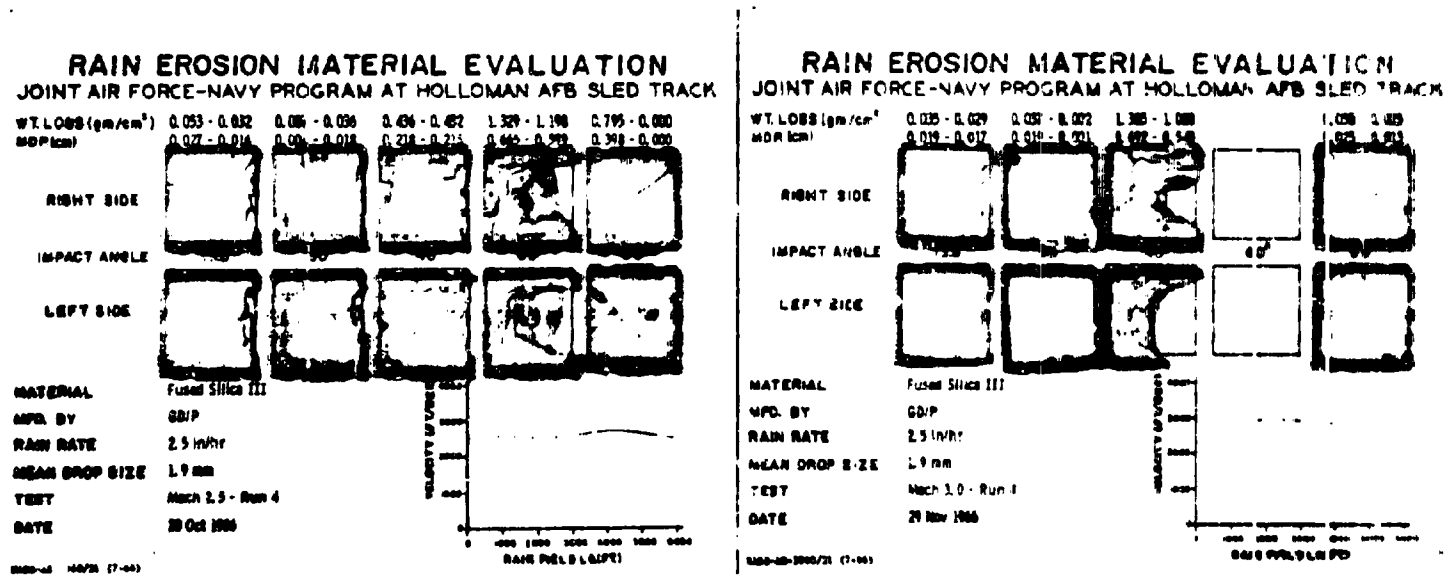

Figure 28. Rain Erosion Damage Data for GD/P Fused Silica (Type III)

[illegible] SANDWICH CERAMICS

[illegible]

The "A" sandwich aluminum oxide radome construction has been developed as a potential means of extending the thermal capability of aluminum oxide, for reduced radome weights, and for certain broadband applications. Practical electrical designs of wall constructions in this material necessitate relatively thin skins (0.020-0.040") and low dielectric cores for skin-core matching. The overall best compromise in achieving good electrical performance and satisfactory thermal shock resistance necessitates the use of about a 1 gm/cc foamed core with a 4 gm/cc high density skin. This combination allows thermal fracture within the core rather than the skins under severe heating rates yet allows for reasonably high skin strengths.

Alumina "A" sandwich samples having 0.020 inch skins were supplied by the Brunswick Corporation for evaluation at all four Mach numbers. Two additional sets having 0.040 inch skins but with the same core density were furnished, one each from Brunswick and Narmco, for evaluation at Mach 1.5.

The fabrication technology for construction of small radomes by this method has been developed by several companies. Although there are certain disadvantages inherent within a ceramic sandwich construction, it should be considered as a manufacturing method which is achievable.

There are no significant erosion differences between the Materials B-1, B-2, and B-3 from two suppliers and constructed by different techniques. The same 0.040 inch skins and similar core densities of the two materials result in very similar damage [illegible]ted at Mach 1.5.

The B-2 alumina sandwich with a 1 gm/cc core density with 0.020 inch skins was evaluated between Mach 1.5 and 3.0. Except for very low impact angles, this material was severely damaged at Mach 2.0 and above. The cause of failure of these composites is the low compression strength of the core material allowing impact failure of the thin outer skin. Weight losses for these materials are not conveniently presentable in graphical or equation form.

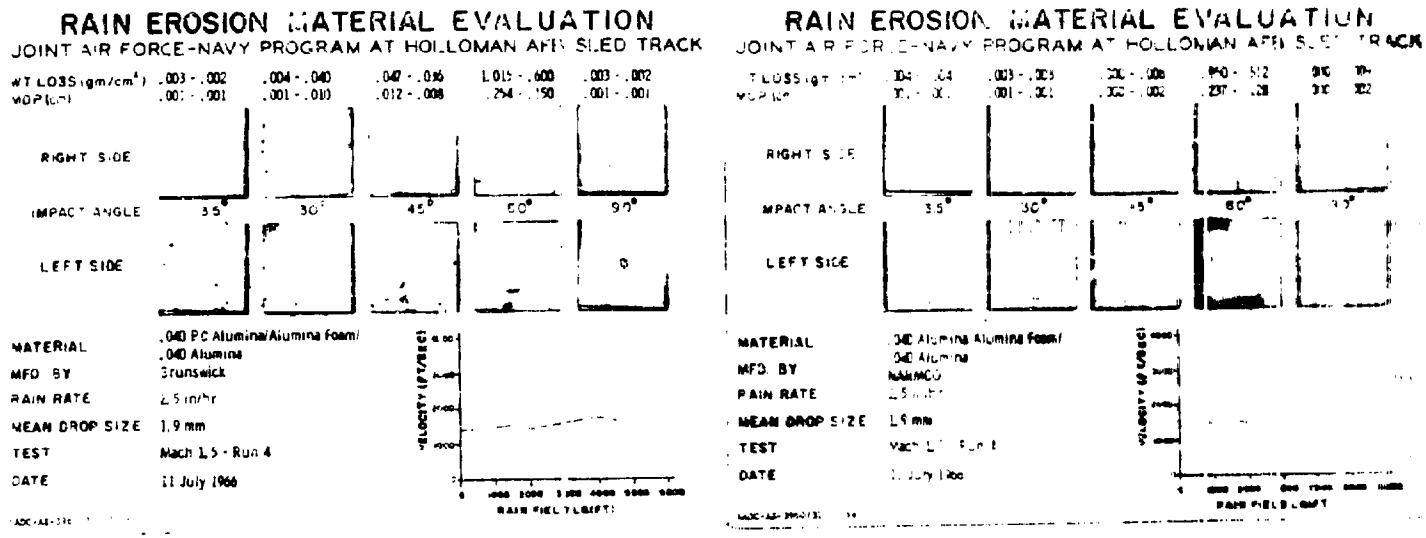

Figure 29. Rain Erosion Damage Data for 0.040 Inch Alumina/Alumina Foam/ 0.040 Inch Alumina

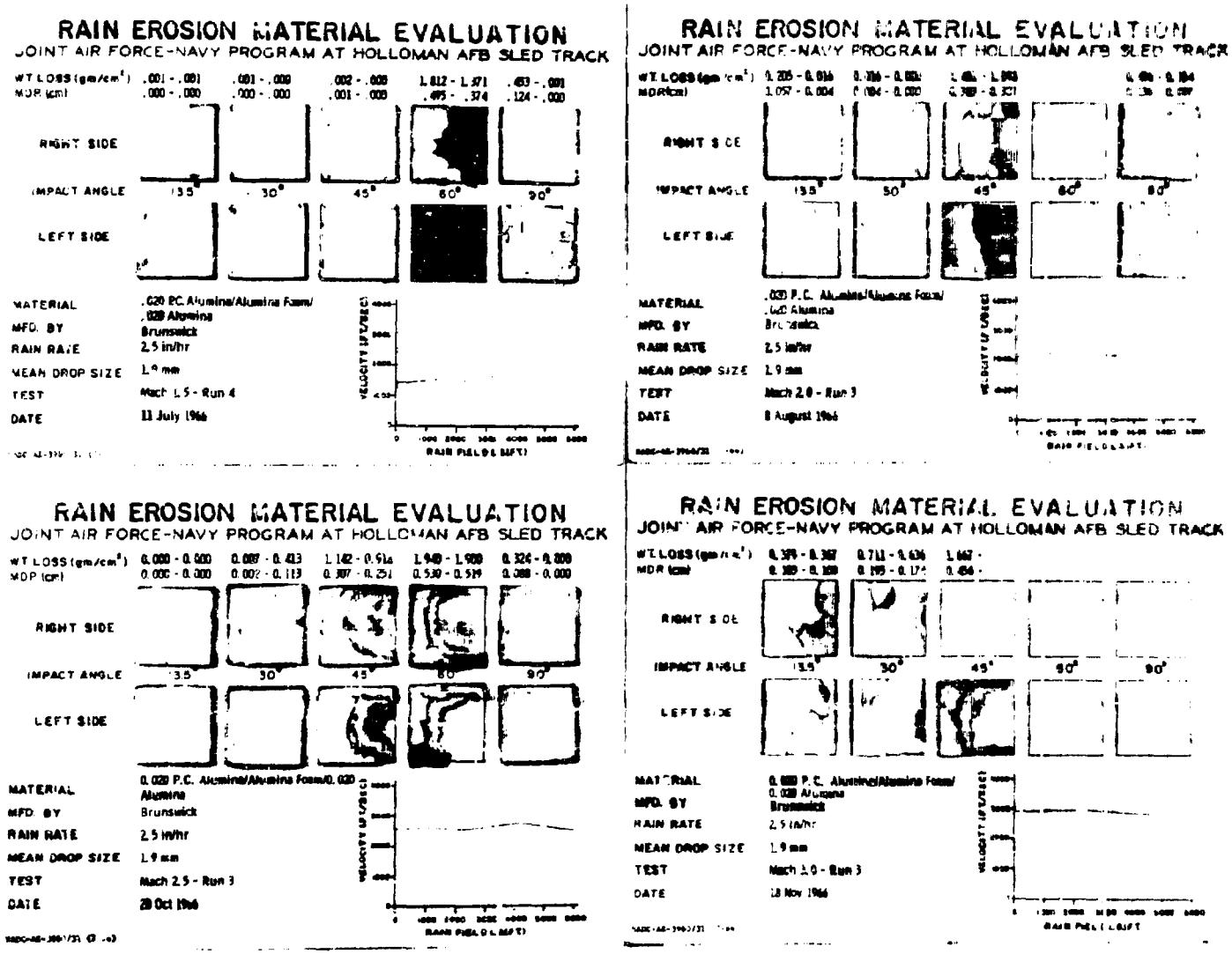

Figure 30. Rain Erosion Damage Data for 0.020 Inch Alumina/Alumina Foam/ 0.020 Inch Alumina

3. CLASS C - PLASTIC LAMINATES

C-1 Polybenzimidazole (PBI) Laminate

Several high temperature resins are being considered for laminate applications in the 600°F range and polybenzimidazole is one. These laminates are processed from preimpregnated sheets of glass cloth which contain a prepolymer of the benzimidazole. By a combination of various catalysts, high temperature and moderate pressure, the prepreg sheets are formed into laminates. A post cure of several hundred degrees Fahrenheit is normally employed to fully develop properties of the finished laminate. A dark brown color is characteristic of the cured laminate. Poor wetting of the glass cloth by the polybenzimidazole resin results in laminates which are dry; i. e., not rich in resin. These laminates typically possess 10 to 20% porosity with excellent flexural and tensile strengths. The PBI (Imidite) laminate specimens were furnished by Narmco R and D Division of the Whittaker Corporation.

The PBI laminates were evaluated at velocities from Mach 1.5 to Mach 3.0 with increasing erosion as the speed increased. Erosion of these laminates was found to obey the high velocity-short exposure time equation developed in Section V-B. Figure 13 shows the mean depth of penetration rate as a function of the sine of the impact angle and the constants for this PBI material are summarized in Table VIII.

The erosion of the PBI laminate was more severe than that of the epoxy laminates, comparable to the polyimides and less severe than the silicone or inorganic laminates.

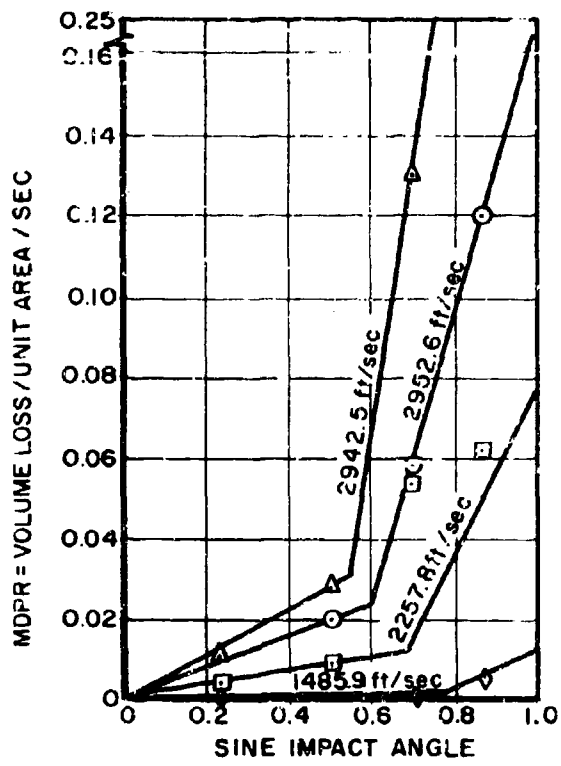

Figure 31. MDPR vs Sine Impact Angle - PBI (Imidite) Laminate

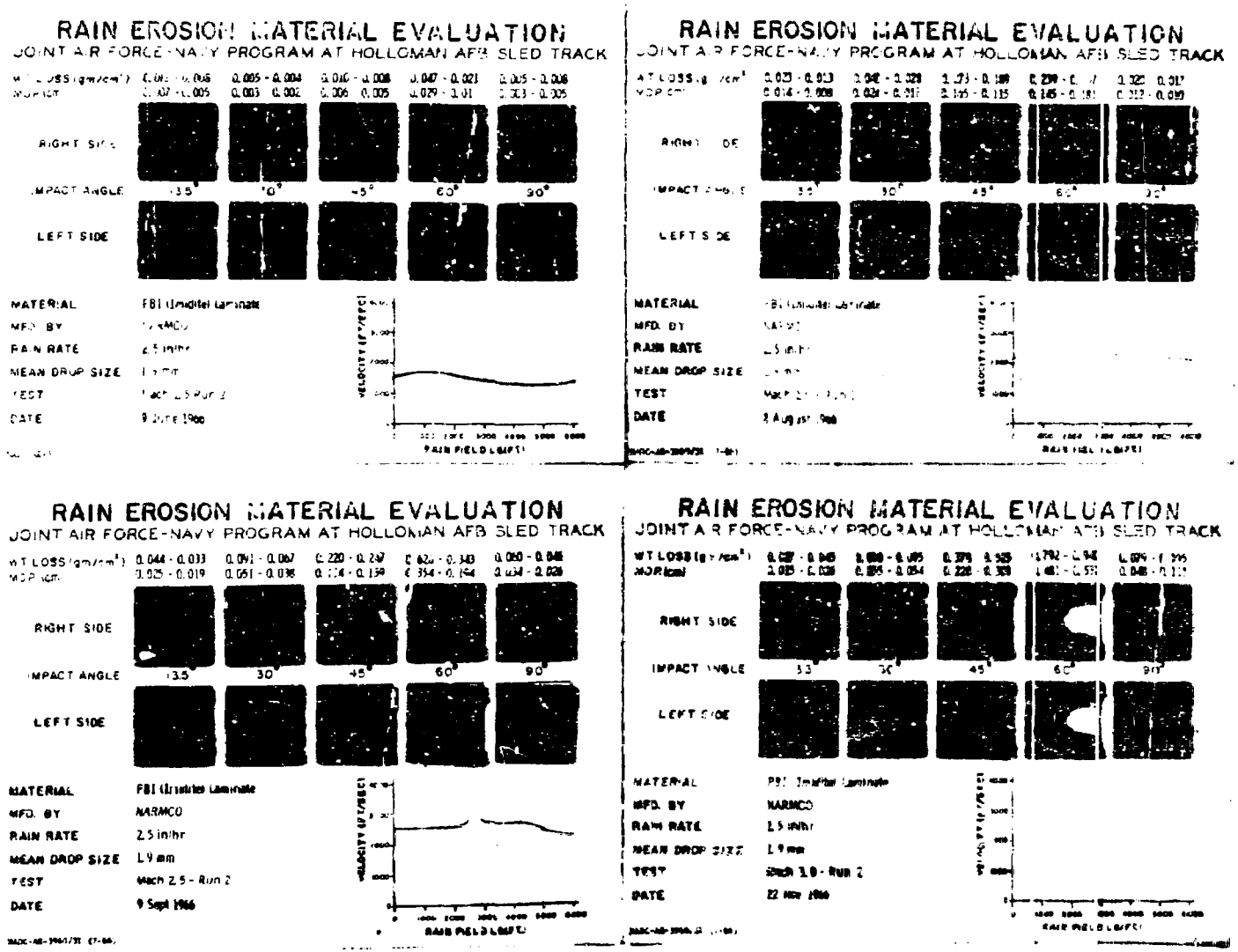

Figure 32. Rain Erosion Damage Data for PBI (Imidite) Laminate

C-2 Furane 8265 Epoxy Laminate

Epoxy resins are widely used for many applications and their utilization for radome laminates is extensive. Interest in higher use temperatures has prompted a number of companies to develop epoxies with good temperature capabilities. One such resin is the Furane 8265 epoxy of the Furane Plastics Company which, although dark brown in color, retains its structural properties for long periods up to 450°F.

Laminates can be prepared by conventional press techniques with zero porosity and good flexural and compressive strengths. The loss tangent of this laminate is reasonably high at 0.019. The specimens which were evaluated in this series were provided by General Dynamics/Fort Worth Division.

The performance of the Furane laminate was outstanding at Mach 1.5 with no measurable erosion. As with the PBI laminate, erosion increased with increasing velocity and the erosion rate (MDPR) was found to vary directly with the normal component ($\sin\theta$) of the velocity of impact. The constants for Furane laminates are found in Table VIII and agreement with the equation was excellent. The Furane epoxy laminate along with the Epon 828 epoxy had the best erosion resistance of the uncoated laminates evaluated.

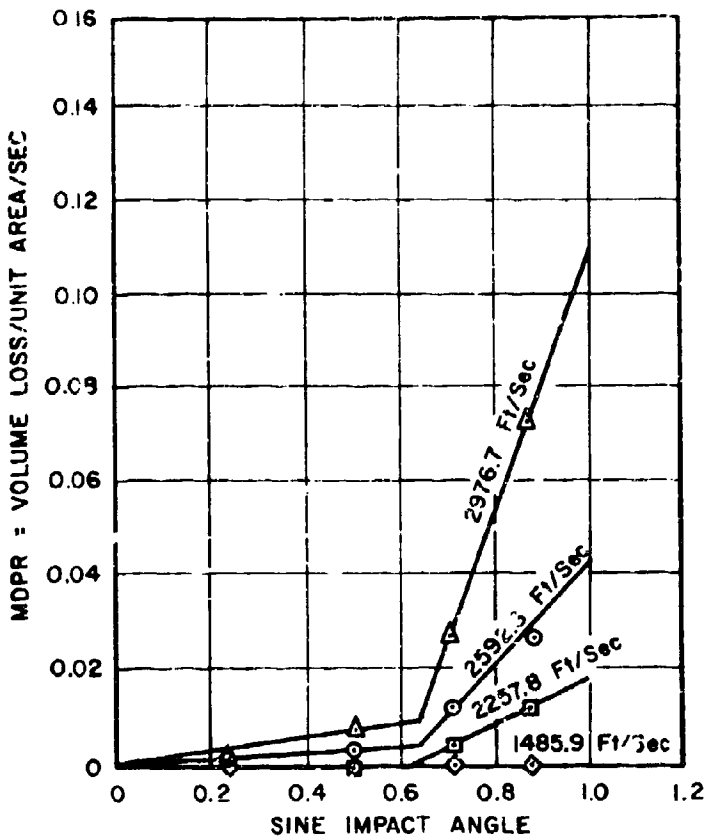

Figure 33. MDPR vs Sine Impact Angle - Furane Epoxy Laminate

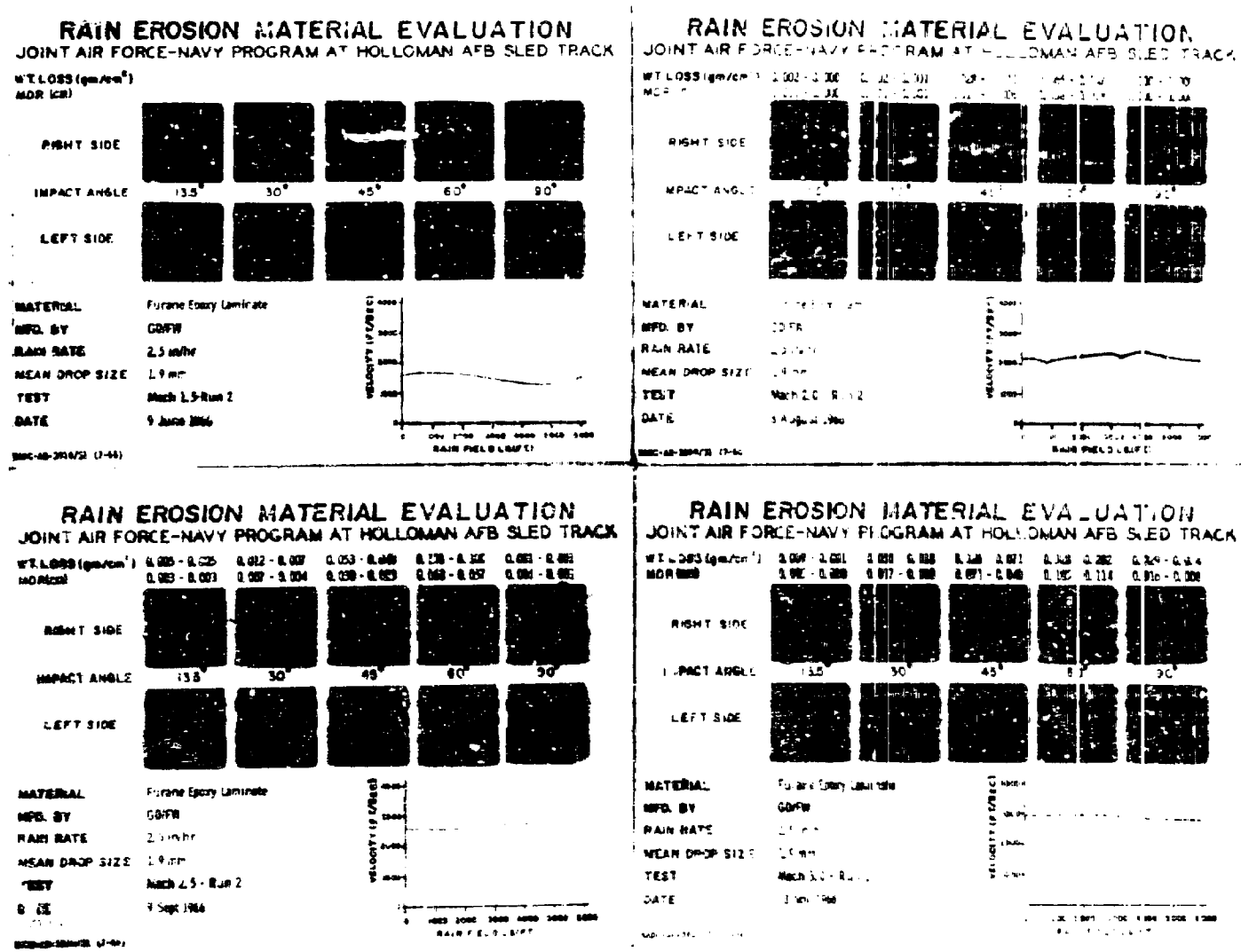

Figure 34. Rain Erosion Damage Data for Furane Epoxy Laminate

C-3 Epon 828 Epoxy Laminate

Perhaps the most widely used epoxy laminating resin is the Epon 828 resin of Shell Chemical Company. This epoxy is normally press formed with an amine catalyst to promote cure. Laminates of this epoxy are good to 450°F for up to 500 hours with retention of physical properties. Zero porosity, dark green laminates can be fabricated which have a density of 1.6 g/cm^3.

The Epon 838 laminate is so widely used that it was selected as standard substrate on which to evaluate elastomeric, ceramic and nickel coatings. All Epon 828 laminates were furnished by NAVAIRDEVCEN.

The uncoated Epon 828 laminate was second only to the Furane in resistance to rain impact. At Mach 1.5, there was only a trace of erosion in the 0° samples with all others untouched. At Mach 2.0 and 2.5 the erosion rate was comparable to the Furane epoxy. Agreement with the rain erosion equation was once again good and constants were derived (see Table VIII).

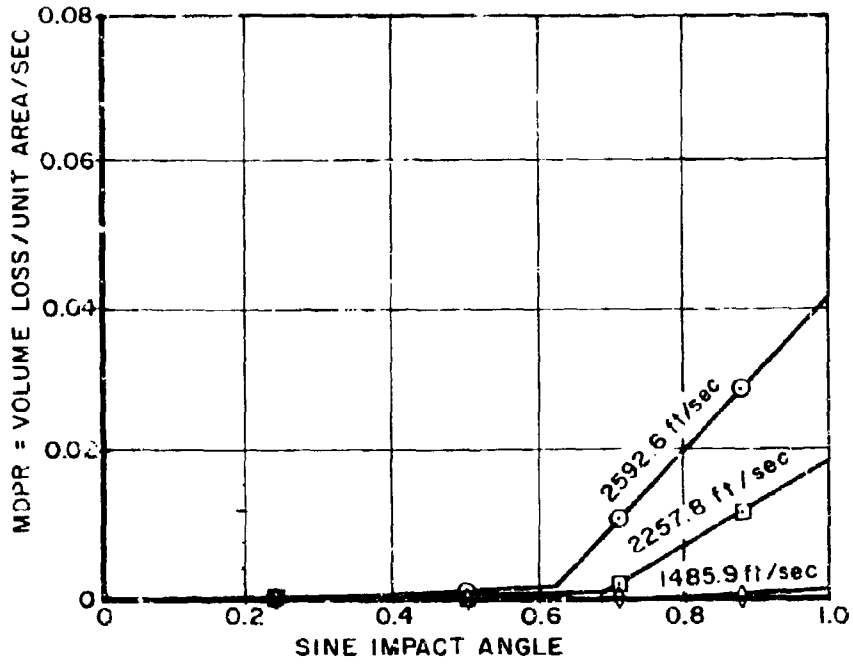

Figure 35. MDPR vs Sine Impact Angle - Epon 828 Epoxy Laminate

C-4 No Specimens

This number was assigned to an epoxy laminate with the upper plies loaded with alumina. However, fabrication difficulties forced its elimination from the program.

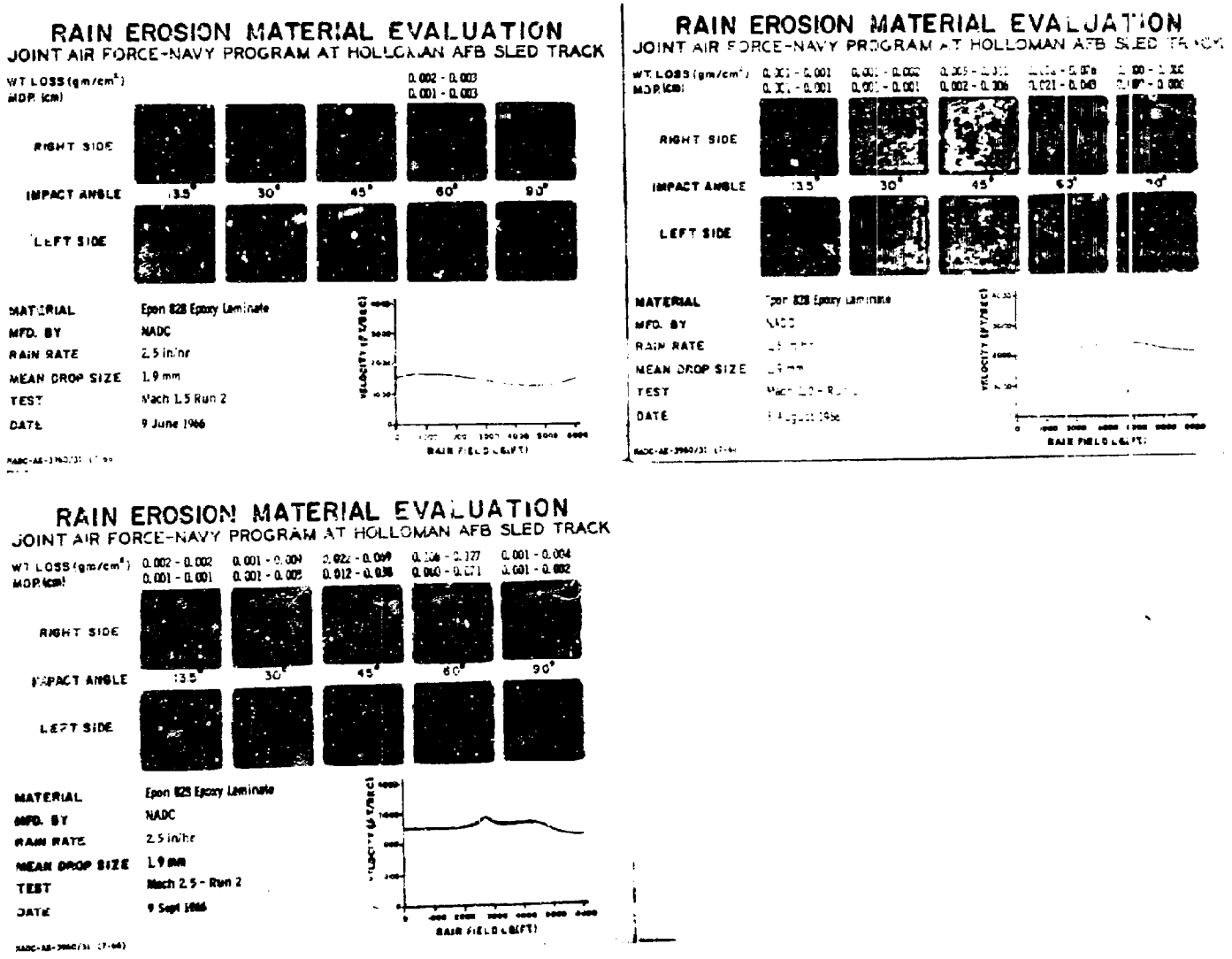

Figure 36. Rain Erosion Damage Data for Epon 828 Epoxy Laminate

C-5 Polyimide Laminate BMEC 1937 Sealer

The polyimide laminate is another 600°F plastic structural material being considered for supersonic transport (and advanced missile) applications. These laminates are fabricated using a prepreg cloth, high temperature and pressure cure and post cure. The polyimide laminate has better oxidative stability than the PBI laminate and hence retains its physical properties as well or better than the PBI although its initial physical properties are lower.

The polyimide resins resemble the PBI in dark brown color and poor wetting of the glass cloth. In order to overcome the porosity which results, a sealer such as a silicone resin to fill the pores is advantageous. The polyimide laminates with BMEC 1937 silicone sealer were supplied by Boeing/Airplane Division.

The data for the sealed polyimide laminate once again followed the rain erosion equation developed earlier. However the sealer inhibited the erosion of the laminate as compared to the uncoated polyimide laminate (Specimen C-6). At Mach 1.5 the sealer was partially removed on the 45° and 60° samples. This removal was considerably more pronounced at Mach 2.0 but there was little or no damage to the laminate itself. Constants for this material in the rain erosion equation are located in Table VIII.

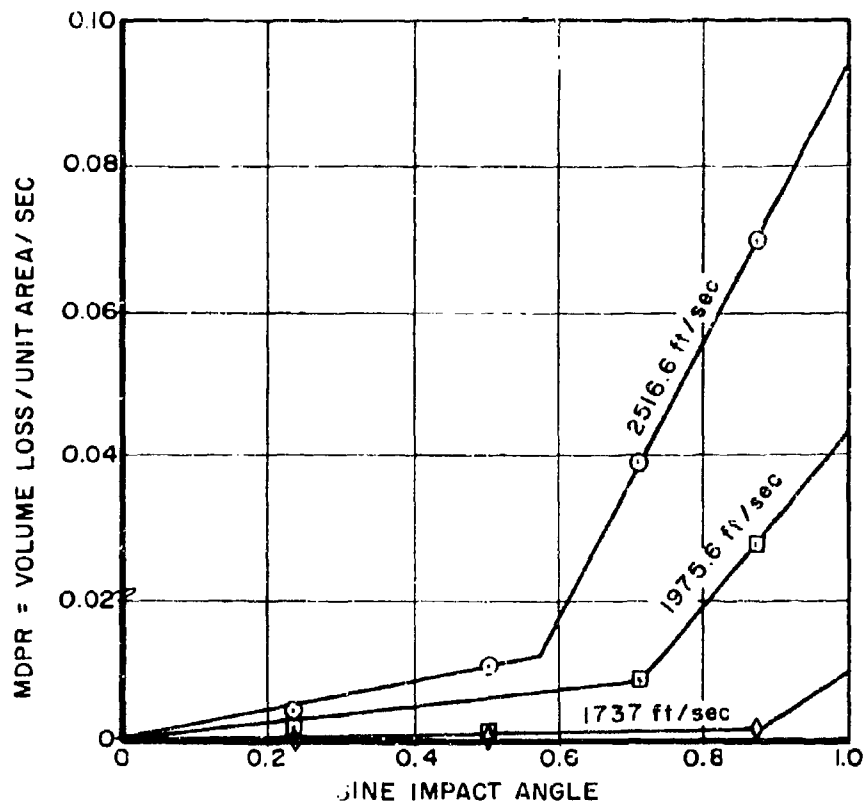

Figure 37. MDPR vs Sine Impact Angle — Polyimide Laminate BMEC 1937 Sealer

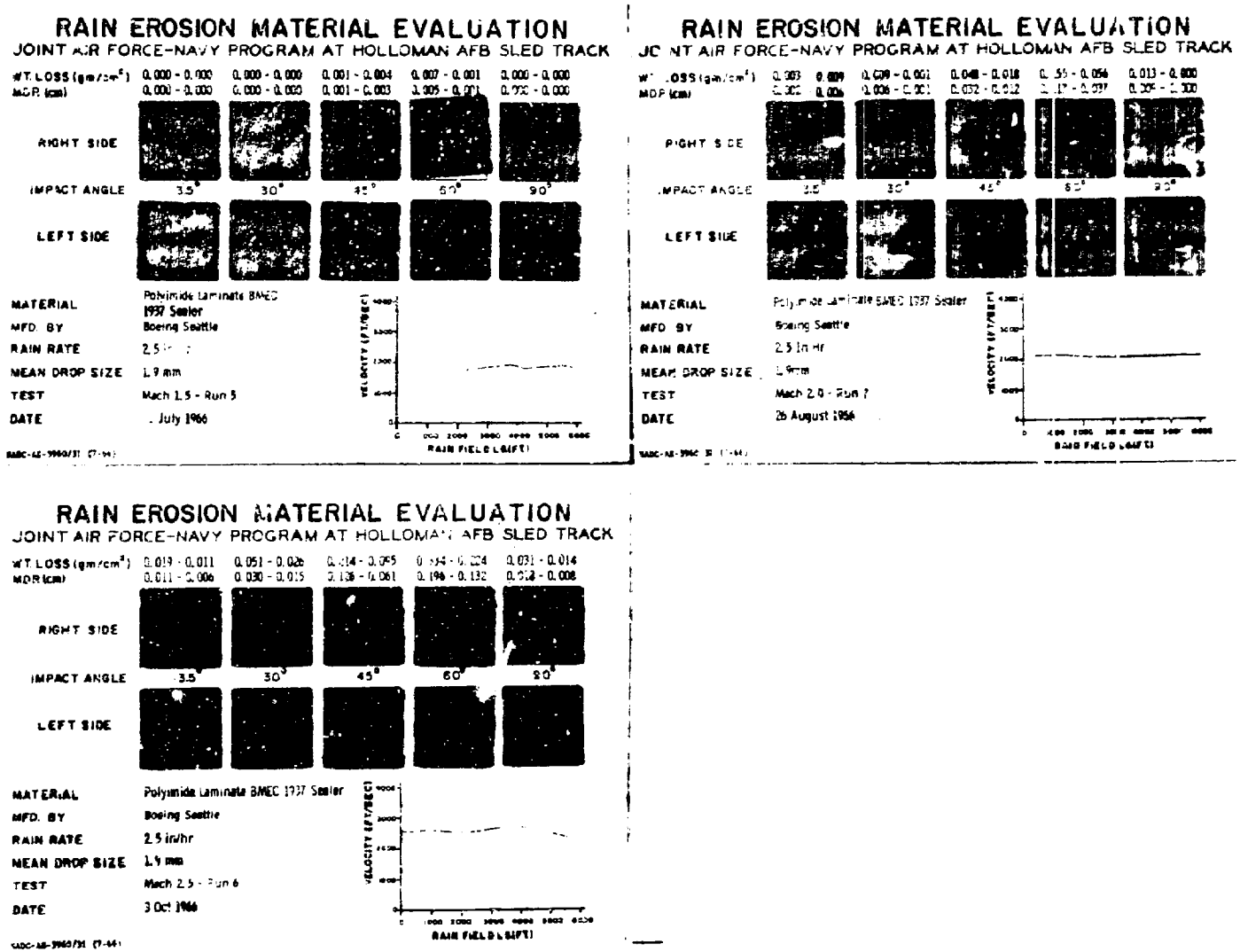

Figure 38. Rain Erosion Damage Data for Polyimide Laminate BMEC 1937 Sealer

C-6 Polyimide Laminate (Uncoated)

Another advantage of the polyimide resin over the PBI is its processability. The laminates from polyimide are more easily fabricated using previously described techniques. A commercially available polyimide is Skyguard 700 of Monsanto. Laminates of this resin were prepared by Brunswick Corporation with density of 1.7 g/cm^3, flexural strength of 60,000 psi and loss tangent of 0.015. These laminates still appeared dry, not as rich in resin as the epoxies, but richer than the PBI.

The erosion of the uncoated polyimide laminate falls between that of the PBI laminate and the sealed polyimide in severity. The damage was moderate at Mach 1.5 and increasingly severe at higher speeds. Constants were once more derived which fit the high velocity-short exposure time equation.

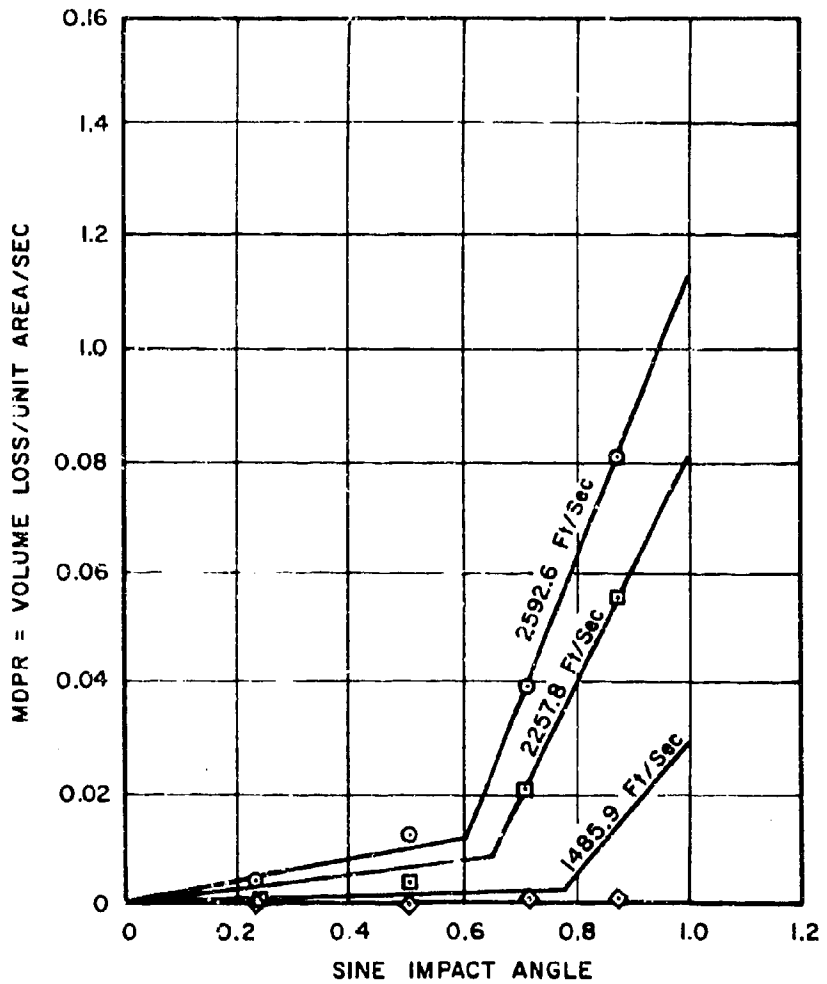

Figure 39. MDPR vs Sine Impact Angle - Polyimide Laminate - Skyguard 700

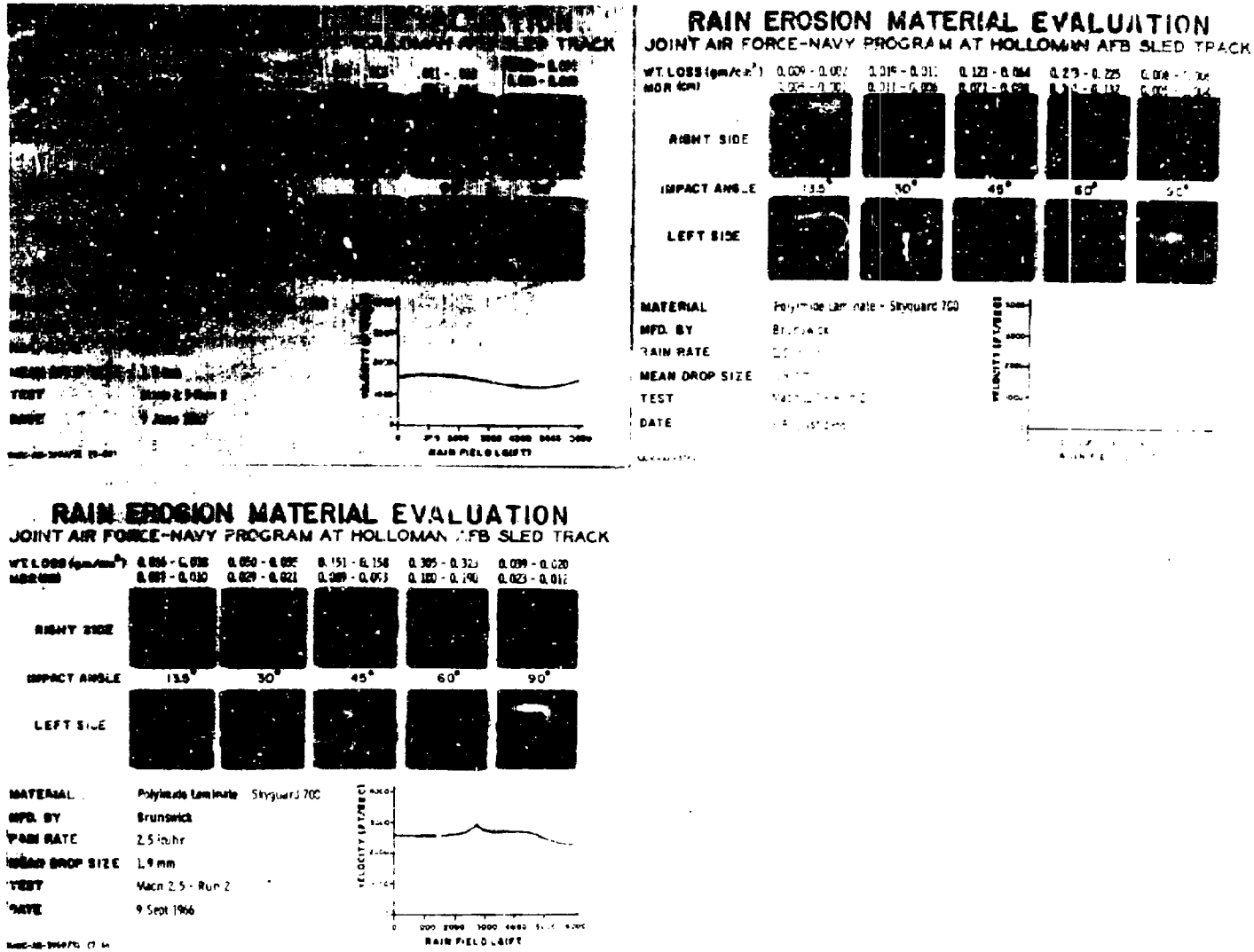

Figure 40. Rain Erosion Damage Data for Polyimide Laminate - Skyguard 700

C-7 Nomex Epoxy Laminate

The Nomex Nylon fabric is widely utilized in many laminate applications because of its fabricability. The Nomex impregnated with a Bakelite epoxy resin is being considered for some advanced missile applications. Although possessing low density (1.38), Nomex laminates have zero porosity and a light tan color. Specimens from Boeing/Aerospace Division were evaluated.

The erosion rates for the Nomex epoxy laminates were slightly greater than the Furane and Epon 828 epoxies at Mach 1.5 and 2.0. At Mach 2.5 the mean depth of penetration rate was still greater than the other epoxies but less than the high temperature plastic laminates (PBI, polyimide, and silicone). Constants for the Nomex laminate in the equation were determined. (See Table VIII.)

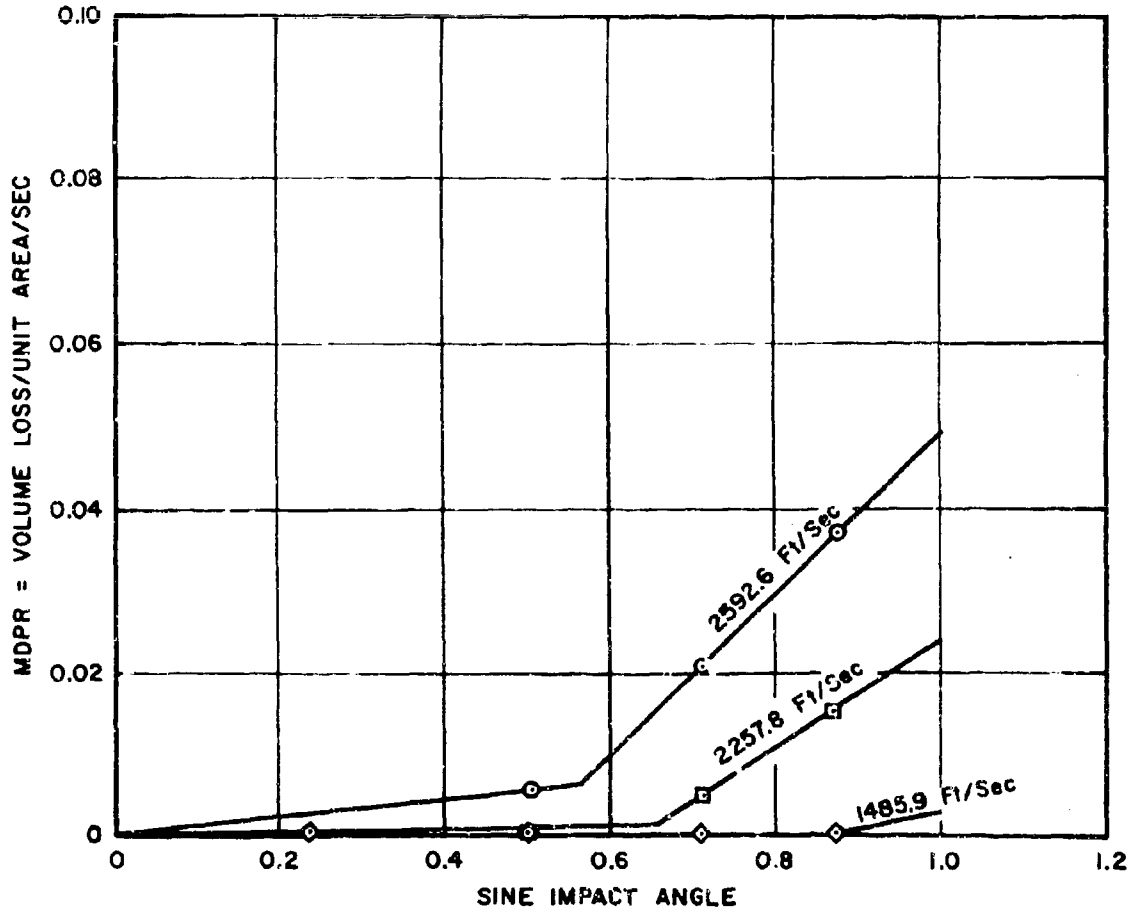

Figure 41. MDPR vs Sine Impact Angle - Nomex Epoxy Laminate

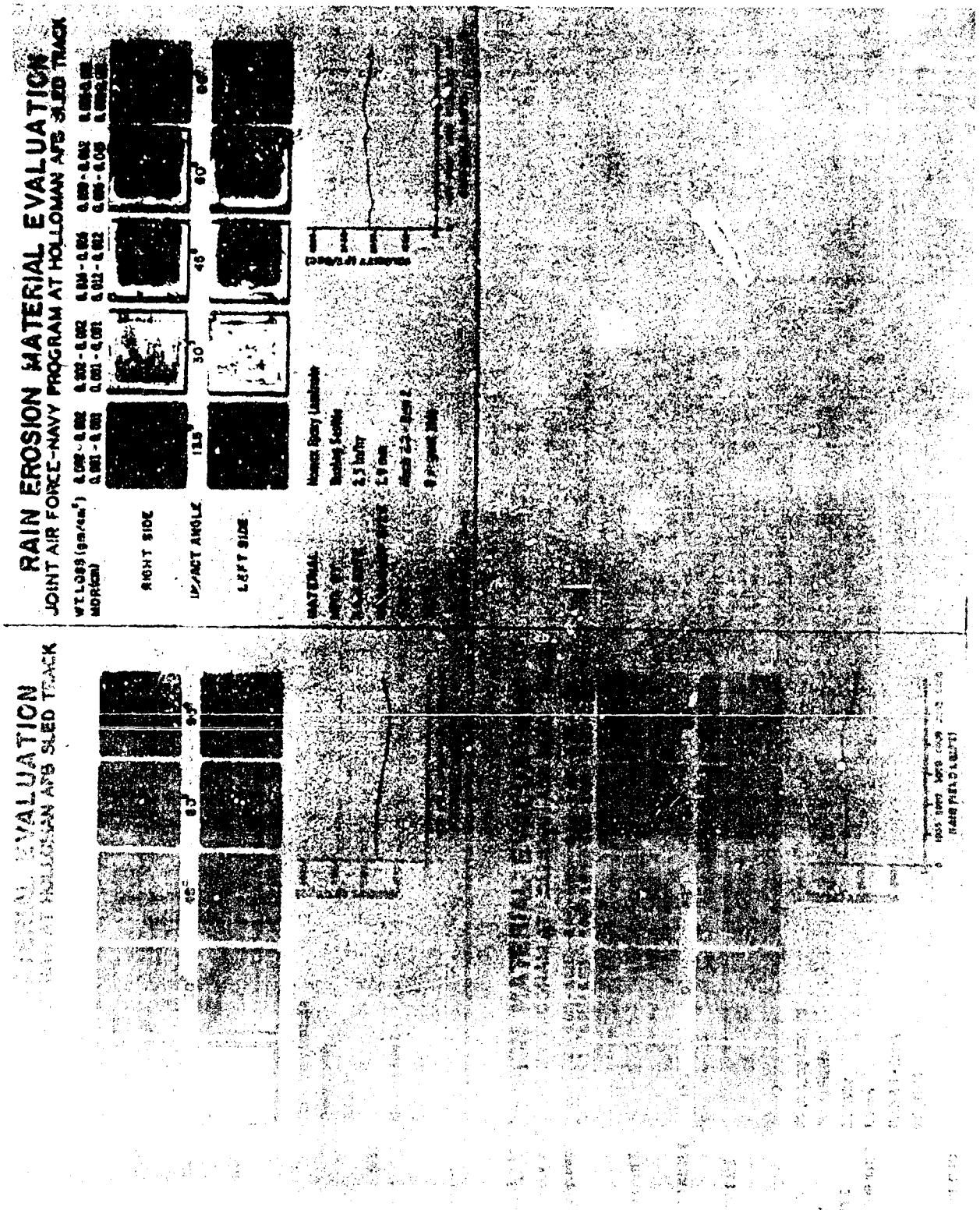

Figure 42. Rain Erosion Damage Data for Nomex Epoxy Laminate

Best Available Copy

C-8 DC 2106 Silicone Laminate

Silicone resins for laminating purposes have not been too widely employed but the most extensively used is the Dow Corning DC-2106 silicone. A set of specimens provided by NAVAIRDEVCEN was evaluated at Mach 1.5 only and erosion resistance was the poorest for any plastic laminate evaluated. Specimens even at 30° were moderately eroded at Mach 1.5 and this was not noted on any other plastic laminates at this speed.

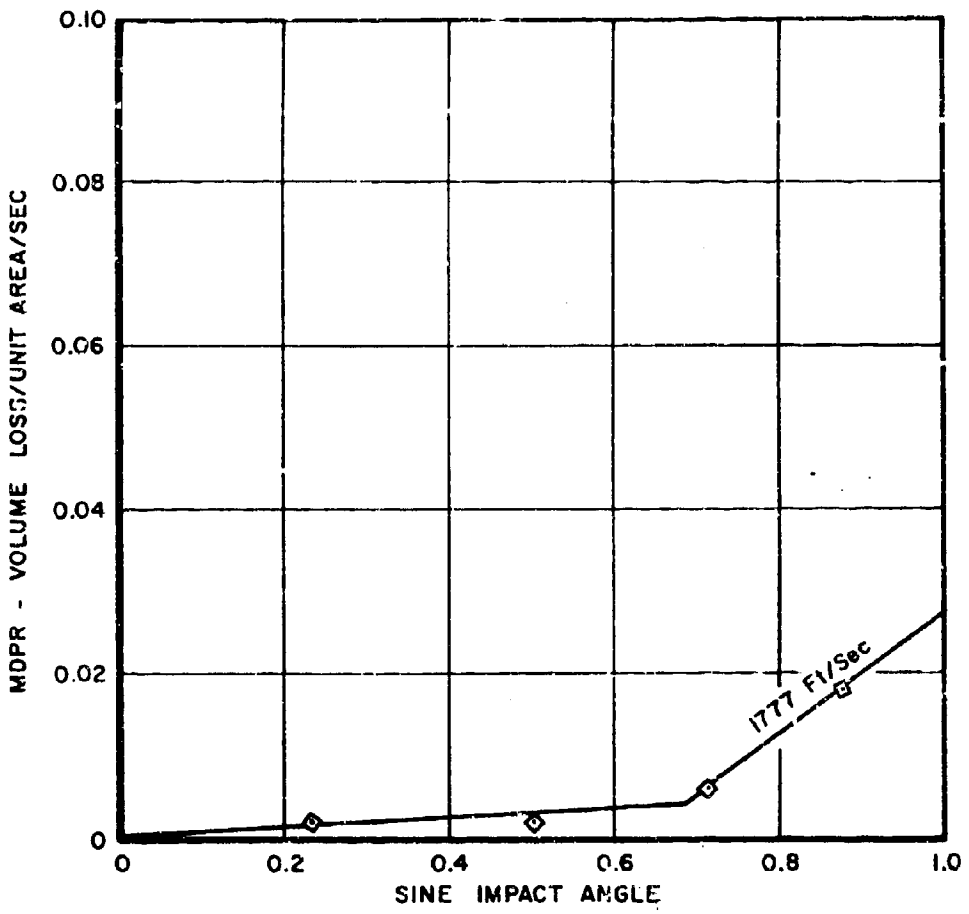

Figure 43. MDPR vs Sine Impact Angle - DC 2106 Silicone Laminate

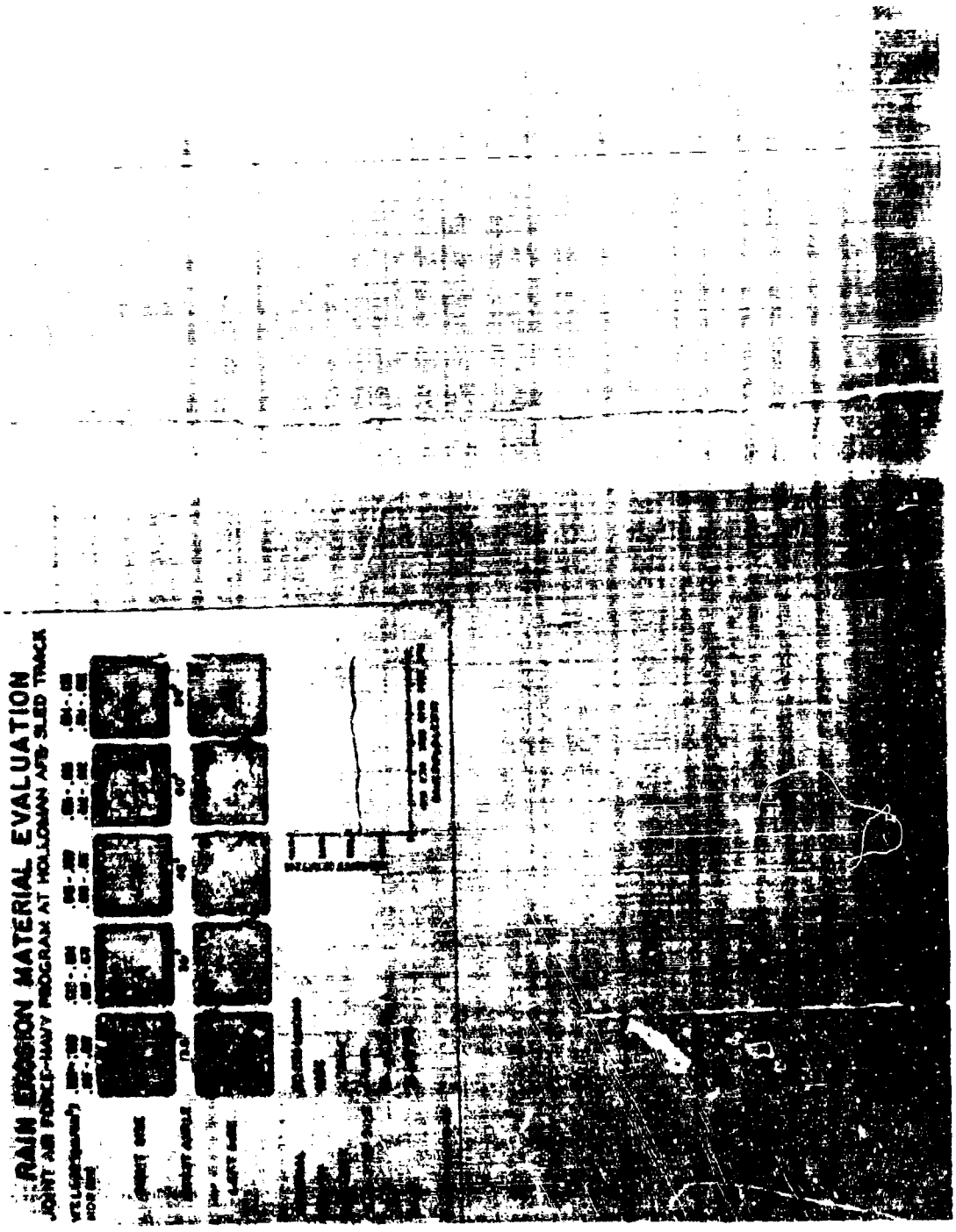

Figure 44. Rain Erosion Damage Data for DC 2106 Silicone Laminate

4. CLASS D - INORGANIC LAMINATES

D-1 Filament Wound Alumina-Silica/S Glass

The inorganic laminates are of interest because of their very high temperature capabilities (up to 1000°F). These laminates are processed in much the same way as the plastic laminates except an inorganic impregnating binder is used. One such structural material is continuous filament wound S-glass laminate in which the binder is an alumina-silica mixture. The laminates prepared from this combination are cured at high temperature but are poorly formed and contain noticeable voids with a grainy, oriented surface. Lockheed Company, Missiles and Space Division provided samples for evaluation.

Of all laminated construction examined in this program, the filament wound alumina-silica-S glass was eroded most severely. This is in part to be expected because the orientation of glass fibers introduced by the winding process would reduce the strength of the overall composite.

At Mach 1.5 damage was observed on the 60° specimens with only slight erosion at 45°. At Mach 2.0 and 2.5 the 60° specimens were completely gone after exposure, the 45° specimens were penetrated and the 30° and 90° samples damaged badly.

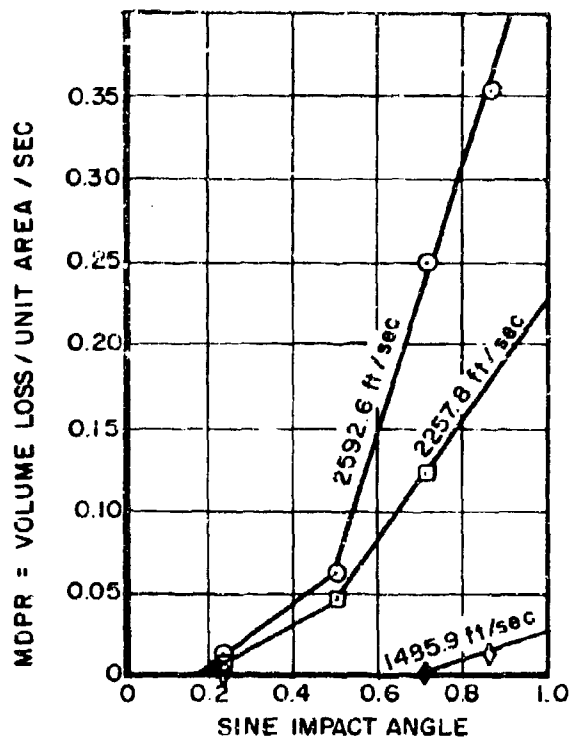

Figure 45. MDPR vs Sine Impact Angle - Filament Wound Alumina - Silica/S Glass Laminate

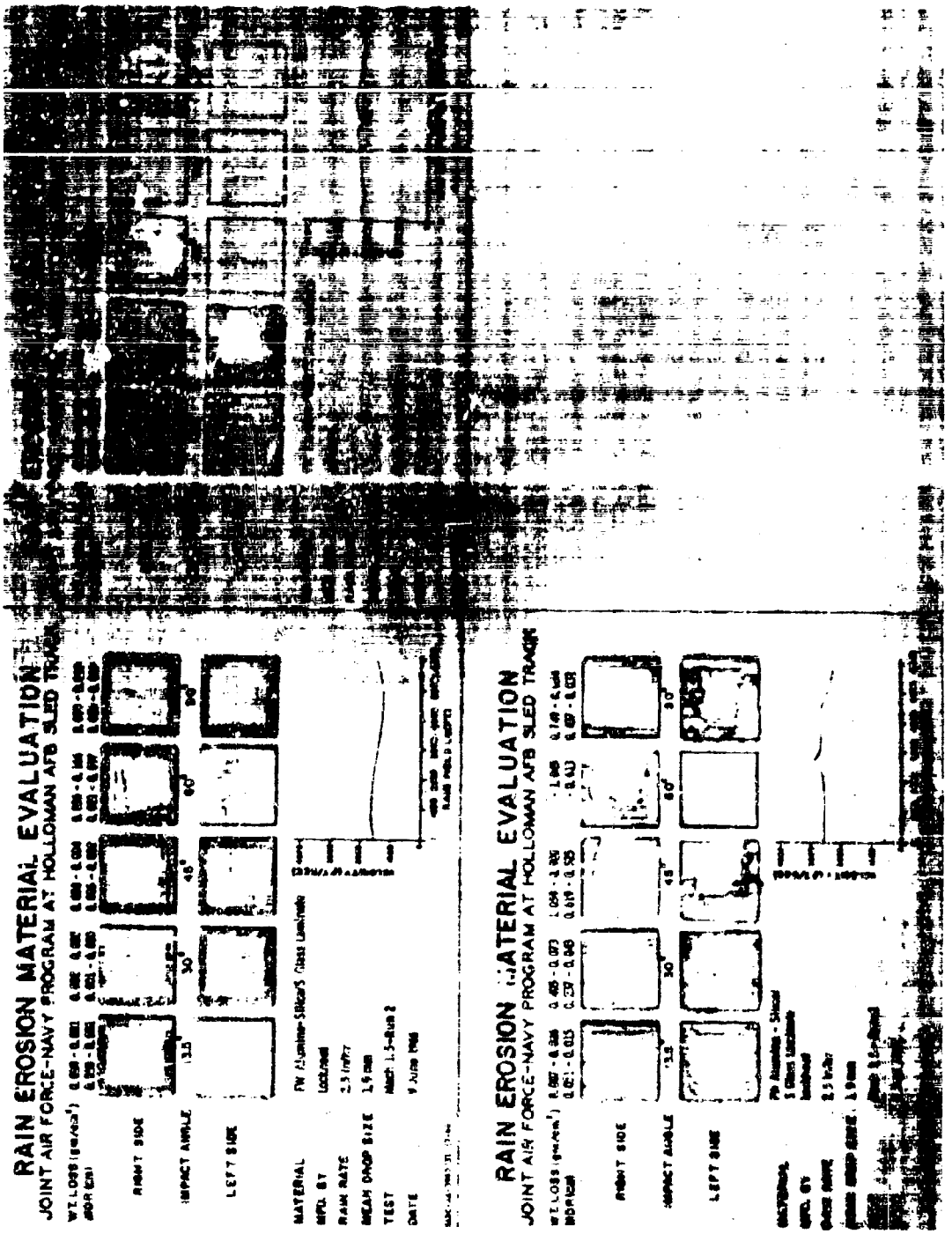

Figure 46. Rain Erosion Damage Data for Filament Wound Alumina - Silica 'S Glass Laminate

D-2 Aluminum Phosphate - S Glass Laminate

The aluminum phosphate - S glass laminate is another inorganic composition which has received wide consideration because of good thermal stability. This laminate is prepared from an acid solution which reacts with the glass cloth and then is fired to complete the cure.

The high porosity and low compressive strength of $AlPO_4$ laminates make them highly susceptible to rain erosion damage even subsonically. Specimens of aluminum phosphate-S glass were supplied by Brunswick Corporation.

Evaluations at Mach 1.5 indicated the $AlPO_4$ laminates to be comparable to the DC-2106 silicone at this velocity and slightly better than the alumina silica-S glass materials. At Mach 2.0 and above, the 60° samples were completely penetrated with the other positions showing progressively greater erosion at higher speeds. The rubber pads with which these materials were backed up were also eroded at the higher velocities after the phosphate was gone. It can be stated that the better wetting, higher physical properties and improved integrity of the plastic (organic and semi organic) laminates are essential for rain erosion resistance. It is the lack of these properties which are the weakness of inorganic laminates.

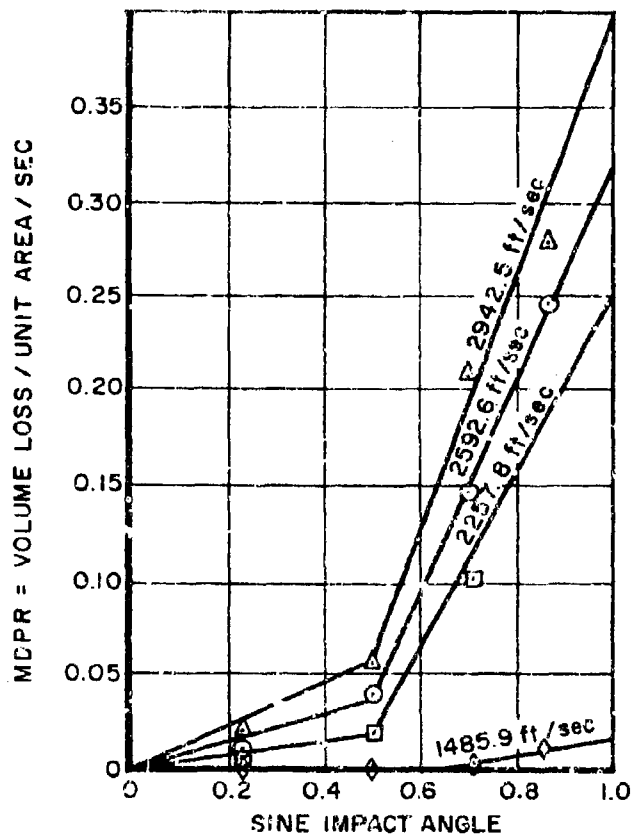

Figure 47. MDPR vs Sine Impact Angle - Aluminum Phosphate Laminate

Figure 48. Rain Erosion Damage Data for Aluminum Phosphate Laminate

5. CLASS E - CERAMIC-COATED LAMINATES

E-1 and E-15 Precast Alumina/$AlPO_4$ Laminate

The casting technique for depositing thin dense ceramic coatings is used for a number of materials including silica and alumina. The alumina is cast on a high temperature substrate and then sintered to densify it. For flat plates, thickness control is good but thin wall casting in radome shapes involves intricate metal molds.

The thin precast coatings are then bonded to the laminate substrate using an adhesive or the laminate may be laid up directly on the cast coating. The over-all protection of this system depends directly upon the quality of this adhesive bond. Further, as with thin ceramic coatings prepared by any technique, the modulus and strength of the substrate compared with the ceramic coating also has a significant effect on the erosion resistance of the entire system. These samples were submitted by the Brunswick Corporation.

The 0.020 inch thickness of precast alumina (Specimen E-1) was evaluated at all velocities, to Mach 3.0 with increasing erosion at higher speeds. Limited protection was afforded the aluminum phosphate at Mach 1.5; the coating was gone at 60° with minor damage to the laminate and the other positions were intact. At Mach 2.0 the laminate was more damaged at 60° but the other positions were only slightly damaged. The 60° samples at Mach 2.5 and 3.0 were completely penetrated through the laminate and the 45° specimens had the coatings removed.

An 0.040 inch thickness of precast alumina (Specimen E-15) over $AlPO_4$ was evaluated at Mach 2.5 only and showed similar performance to and slightly better protection than the 0.020 inch thickness. In general, the adhesive bond on these specimens was quite satisfactory with small pieces remaining on the laminate even after considerable erosion had occurred.

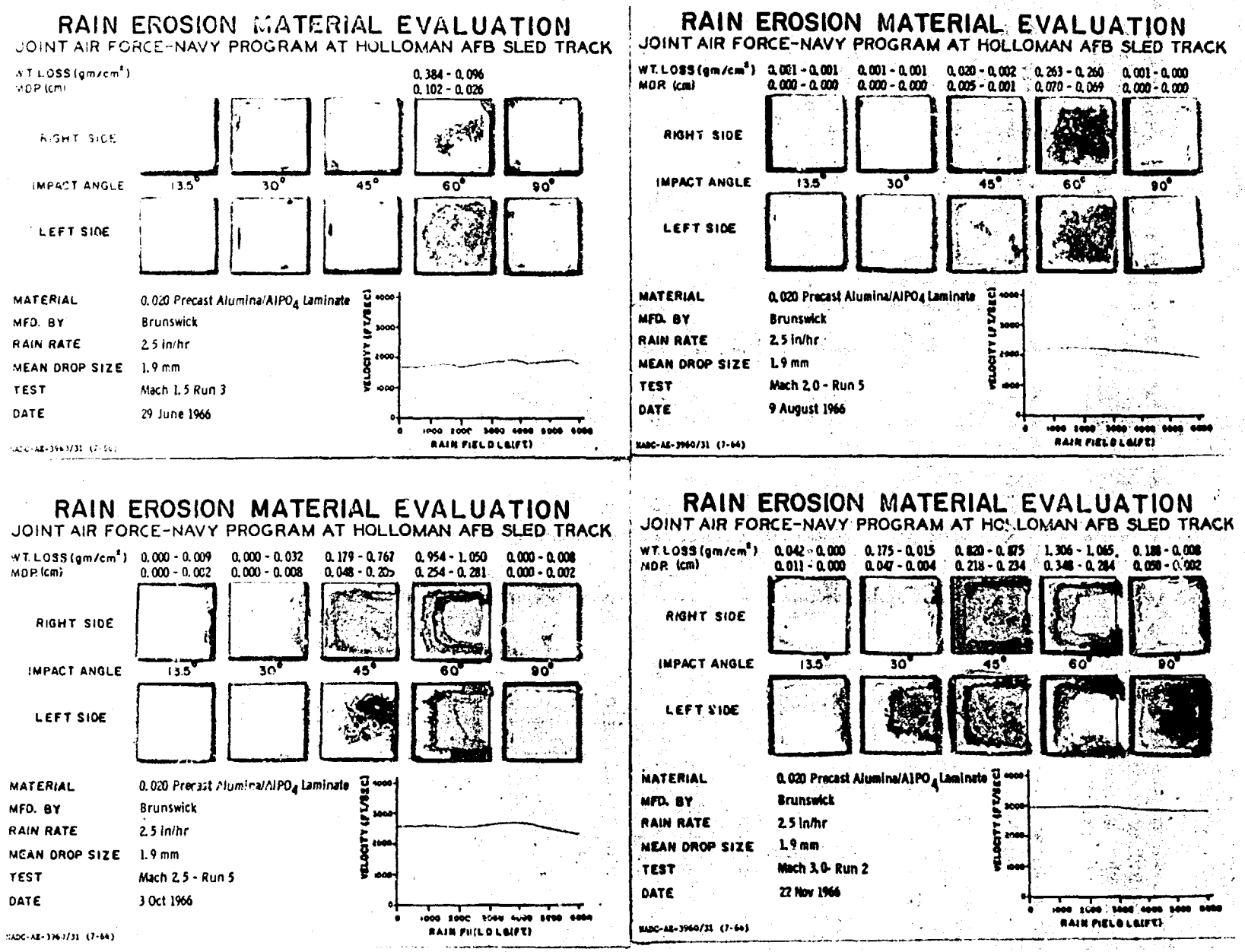

Figure 49. Rain Erosion Damage Data for 0.020 Inch Precast Alumina/$AlPO_4$ Laminate

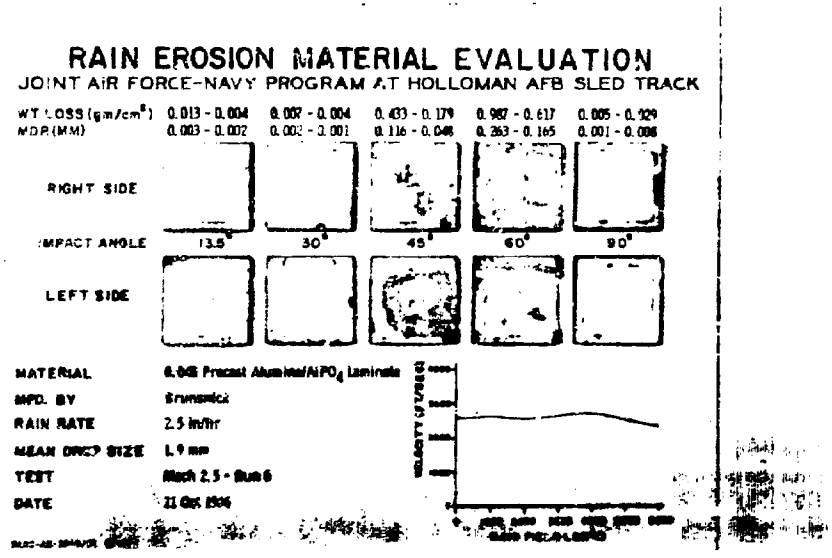

Figure 50. Rain Erosion Damage Data for 0.040 Inch Precast Alumina/$AlPO_4$ Laminate

E-2, E-3, E-4, E-11, E-12 Plasma-Sprayed Alumina Over $AlPO_4$, Silica-Alumina- S Glass or Polyimide

The plasma spraying technique is another method being widely employed for preparing thin, dense coatings of ceramics and metals. In this process, ceramic particles are injected into an electrically heated, very high temperature inert gas stream which melts and accelerates the particles so that upon impact with the substrate they deform and bond to the surface. The degree of melting of the particles depends on the particle diameter, density and thermal properties and the enthalpy of the gas stream. Not only can a number of materials be deposited on a number of substrates, but composite coatings of several materials can be applied simultaneously. The coating can be applied directly to a laminate substrate if it has high temperature capability or on a high temperature mold and the laminate laid up or secondarily bonded. The performance of these coatings is once again highly dependent upon the strength of the substrate. The plasma sprayed coatings over aluminum phosphate and polyimide were supplied by Brunswick and those over alumina-silica-quartz glass were furnished by Lockheed.

Two thicknesses (.020 inch and 0.040 inch) of plasma sprayed alumina over aluminum phosphate laminate were evaluated at all velocities to Mach 3.0. The aluminum phosphate was used because its high temperature stability enabled direct deposition of the alumina on the laminate. In general the plasma sprayed coatings were eroded more severely than the precast or flame sprayed coatings even at the 0.040 inch thickness. The thicker coating did yield more protection at Mach 1.5 and 2.0, but at Mach 2.5 and above this effect was negligible with little additional protection afforded by the extra thickness.

Plasma sprayed alumina over alumina-silica-quartz glass and polyimide laminates were evaluated at Mach 1.5 and 2.0 respectively. The alumina over alumina-silica-quartz glass exhibited the lowest erosion resistance of the plasma sprayed coating-substrate combinations. The alumina over polyimide performed better than the alumina over $AlPO_4$. Once again this erosion resistance can be tied directly to the substrate strength (polyimide stronger than $AlPO_4$ stronger than alumina-silica-quartz glass).

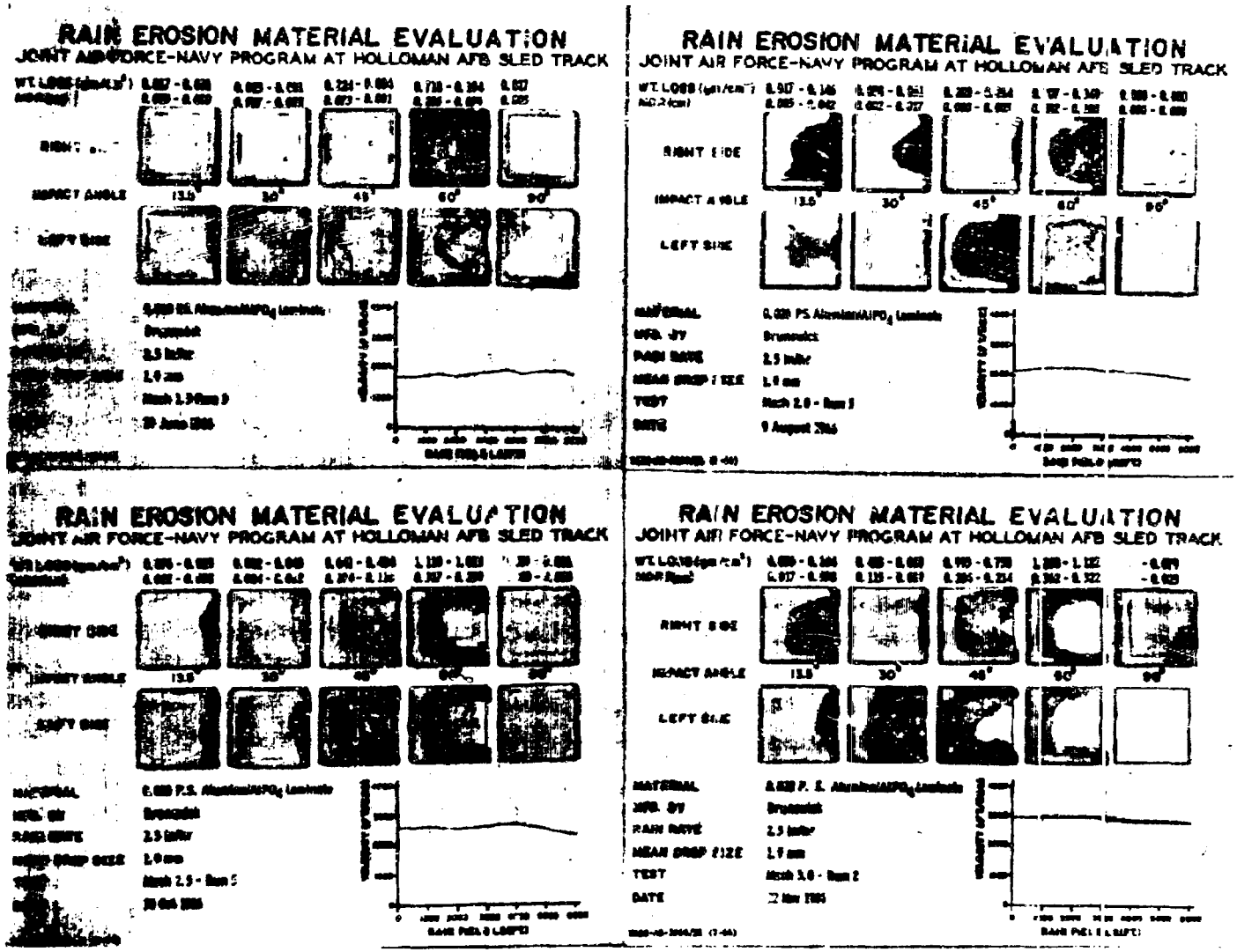

Figure 51. Rain Erosion Damage Data for 0.020 Inch PS Alumina/$AlPO_4$ Laminate

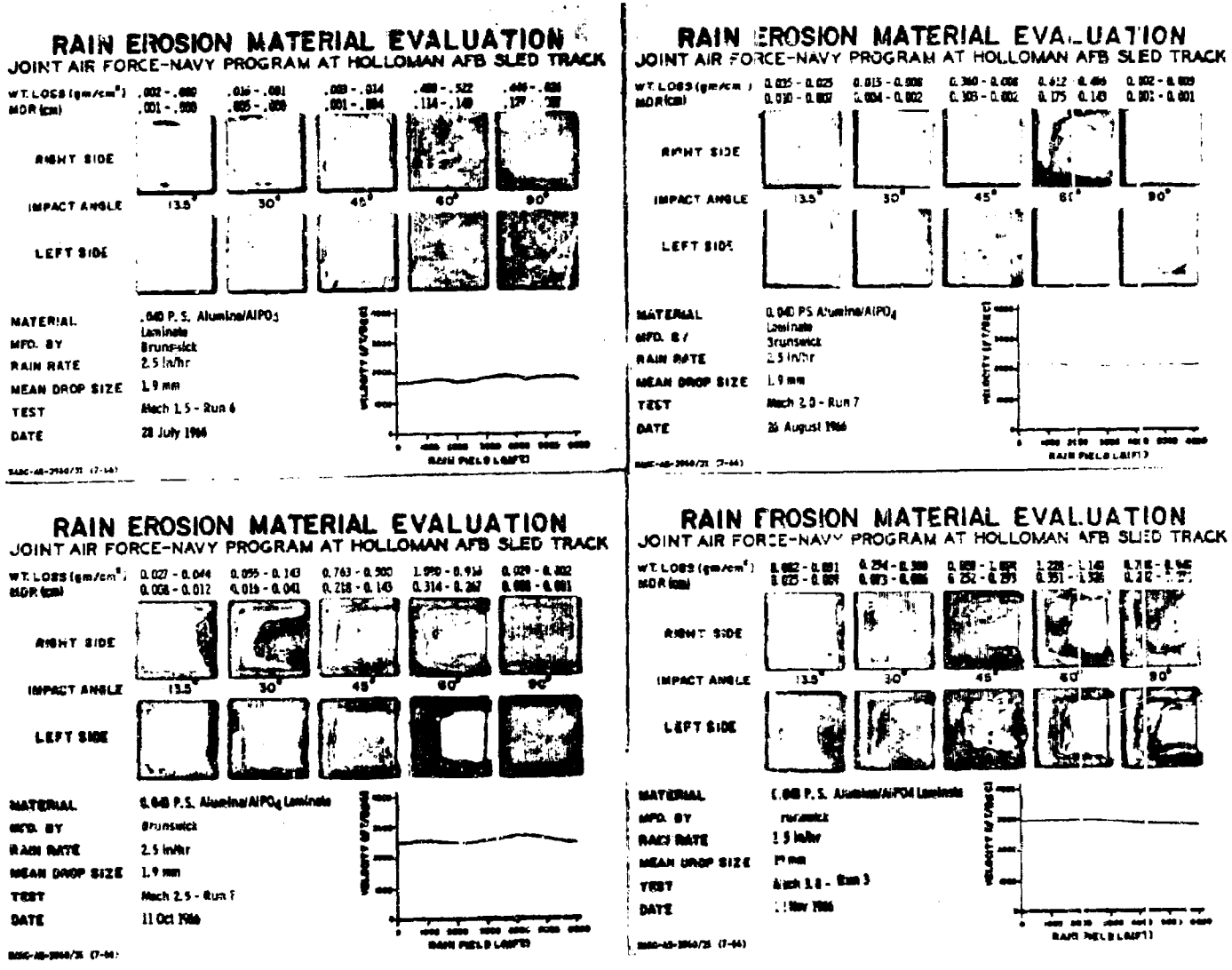

Figure 52. Rain Erosion Damage Data for 0.040 Inch PS Alumina/$AlPO_4$ Laminate

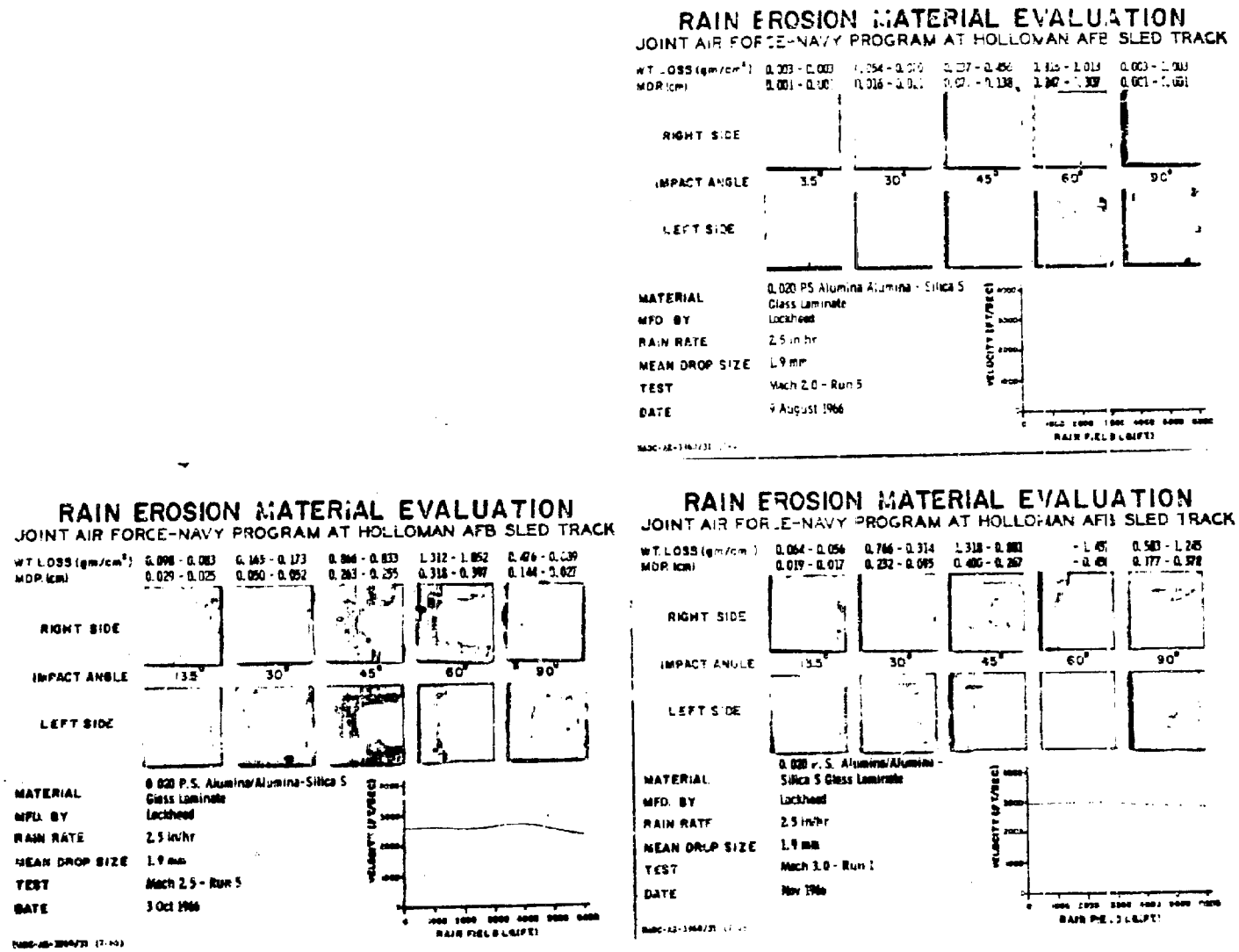

Figure 53. Rain Erosion Damage Data for 0.020 Inch PS Alumina/Alumina - Silica S Glass Laminate

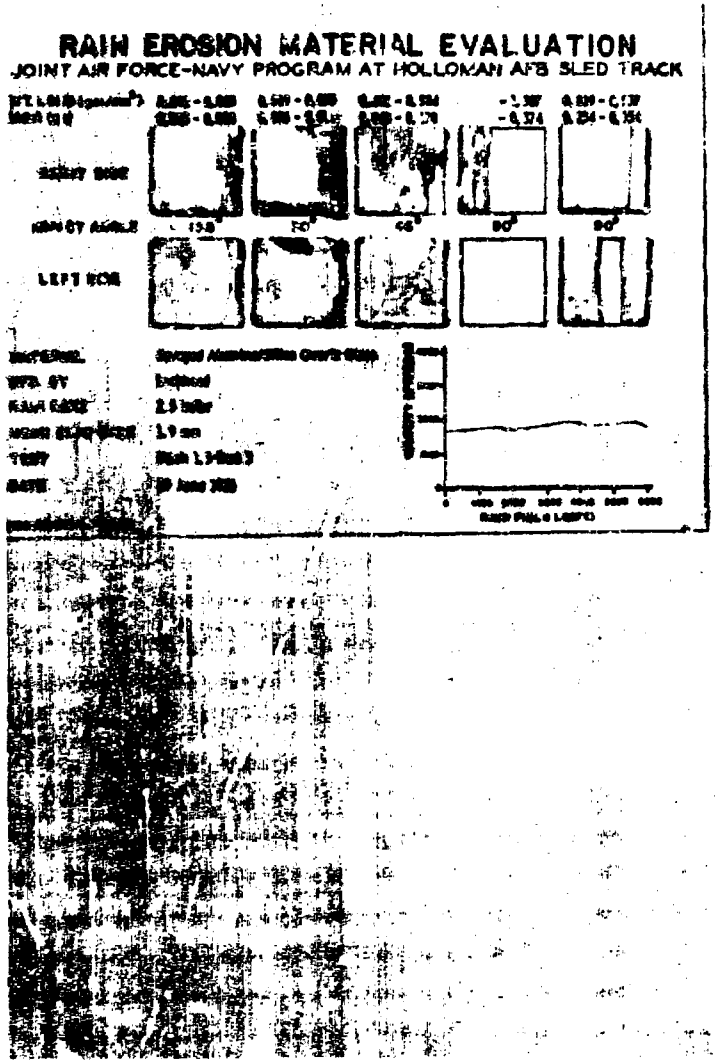

Figure 54. Rain Erosion Damage Data for Sprayed Alumina/Silica Quartz Glass

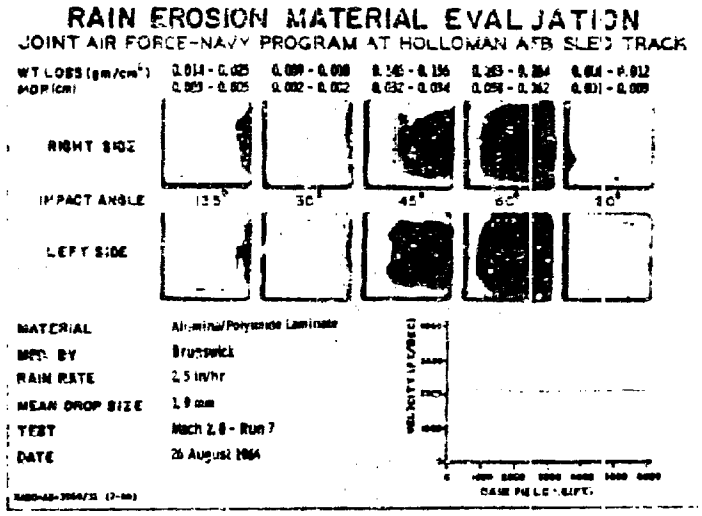

Figure 55. Rain Erosion Damage Data for Alumina/ Polyimide Laminate

E-5, E-6, E-9, E-10 Flame Sprayed Alumina Over PBI and Polyimide Laminates

The flame spraying of ceramic materials has been widely used for coatings on radomes, compressor blades and many industrial applications. In this technique which is similar to plasma spraying the spraying gas is oxidizing rather than inert and combustion of these gases produces the heat for melting the particles. Oxygen and acetylene are the fuel gases and the materials may be fed in the powder, wire, or rod form. The principal difference in the alumina coatings produced by these two methods is that the flame spraying produces alumina in the gamma form which is a crystalline, low density form while plasma spraying produces primarily alpha alumina, the high density phase. In the Rokide "A" process of flame spraying, the coating material is fed in the rod form. Once again combinations of materials to achieve specific compositions can be sprayed together. The flame sprayed alumina over PBI specimens were furnished by Narmco and the alumina over polyimide was supplied by Goodyear Aerospace Corporation.

Flame sprayed alumina coatings in two thicknesses over PBI laminates and with and without chromic oxide over polyimide laminates were evaluated up to Mach 3.0. The coatings over PBI were produced by powder spraying directly on the laminate. The chromic oxide addition to the alumina forms a eutectic with considerably improved properties and better strength. The coatings on polyimide were sprayed on a metal die using the Rokide "A" (rod) process and then the laminates were laid up afterward.

The flame sprayed coatings over PBI performed reasonably well in the rain; however, at 60° the coating was gone even at Mach 1.5. In these specimens the effect of coating thickness was less pronounced than with plasma sprayed coatings.

The Rokide "A" coatings with and without chromic oxide were comparable at all speeds and yielded better protection than the powder sprayed coatings or the plasma sprayed coatings (although this may be due to a better bond).

E-7 No Specimens

This number was originally assigned to a vapor deposited alumina coating over a PBI laminate. However, no specimens were obtainable for evaluation.

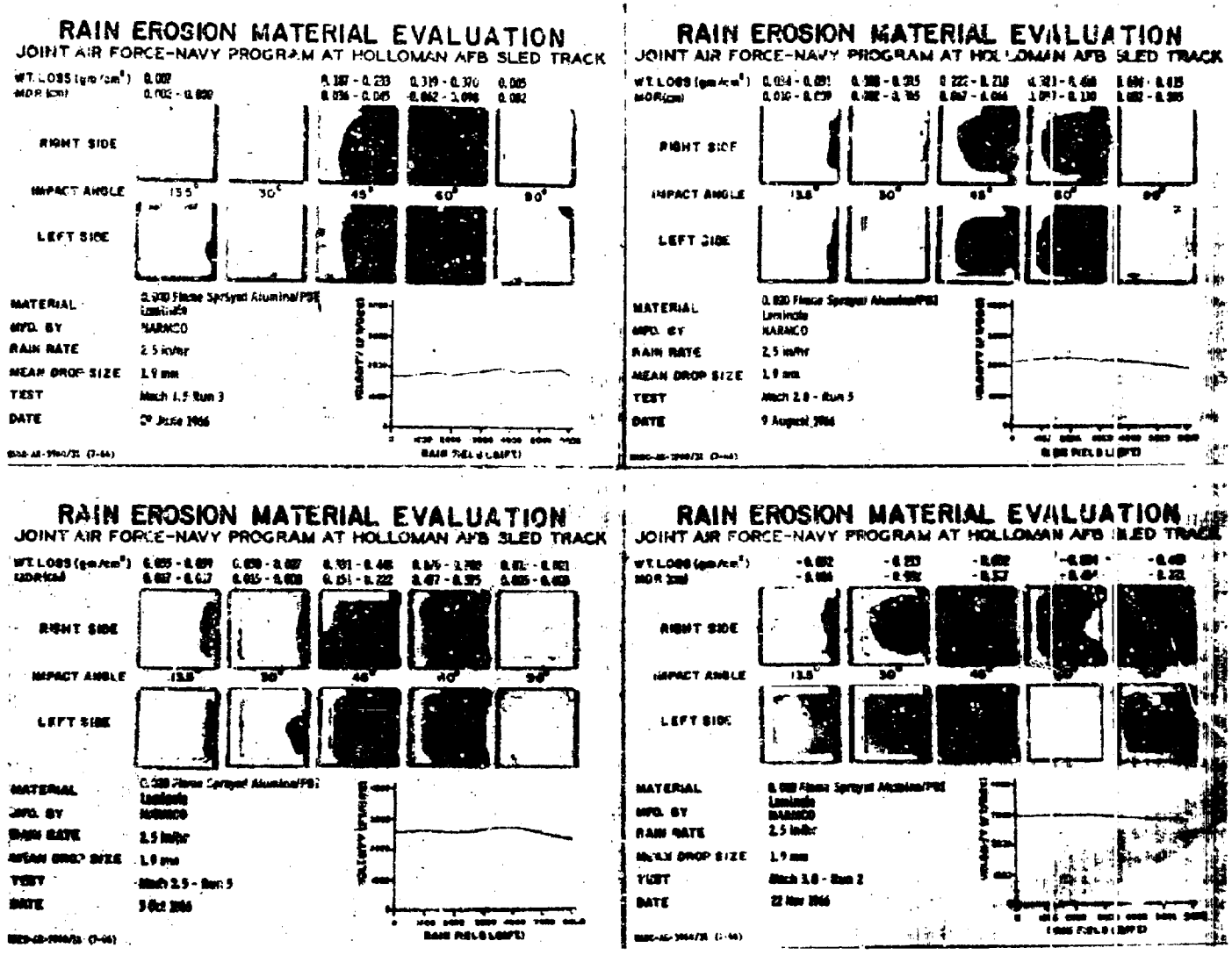

Figure 56. Rain Erosion Damage Data for 0.020 Inch Flame Sprayed Alumina/FBI Laminate

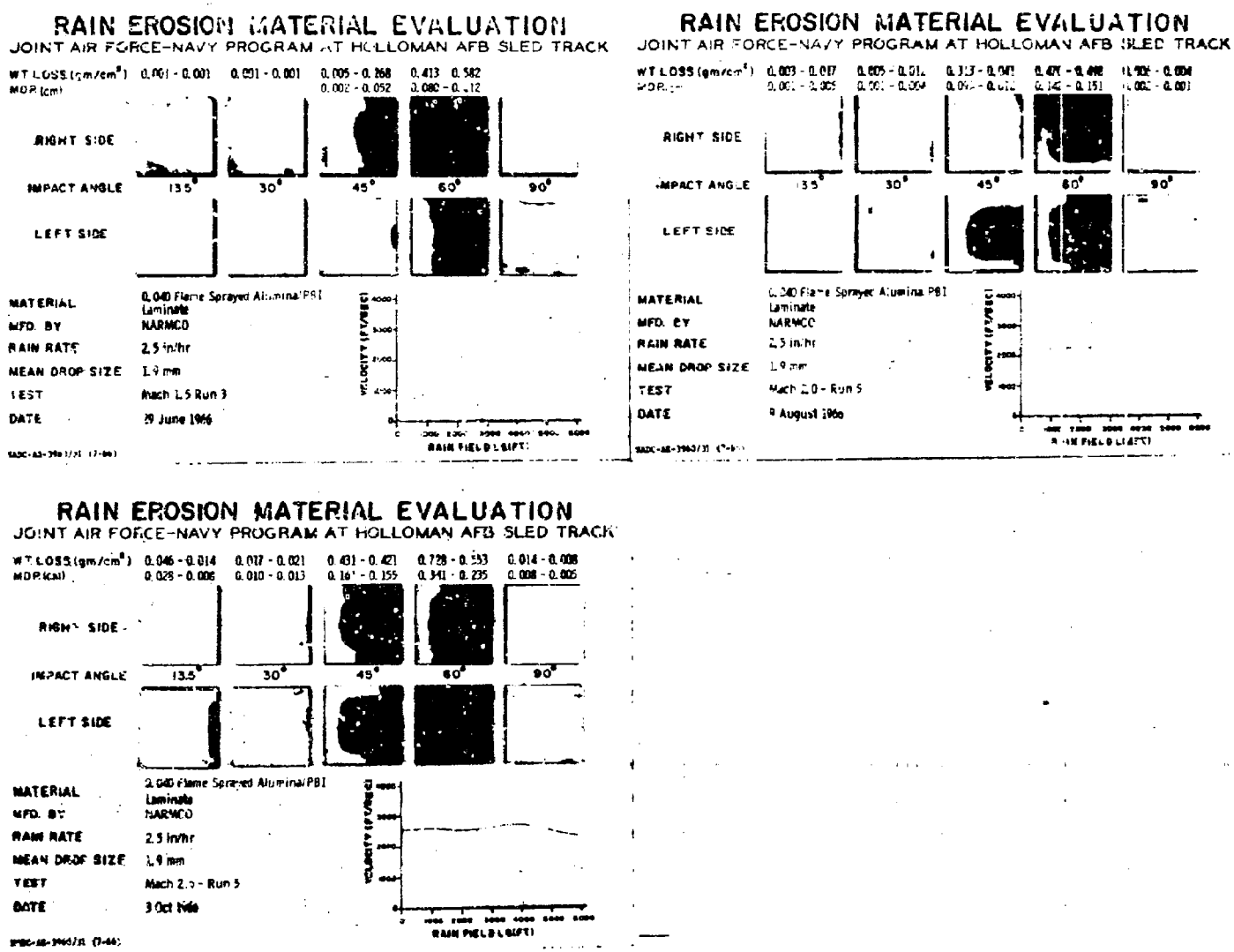

Figure 57. Rain Erosion Damage Data for 0.040 Inch Flame Sprayed Alumina/PBI Laminate

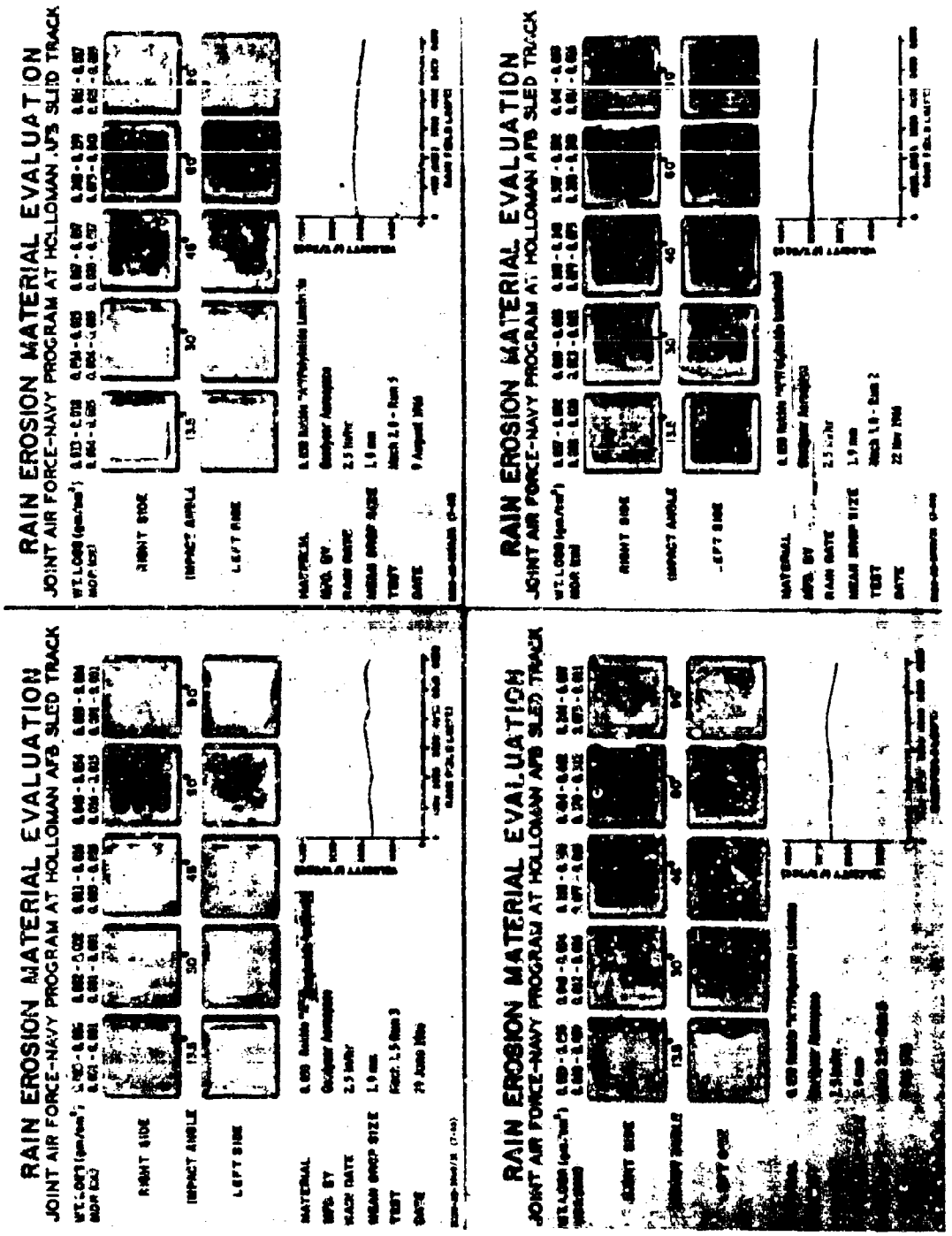

Figure 58. Rain Erosion Damage Data for 0.030 Inch Rohide "A"/Polyimide Laminate

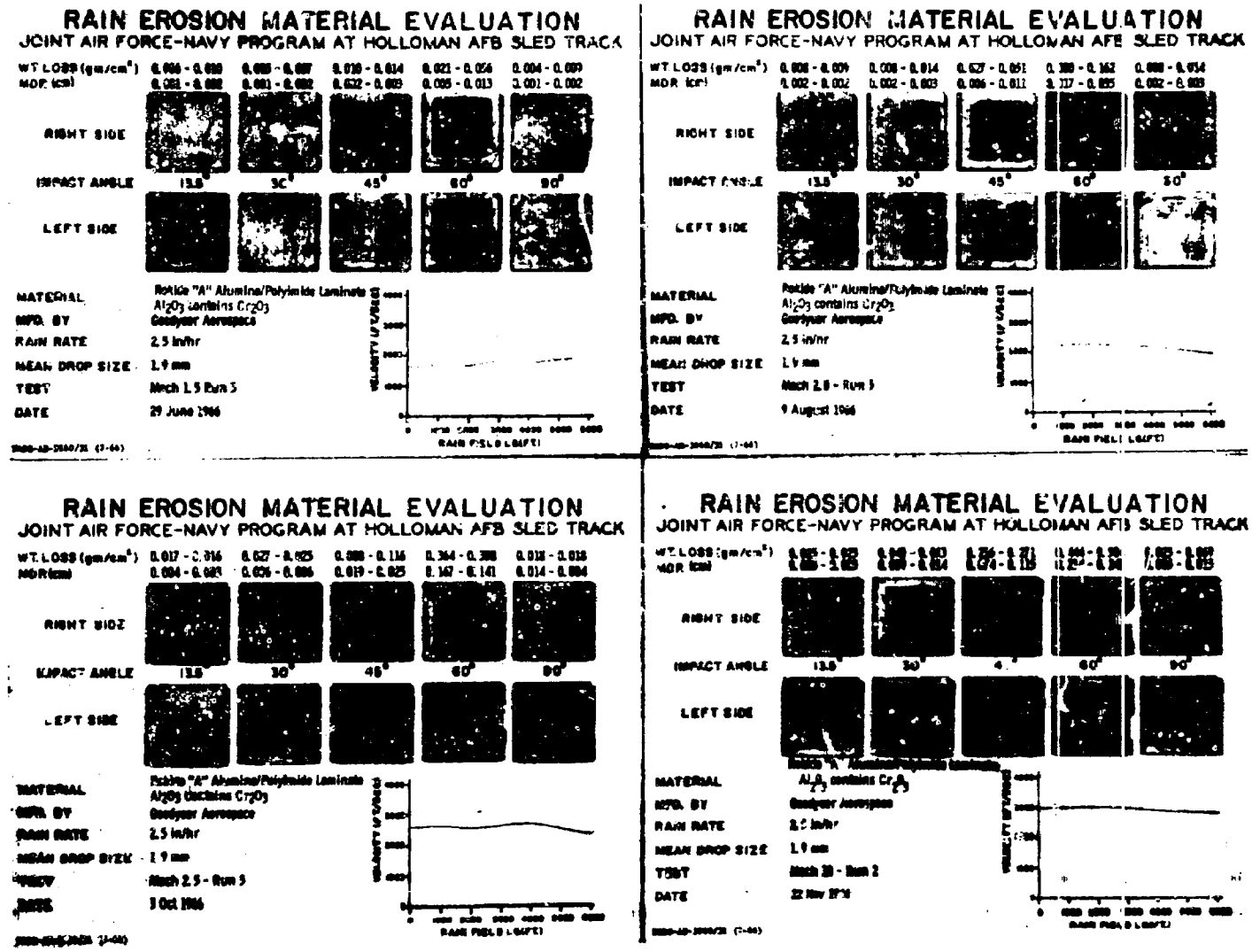

Figure 59. Rain Erosion Damage Data for Rokide "A" Alumina/Polyimide Laminate Al_2O_3 Contains Cr_2O_3

PRECEDING PAGE BLANK - NOT FILMED.

E-8 Alumina/RTV521/Polyimide Laminate

An interesting composition of alumina filled with a vitreous clay is being considered for radome applications on advanced aircraft. The addition of clay greatly improves the hardness of the alumina coating (to Knoop 1000) and facilitates fabrication of radomes with it. The application of this material over an RTV silicone which acts as an interlayer with low modulus to counteract thermal expansion differences and as an adhesive and then backed up with a thin polyimide laminate is now being evaluated. Samples of this composition were provided by Boeing/Airplane Division.

The dielectric design of this structure would be difficult because of the differences in dielectric constants for the three materials. Considerable experimentation would be required to establish operating capability of such a system. Tapered construction of two layers might also be required.

At Mach 1.5 a coating of 0.125 inch thick alumina (71.5%) filled with clay over 0.030 inch RTV521 silicone over 0.100 inch polyimide laminate was undamaged after exposure. At Mach 2.0 the 60° specimens were diced into many small pieces but the adhesion to the polyimide through the silicone was maintained. At Mach 2.5 and 3.0 the 60° specimens were completely penetrated and the other positions increasingly eroded.

E-13 No Specimens

Plasma sprayed alumina over a filament wound silica quartz glass laminate were planned for this number. This would be in distinction to the plasma sprayed alumina over the silica quartz glass laminates prepared by lay-up techniques (Specimen E-11). No specimens were obtained for evaluation.

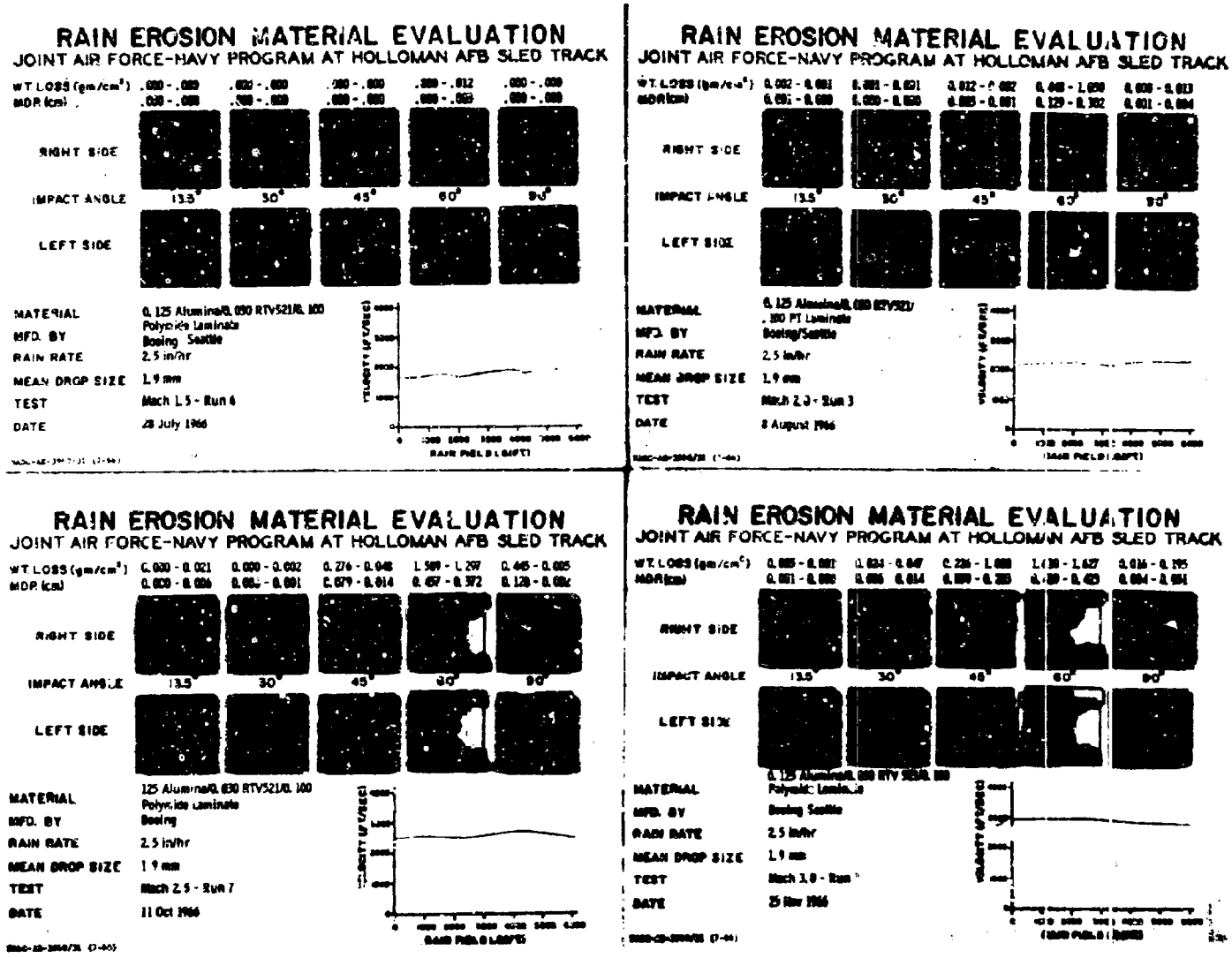

Figure 60. Rain Erosion Damage Data for 0.125 Inch Alumina/0.030 Inch RTV521/0.100 Inch Polyimide Laminate

E-14 Rokide A Alumina (Epoxy Impregnated)/Epoxy Laminate

For lower temperature substrates such as epoxies, the "pick-up" technique in which the ceramic is sprayed on a mold and the coating is picked up by laminating directly onto it can be used. This maximizes the adhesive bond obtainable for this coating-substrate combination.

A technique which is useful for sealing the pores in a sprayed coating is to impregnate the sprayed ceramic with an organic resin. This resin can then be room temperature cured or heat cured to seal it.

Specimens consisting of a flame sprayed alumina (Rokide "A" process) onto which an Epon 828 epoxy laminate had been laid up and on which the surface had been impregnated with Epon 828 epoxy resin were furnished by the Naval Ordnance Laboratory.

The Rokide "A" alumina coatings (0.030 inch) which had been impregnated with Epon 828 epoxy resin and picked up on an 828 epoxy laminate yielded the best protection of any ceramic coating in the rain field. At Mach 1.5 no damage was observed; at Mach 2.0 the coating was partially removed at 60° with no other damage, and at Mach 2.5 the 45° and 60° positions were damaged but the others were untouched.

The combination of no porosity of the coating (via impregnation) and the good bonding of the pick-up technique resulted in a ceramic coated laminate with good resistance.

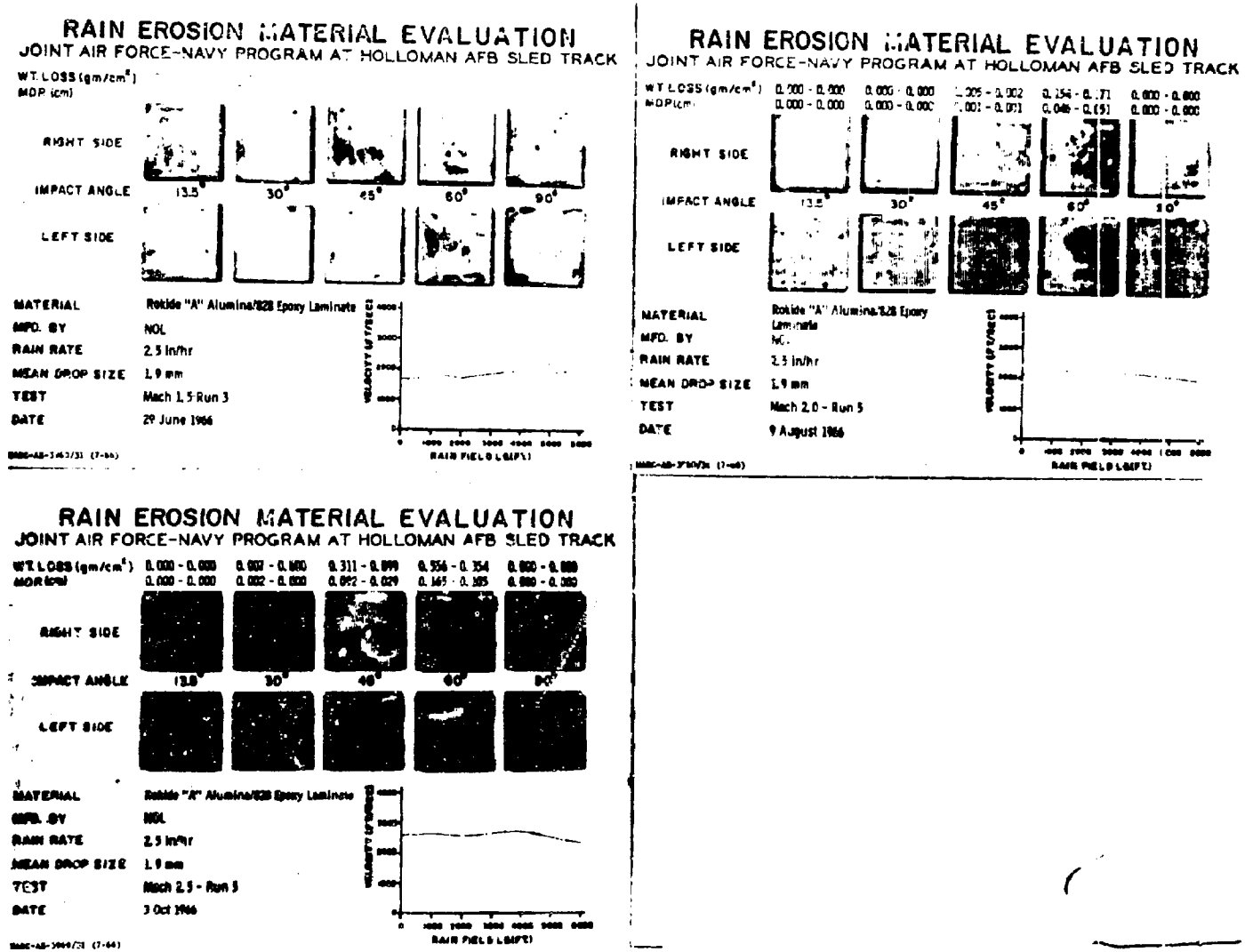

Figure 61. Rain Erosion Damage Data for Rokide "A" Alumina/828 Epoxy Laminate

E-16 Plasma Sprayed Alumina (H_3PO_4-Treated)/Epoxy Laminate

The plasma sprayed alumina coatings have been investigated thoroughly in a recent Air Force program (Reference 8). An interesting development of this research was that treatment of the as-sprayed alumina coatings with phosphoric acid reduced the porosity, improved the hardness and greatly enhanced the subsonic rain erosion resistance of this coating. The phosphoric acid reacts chemically with the alumina particles to give an aluminum phosphate which seals the pores.

A set of these H_3PO_4-treated specimens were prepared by secondarily bonding a treated alumina coating (sprayed on a metal mold) to an epoxy laminate using an epoxy adhesive. These specimens were prepared by Brunswick Corporation under Contract AF 33(615)-3342.

The erosion resistance of this phosphoric acid-treated, plasma-sprayed alumina (0.030 inch) was as good as the epoxy-impregnated Rokide "A" alumina; that is, the best of any ceramic coating. At Mach 1.5 the specimens were undamaged and at Mach 2.0, the 60° specimens were the only ones damaged. The coating was partially removed but the adhesion to the epoxy laminate was excellent.

Once again these results point out the need for reducing the porosity of sprayed coatings and the requirement of optimizing the adhesive bond between ceramic and laminate.

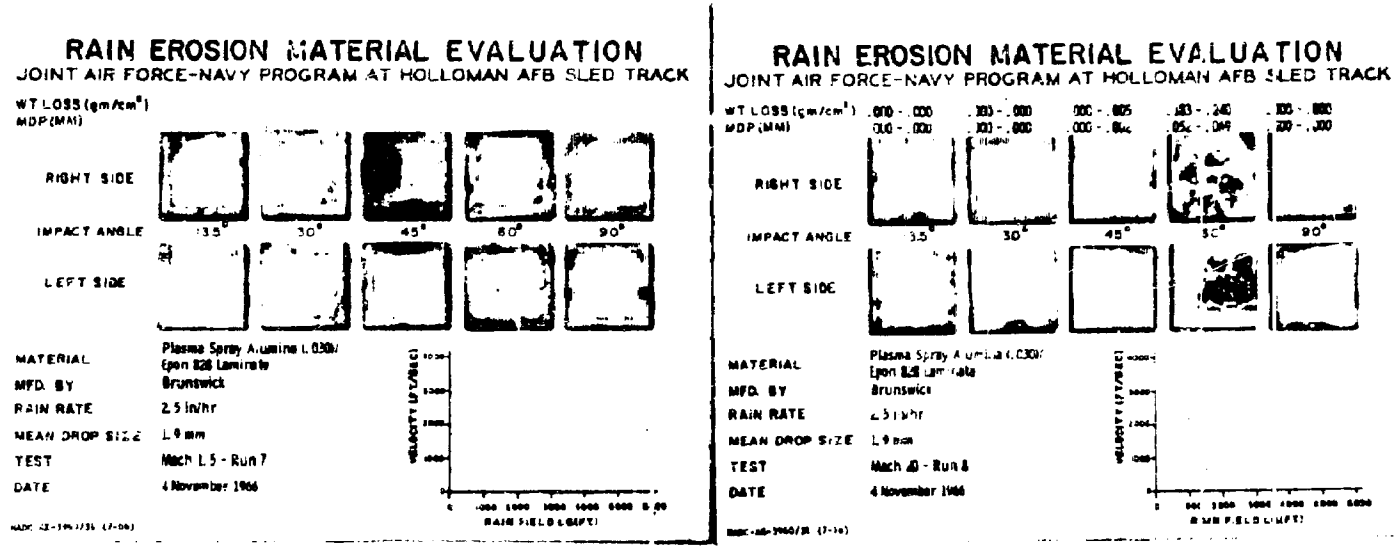

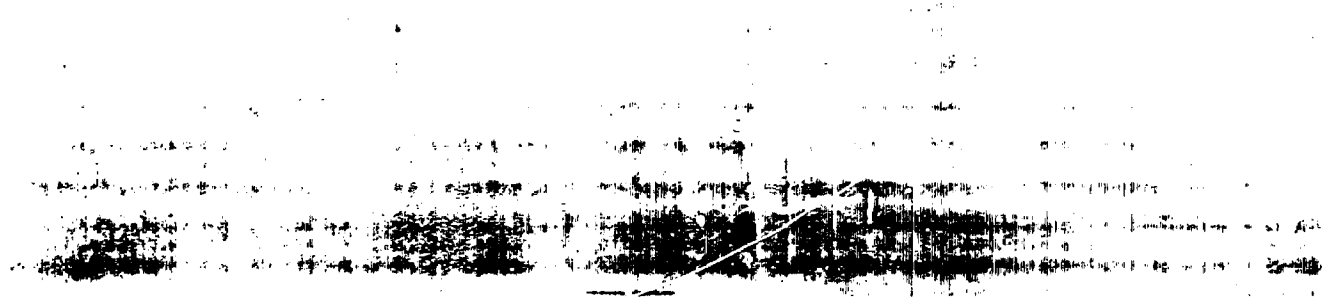

Figure 62. Rain Erosion Damage Data for Plasma Sprayed Alumina (0.030 Inch)/ Epon 828 Laminate

6. CLASS F - ELASTOMERIC-COATED LAMINATES

F-1 and F-2 0.010 and 0.020 Inch Sprayed Neoprene/Epon 828 Laminate

Although elastomeric coatings are usually used for subsonic rain erosion protection because of their good protective abilities in that environment, they are not widely considered for supersonic purposes because of temperature limitations and poor resistance to supersonic rain impact. In a subsonic environment the resiliency and recovery ability of the elastomers enables them to withstand repeated raindrop impact. At higher velocities the increased severity and rapidity of impact causes them to fail.

It was felt that several representative elastomeric coatings should be examined at Mach 1.5 to 2.5. Two such coatings were two thicknesses of a sprayed neoprene (Gates Engineering Company) applied over an Epon 828 epoxy laminate made by the Naval Air Development Center. The 0.010 inch thickness lies within the rain erosion specification coating thickness (Mil-C-7439B) and the 0.020 inch thickness represents an upper limit for sprayed neoprene (because of electrical characteristics and application difficulties). The Epon 828 laminate was prepared in the same manner as the uncoated laminate (Specimen C-3).

Exposure of the sprayed neoprene resulted in no detectable erosion at Mach 1.5 with increasing damage at Mach 2.0 and 2.5. The 0.010 inch thickness was sufficient to provide protection and the addition of an extra 10 mils did not improve the resistance. At Mach 2.5 there was less substrate damage at the 45° position with the 0.020 inch coating but the 60° position eroded comparably at all speeds.

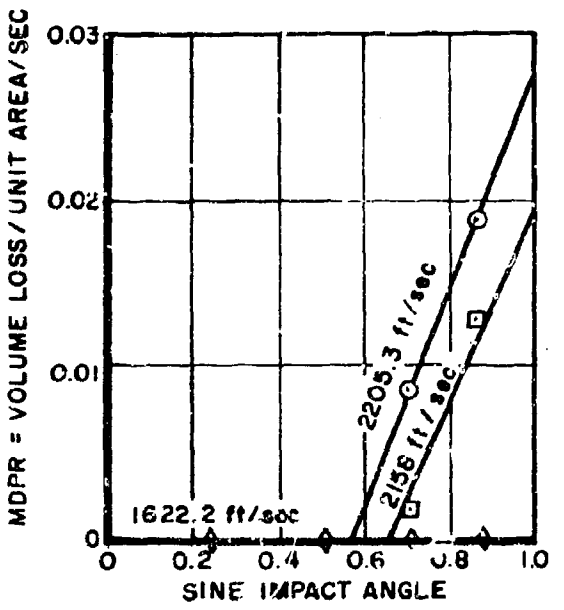

Figure 63. MDPR vs Sine Impact Angle - 0.010 Inch Gaco/Epon 828 Epoxy Laminate

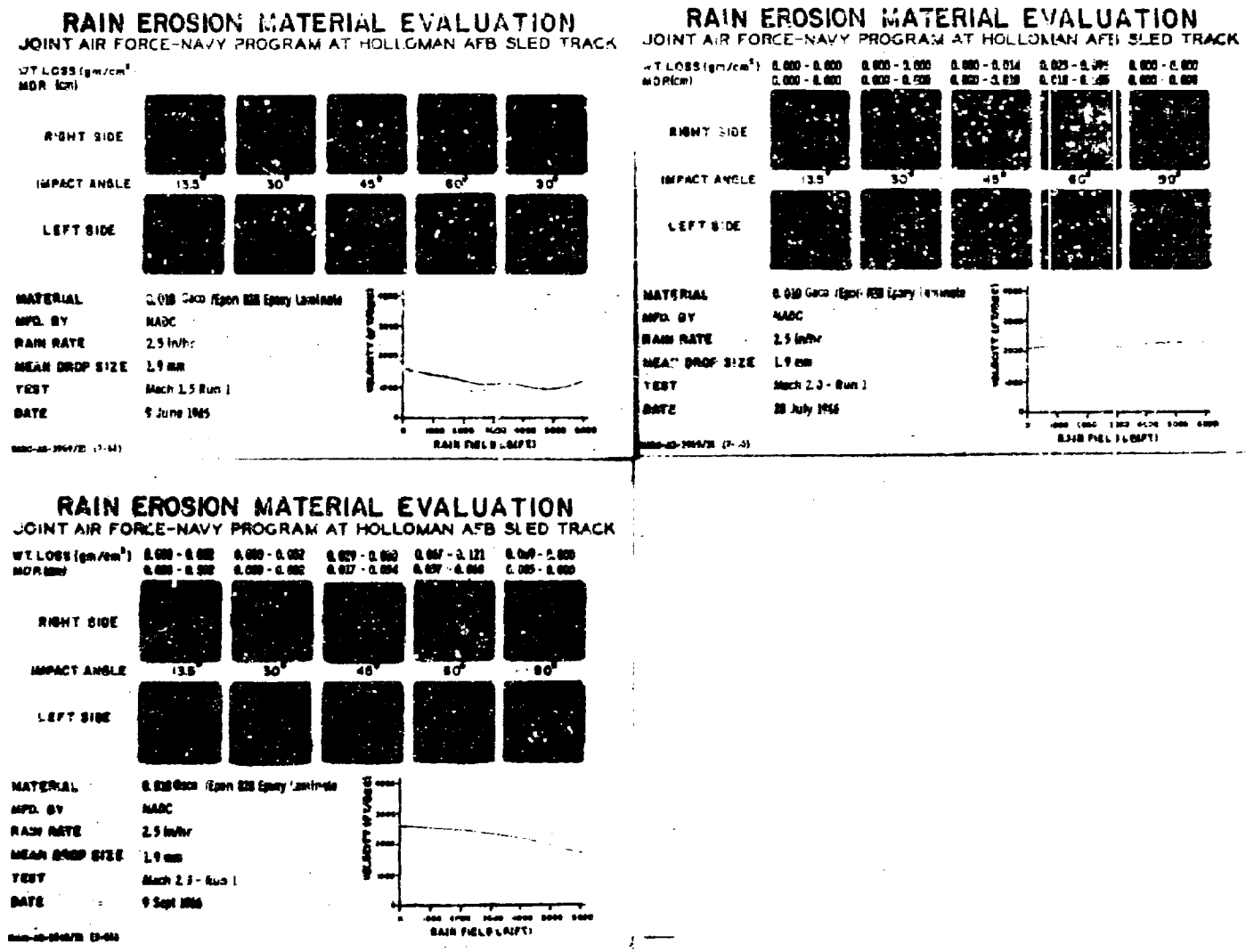

Figure 64. Rain Erosion Damage Data for 0.010 Inch Gaco/ Epon 828 Epoxy Laminate

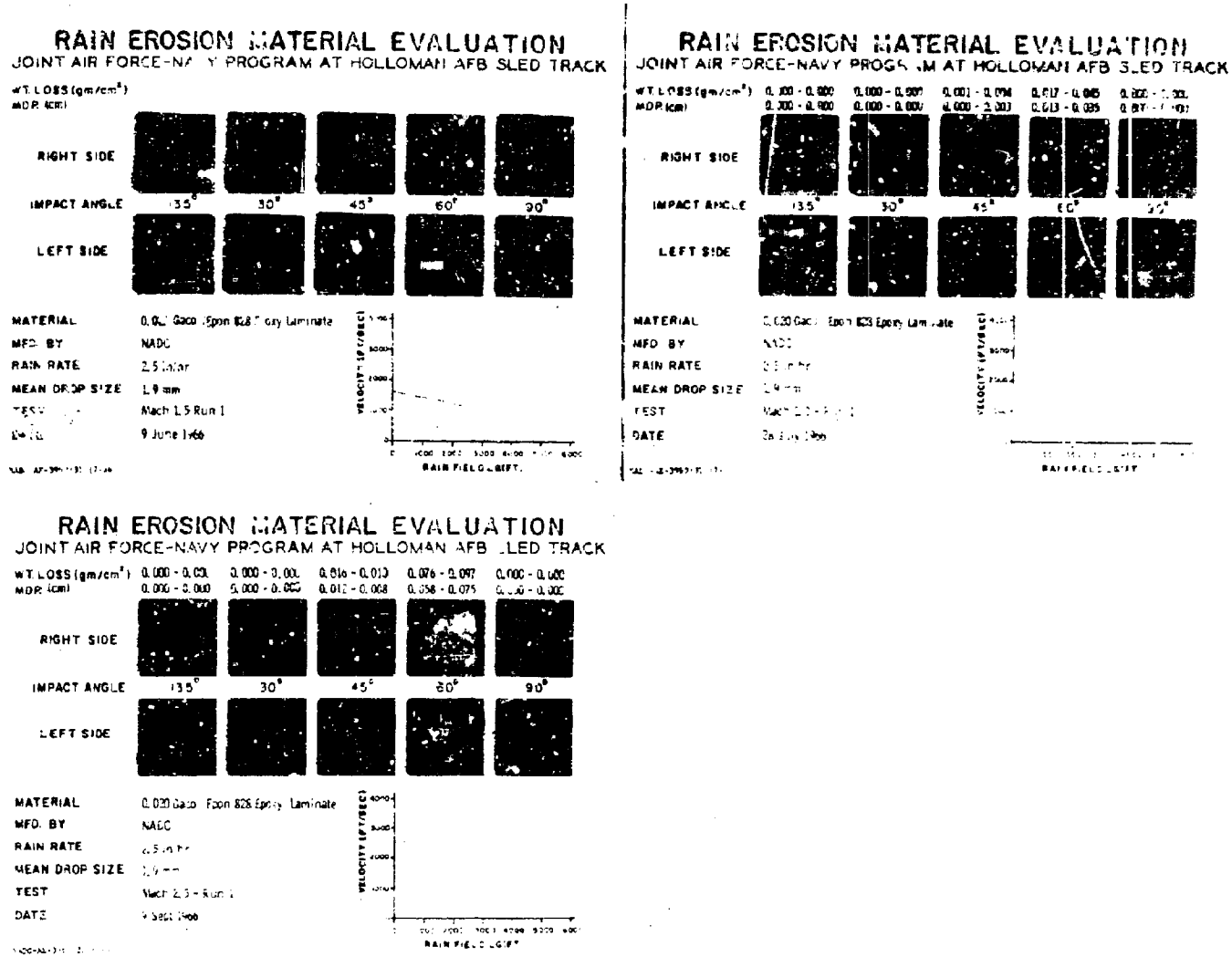

Figure 65. Rain Erosion Damage Data for 0.020 Inch Gaco/Epon 828 Epoxy Laminate

F-3, F-4, F-5 0.010, 0.020, and 0.030 Inch Neoprene/Dacron Cloth/Epon 828 Laminate

To determine the effects of elastomeric coating thickness and to compare prefabricated bonded neoprene to the conventional sprayed neoprene, three thicknesses, 0.010, 0.020, and 0.030 inch of a neoprene over Dacron cloth boot material from B. F. Goodrich were applied to Epon 828 epoxy laminates by NAVAIRDEVCEN. These neoprene boots have a specific gravity of 1.30, Shore "A" hardness of 56, percent elongation of 570 at break, tensile strength of 3090 psi, and a dielectric constant and loss tangent of 3.1 and 0.029 respectively.

The laminates were once again prepared by the press technique and after cure the materials were adhesively bonded with a two-part, low temperature cure epoxy adhesive.

Neoprene boots are widely used in many commercial aircraft but are not accepted for many military applications. Field maintenance and application are considerably easier than the sprayed neoprene which is difficult to work with in the field.

The prefabricated boots of neoprene over Dacron cloth protected the epoxy laminate substrates almost as well as the sprayed neoprene coatings. There was no thickness effect with these coatings and the 0.010 inch boot resisted erosion as well as the 0.020 or 0.030 inch thickness. The adhesive bond was satisfactory and failure appeared to be by tearing and wearing away of the coating. No erosion was evident at Mach 1.5 and it became progressively worse at higher velocities.

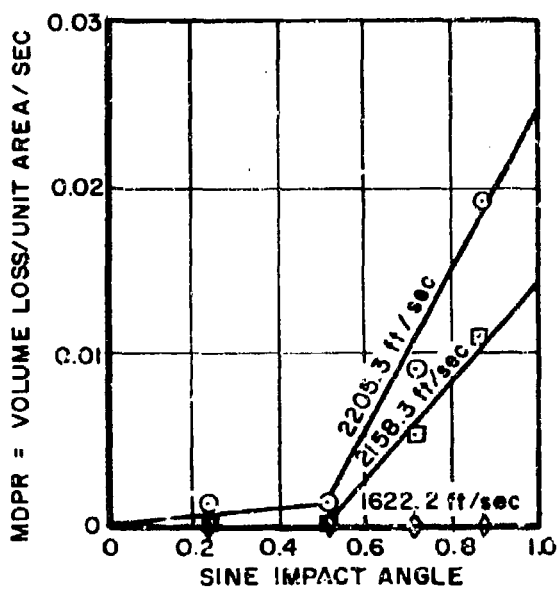

Figure 66. MDPR vs Sine Impact Angle - 0.010 Inch Neoprene/Dacron/Epon 828 Epoxy Laminate

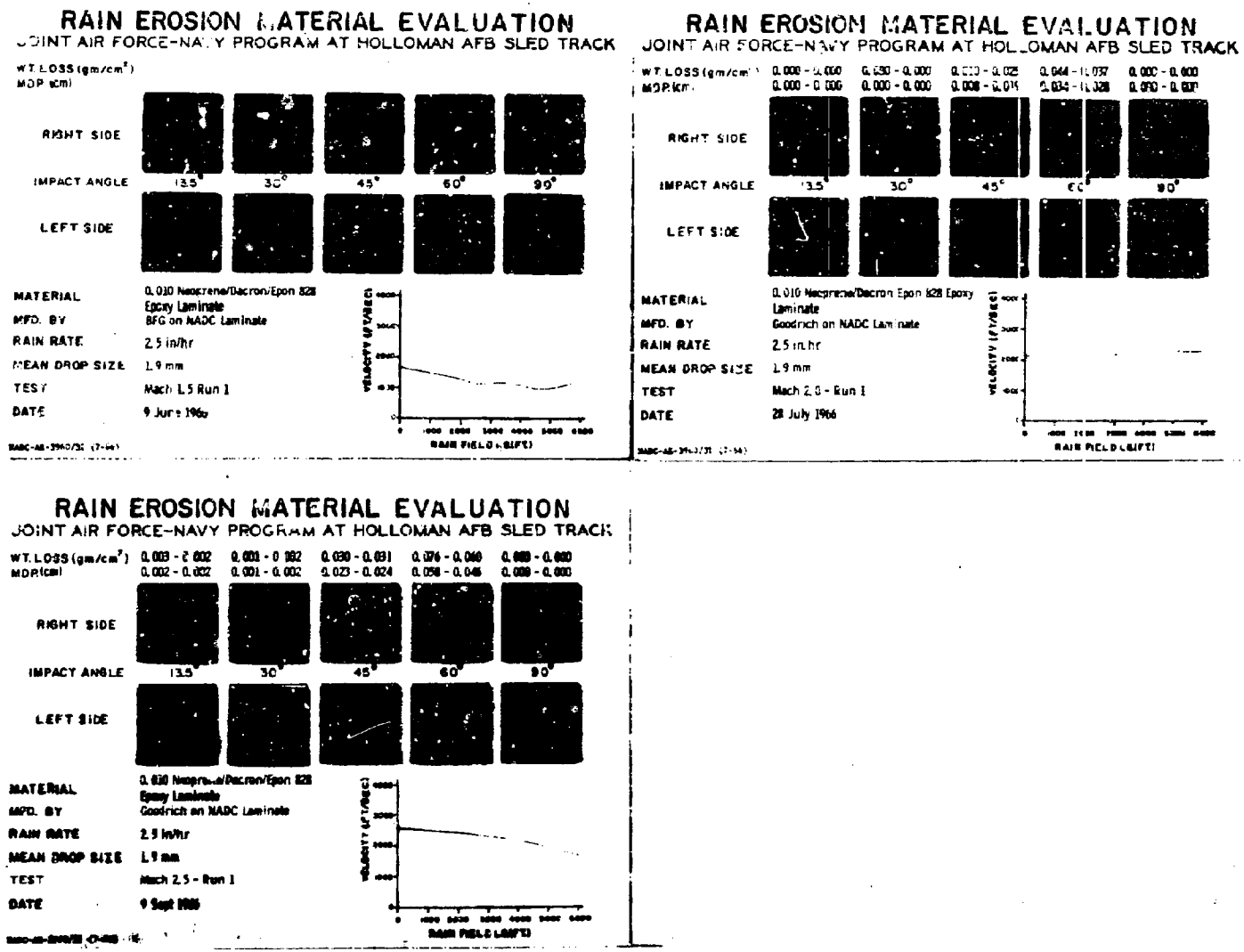

Figure 67. Rain Erosion Damage Data for 0.010 Inch Neoprene/Dacron/Epon 828 Epoxy Laminate

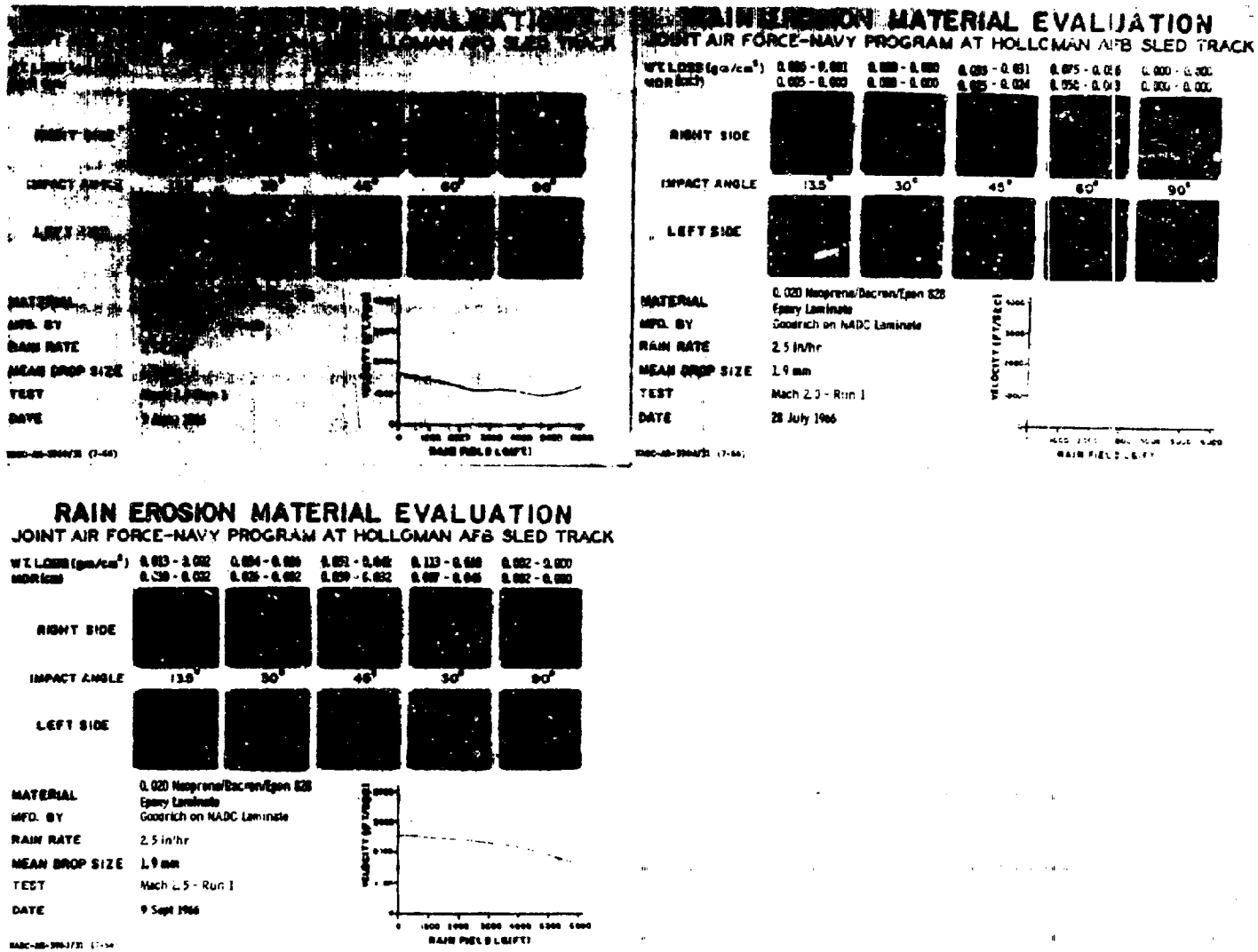

Figure 68. Rain Erosion Damage Data for 0.020 Inch Neoprene/Dacron/Epon 828 Epoxy Laminate

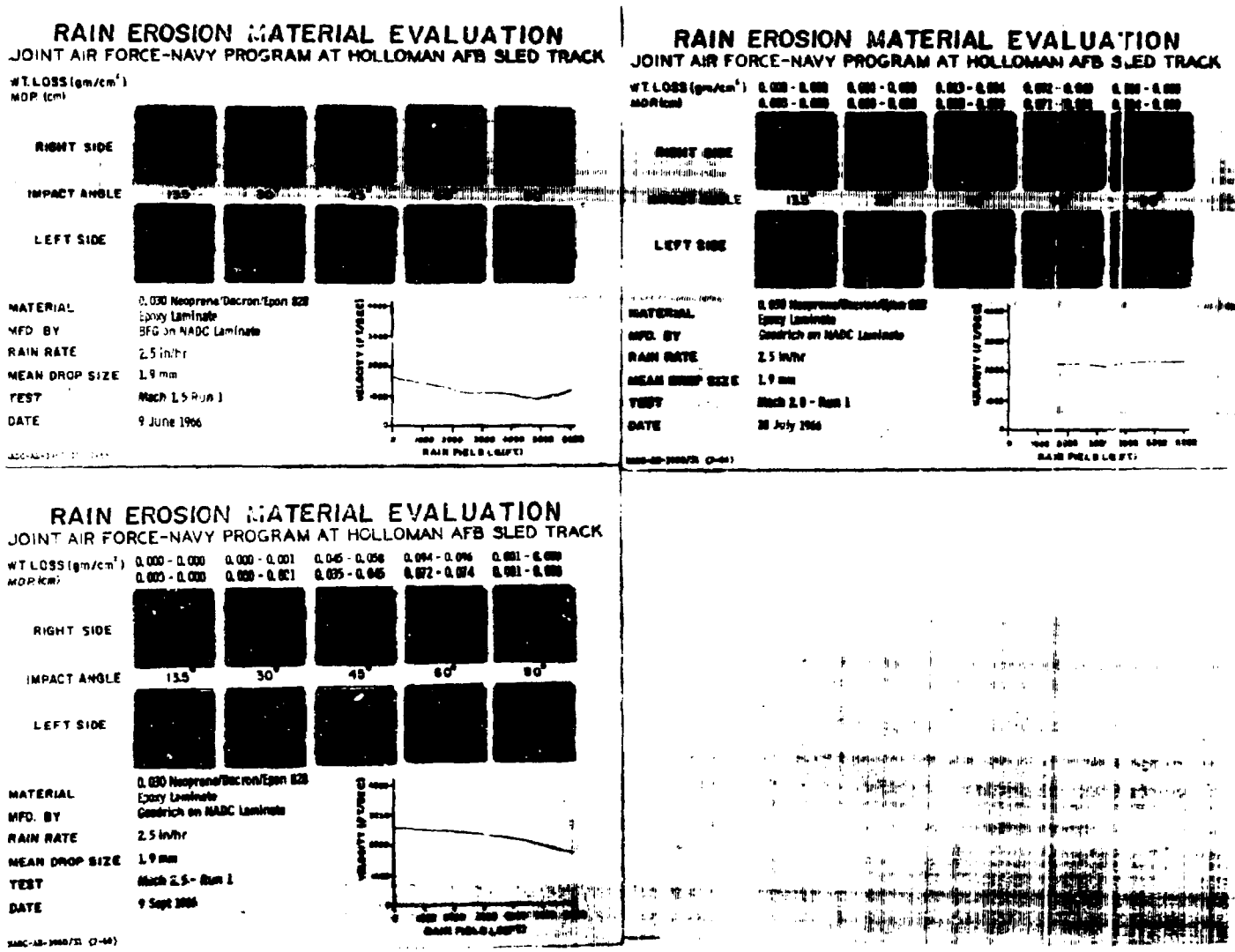

Figure 69. Rain Erosion Damage Data for 0.030 Inch Neoprene/Dacron/Epon 828 Epoxy Laminate

F-6, F-7, F-8 0.014, 0.026, and 0.038 Inch Polyurethane/Epon 828 Laminate

Three thicknesses of an unfilled polyurethane elastomer were supplied by B. F. Goodrich and applied to Epon 828 epoxy laminates by NAVAIRDEVCEN using an epoxy adhesive. The polyurethanes are another class of elastomeric materials which exhibit excellent resistance to subsonic rain erosion. These coatings possessed a specific gravity of 1.22, Shore "A" hardness of 78, 640% elongation at break and tensile strength of 3450 psi. The electrical properties were not too favorable with a dielectric constant of 5.5 and a loss tangent of 0.05.

The polyurethane elastomers erode by a sudden structural failure in an isolated area rather than a gradual eroding away of the surface. Adhesion of polyurethane elastomeric sheets has always been a continuing problem.

The polyurethanes have excellent sand erosion resistance and are being widely considered for rain erosion protection as well. In-house research at the Air Force Materials Laboratory has indicated an order of magnitude in erosion resistance improvement with urethanes over neoprene.

The particular polyurethanes evaluated in thicknesses of 0.014, 0.026, and 0.038 inch were comparable to corresponding thicknesses of neoprene boots in erosion resistance but less resistant than the sprayed neoprene. Once again no thickness effect was evident and the 0.014 inch polyurethane was as resistant as the others. There was no damage at Mach 1.5 once again; the erosion at Mach 2.0 and 2.5 took the form of cold flow in the surface where it was not completely broken through. This deformation of the surface into many small protrusions is characteristic of some unfilled urethanes.

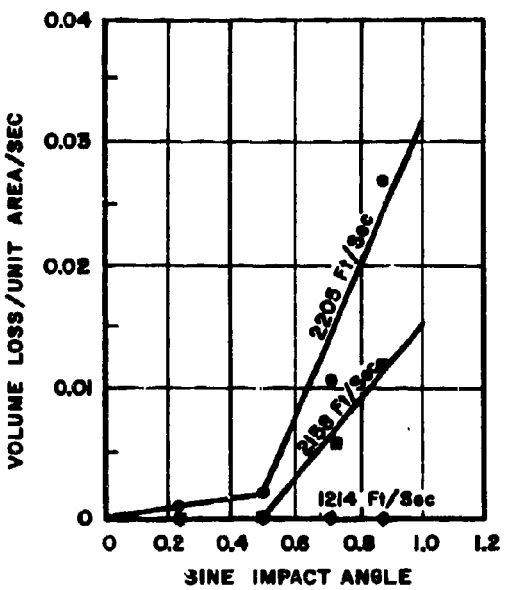

Figure 70. MDPR vs Sine Impact Angle - 0.014 Inch Polyurethane/Epon 828 Epoxy Laminate

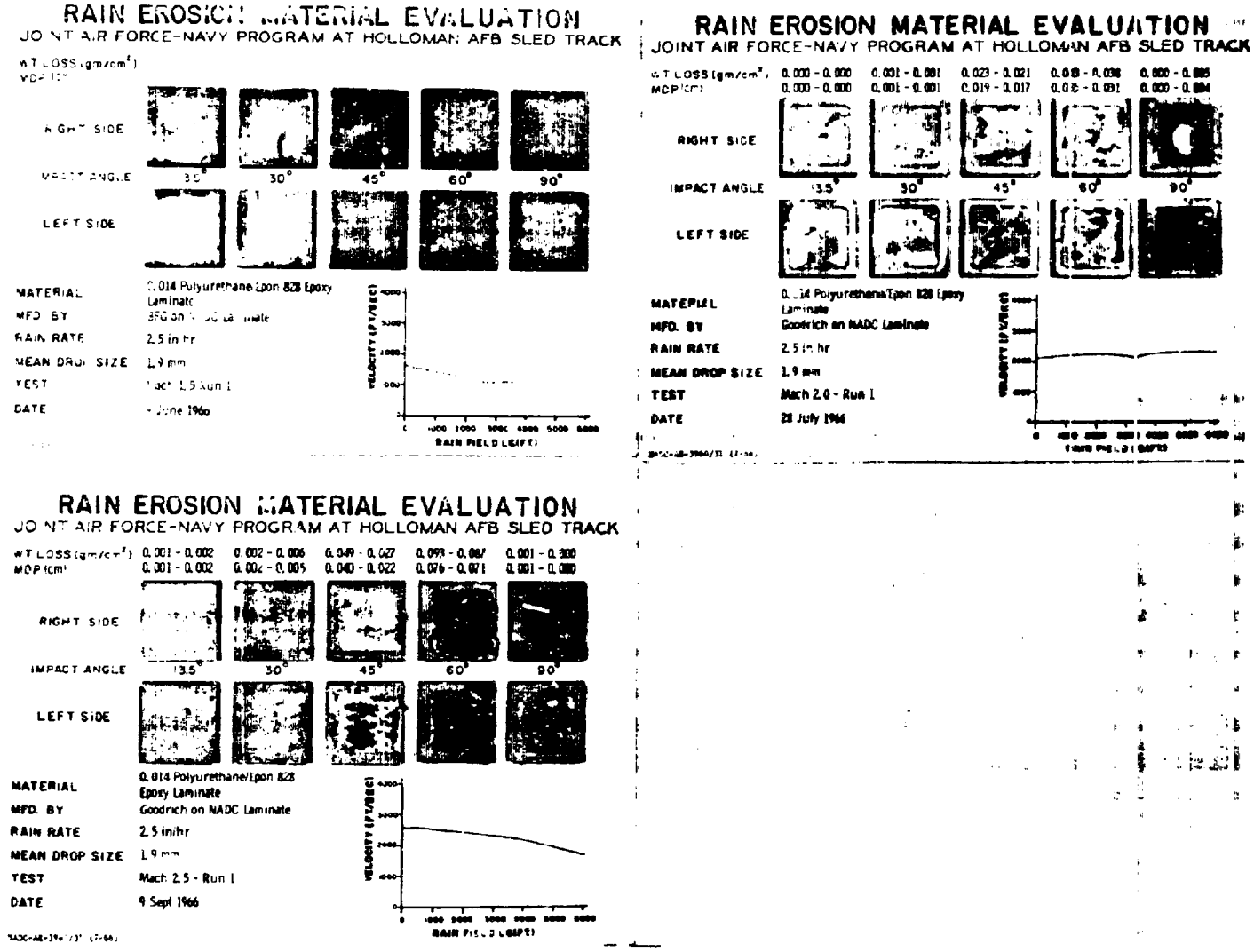

Figure 71. Rain Erosion Damage Data for 0.014 Inch Polyurethane/Epon 828 Epoxy Laminate

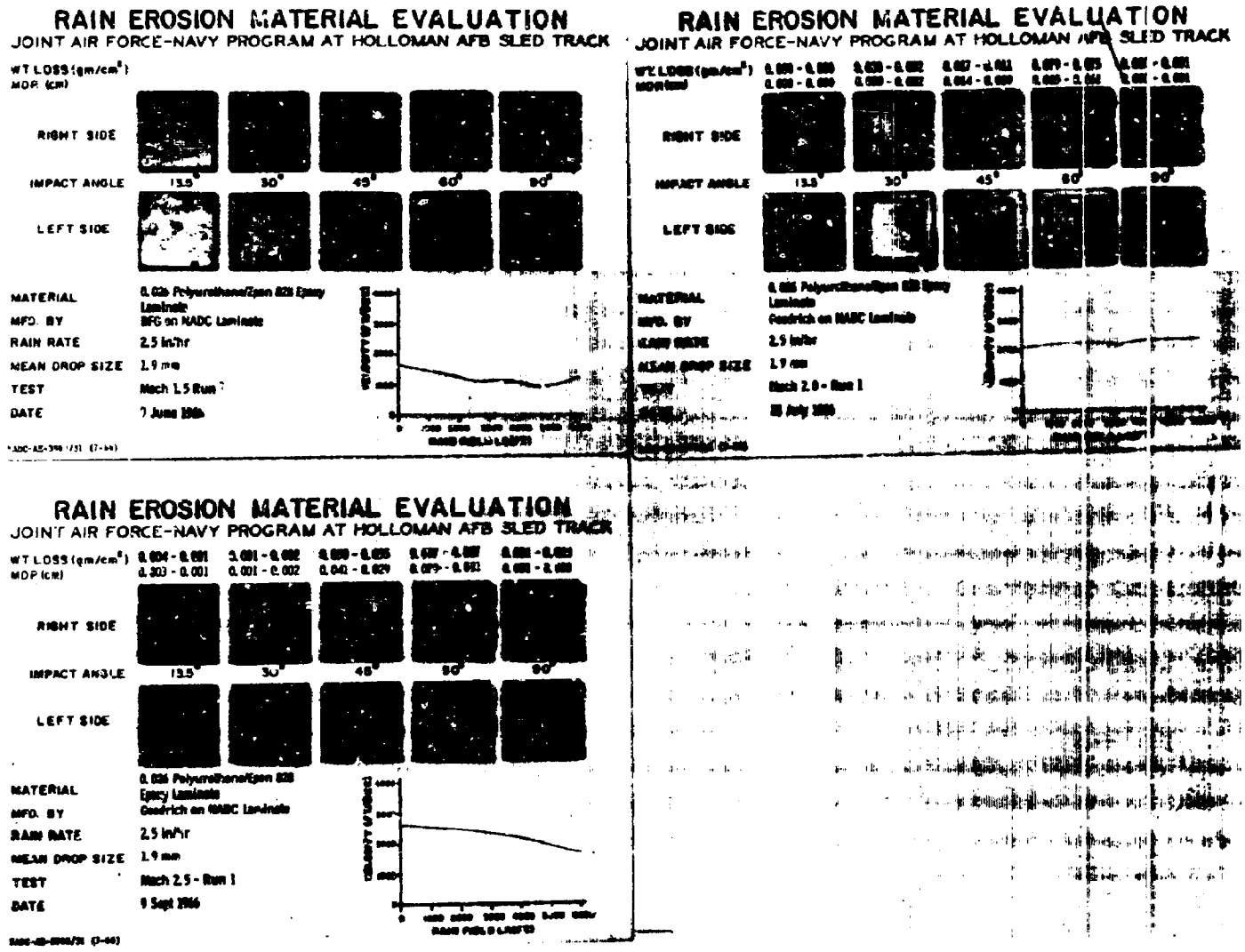

Figure 72. Rain Erosion Damage Data for 0.026 Inch Polyurethane/Epon 828 Epoxy Laminate

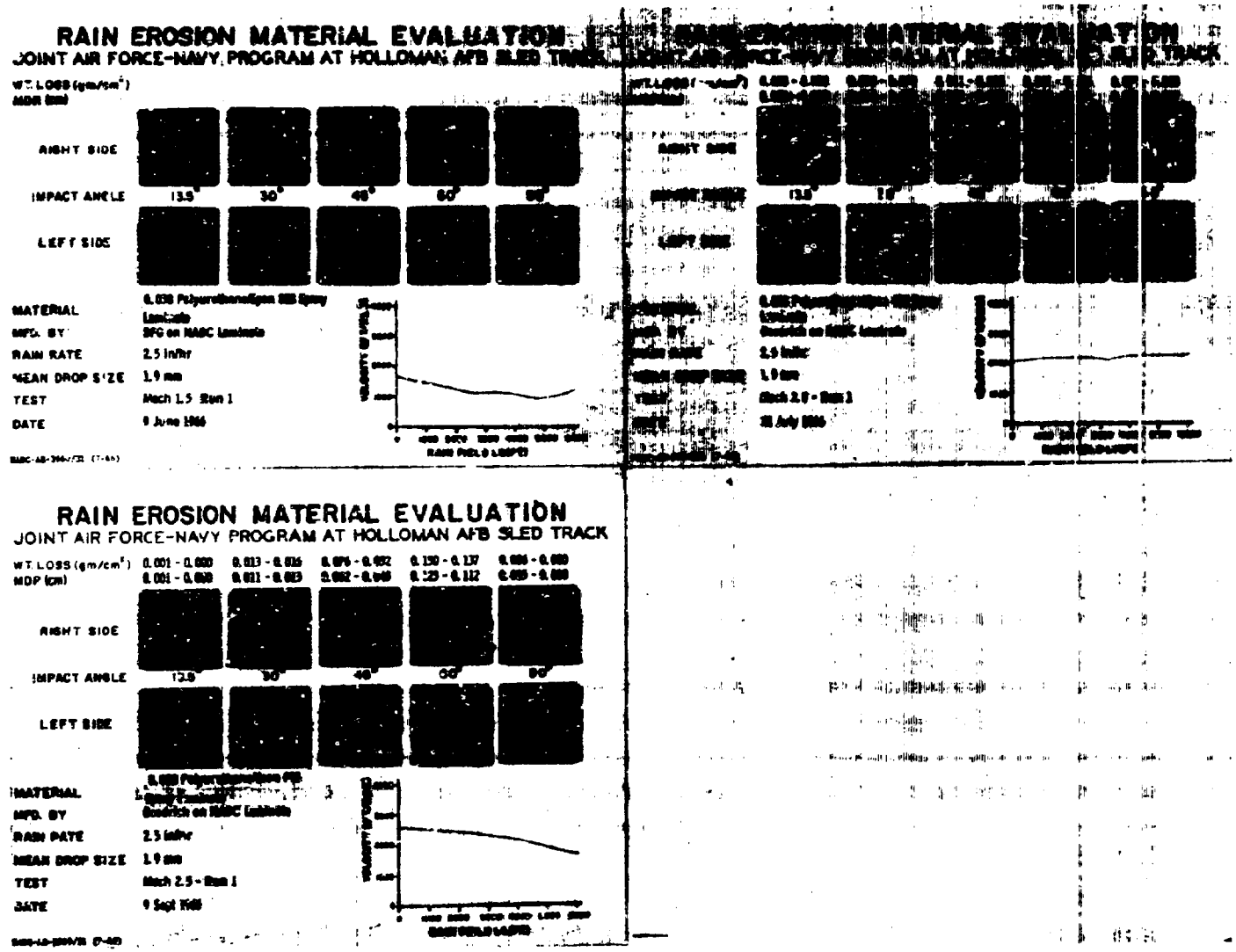

Figure 73. Rain Erosion Damage Data for 0.038 Inch Polyurethane/Epon 828 Epoxy Laminate

F-9, F-10, F-11 0.010, 0.020, and 0.030 Inch Hycar Rubber/Epon 828 Laminate

As representative of an elastomer with high hardness, tear strength and modulus at 100% elongation, three thicknesses of a Hycar rubber were chosen. These coatings had a specific gravity of 1.368, Shore "A" hardness of 94, tear strength of 775 lb/inch, 430% elongation at break, and 4030 psi tensile strength. Once again the electrical properties were poor with dielectric constant of 5.0 and loss tangent of 0.05.

These coatings were bonded to the Epon 828 epoxy laminates by use of the two-part epoxy adhesive previously mentioned. The Hycar sheets which had no cloth backing were supplied by B. F. Goodrich and the epoxy laminate substrates were furnished by NAVAIRDEVCEN.

The high hardness and 100% modulus of the Hycar rubber are not desirable in an elastomeric erosion resistant coating. These coatings suffered no weight loss at Mach 1.5 but the surface underwent compression. This compression at the higher velocities resulted in loss of adhesive bond and failure through tearing of the loosened coating. Once again no thickness effect was noted but the damage progressed with velocity.

Specimens of F-9 (0.010" Hycar) were not evaluated because damage to the 0.020 and 0.030 inch thicknesses was so severe that their omission from exposure was warranted.

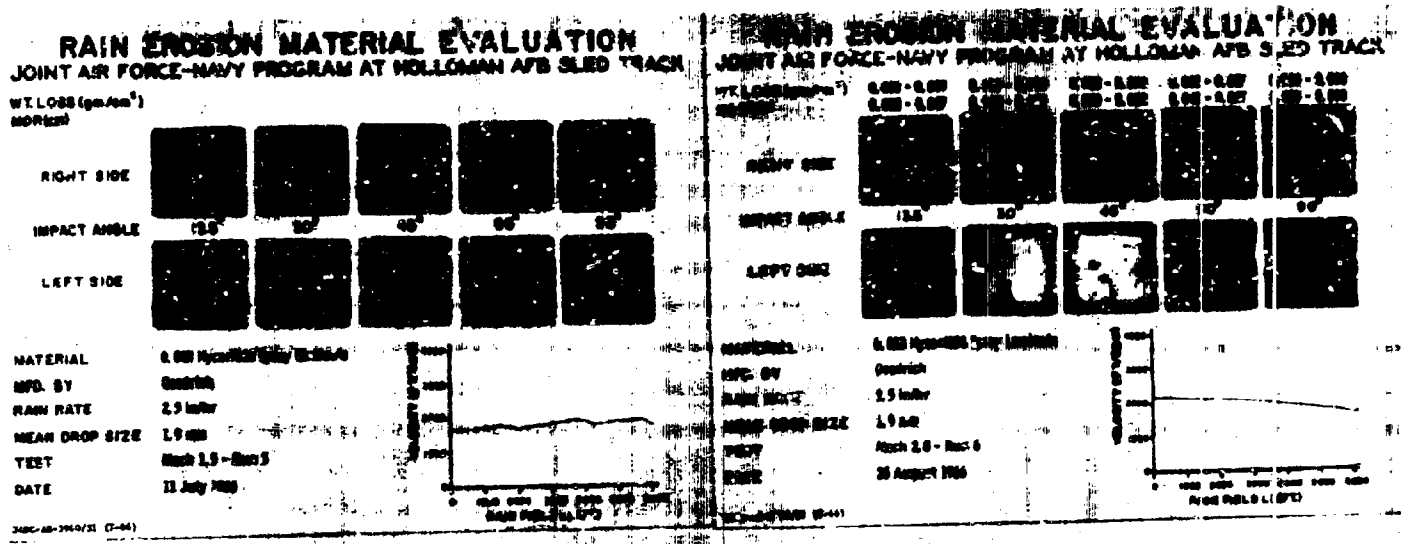

Figure 74. Rain Erosion Damage Data for 0.020 Inch Hycar/828 Epoxy Laminate

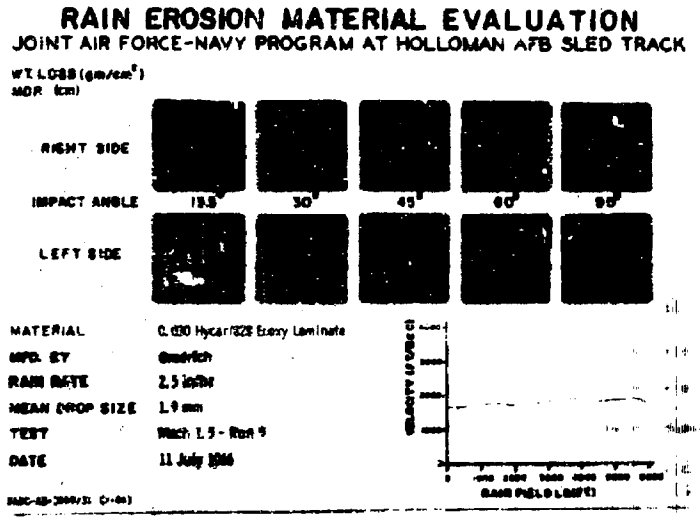

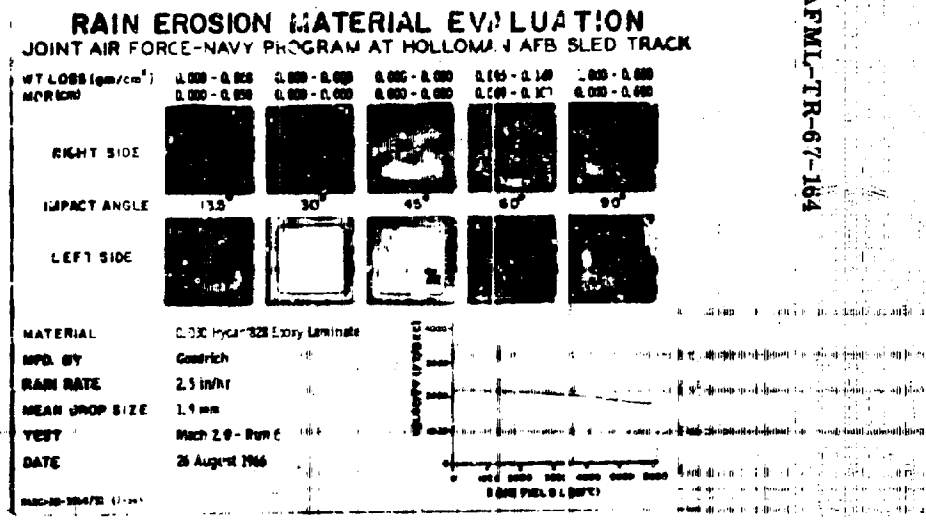

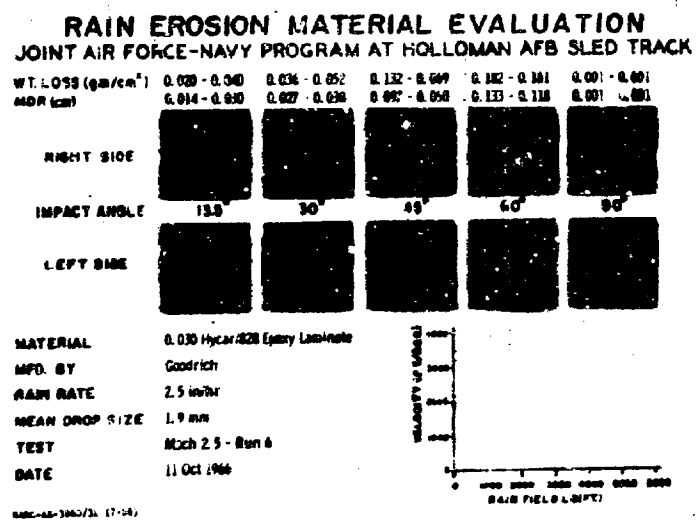

Figure 75. Rain Erosion Damage Data for 0.030 Inch Hycar/828 Epoxy Laminate

PRECEDING PAGE BLANK - NOT FILMED.

7. CLASS G - GLASSES

G-1, G-2, G-3, G-4 Glass

Four glass materials were submitted for evaluation. These included two Corning Chemcor glasses (0313 and 0315), 9753 IR Glass, and the Owens Illinois C106 CER-VIT. These materials are of particular interest for aircraft windshields, infrared domes, and radome applications.

The Chemcor materials (G-1, G-4) are surface strengthened glasses in which the outside surfaces have been put into compression. These materials have extremely high flexural strengths, zero porosity and are good optical glasses when polished. Unless the compression layer is scratched or abraded these glasses defy breakage by ordinary abuse.

The 9753 IR Glass is a relatively new material for use with infrared systems between one and four microns wavelength. The samples submitted were ground and are therefore translucent; only polished specimens are transparent.

The fourth glass evaluated was the G-3 material, Owens Illinois C106 CER-VIT, submitted by the Boeing Co. It is opaque and milky white in color with extremely smooth surfaces when polished. The elastic modulus, shear modulus, and flexural strength are good for this class of materials.

The catastrophic type of fracture experienced by all the glass materials tested does not lend itself to MDPR curves and equation fitting. Generally these materials have less rain erosion resistance than the ceramics. As is typical for all glass materials the greater the strength, the more complete the breakage upon fracture.

The Chemcor glass, while stronger than most grades of steel, is destroyed by internal stress relieving after the rain erosion degradation of the outside compression layer. The G-3 glass showed somewhat less serious damage than the other materials tested at Mach 2.0 and low impact angles.

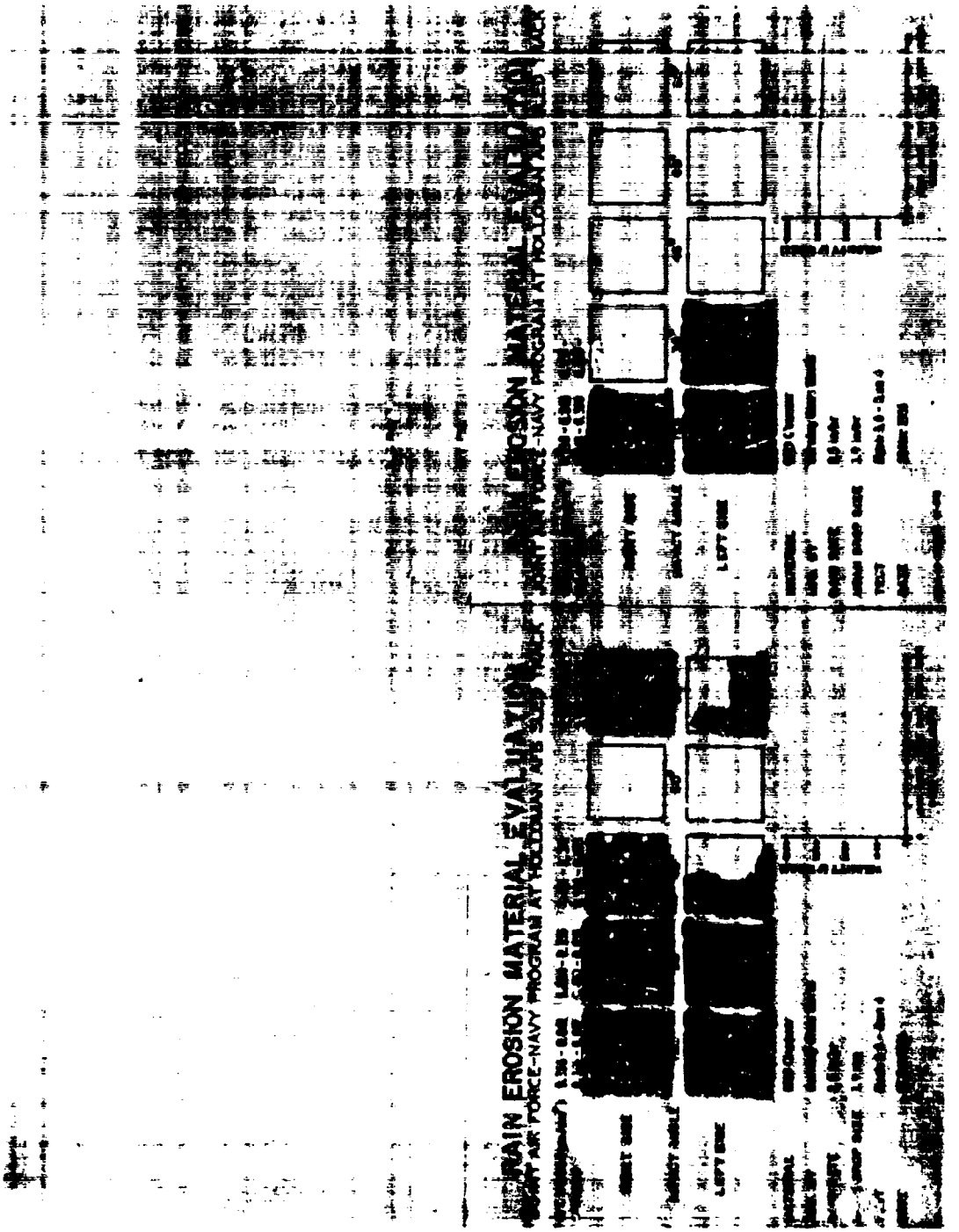

Figure 76. Rain Erosion Damage Data for 0313 Chemcor Glass

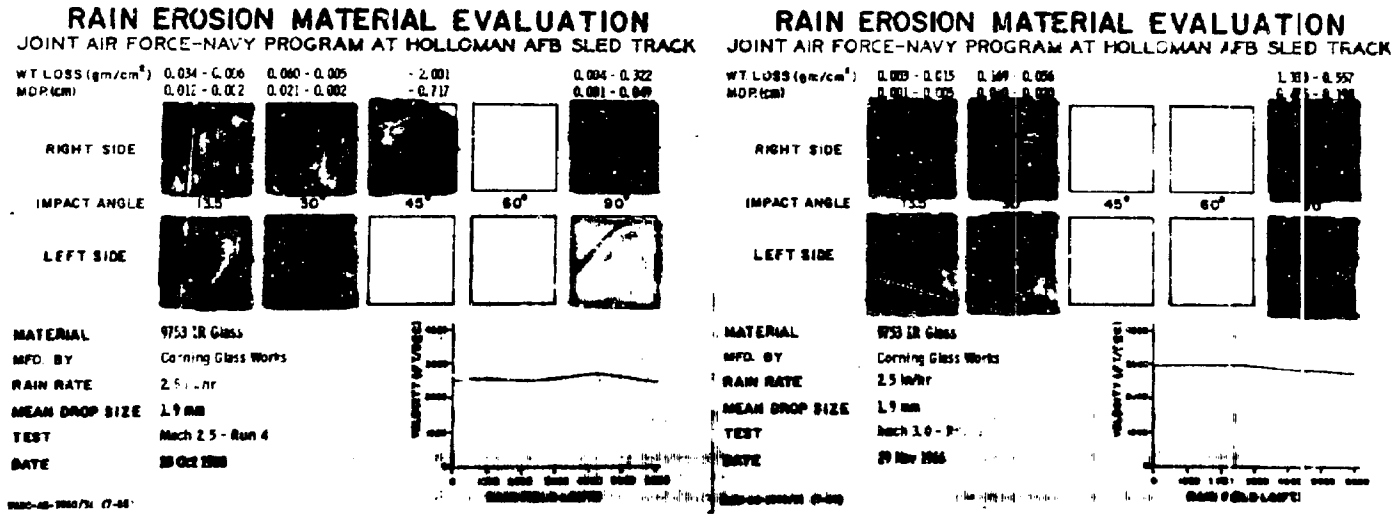

Figure 77. Rain Erosion Damage Data for 9753 IR Glass

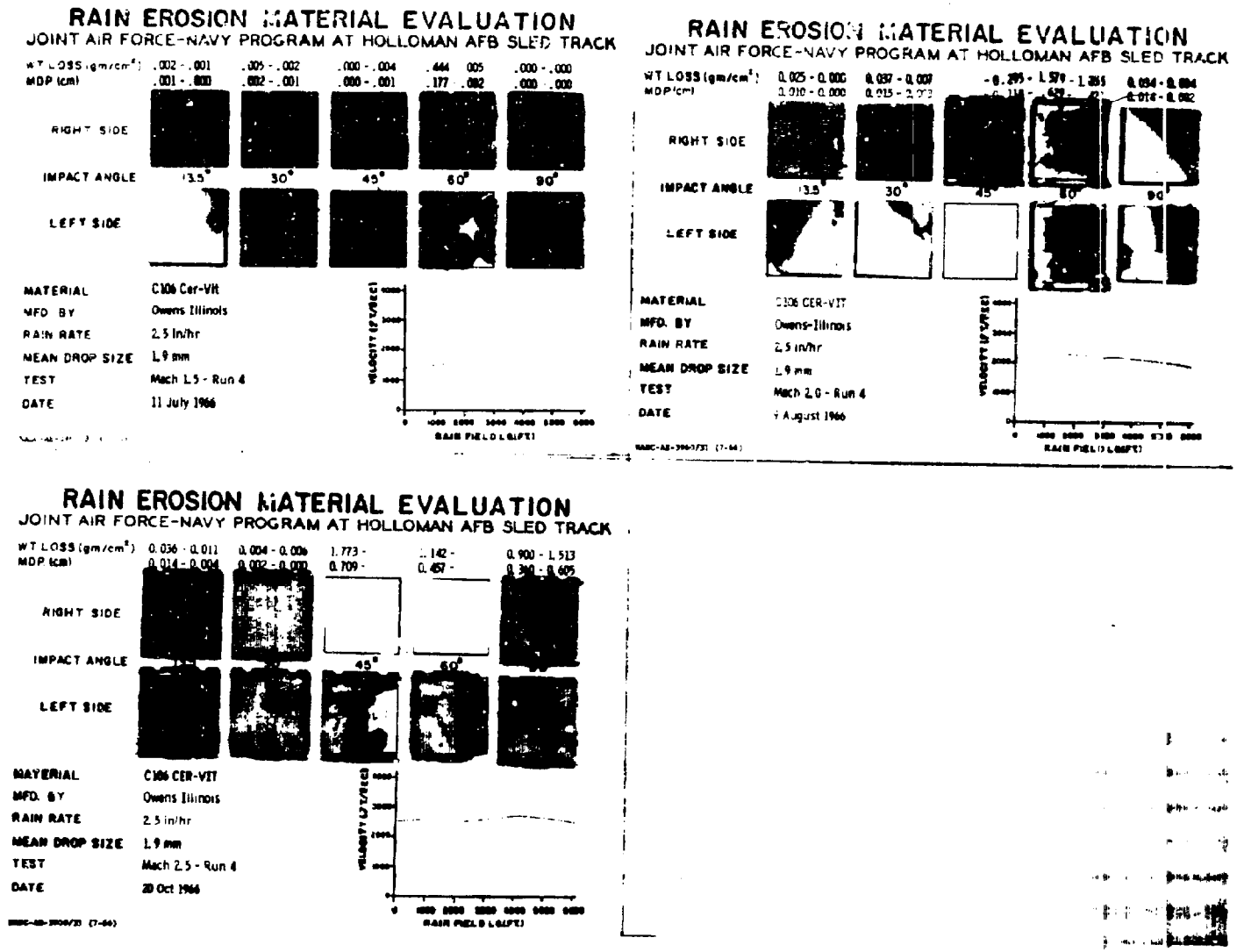

Figure 78. Rain Erosion Damage Data for C106 CER-VIT Glass

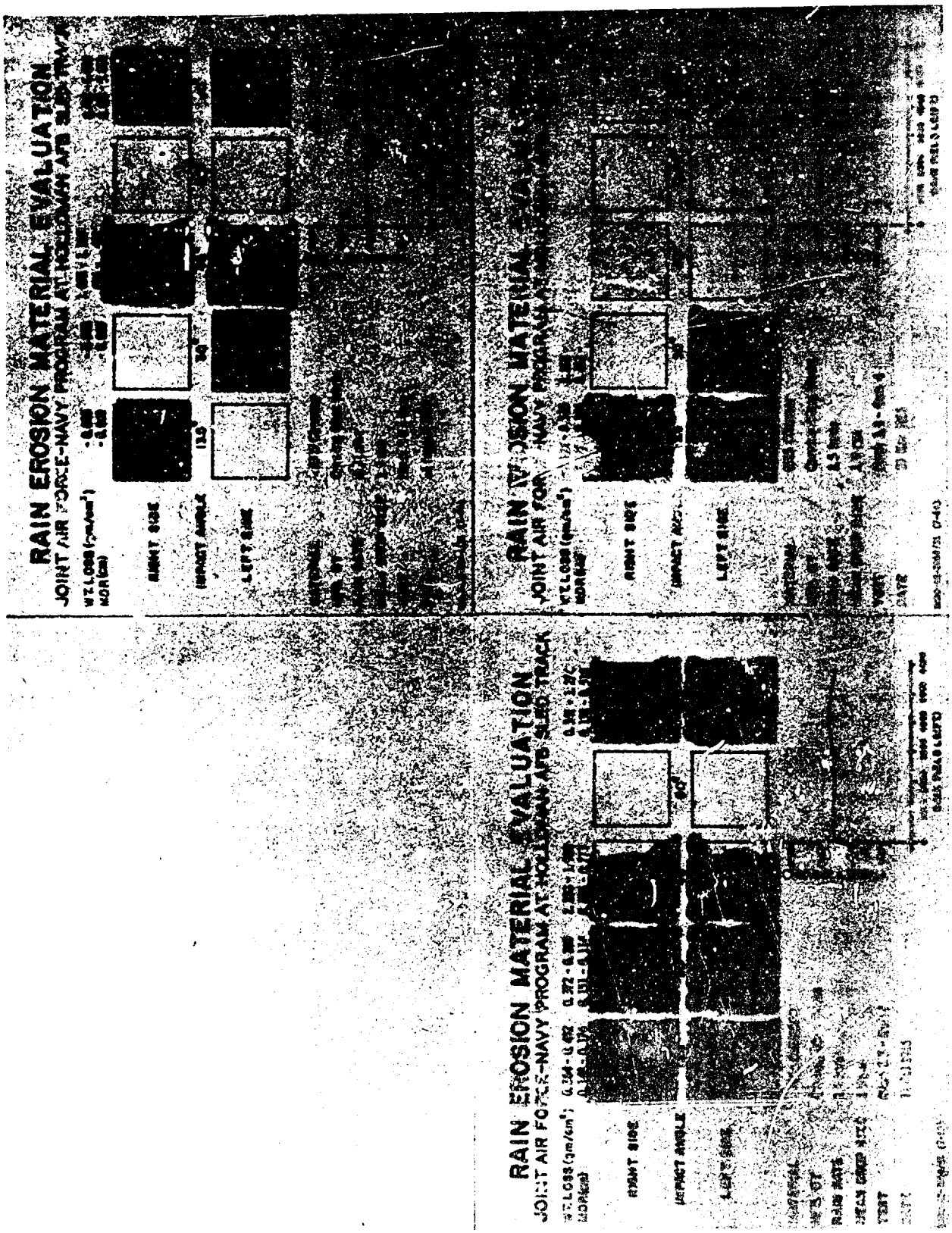

Figure 79. Rain Erosion Damage Data for 0315 Chemcor Glass

Best Available Copy

PRECEDING PAGE BLANK - NOT FILMED.

8. CLASS H - SANDWICH PLASTICS

H-1, H-2, H-3 Honeycomb Sandwiches

In the interest of trying to develop some quantitative data for lightweight plastic and metal sandwich structures, the materials H-1, H-2, and H-3 were included for evaluation.

Material H-1 consists of a preformed 0.030 inch autoclaved skin having 3 plys of No. 181 cloth. The overexpanded core was then bonded to the skin. The resin system is Furane 8265 epoxy. A 0.010 inch sprayed Gaco coating was then applied.

Material H-2 uses a 0.020 inch preformed Polyimide skin bonded to a 3/16 inch cell polyimide core material. No coating or sealer has been used on the face of the samples.

The H-3 material is a structural sandwich made from 0.010 inch 6-4 titanium skins and 3/16 inch polyimide core honeycomb.

The 8265 Furane epoxy sandwich showed better rain erosion performance than the polyimide sandwich. This would be expected inasmuch as the skin thickness was greater for the Furane epoxy; but modulus and strength are also higher for the epoxy systems. Although the data for these two plastic composites is not plotted, the card photographs qualitatively show the effects of both velocity and angle.

The 0.010 inch 6-4 titanium skin/polyimide honeycomb combination, while not eroded, was highly susceptible to drop impact damage at the higher velocities and angles. It is likely that this combination could be greatly improved by using 0.015 to 0.020 inch outside skin thickness and a 1/8 inch cell honeycomb with stronger cell walls.

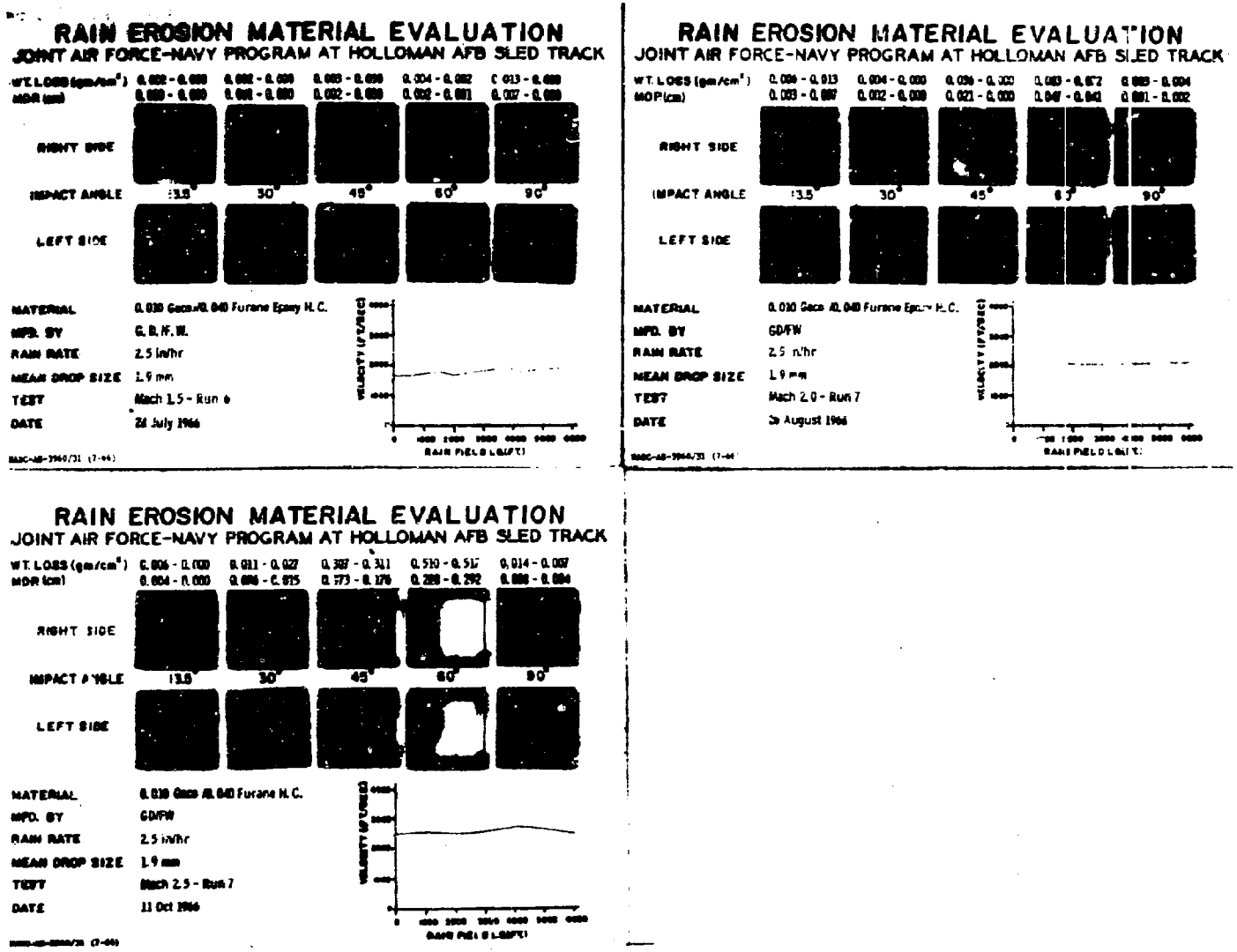

Figure 80. Rain Erosion Damage Data for 0.010 Inch Gaco/0.040 Furane Epoxy Honeycomb

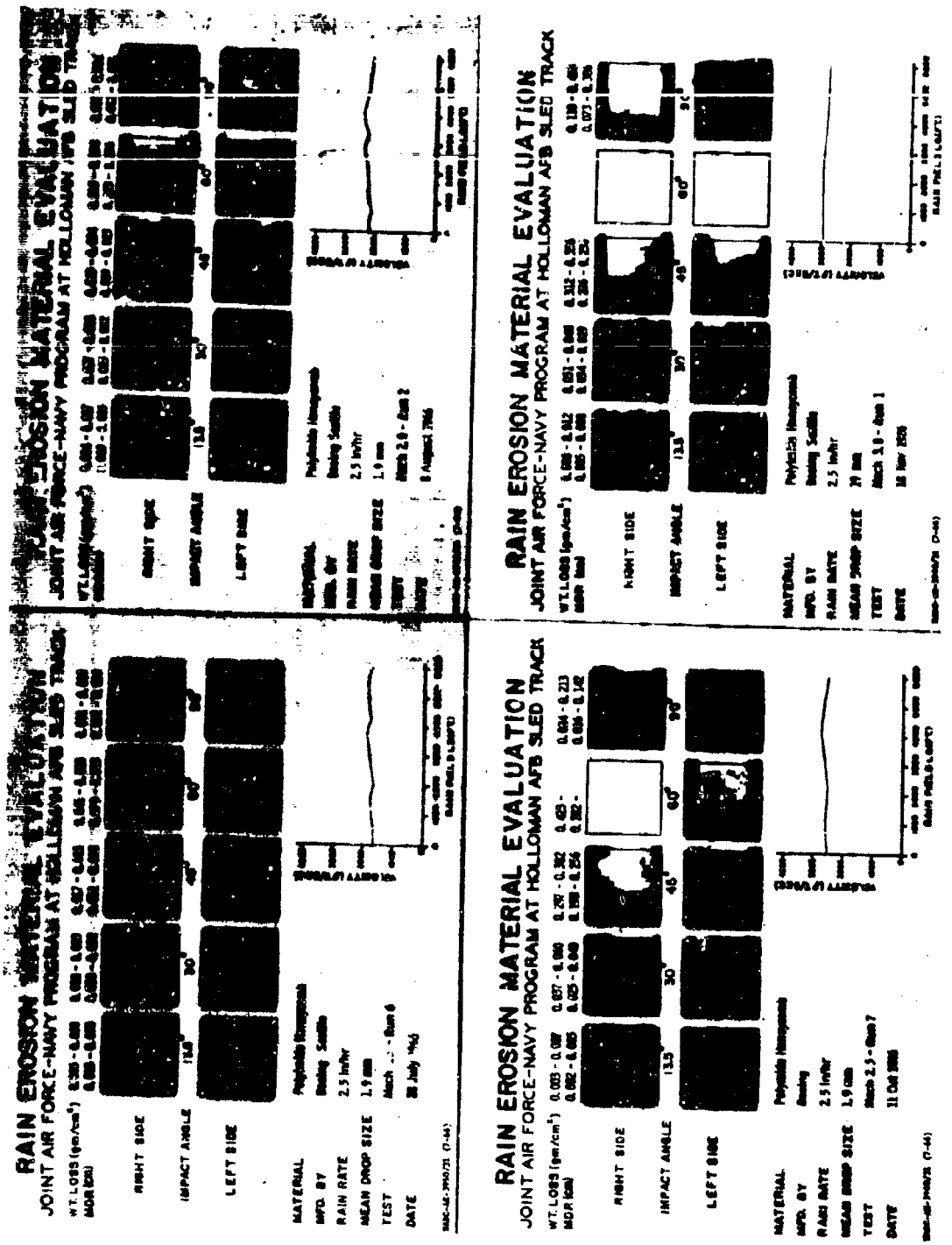

Figure 81. Rain Erosion Damage Data for Polyimide Honeycomb

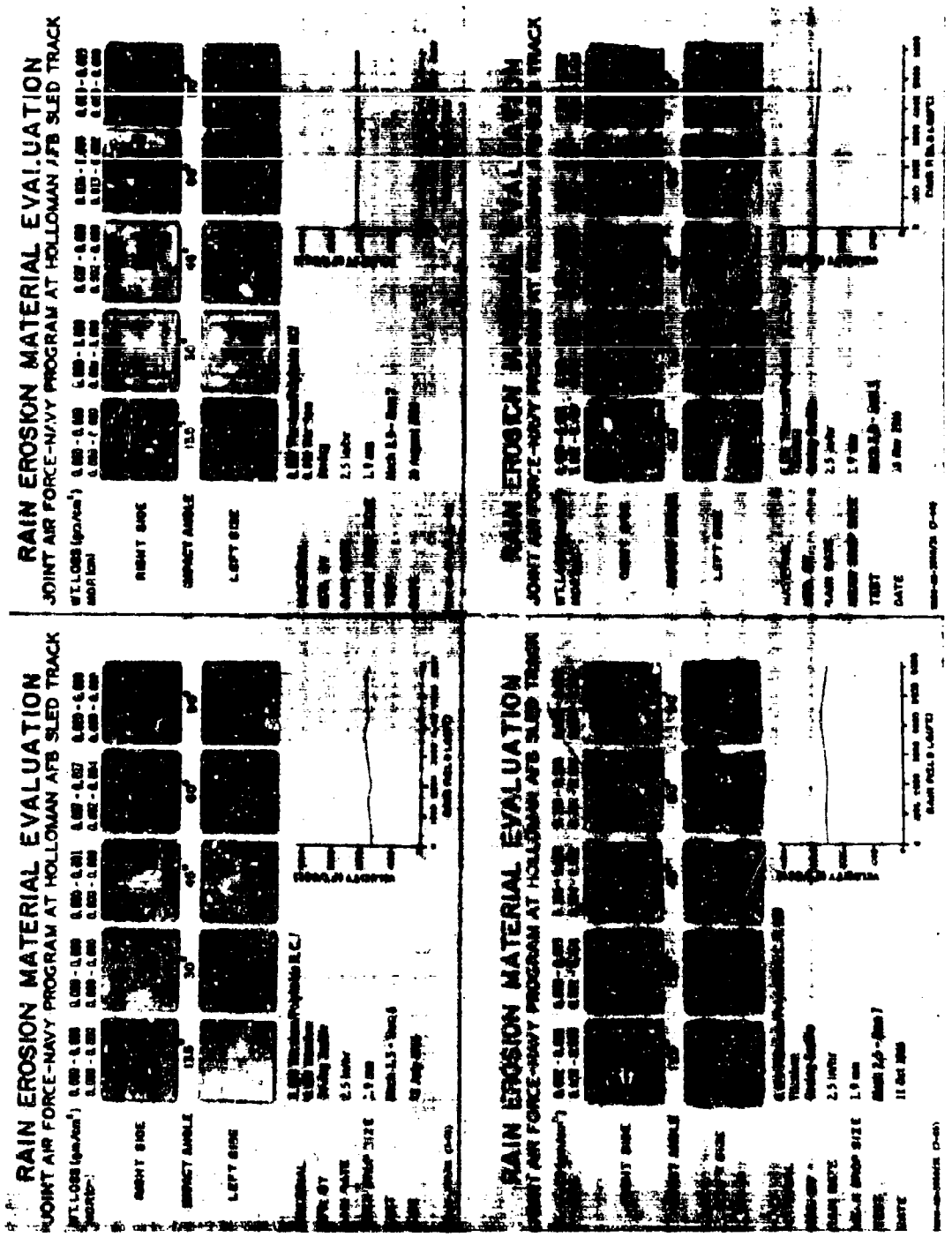

Figure 82. Rain Erosion Damage Data for 0.010 Inch Titanium/Polyimide Honeycomb/0.010 Inch Titanium

H-4 and H-5 Teflon or Cork/Nomex Epoxy Laminate

Ablative coatings which char at uniform rates to give a protective layer are widely used for thermal protection of high temperature missile and reentry systems. Two materials with good ablative characteristics are Teflon and cork. Thin coatings of these materials over an epoxy laminate such as the Nomex were selected for exposure to rain.

Teflon sheet was supplied by AFML and adhesively bonded with an epoxy to a Nomex epoxy laminate from Boeing/Aerospace Division. A coating of Armstrong Cork AC-2755 sometimes used as an ablative material over the Nomex epoxy laminate was also furnished by Boeing.

Teflon and cork have exhibited poor erosion resistance subsonically and this was borne out by the supersonic exposures. The cork coating was more severely damaged at each velocity than the Teflon and this was expected because of its high porosity and lack of strength. It can be stated unequivocally that cork has very poor rain erosion resistance for exposure angles above 15° at velocities of Mach 2.0 or greater.

The erosion resistance of cork and Teflon is very low by comparison with other coatings like neoprene and polyurethane. The adhesive bond of both materials to the Nomex epoxy was satisfactory.

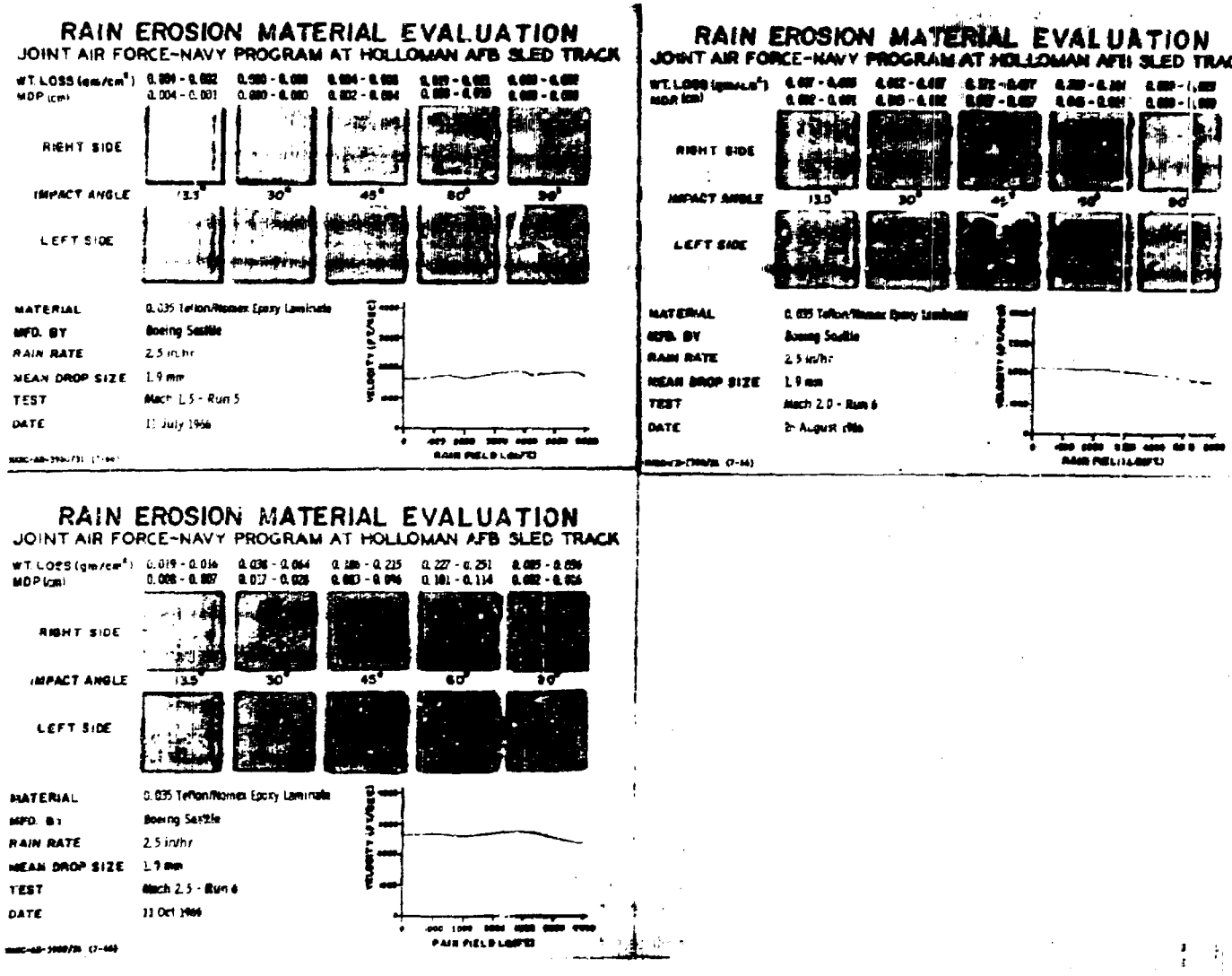

Figure 83. Rain Erosion Damage Data for 0.035 Inch Teflon/Nomex Epoxy Laminate

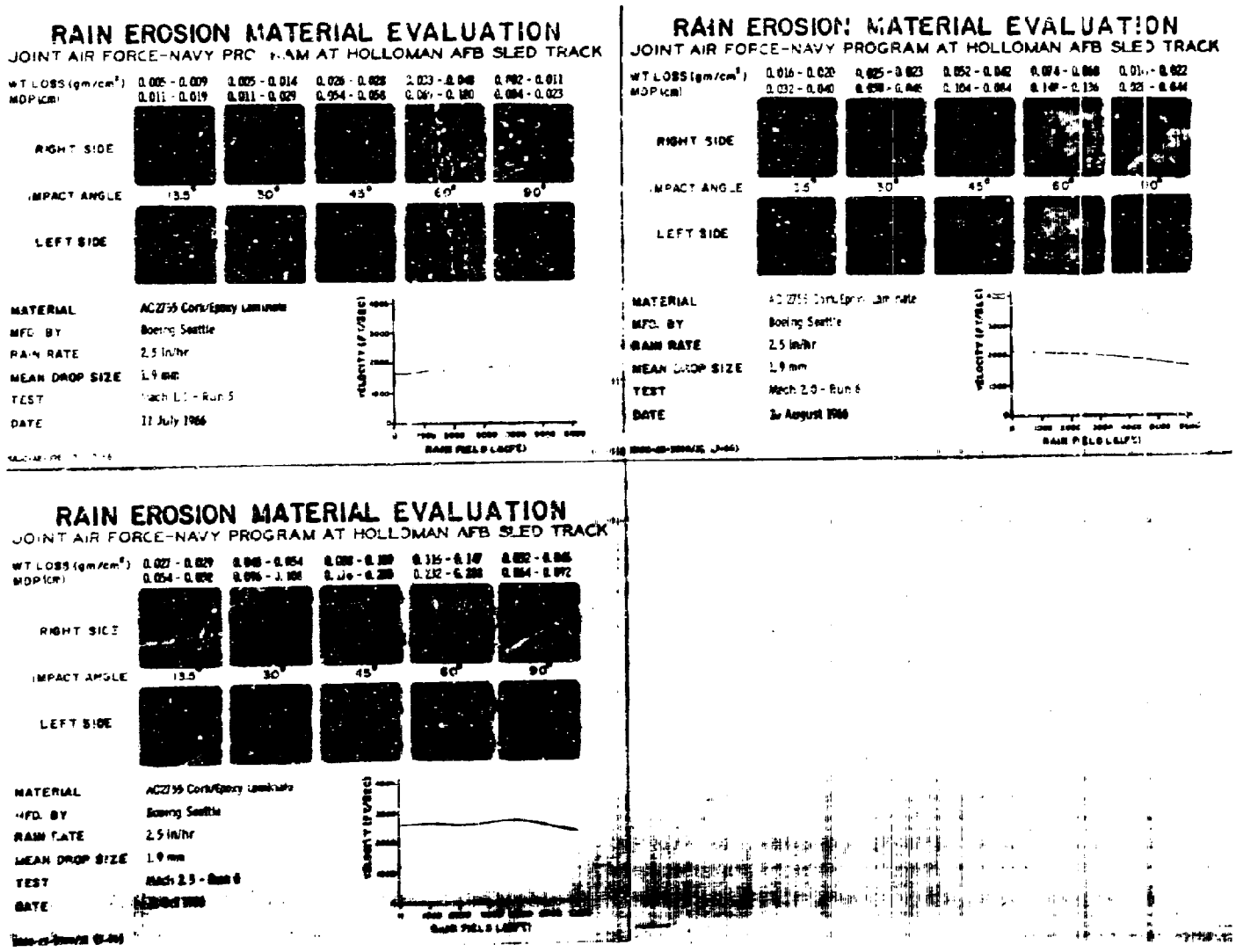

Figure 84. Rain Erosion Damage Data for AC-2755 Cork/ Epoxy Laminate

PRECEDING PAGE BLANK - NOT FILMED.

H-6 0.010 Inch Electroplated Nickel/Epon 828 Epoxy Laminate

Not all laminate structures need be electrically transparent for radar purposes. For structural applications where metal coatings are permissible, such as lightweight, high speed compressor blades, the use of nickel plated coatings is feasible. In a recent research effort (Reference 9), the Air Force Materials Laboratory developed nickel coatings which can be plated directly on the laminate itself. This plating is accomplished by sensitizing the laminate surface, making it conductive with electroless copper and then electrolytically depositing nickel on the copper. The erosion resistance of these coatings is highly dependent on thickness and 0.010 inch was selected as a representative thickness.

Subsonic evaluations of these nickel coatings have indicated 10 times the resistance over the elastomeric and ceramic coatings. The ductility of the nickel (elongation up to 20%) is felt to be responsible for this resistance.

The electroplated nickel coatings were the most erosion resistant thin (40 mils or less) coatings at supersonic velocities. At Mach 1.5 and 2.0 the coatings appeared unexposed after their firings. At Mach 2.5 specimens at all positions except 60° appeared the same way. At 60° the surface of the nickel had been deformed and ridges appeared where it had been pushed up by the radially flowing water. This phenomenon was also observed on the polyphenylene oxide plastic which likewise was deformed on the surface. The 60° nickel plated samples had lost adhesion but were not penetrated by the water drops.

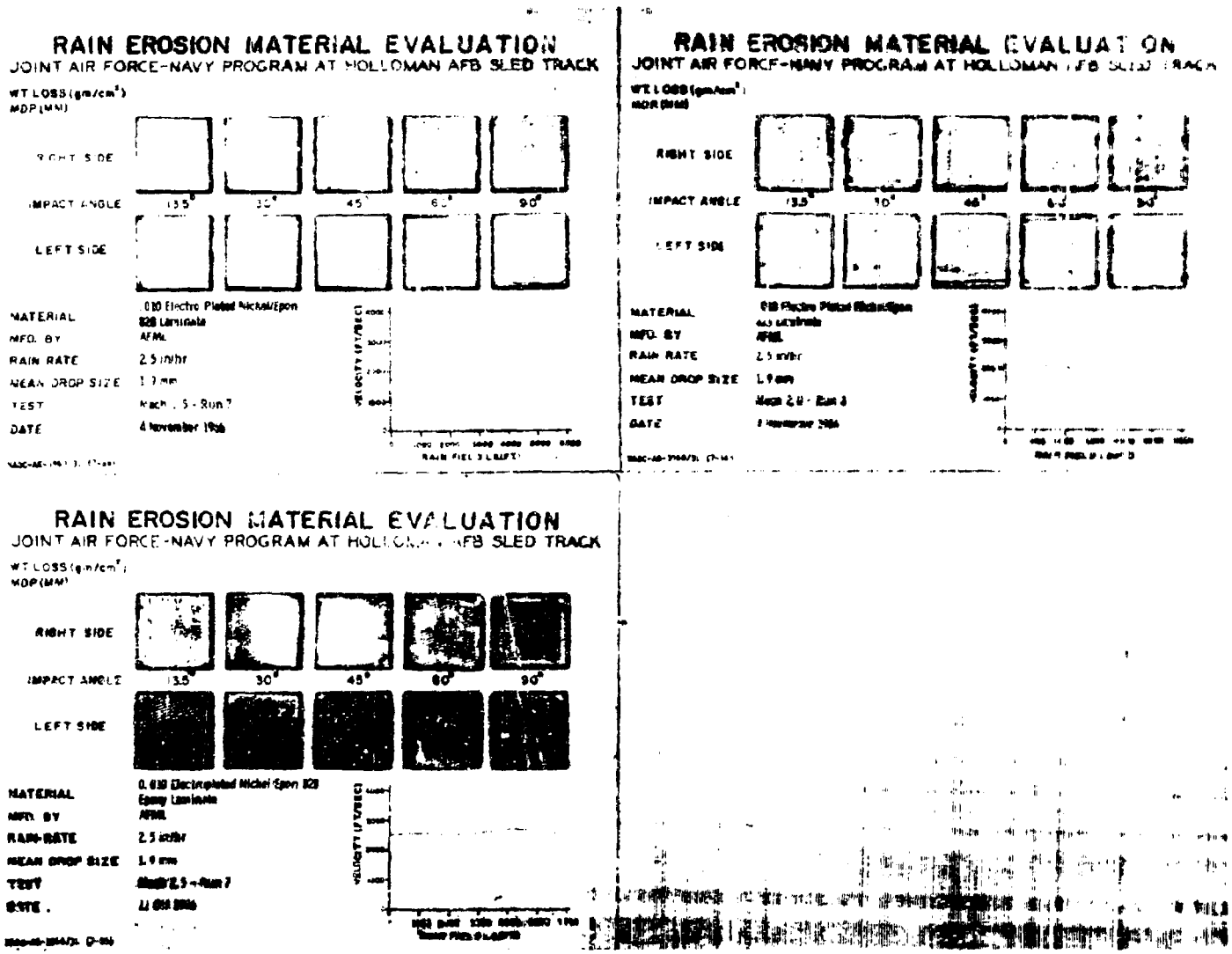

Figure 85. Rain Erosion Damage Data for 0.010 Inch Electro Plated Nickel / Epon 828 Laminate

9. CLASS I - THERMAL PLASTICS

I-1 Polyphenylene Oxide (PPO)

An interesting new thermoplastic material which has been recently developed is the polyphenylene oxide of General Electric. This material has good mechanical properties with tensile modulus of 370,000 psi and low creep properties. The electrical properties are also quite good with low dielectric constant and loss tangent.

The material selected for evaluation was grade 531-801 which was light beige in color. This material had a shear strength of 10,900 psi which is reasonably high for a plastic. The specimens were furnished by General Electric.

The polyphenylene oxide plastic resisted the erosion completely below Mach 2.5 with only superficial deformation of the surface and no weight loss at Mach 2.5. This resistance was most surprising and one of the significant developments of these evaluations. The slight distortion of the surface was much like that of the plated nickel. It is believed the high shear strength of the PPO is largely responsible. In general, results were promising enough to warrant evaluations up to Mach 5.0 and the use of this resin for laminating purposes and possibly as a thin protective coating.

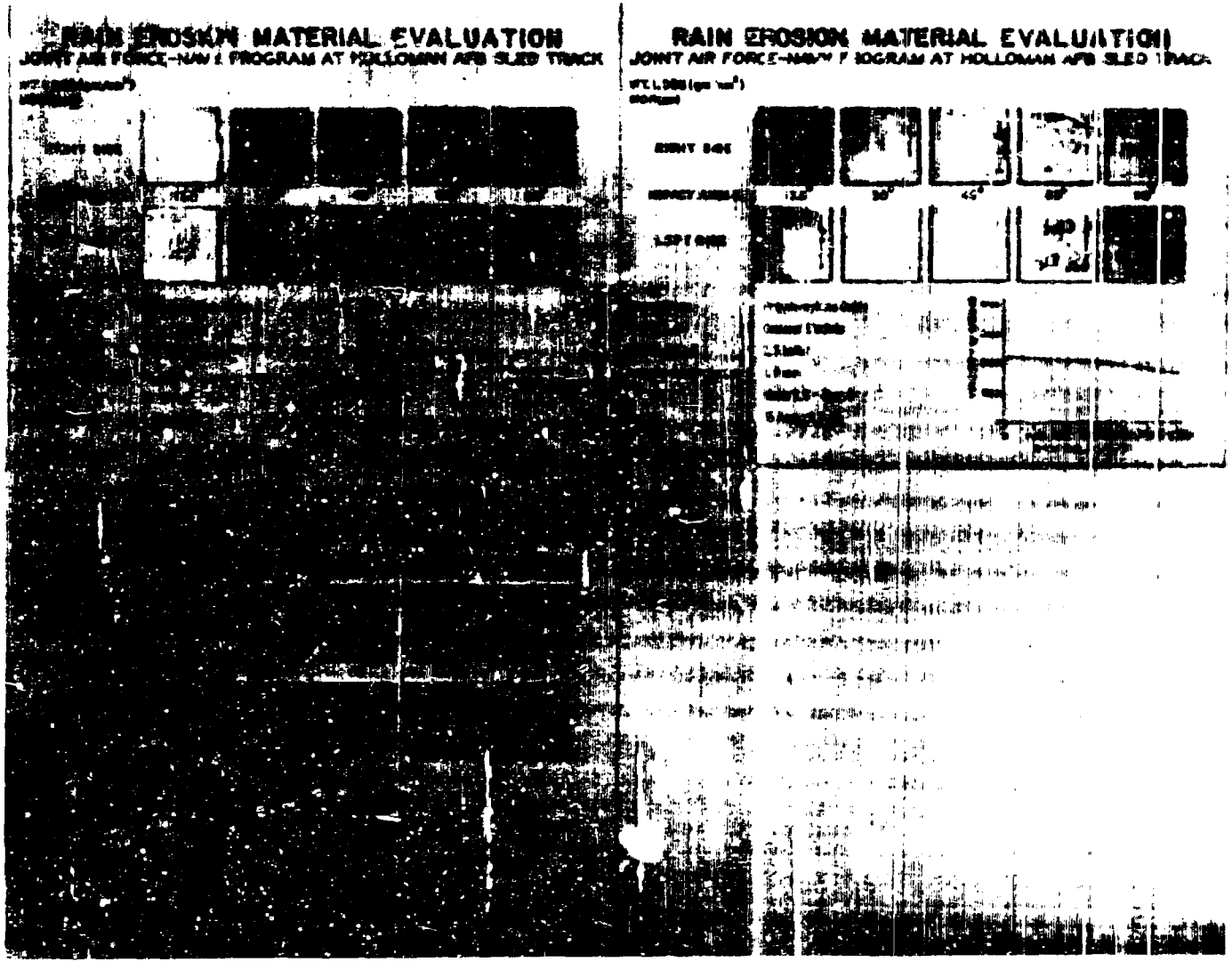

Figure 86. Rain Erosion Damage Data for Polyphenylene Oxide

1-2 Polymethylmethacrylate (Plexiglas)

Polymethylmethacrylate (Plexiglas) has been used for years as an erosion reference material because of its uniform composition. The type evaluated in this series was Type II-UVA of Rohm & Haas Company which conforms to Mil Spec-P-5425B. The specimens were furnished by AFML. This is the same grade of Plexiglas used for the calibration runs at each velocity.

The material has zero porosity, a density of 1.19 and moderate physical properties. Its widespread application for a variety of purposes makes it of interest for rain erosion, particularly with its use in low speed aircraft canopies.

The erosion of Plexiglas is in the form of chipping into granules. This increases with angle of impact and velocity. At Mach 1.5 the 60° specimens are surface damaged with no weight loss. The damage at Mach 2.0 is noticeable at 60°, very minor at 45°, and slight otherwise. At Mach 2.5, the erosion was progressively greater.

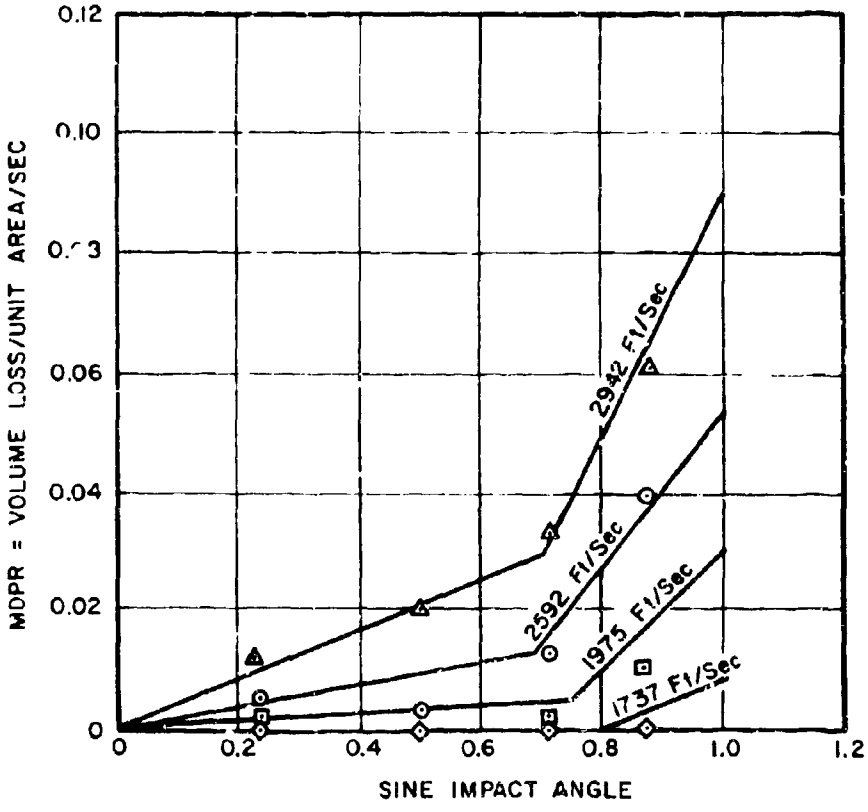

Figure 87. MDPR vs Sine Impact Angle - Plexiglas

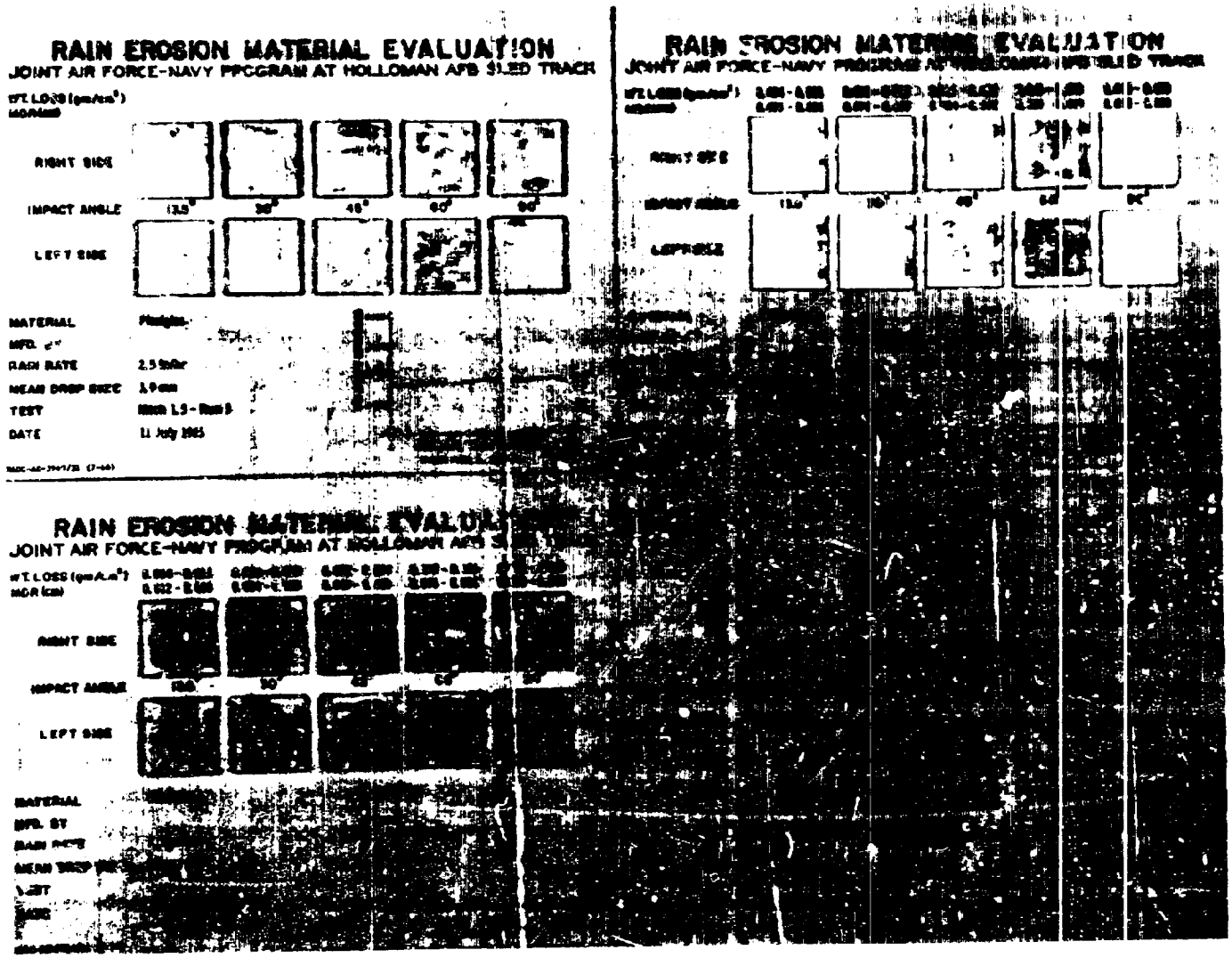

Figure 88. Rain Erosion Damage Data for Plexiglas

I-3 Teflon (TFE)

Bulk polytetrafluoroethylene (Teflon) was selected for evaluation because of its many uses as an ablator protective covering, and gasket or seal material. The Teflon evaluated was similar to the thin coating applied over epoxy laminates (Specimen H-4).

The material has a density of 2.25 and physical properties which are poorer than Plexiglas.

The erosion of Teflon is relatively uniform and was considerable even at Mach 1.5. With increasingly greater penetration at higher velocities, the Teflon rates as the poorest thermal plastic evaluated.

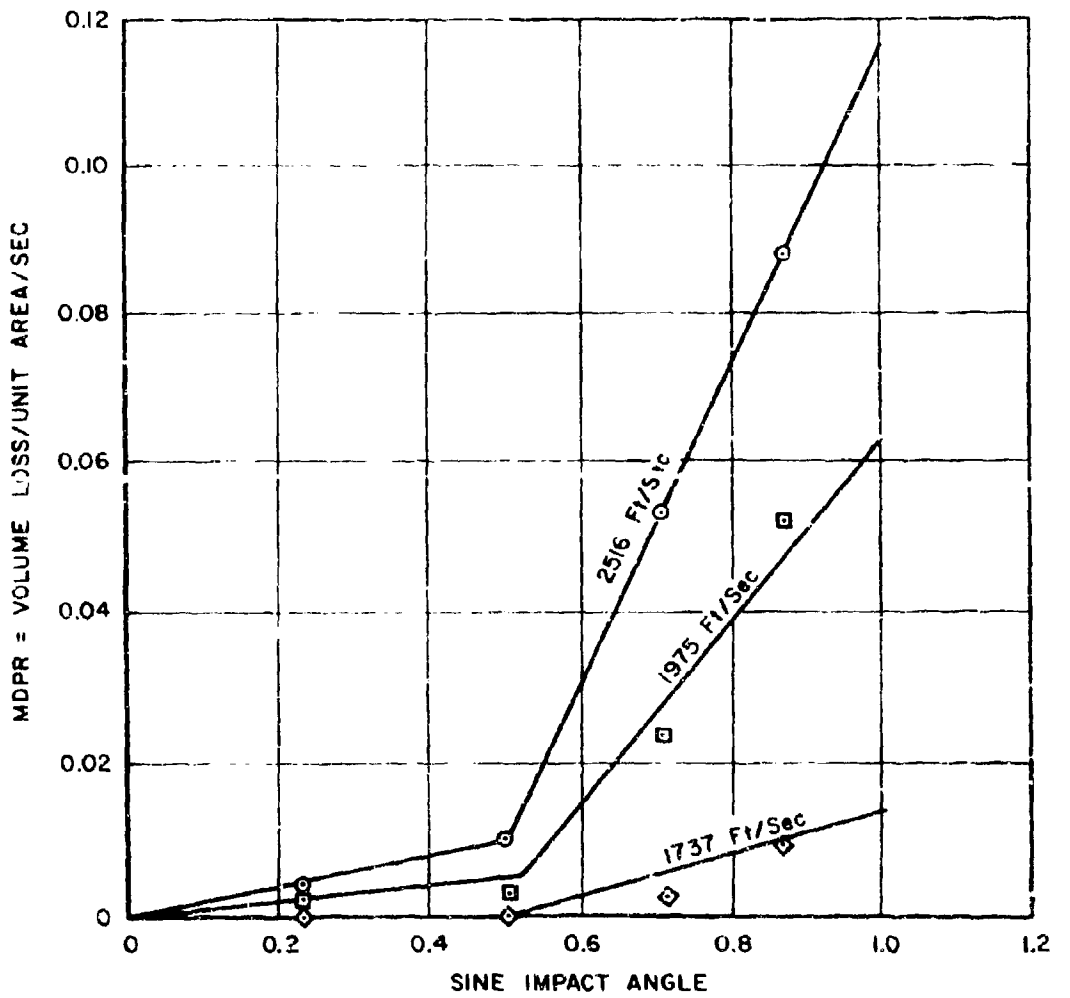

Figure 89. MDPR vs Sine Impact Angle - Teflon

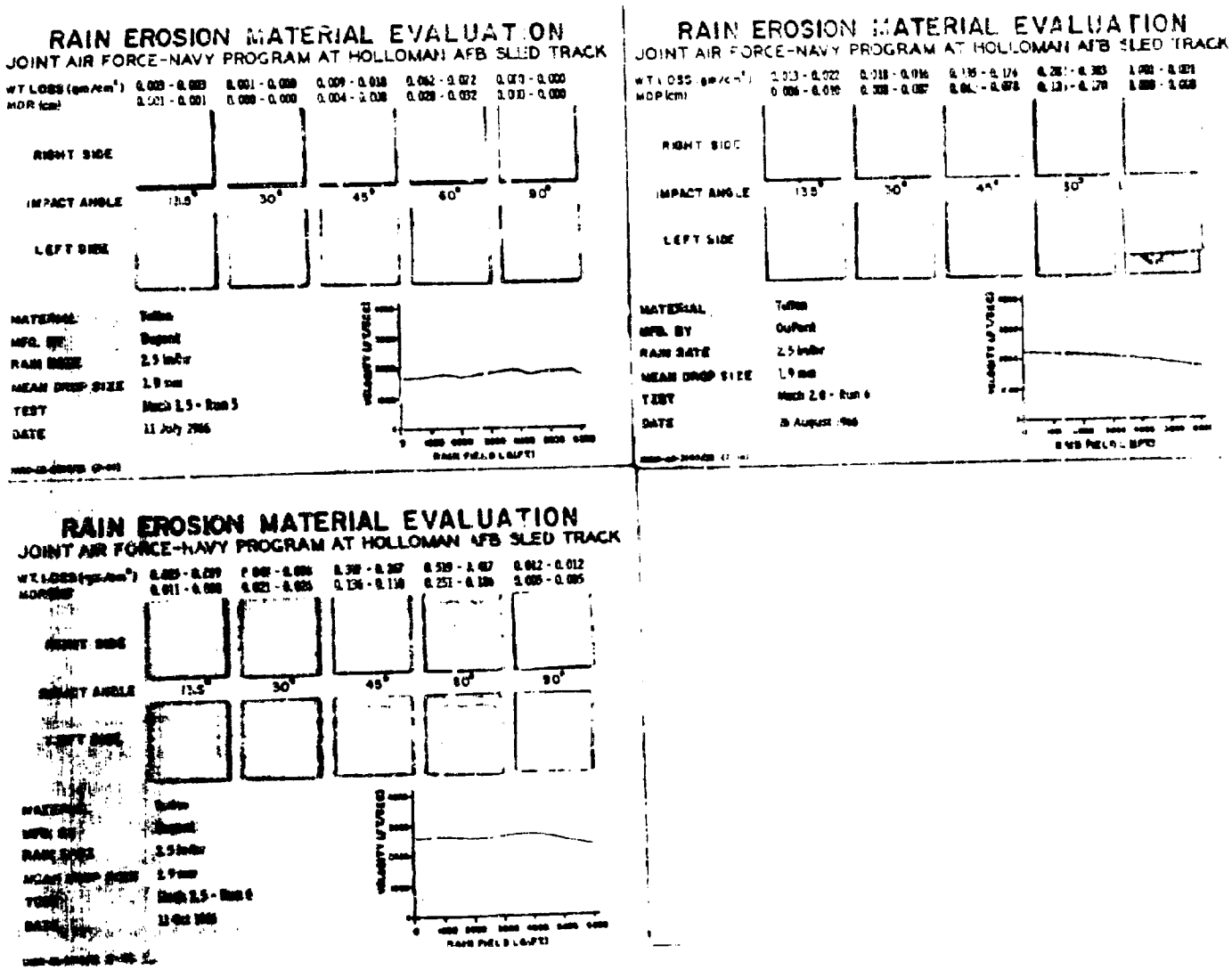

Figure 90. Rain Erosion Damage Data for Teflon

10. CLASS J - METALS

J-1, J-2, J-3 Aluminum and Copper

Two aluminum alloys and annealed copper were selected for the program. The aluminum alloys are 2024-T3, widely used in aerospace vehicle construction, and 6061-T6, a weldable alloy. The annealed copper was selected to include one softer more ductile metal. These metals are of special interest to researchers in the field of cavitation damage for some possible correlation with rain erosion damage.

Of the two aluminum alloys the 2024-T3 aluminum is harder and has greater yield and tensile strengths. It also has somewhat greater ductility. The annealed copper has lower tensile strength but much greater ductility.

All three metals were run at all Mach numbers up through Mach 3.0. Post-run sample processing showed no weight losses with the exception of very small losses for the 6061-T6 at Mach 3.0. At the higher Mach numbers and impact angles these materials did experience a change of surface condition which is best termed as roughening.

The surface of the copper was measurably compressed and dented. The high ductility allowed the surface layer to work harden. Greater exposure times or higher velocities obviously would result in loss of material.

The test results for the metals cannot be graphed as was possible for most other materials.

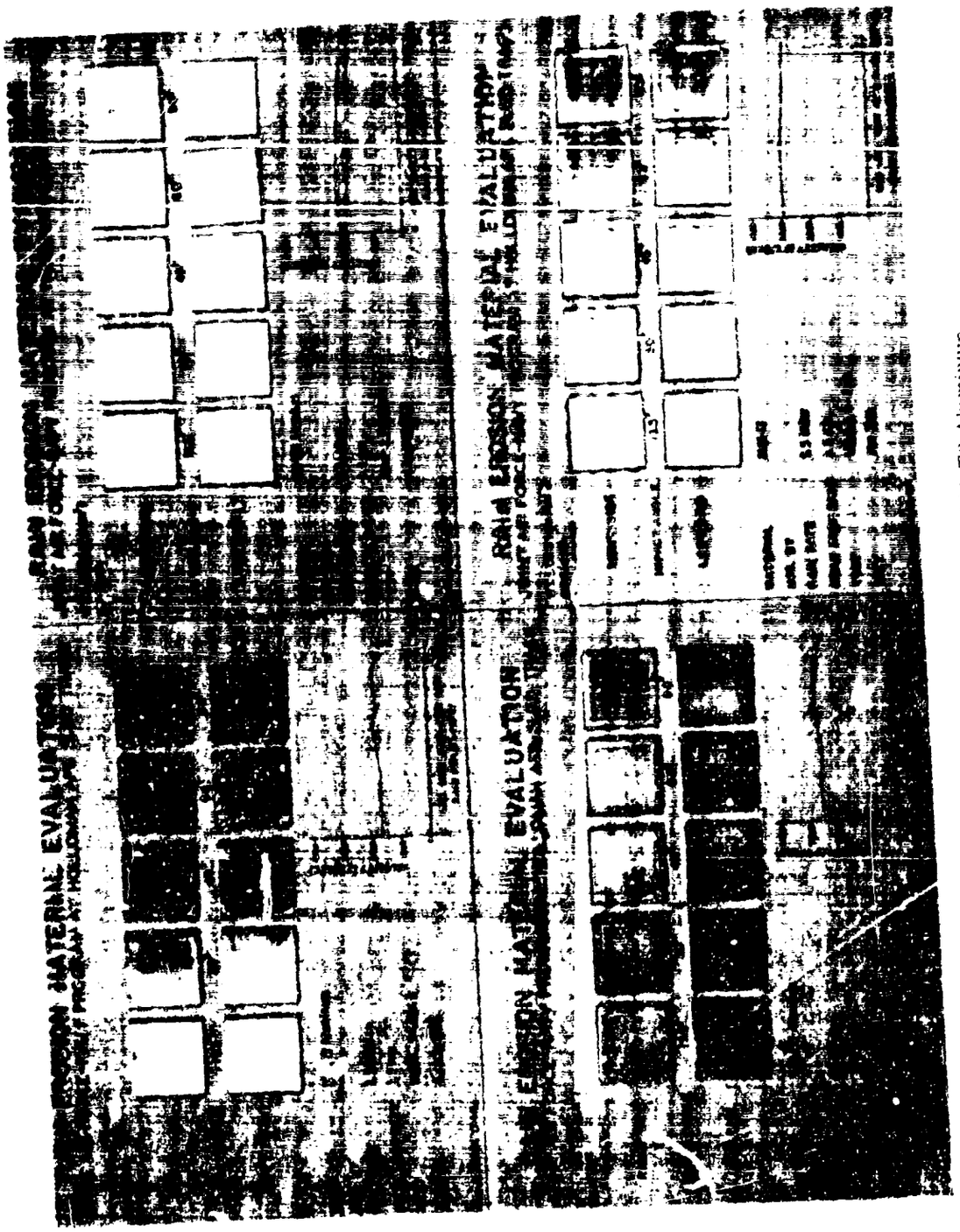

Figure 91. Rain Erosion Damage Data for 7024-T3 Aluminum

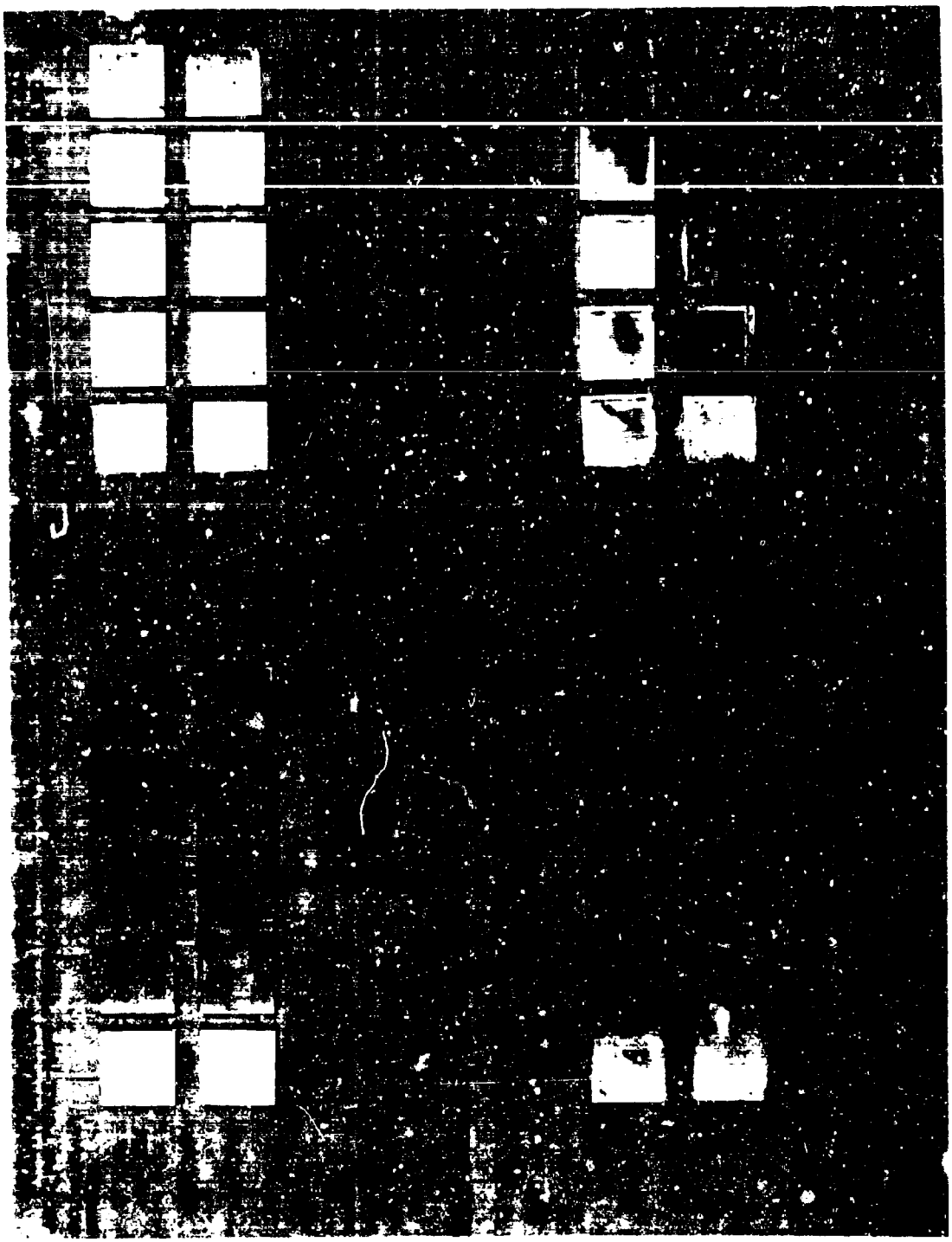

Figure 92. Rain Erosion Damage Data for 6061-T6 Aluminum

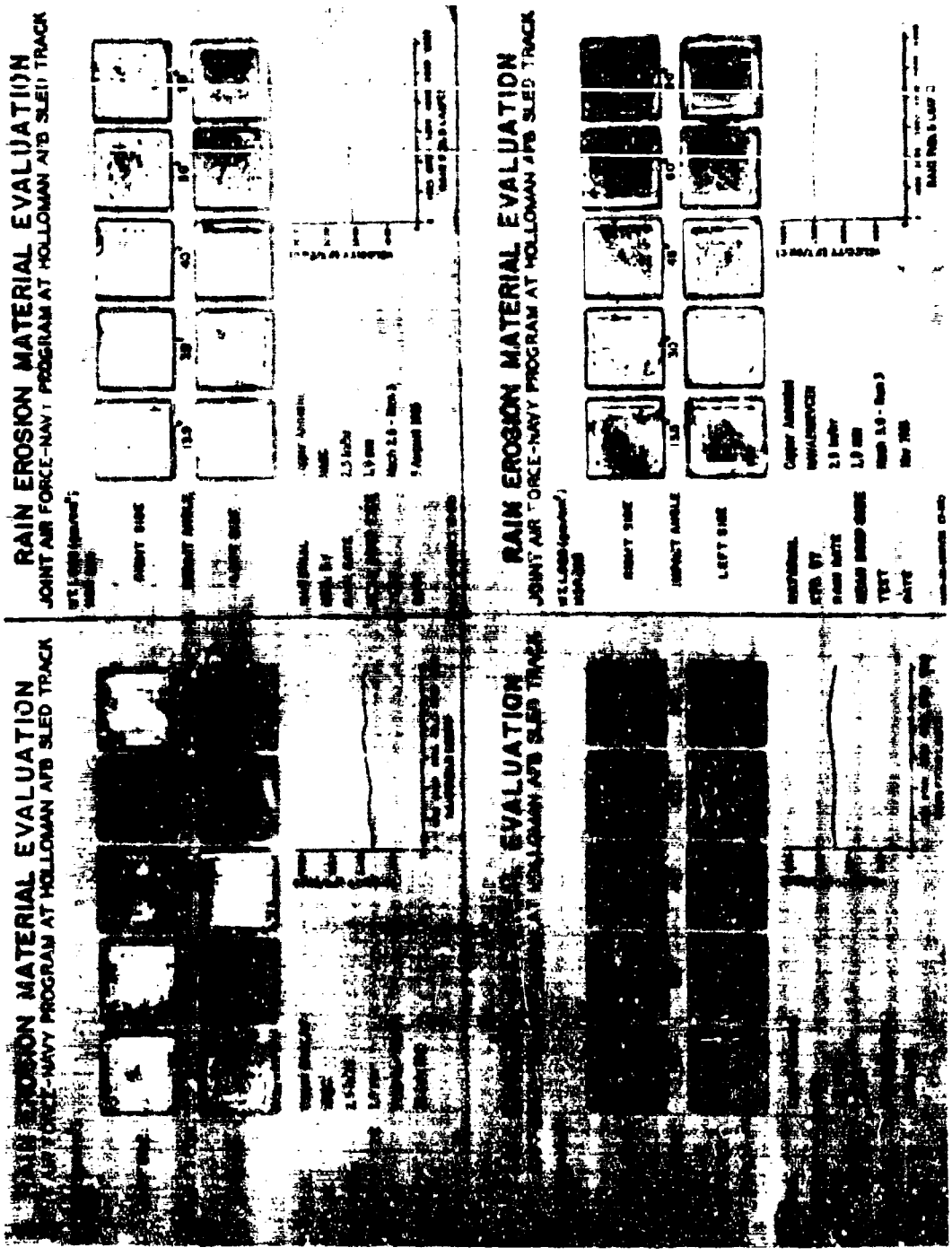

Figure 93. Rain Erosion Damage Data for Annealed Copper

SECTION IX

DISCUSSION OF RESULTS

It must be emphasized that the exposures in these evaluations were for short periods only but even these brief encounters with the rain were sufficient to indicate considerable differences in the supersonic rain erosion resistance of various materials. The average velocities and times in rain for each of the four Mach numbers were as follows:

Mach Number	Average Velocity (ft/sec)	Average Time in Rain (sec)
1.5	1613.6 (8 runs)	3.72
2.0	2126.4 (9 runs)	2.82
2.5	2484.4 (8 runs)	2.41
3.0	3047.8 (4 runs)	1.97

The alumina and beryllia isotropic ceramics were expected to be highly resistant to rain impingement supersonically based on previous studies and they were found to be usable at all angles of impingement up to Mach 3.0. The cordierite was useful for angles below 60° up to Mach 3.0 and the fused silicas were limited to 30° and below at all velocities.

The sandwich ceramic construction is not suitable for supersonic applications where rain will be encountered. The foam core which gives lightweight and good electrical characteristics also contributes to failure in rain by virture of its low strength.

The erosion of the plastic laminates was increasingly severe with greater impingement angle and higher velocities. The discontinuity in the plots of erosion rate (mean depth of penetration rate) as a function of the sine of the impact angle may be explained as follows. The low rates initially result from a gradual eroding away of the surface resin until a point is reached where the laminate plies are penetrated and a greater rate of erosion occurs. This penetration of the upper resin layer occurs more rapidly at smaller angles with increasing velocity and hence the increasing rate at higher speeds. The resins such as PBI and polyimide which result in "dry" laminates also erode more rapidly than do epoxy laminates because of a lack of outer resin layer and hence quicker penetration of the plies. This lack of surface layer is also true for the inorganic laminates.

All laminates should be covered with a protective coating for supersonic applications. In general, they are useful uncoated at 15° impingement angles or less but exhibit increasing damage at 30° and above at Mach 2.0 or greater. The epoxy laminates are not damaged severely in any position after one exposure at Mach 1.5. However, they would be eroded with further exposure at this velocity.

Ceramic coatings demonstrated limited protectiveness for laminate substrates in a supersonic rain environment. Casting, flame spraying, and plasma spraying are effective ways of preparing these coatings. However, unless the surface of the sprayed coating is treated chemically or impregnated with a sealer of some kind, the ceramic coated laminates are eroded at angles of 45° and above, even at Mach 1.5. The reduction of coating porosity and the quality of ceramic-laminate adhesion are the most important factors in erosion resistance. With proper preparation ceramic coatings are erosion resistant at angles of 60° or less up to Mach 2.0.

If the exposure time is short enough at Mach 1.5, the elastomeric coatings such as neoprene and urethane are resistant to rain erosion. However, at Mach 2.0 or faster even 2 seconds was sufficient to erode completely through the 60° specimens. The positions which were damaged at Mach 2.5 were all angles of 45° or more. The damaging effect of drop impingement at the higher incidence angles is not mitigated at all by thicker elastomeric coatings; the damage is comparable for thicknesses of a particular material up to 30 mils. The shear and impact stresses are of such a magnitude at Mach 2.0 and above that they are transmitted through any of these coatings to the laminate, breaking the bond and initiating erosion.

Surface strengthening of glasses improves their properties for conventional applications but it does not enhance their supersonic rain erosion resistance. The catastrophic failure once rain penetrates the surface layer is so extreme that these glasses would have utility only in designs of less than 13.5° incidence angle.

Honeycomb structures even with very strong skins possess poor erosion resistance for the same reasons as the sandwich ceramics. The physical properties of ablative coatings are so low that they have poor subsonic erosion resistance as well as poor supersonic resistance.

The use of electroplated nickel coatings applied directly to plastic laminates is a definite improvement for protection of surfaces where radar compatibility is not a concern. These coatings were unaffected at all impingement angles at Mach 1.5 and 2.0, and only the 60° specimens began to lose adhesion at Mach 2.5.

The erosion resistance of polyphenylene oxide at Mach 2.5 and below was somewhat unexpected because its overall physical strengths are not greatly different from Plexiglas. However, its shear strength of 10,900 psi is higher than the other thermal plastics and thus imparts "ductility" to the bulk plastic.

The ductility of annealed copper and the aluminum alloys enables their surfaces to be considerably deformed without measurable weight losses. These metals would eventually be pitted with material loss after longer rain exposure times at supersonic velocities.

SECTION X

CONCLUSIONS

1. CLASS A - ISOTROPIC CERAMICS

The highly dense alumina and beryllia were the most erosion resistant materials evaluated. Other ceramics ranked in decreasing order after them: Pyroceram 9606, cordierite and fused silica. Erosion rate equations were developed for the fused silica materials. The density and compressive strength of the alumina and beryllia are believed to contribute to their erosion resistance.

2. CLASS B - SANDWICH CERAMICS

The sandwich ceramics are inherently low in supersonic rain erosion resistance because the low compression strength of the foam core permits the dense skin to fail by impact fracture.

3. CLASS C - PLASTIC LAMINATES

Epoxy laminates were found to be the most erosion resistant laminate construction. Other organic and semiorganic laminates were decreasingly resistant as follows: polyimide, polybenzimidazole (PBI), and silicone. Erosion rates (mean depth of penetration per second) were discovered to be directly proportional to the normal component of the impact velocity (sine of the impact angle) and exponentially proportional to the velocity itself. Constants were determined for equations describing the erosion of these plastic laminates in a supersonic rain environment.

4. CLASS D - INORGANIC LAMINATES

Inorganic laminates were found to be less resistant than any of the organic or semiorganic laminates. This may be attributed to their lower strength.

5. CLASS E - CERAMIC-COATED LAMINATES

The porosity of ceramic coatings and the strength of the laminate substrate are the most important factors in the erosion resistance of the overall composite. Sealing of the pores can be effectively accomplished by physical impregnation with a resin or by chemical treatment of the surface. The coating-laminate interfacial adhesion is another important factor. Precasting, plasma spraying, and flame spraying have been shown to be effective techniques for producing erosion resistant ceramic coatings.

6. CLASS F - ELASTOMERIC-COATED LAMINATES

Elastomeric coatings have exhibited good erosion resistance at Mach 1.5 for very short exposure times. The effect of coating thickness on erosion protection is negligible at Mach 2.0 and above with 0.010 inch elastomeric coatings offering as much protection as 0.030 inch coatings. The quality of the bond is very important in the protection provided by these coatings.

7. CLASS G - GLASSES

The glasses are characterized by less erosion resistance than the ceramics and catastrophic failure upon exposure to rain supersonically. This failure is intensified by internal stress relieving after the surface compression layer is degraded. The greater the strength of these glasses, the more catastrophic is their failure.

8. CLASS H - SANDWICH PLASTICS

Honeycomb sandwiches are poor in erosion resistance because of weaknesses inherent in the thin-skin-over-cellular structure. Thicker skins, smaller cells, and thicker cell walls improve the erosion resistance in a limited manner.

Ablative coatings such as cork and Teflon are poor in erosion resistance because of high porosity and low strength.

Electroplated nickel coatings are the most erosion resistant thin coatings over laminates evaluated. The ductility of the nickel is responsible for its supersonic rain erosion protective ability.

9. CLASS I - THERMAL PLASTICS

Polyphenylene oxide resists supersonic erosion because its high shear strength enables considerable surface deformation and rearrangement without measurable erosion. Plexiglas and Teflon in bulk form are eroded because of low shear strength.

10. CLASS J - METALS

Soft ductile metals such as aluminum alloys and copper are damaged by supersonic rain impact but, for short exposure times, this damage takes the form of denting and surface deformation without material weight loss.

PRECEDING PAGE BLANK - NOT FILMED.

SECTION XI

FUTURE WORK

1. The velocity range of evaluations will be extended to Mach 4 and Mach 5 for the isotropic ceramics, thermal plastics, metal coatings, and bulk metals.

2. A series of repeated runs on particular materials will be made at a specific velocity (Mach 1.5) to accumulate exposure time on these materials for comparing damage at longer times at lower velocity with short times at high velocity.

3. New improved materials such as pyrolytic boron nitride in the isotropic ceramics class and polycarbonate in the thermal plastics class will be evaluated. Metals such as titanium and A-1100 pure aluminum will be evaluated along with improved urethane elastomeric and other ceramic coatings. Increased emphasis will also be placed on glasses because of problems with these materials.

TABLE I

PROPULSION SYSTEMS

Mach Number	Boost		Sustain		
	1st Stage	2d Stage	1st Stage	2d Stage	3d Stage
1.5	1 Genie	-	2 M-58	2 M-58	2 M-58
2.0	1 Nike	-	3 M-58	3 M-58	-
2.5	1 Genie	1 Genie	4 M-58	3 M-58	-
3.0	1 Nike	1 Nike	6 M-58	-	-

TABLE II

RUN RECORD - MACH 1.5

NAVAIRDEVCEN-AFML Run No.	Holloman Run No.	Date	Time	V Avg (ft/sec)	Winds	Samples
1	5R-A2	15 Jun	0245	1214.2	Calm 2 k at 30° 2 k at 20°	F1, F2, F3, F4, F5, F6, F7, F8
2	5R-A3	15 Jun	0554	1460	Calm	G3, J2, C2, G1, D1, C6, C7, D2
3	5R-A5	29 Jun	0605	1769	2 k cross track	E10, E9, E11, E5, E2, E1, E14, E6
4	5R-A6	11 Jul	0215	1580	1 k at 10° 1 k at 20° 2 k at 15°	A1, A2, B1, A8, B2, G3, G5, B3
5	5R-A7	11 Jul	0603	1737	Calm	H5, H4, F10, F11, I1, I2, I3, G5
6	5R-A8	28 Jul	0205	1777	2 k at 90° Calm 3 k at 90°	H3, H1, H2, J3, J1, E8, C8, D3
7	5R-B9A	13 Dec	0934	1758.0	Calm	E16 H6, remaining six Plexiglas

TABLE III

RUN RECORD - MACH 2.0

NAVAIRDEVCEN-AFML Run No.	Holloman Run No.	Date	Time	V Avg	Winds	Samples
1	5R-B1	28 Jul	0520	2158.3	NW at 2 k	F1, F2, F3, F4, F6, F-7, F-8, F5
2	5R-B2	8 Aug	0342	2257.8	Calm	C6, C2, C3, C1, C7, D1, D2, H2
3	5R-B3	8 Aug	0657	2197.1	4 k at 20°	E8, B2, A1, A2, A3, A6, A7, J3
4	5R-B4	9 Aug	0245	2110.3	Calm	A8, A9, A10, A11, G1, G2, G3, J1
5	5R-B5	9 Aug	0511	2095.5	Calm	E1, E2, E4, E5, E6, E9, E10, E14
6	5R-B6A	26 Aug	0347	1975.6	Calm	F9, F10, H4, H5, I1, I3, I2, C5
7	5R-B7A	26 Aug	0714	2123.5	2 k at 210°	E3, E12, A12, G4, H3, H6, H1, J2, A1
8	5R-B8A	8 Dec	0802	2116.9	140° at 2 k	E-16, H6, rest Plexiglas
9	5R-B10A	22 Dec	0900	2109.3	4 k at 355°	All Plexiglas and reruns

TABLE IV

RUN RECORD - MACH 2.5

NAVAIRDEVCEN-AFML Run No.	Holloman Run No.	Date	Time	V Avg	Winds	Samples
1	5R-C2A	9 Sep	0344	2205.3	Calm	F1, F2, F3, F4, F6, F7, F8, F5
2	5R-C3A	9 Sep	07500	2592.6	Calm	C6, C2, C3, C1, C7, D1, D2, I2
3	5R-C8A	20 Oct	0805	2594.8	Calm	B2, A1, A2, A3, A6, A7, J3, C3
4	5R-C7A	20 Oct	0529	2561.1	Calm	A8, A9, A10, A11, G1, G2, G3, J1
5	5R-C4A	30 Oct	0537	2243.4	3 k at 250°	E1, E2, E4, E5, E6, E9, E10, E14
6	5R-C5A	11 Oct	0448	2516.6	Calm	C5, F10, N4, H5, I1, I3, I2, E15
7	5R-C6A	11 Oct	0815	2612.5	Calm	E3, E8, G4, H1, H2, H3, H6, J2
8	5R-C1A	8 Sep	0720	2549.0	3 k at 60°	All Plexiglas

TABLE V

RUN RECORD - MACH 3.0

NAVAIRDEVCEN-AFML Run No.	Holloman Run No.	Date	Time	V Avg	Winds	Samples
1	5R-D5A	23 Nov	0713	2905.8	N at 1 k	E8, A1, A2, A3, A5, A4, A6, A7
2	5R-D4A	22 Nov	0817	2942.5	Calm	E1, E2, E5, E9, E10, C1, D2, plexiglas
3	5R-D3A	18 Nov	0800	2976.7	Calm	E3, B2, C2, H2, H3, J3, J1, H1
4	5R-D1A	4 Nov	4 Nov	3366.4	-	All Plexiglas

TABLE VI

MATERIALS LIST

Class	Material	Supplier	Test Mach No.
Isotropic Ceramics			
A-1	9606 Pyroceram	CGW	1.5, 2.0, 2.5, 3.0
A-2	9611 Pyroceram	CGW	1.5, 2.0, 2.5, 3.0
A-3	753 Alumina	Alsimag	2.0, 2.5, 3.0
A-4	Wearox Alumina	Wesgo	3.0
A-5	Al-300 Alumina	Wesgo	3.0
A-6	754 Beryllia	Alsimag	2.0, 2.5, 3.0
A-7	701 Cordierite	Alsimag	2.0, 2.5, 3.0
A-8	7941 Fused Silica	CGW	1.5, 2.0, 2.5, 3.0
A-9	Fused Silica-I (coated with silicon)	GD/P	2.0, 2.5, 3.0
A-10	Fused Silica-II (coated with Teflon)	GD/P	2.0, 2.5, 3.0
A-11	Fused Silica-III (uncoated)	GD/P	2.0, 2.5, 3.0
A-12	Fused Silica	Brunswick	2.0
Sandwich Ceramics			
B-1	0.040" Alumina Sandwich	Narmco	1.5
B-2	0.020" Alumina Sandwich	Brunswick	1.5, 2.0, 2.5, 3.0
B-3	0.040" Alumina Sandwich	Brunswick	1.5
Plastic Laminates			
C-1	Polybenzimidazole (Imidite)	Narmco	1.5, 2.0, 2.5, 3.0
C-2	8265 Epoxy	Furane	1.5, 2.0, 2.5, 3.0

TABLE VI (CONTD)

Class	Material	Supplier	Test Mach No.
Plastic Laminates			
C-3	828 Epoxy	Shell	1.5, 2.0, 2.5
C-4	No samples submitted		
C-5	Polyimide/BMEC 1937 Sealer	Boeing/ Airplane	1.5, 2.0, 2.5
C-6	Polyimide (Skygard 700)	Brunswick	1.5, 2.0, 2.5
C-7	Nomex Epoxy	Boeing/ Aerospace	1.5, 2.0, 2.5
C-8	DC2106 Silicone	NAVAIRDEVCEN	1.5
Inorganic Laminates			
D-1	Alumina/Filament Wound S glass	Lockheed	1.5, 2.0, 2.5, 3.0
D-2	Aluminum Phosphate/S glass	Brunswick	1.5, 2.0, 2.5
Ceramic Coated Plastic Laminates			
E-1	0.020" Precast Alumina/Aluminum Phosphate	Brunswick	1.5, 2.0, 2.5, 3.0
E-2	0.020" Plasma Sprayed Alumina/ Aluminum Phosphate	Brunswick	1.5, 2.0, 2.5, 3.0
E-3	0.040" Plasma Sprayed Alumina/ Aluminum Phosphate	Brunswick	1.5, 2.0, 2.5, 3.0
E-4	0.020" Plasma Sprayed Alumina/ Alumina-Silica-S glass	Lockheed	2.0, 2.5, 3.0
E-5	0.020" Flame Sprayed Alumina/PBI	Narmco	1.5, 2.0, 2.5, 3.0

TABLE VI (CONTD)

Class	Material	Supplier	Test Mach No.
Ceramic Coated Plastic Laminates			
E-6	0.040" Flame Sprayed Alumina/PBI	Narmco	1.5, 2.0, 2.5, 3.0
E-7	No samples submitted		
E-8	0.125" Alumina/ 0.030" RTV521/ Polyimide	Boeing/ Airplane	1.5, 2.0, 2.5, 3.0
E-9	0.030" Rokide "A" Alumina/Polyimide	Goodyear	1.5, 2.0, 2.5, 3.0
E-10	0.030" Rokide "A" Alumina with Cr_2O_3/Polyimide	Goodyear	1.5, 2.0, 2.5, 3.0
E-11	Plasma Sprayed Alumina/Silica/ quartz glass	Lockheed	1.5
E-12	Flame Sprayed Alumina/Polyimide	Brunswick	2.0
E-13	No samples submitted		
E-14	0.030" Rokide Alumina/ 828 Epoxy	NOL	1.5, 2.0, 2.5
E-15	0.040" Precast Alumina/Aluminum Phosphate	Brunswick	2.5
E-16	0.030" Plasma Sprayed Alumina (H_3PO_4 treated)/ 828 Epoxy	Brunswick	1.5, 2.0
Elastomeric Coated Plastic Laminates			
F-1	0.010" GACO/828 Epoxy	Gates Engineering/ NAVAIRDEVCEN	1.5, 2.0, 2.5

TABLE VI (CONTD)

Class	Material	Supplier	Test Mach No.
Elastomeric Coated Plastic Laminates			
F-2	0.020" GACO/828 Epoxy	Gates Engineering/ NAVAIRDEVCEN	1.5, 2.0, 2.5
F-3	0.010" Neoprene on Dacron/828 Epoxy	B. F. Goodrich/ NAVAIRDEVCEN	1.5, 2.0, 2.5
F-4	0.020" Neoprene on Dacron/828 Epoxy	B. F. Goodrich/ NAVAIRDEVCEN	1.5, 2.0, 2.5
F-5	0.030" Neoprene on Dacron/828 Epoxy	B. F. Goodrich/ NAVAIRDEVCEN	1.5, 2.0, 2.5
F-6	0.014" Polyurethane on Dacron/828 Epoxy	B. F. Goodrich/ NAVAIRDEVCEN	1.5, 2.0, 2.5
F-7	0.026" Polyurethane on Dacron/828 Epoxy	B. F. Goodrich/ NAVAIRDEVCEN	1.5, 2.0, 2.5
F-8	0.038" Polyurethane on Dacron/828 Epoxy	B. F. Goodrich/ NAVAIRDEVCEN	1.5, 2.0, 2.5
F-10	0.020" Hycar on Dacron/828 Epoxy	B. F. Goodrich/ NAVAIRDEVCEN	1.5, 2.0, 2.5
F-11	0.030" Hycar on Dacron/828 Epoxy	B. F. Goodrich/ NAVAIRDEVCEN	1.5, 2.0, 2.5
Glasses			
G-1	0313 Chemcor	CGW	2.0, 2.5, 3.0
G-2	9753 I/R Glass	CGW	2.0, 2.5, 3.0
G-3	C106 CER - VIT	Owen-Illinois	1.5, 2.0, 2.5
G-4	0315 Chemcor	CGW	2.0, 2.5, 3.0
G-5	0312 Chemcor	CGW	1.5

TABLE VI (CONCLUDED)

Class	Material	Supplier	Test Mach No.
Sandwich Plastics			
H-1	8265 Furane Epoxy Sandwich	GD/FW	1.5, 2.0, 2.5
H-2	Polyimide Sandwich	Boeing/ Airplane	1.5, 2.0, 2.5, 3.0
H-3	Titanium/Polyimide Sandwich	Boeing/ Airplane	1.5, 2.0, 2.5, 3.0
H-4	0.035" Teflon/Nomex Epoxy	Boeing/ Aerospace	1.5, 2.0, 2.5
H-5	Cork/Epoxy	Boeing/ Aerospace	1.5, 2.0, 2.5
H-6	Nickel Plate/Epoxy	AFML	1.5, 2.0, 2.5
Thermal Plastics			
I-1	PPO	GE	1.5, 2.0, 2.5
I-2	Plexiglas	AFML	1.5, 2.0, 2.5, 3.0
I-3	TFE Teflon	AFML	1.5, 2.0, 2.5
Metals			
J-1	2024-T3 Aluminum	NAVAIRDEVCEN	1.5, 2.0, 2.5, 3.0
J-2	6061-T6 Aluminum	NAVAIRDEVCEN	1.5, 2.0, 2.5, 3.0
J-3	Annealed Copper	NAVAIRDEVCEN	1.5, 2.0, 2.5, 3.0

PRECEDING PAGE BLANK - NOT FILMED.

MATERIALS

Material	Porosity-% ASTM 373-56	Density-gm/cc ASTM 373-56	Hardness Knoop	Modulus of Elasticity psi Sonic Resonance Method	S
A. Isotropic Ceramics					
A-1 9606 Pyroceram-CGW	.00	2.6	500 gm load 619	17.2×10^6	
A-2 9611 Pyroceram-CGW	.00	2.93	100 gm load 644	17.0×10^6	
A-3 Alumina-Alsimag No. 753	0	3.85	Rockwell 45N 80		
A-4 Alumina-Wearox-Wesgo					
A-5 Alumina-Wesgo AL-300	0	3.76	MOH scale 9		
A-6 Beryllia-Alsimag No. 754	0	2.88	Rockwell 45N 65		
A-7 Cordierite-Alsimag No. 701	.02-1.0	2.3	MOH Scale 8		
A-8 Fused Silica-No. 7941 CGW	2.5-12.0	1.9-2.1	Rockwell 15N 84	8.4×10^6	
A-9 Fused Silica-GD/P I (coated)	12.0	2.0	500 gm load 190	3.5×10^6	
A-10 Fused Silica-GD/P II (coated)	12.0	2.0	500 gm load 190	3.5×10^6	
A-11 Fused Silica-GD/P III	12.0	2.0	500 gm load 190	3.5×10^6	
A-12 Fused Silica-Brunswick					

TABLE VII

'IALS PROPERTIES SUMMARY

ce	Shear Modulus psi Sonic Resonance Method	Shear Strength psi	Flexural Strength-psi Cyl. Spec. 4Pt. Loading 100,000 psi/min	Tensile Strength psi Supplier Method	Compressive Strength psi	Poisson's Ratio Sonic Resonance Method	Dielectric Constant (8.6-10.0 KMC) ATC Rept. ARTC 4	Loss Tangent (8.6-10.0 KMC) ATC Rept. ARTC 4
	6.9×10^6		$35. \times 10^3$	$26. \times 10^3$	340×10^3	.245	5.5	.0003
	7.0×10^6		$14. \times 10^3$	$10. \times 10^3$	125×10^3	.22	6.9	.0004
			$50. \times 10^3$	$28. \times 10^3$	375×10^3		9.6	.0019
			$46. \times 10^3$		250×10^3		9.9	.0015
			35×10^3	$11. \times 10^3$	185×10^3		6.1	.0001
			15×10^3	$6. \times 10^3$	50×10^3		5.5	.005
	3.6×10^6		6,300	4.7×10^3	50×10^3	.15	3.3	.0016
			4,000			.17	3.2	.0002
			4,000			.17	3.2	.0002
			4,000			.17	3.2	.0002

2

TABLE VII (CON

Material	Porosity-% ASTM 373-56	Density-gm/cc ASTM 373-56	Hardness Knoop	Modulus of Elasticity psi Sonic Resonance Method	Shear Modu psi Sonic Reson Method
B. Sandwich Ceramics					
B-1 "A" Sandwich Alumina 0.040" Alumina Skins/Alumina Foam Core Narmco	10 - 15 20 - 25	4.07 1.0	970 500 gm load		
B-2 "A" Sandwich Alumina 0.020" PC Alumina Skins/Alumina Foam Core Brunswick	<7	3.66	Rockwell "A"89	43.3×10^6	
B-3 "A" Sandwich Alumina 0.040" PS Alumina Skins/Alumina Foam Core Brunswick					
G. Glasses					
G-1 Chemcor- CGW No. 0313	0	2.45	100 gm load 540(est)	10.6×10^6	4.4 x 1(
G-2 I/R Glass No. 9753, CGW	0.00	2.798	601		5.6 x 1(
G-3 C106 CER-VIT Owens Illinois, Boeing	0	2.51	200 gm load 600	13.3×10^6	5.3 x 1(
G-4 No. 0315 Chemcor-CGW	0.00	2.458	100 gm load 590	10.3×10^6	4.3 x 1(
G-5 No. 0312 Chemcor-CGW					
D. Inorganic Materials					
D-1 FW Alumina-Silica S Glass Lockheed		1.71			
D-2 Alumina Phosphate-S Glass Laminate Brunswick	15	FTM Std 406 1.8	Barcol 60	2.82×10^6	

/11 (CONTD)

ar Modulus psi c Resonance Method	Shear Strength psi	Flexural Strength-psi Cyl. Spec. 4Pt. Loading 100,000 psi/min	Tensile Strength psi Supplier Method	Compressive Strength psi	Poisson's Ratio Sonic Resonance Method	Dielectric Constant (8.6-10.0 KMC) ATC Rept. ARTC 4	Loss Tangent (8.6-10.0 KMC) ATC Rept. ARTC 4	
						8.6		Skin
	220		500-1000			2.43	.00125	Core
		Composite 34.5×10^3	20×10^3	30×10^4		8.8	.0007	Skin
						2.5	.0011	Core
4.4×10^6		40×10^3			.22			
5.6×10^6					.28	8.59	.01	
5.3×10^6		1.8×10^4			.25	5.4 at 1MC	.026 at 1MC	
4.3×10^6		85,000			.21			
	MTD 1042 400	16×10^3	28×10^3	6×10^3		3.44	.008	

2

TABLE VII (C

Material	Porosity-% ASTM 373-56	Density-gm/cc ASTM 373-56	Hardness Knoop	Modulus of Elasticity psi Sonic Resonance Method	Shear p Sonic R Me
E. Ceramic Coated Laminates					
E-1 Precast Alumina (0.020") on Al PO_4 - Brunswick	<5	3.75	Rockwell 'A' 88	43.9×10^6	
E-2 Plasma Spray Alumina* (0.020") onAl PO_4 Brunswick	8	FTM Std 406 3.5	Rockwell 'C' 70	40×10^6	
E-3 Plasma-Spray Alumina (0.040") on Al PO_4 Brunswick	8	FTM Std 406 3.5	Barcol 60	40×10^6	
E-4 0.020" PS Alumina/Alumina-Silica S Glass Laminate-FW Lockheed		3.3			
E-5 0.020" PS Alumina/PBI Laminate- Na mco	12 15	3.3 1.65	1450 70	32×10^6 4.75×10^6	N 2.0
E-6 0.040" PS Alumina/PBI Laminate- Narmco	12 15	3.3 1.65	1450 70	32×10^6 4.75×10^6	N 2.0
E-7 Vapor Deposited Alumina/ PBI Laminate GTC					
E-8 0.125" Alumina/0.030" RT V521/ 0.100" Polyimide Laminate Boeing Seattle	.6	3.48	500 gm load 1000	25.7×10^6	10.2
E-9 0.030" P3 Rokide "A" PI Laminate-Goodyear Aerospace	7	3.3 FTM Std 406 11755	2000 gm load Barcol 48	2.73×10^6	N
E-10 PS Rokide "A" Alumina/ PI Laminate-Al_2O_3 contains CR_2O_3 - Goodyear Aerospace	2	4.6/1.755	2000 gm load	3.12×10^6	

*Properties for costing - See D-2 for laminate

'II (CONTD)

ear Modulus psi ic Resonance Method	Shear Strength psi	Flexural Strength-psi Cyl. Spec. 4Pt. Loading 100,000 psi/min	Tensile Strength psi Supplier Method	Compressive Strength psi	Poisson's Ratio Sonic Resonance Method	Dielectric Constant (8.6-10.0 KMC) ATC Rept. ARTC 4	Loss Tangent (8.6-10.0 KMC) ATC Rept. ARTC 4	
		23.3×10^3				8.8	.0007	
		35×10^3	25×10^3			9.0	.003	
		35×10^3	25×10^3			9.0	.003	
N/A 2.0×10^6	6×10^3	5×10^3 11×10^4	2×10^3 87×10^3	4×10^4 7×10^4		7.0 4.2-4.8	.001 .007	Ceramic Plastic
N/A 2.0×10^6	6×10^3	5×10^3 11×10^4	2×10^3 87×10^3	4×10^4 7×10^4		7.0 4.2-4.8	.001 .007	Ceramic Plastic
					.26			
10.2×10^6								
N/A	FTMS 406 1059	FTMS 406 59,300	FTMS 406 15,600	37,000 -37,600				
N/A	1380	65,800	33,650	87,000-A 103,000-C/ 47,500				

2

TABLE VII

Material	Porosity-% ASTM 3 3-56	Density-gm/cc ASTM 373-56	Hardness Knoop	Modulus of Elasticity psi Sonic Resonance Method	Shear M Sonic Re Met
E-11 Sprayed Alumina/Silica quartz glass - Lockheed					
E-12 Plasma Sprayed Alumina/ PI Laminate - Brunswick					
E-13 0.020" PS Alumina/FW Silica Quartz glass Laminate - Lockheed					
E-14 PS Rokide "A" Alumina/ 828 Epoxy Laminate NOL	13.3	3.37	1950	15.8×10^6	7.3
E-15 0.040" Precast Alumina/ Al PO_4 Laminate - Brunswick		3.75			
E-16 0.030" Plasma Sprayed Alumina (H_3PO_4 treatment)/ Epon 828 Laminate	7	3.5	520		

TABLE VII (CONTD)

Shear Modulus Sonic Resonance Method	Shear Strength psi	Flexural Strength-psi Cyl. Spec. 4Pt. Loading 100,000 psi/min	Tensile Strength psi Supplier Method	Compressive Strength psi	Poisson's Ratio Sonic Resonance Method	Dielectric Constant (8.6-10.0 KMC) ATC Rept. ARTC 4	Loss Tangent (8.6-10.0 KMC) ATC Rept. ARTC 4
7.3×10^6					.08		

Material	Specific Gravity	Hardness Shore "A" Durometer ASTM-D-676	Tear lbs/in. Thickness	% Elonga at bre ASTM-D-
F. Elastomeric Coated Laminates				
F-1 0.010" Gaco/Epon 828 Epoxy Laminate Navairdevcen	1.77			
F-2 0.020" Gaco/828 Epoxy Laminate-Navairdevcen	1.77			
F-3 0.010" Neoprene/Dacron/828 Epoxy Laminate-Goodrich	1.30	56	137	570
F-4 0.020" Neoprene/Dacron/828 Epoxy Laminate-Goodrich	1.30	56	137	570
F-5 0.030" Neoprene/Dacron/828 Epoxy Laminate-Goodrich	1.30	56	137	570
F-6 0.014" Polyurethane/828 Epoxy Laminate-Goodrich	1.22	78	335	640
F-7 0.026" Polyurethane/828 Epoxy Laminate-Goodrich	1.22	78	335	640
F-8 0.038" Polyurethane/828 Epoxy Laminate-Goodrich	1.22	78	335	640
F-9 0.010" Hycar/828 Epoxy Laminate	1.368	94	775	430
F-10 0.020" Hycar/828 Epoxy Laminate	1.368	94	775	430
F-11 0.030" Hycar/828 Epoxy Laminate	1.368	94	775	430

TABLE VII (CONTD)

ear s/in. ckness	% Elongation at break ASTM-D-412	Modulus at 100% Elongation-psi-ASTM-D-412	Modulus at 300% Elongation-psi-ASTM-D-412	Tensile Strength psi ASTM-D-412	Dielectric Constant (8.6-10.0 KMC) ATC Rept. ARTC 4	Loss Tangent (8.6-10.0 KMC) ATC Rept. ARTC 4
137	570	220	900	3090	3.1	.029
137	570	220	900	3090	3.1	.029
137	570	220	900	3090	3.1	.029
35	640	560	1380	3450	5.5	.05
335	640	560	1380	3450	5.5	.05
35	640	560	1380	3450	5.5	.05
5	430	1350	3240	4030	5.0	.05
5	430	1350	3240	4030	5.0	.05
5	430	1350	3240	4030	5.0	.05

2

TABLE VII (CONTD)

Material	Porosity-% FTM Std No. 406 MTD 5021	Density-Gm/cc FTM Std No. 406 MTD 5011	Hardness Barcol	Modulus of Elasticity-psi Slope of Tau at Low End of Stress Strain Curve	Shear Modulus psi	Sh Stren FTM No. MTD
C. Plastic Laminates						
C-1 PBI (Imidite) Laminate -Narmco	15	1.65	70	4.75×10^6	2.0×10^6	6 x
C-2 Furane Epoxy Laminate-No. 8265 GD/FW	0	1.77	60 (min.)	3.2×10^6		
C-3 Epon 828 Epoxy Laminate-Navairdevcen (All Epon 828 is good for 450°F/500 hrs)	0	1.6				
C-4 Epon 828 Epoxy 50% Alumina Loaded-Navairdevcen						
C-5 Polyimide Laminate BMEC 1937 Sealer-Boeing	7.9 (1)	1.51 (Sp. Gr.)	50 (2)	2.7×10^6		150
C-6 Polyimide Laminate-Skyguard 700-Brunswick		1.7	55	2.7×10^6		
C-7 Nomex Epoxy Laminate Boeing Seattle	0	1.38	45-50	$4-6 \times 10^6$		
C-8 DC2106 Laminate Navairdevcen Silicone						

BLE VII (CONTD)

ar tus i	Shear Strength-psi FTM Std No. 406 MTD-1040	Flexural Strength-psi FTM Std No. 406 MTD 1031	Tensile Strength-psi FTM Std No. 406 MTD 1011	Compressive Strength-psi FTM Std No. 406 MTD 1021	Poisson's Ratio Supplier Method	Dielectric Constant (8.6-10.0 KMC) ATC Rept. ARTC 4	Loss Tangent (8.6-10.0 KMC) ATC Rept. ARTC 4	
$\times 10^6$	6×10^3	11×10^4	87×10^3	7.0×10^3		4.2-4.8	.007	Laminate only
		70×10^3	50×10^3	45×10^3		4.86*	.019*	*at 350°F
	1500	45×10^3	35×10^3	28×10^3		4.1	.009	
		60×10^3	40×10^3	40×10^3		4.2	.015	
			$15-25 \times 10^3$					

2

TABLE VII (CONCL

	Porosity-% FTM Std No. 406 MTD 5021	Density-gm/cc FTM Std No. 406 MTD 5021	Hardness Barcol	Modulus of Elasticity-psi Slopes of Tan at Low End of Stress Strain Curve	Shear Modulus psi	
H. Sandwich Plastics						
H-1 0.010" Gaco/0.040" Furane Epoxy HC-GD/FW	0	1.77	60 (min)	3.2×10^6		
H-2 Polyimide HC - Boeing	7.9	1.51	50	2.7×10^6		1
H-3 0.010" Titanium/Polyimide HC/ 0.010" Titanium - Boeing	0	4.43		16×10^6	6.2×10^6	
H-4 0.035" Teflon/Nomex Epoxy Laminate		2.25	Shore 55-56	9.5×10^4		2.
H-5 0.035" Armstrong Cork AC-2755 Over Nomex Epoxy Laminate-Boeing Seattle	50	.48		7×10^3		
H-6 0.010" Electroplated nickel/Epon 828 Laminate-AFML		8.90	Vickers 163-332			
I. Thermal Plastics						
I-1 PPO-GE (polyphenylene oxide)	0	1.06	Rockwell R-120	37×10^4		10
I-2 Plexiglas (Type II- UVA)-AFML	0	1.19	45-49	4.36×10^5		
I-3 Teflon - DuPont	0	2.25	Shore 55-56	9.5×10^4		25
J. Metals						
J-1 2024-T3 Aluminum		2.77	Brinell 120			
J-2 6061 T6 Aluminum		2.70	95			
J-3 Copper-Annealed		8.96				

TABLE VII (CONCLUDED)

Shear Modulus psi	Shear Strength-psi FTM Std No. 406 MTD 1040	Flexural Strength-psi FTM Std No. 406 MTD 1031	Tensile Strength-psi FTM Std No. 406 MTD 1011	Compressive Strength-psi FTM Std No. 406 MTD 1021	Poisson's Ratio Supplier Method	Dielectric Constant (8.6-10.0 KMC) ATC Rept. ARTC 4	Loss Tangent (8.6-10.0 KMC) ATC Rept. ARTC 4	
		70×10^3	50×10^3	45×10^3		4.86*	.019*	*at 350°F
	1.5×10^3	45×10^3	35×10^3	28×10^3		4.1 *	.009*	*at 75°F-937mc
6.2×10^6	78×10^3		134×10^3	132×10^3	0.30			
	$2.5/3 \times 10^3$	2×10^3	3200/4000	1.7×10^3		2.1	.0002 .0005	
			300/400	150 300		1.8	.05	
			$73\text{-}133 \times 10^3$					Elong. 4-20%
	10.9×10^3	15×10^3	10.5×10^3	11×10^3	0.4	2.58	0.01	
	8600	17.7×10^3	10.8×10^3	18×10^3	0.33	2.2-3.2	0.02-0.03	
	2500/3000	2×10^3	3200/4000 3500/4500	1.7×10^3		2.1	.0002 .0005	Depends on Freq.
			64,000		Yield Strength 42,000	Elong. 15%		
			42,000		35,000	10%		
			32,000		———	40%		

2

TABLE VIII

CONSTANTS FOR THE RAIN EROSION EQUATION

$$(MDPR = Ee^{\alpha v}\sin\theta + Fe^{\gamma v})$$

Material	α	γ	$\theta < \theta_0$ E	$\theta < \theta_0$ F	$\theta > \theta_0$ E	$\theta > \theta_0$ F
C-1 Polybenzimidazole (PBI) Laminate	1.73×10^{-3}	1.45×10^{-3}	3.38×10^{-4}	0	4.11×10^{-3}	-4.65×10^{-3}
C-2 Furane 8265 Epoxy Laminate	2.41×10^{-3}	2.22×10^{-3}	1.34×10^{-5}	0	2.15×10^{-4}	-2.15×10^{-4}
C-3 Epon 828 Epoxy Laminate	1.84×10^{-3}	1.64×10^{-3}	Undetermined	0	9.62×10^{-4}	-8.40×10^{-4}
C-5 Polyimide Laminate-BMEC 1937 Sealer	1.21×10^{-3}	5.12×10^{-4}	9.63×10^{-4}	0	9.48×10^{-2}	-2.75×10^{-2}
C-6 Polyimide Laminate	6.44×10^{-4}	3.41×10^{-4}	3.7×10^{-3}	0	4.9×10^{-2}	$-5.8\times10^{+2}$
C-7 Nomex Epoxy Laminate	1.39×10^{-3}	8.58×10^{-4}	3.26×10^{-4}	0	2.77×10^{-3}	-5.48×10^{-3}
7941 Fused Silica	2.15×10^{-3}	2.66×10^{-3}	0	0	1.79×10^{-3}	0.628×10^{-3}
GD/P Fused Silica	0.896×10^{-3}	0.498×10^{-3}	0	0	0.097	0.155

REFERENCES

1. NAVAIRDEVCEN drawings:

A-40-00281	Drawing List
J-40-00119	Wedge Assembly
A-40-00283	Test Sample
J-40-00109	Wedge Plates
D-40-0011	Wedge Base
C-40-00112	V Bar
D-40-00113	Cover and Bottom Plate
C-40-00115	Remet Cover Strip
A-EH-00539	Remet Spacer
A-EH-00538	Remet Pad

2. Wind Tunnel Tests of a 1/3-Scale Rain Erosion Wedge Model at Mach Numbers of 2.15, 2.86 and 3.75, David Taylor Model Basin Report AL 17.

3. D. C. Jenkins and J. D. Booker, The Time Required for High Speed Airstreams to Disintegrate Water Drops, Royal Aircraft Establishment Technical Note No. Mech. Engr. 401, Farnborough, England, May 1964.

4. Olive G. Engel, "Fragmentation of Water Drops in the Zone Behind an Air Shock," Journal of Research of the National Bureau of Standards, Vol 60, No. 3, March 1958.

5. The Holloman Track - Facilities and Capabilities, MDC-TR-65-2, Air Force Missile Development Center, Holloman Air Force Base, New Mexico, June 1965.

6. Marcel C. Reynolds, Rain Measurement and Simulation for Supersonic Rain Erosion Studies, Sandia Corporation Report SCR-474, February 1962.

7. Transactions, American Geophysical Union 24th Annual Meeting, 23-24 April 1943, Part II.

8. V. A. Chase and R. L. Copeland, Supersonic Rain Erosion Resistant Coating Materials Investigation, AFML-TR-67-62, Air Force Materials Laboratory, Wright-Patterson Air Force Base, Ohio, February 1967.

9. James H. Weaver, Nickel Electroplated Nonconductive Materials for Rain Erosion Protection, AFML-TR-66-398, Air Force Materials Laboratory, Wright-Patterson Air Force Base, Ohio, December 1966.

Unclassified

Security Classification

DOCUMENT CONTROL DATA - R&D

(Security classification of title, body of abstract and indexing annotation must be entered when the overall report is classified)

1. ORIGINATING ACTIVITY *(Corporate author)*
Air Force Materials Laboratory
Wright-Patterson Air Force Base, Ohio 45433

2a. REPORT SECURITY CLASSIFICATION

2b. GROUP

3. REPORT TITLE
JOINT AIR FORCE-NAVY SUPERSONIC RAIN EROSION EVALUATIONS OF MATERIALS

4. DESCRIPTIVE NOTES *(Type of report and inclusive dates)*
January 1966 - December 1966

5. AUTHOR(S) *(Last name, first name, initial)*
Schmitt, George J., Jr., Tatnall, George J., and Fouike, Kenneth W.

6. REPORT DATE	7a. TOTAL NO. OF PAGES	7b. NO. OF REFS
December 1967	166	9

8a. CONTRACT OR GRANT NO.	9a. ORIGINATOR'S REPORT NUMBER(S)
b. PROJECT NO. 7340	AFML-TR-67-164
c. 734007	9b. OTHER REPORT NO(S) *(Any other numbers that may be assigned this report)*
d.	

10. AVAILABILITY/LIMITATION NOTICES This document may be further distributed by any holder only with specific prior approval of the Elastomers and Coatings Branch (MANE), Nonmetallic Materials Div., AF Materials Laboratory, Wright-Patterson AFB, Ohio 45433, or the Radome Antenna Sec (AERT), Radar Div, Naval Air Development Center, Johnsville, Pa 18974

11. SUPPLEMENTARY NOTES

12. SPONSORING MILITARY ACTIVITY
Air Force Materials Laboratory
Wright-Patterson Air Force Base, Ohio 45433

13. ABSTRACT

A comprehensive investigation of sixty-five dielectric and other materials for short exposure time rain erosion resistance at velocities of Mach 1.5, 2.0, 2.5 and 3.0 has recently been accomplished in a joint program of the Elastomers and Coatings Branch, Nonmetallic Materials Division, Air Force Materials Laboratory and the Radome-Antenna Section, Naval Air Development Center. This work was accomplished at the Holloman AFB Test Track Facility, New Mexico.

Multiple samples of each material were mounted in a wedge shaped holder attached to the forward end of a multi-staged rocket sled and exposed to the same rain environment by firing the sled through a 6,000 feet long artificial rainfield. The samples were exposed at five different impact angles and four different velocities and the quantitative rain erosion resistance determined as a function of velocity, time of exposure and impact angle. Although the exposure times were short the materials demonstrated real differences in their rain erosion resistance.

Materials evaluated included isotropic and sandwich ceramics, plastic laminates, nickel electroplated plastics, inorganic laminates, ceramic and elastomeric coated laminates,

DD FORM 1 JAN 64 1473

Unclassified

Security Classification

Unclassified

Security Classification

14. KEY WORDS	LINK A ROLE	LINK A WT	LINK B ROLE	LINK B WT	LINK C ROLE	LINK C WT
Rocket Sled						
Supersonic Rain Erosion						
Materials Evaluations						
Mean Depth of Penetration Rate						
Impact Angle						
Velocity						

INSTRUCTIONS

1. ORIGINATING ACTIVITY: Enter the name and address of the contractor, subcontractor, grantee, Department of Defense activity or other organization *(corporate author)* issuing the report.

2a. REPORT SECURITY CLASSIFICATION: Enter the overall security classification of the report. Indicate whether "Restricted Data" is included. Marking is to be in accordance with appropriate security regulations.

2b. GROUP: Automatic downgrading is specified in DoD Directive 5200.10 and Armed Forces Industrial Manual. Enter the group number. Also, when applicable, show that optional markings have been used for Group 3 and Group 4 as authorized.

3. REPORT TITLE: Enter the complete report title in all capital letters. Titles in all cases should be unclassified. If a meaningful title cannot be selected without classification, show title classification in all capitals in parenthesis immediately following the title.

4. DESCRIPTIVE NOTES: If appropriate, enter the type of report, e.g., interim, progress, summary, annual, or final. Give the inclusive dates when a specific reporting period is covered.

5. AUTHOR(S): Enter the name(s) of author(s) as shown on or in the report. Enter last name, first name, middle initial. If military, show rank and branch of service. The name of the principal author is an absolute minimum requirement.

6. REPORT DATE: Enter the date of the report as day, month, year; or month, year. If more than one date appears on the report, use date of publication.

7a. TOTAL NUMBER OF PAGES: The total page count should follow normal pagination procedures, i.e., enter the number of pages containing information.

7b. NUMBER OF REFERENCES: Enter the total number of references cited in the report.

8a. CONTRACT OR GRANT NUMBER: If appropriate, enter the applicable number of the contract or grant under which the report was written.

8b, 8c, & 8d. PROJECT NUMBER: Enter the appropriate military department identification, such as project number, subproject number, system numbers, task number, etc.

9a. ORIGINATOR'S REPORT NUMBER(S): Enter the official report number by which the document will be identified and controlled by the originating activity. This number must be unique to this report.

9b. OTHER REPORT NUMBER(S): If the report has been assigned any other report numbers *(either by the originator or by the sponsor)*, also enter this number(s).

10. AVAILABILITY/LIMITATION NOTICES: Enter any limitations on further dissemination of the report, other than those imposed by security classification, using standard statements such as:

(1) "Qualified requesters may obtain copies of this report from DDC."

(2) "Foreign announcement and dissemination of this report by DDC is not authorized."

(3) "U. S. Government agencies may obtain copies of this report directly from DDC. Other qualified DDC users shall request through _____."

(4) "U. S. military agencies may obtain copies of this report directly from DDC. Other qualified users shall request through _____."

(5) "All distribution of this report is controlled. Qualified DDC users shall request through _____."

If the report has been furnished to the Office of Technical Services, Department of Commerce, for sale to the public, indicate this fact and enter the price, if known.

11. SUPPLEMENTARY NOTES: Use for additional explanatory notes.

12. SPONSORING MILITARY ACTIVITY: Enter the name of the departmental project office or laboratory sponsoring *(paying for)* the research and development. Include address.

13. ABSTRACT: Enter an abstract giving a brief and factual summary of the document indicative of the report, even though it may also appear elsewhere in the body of the technical report. If additional space is required, a continuation sheet shall be attached.

It is highly desirable that the abstract of classified reports be unclassified. Each paragraph of the abstract shall end with an indication of the military security classification of the information in the paragraph, represented as *(TS)*, *(S)*, *(C)*, or *(U)*.

There is no limitation on the length of the abstract. However, the suggested length is from 150 to 225 words.

14. KEY WORDS: Key words are technically meaningful terms or short phrases that characterize a report and may be used as index entries for cataloging the report. Key words must be selected so that no security classification is required. Identifiers, such as equipment model designation, trade name, military project code name, geographic location, may be used as key words but will be followed by an indication of technical context. The assignment of links, rules, and weights is optional.

Unclassified

Security Classification

DD Form 1473 — Item 13, ABSTRACT (contd)

glasses, thermoplastics, sandwich plastics and metals. The results of these supersonic exposures are summarized and listed according to materials category.

Quantitative data in the form of weight loss per unit area and mean depth of penetration rate (MDPR) are presented. Equations describing the high velocity-short exposure time erosion rates of plastic laminates and fused silica ceramics have been developed. Data for most other materials have been plotted but not fitted to equations. Photographs of all rain-exposed specimens and descriptions of the 65 materials evaluated are included.

Distribution of this Abstract is unlimited.